TRANSLATIONAL STUDIES OF EPIGENETIC INTERVENTIONS FOR POST-TRAUMATIC EPILEPSY

A Dissertation

by

VICTORIA MARIE DUNLAP GOLUB

Submitted to the Office of Graduate and Professional Studies of
Texas A&M University
in partial fulfillment of the requirements for the degree of

DOCTOR OF PHILOSOPHY

Chair of Committee,	D. Samba Reddy
Committee Members,	C. Jane Welsh
	Michelle Hook
	Gerard Toussaint
Head of Department,	Farida Sohrabji

August 2021

Major Subject: Medical Sciences

ABSTRACT

Post-traumatic epilepsy (PTE) is a life-long seizure disorder that can arise from traumatic brain injury (TBI). In addition to the rapid inflammatory response and lesion-site necrosis, TBI induces immediate and long-term changes within the epigenome which contribute to the development of post-traumatic seizures. Animal models of PTE have many limitations to demonstrate a high enough incidence of seizures to design studies which test novel therapeutic strategies. Using a controlled-cortical impact model of severe TBI, we designed a model of PTE which has generated spontaneous seizures in about 80% of mice. In the first aim of this dissertation, we fully characterized the histopathology, electrographic activity, and behavioral changes which are associated with PTE over 120 days after TBI incident.

Currently, there are no pharmacotherapies in use to favorably control seizures, and/or the functional and behavioral outcome of PTE. Epigenetic histone modification can be easily manipulated with the use of HDAC inhibitors which block the removal of acetyl groups from histone proteins, thereby affecting gene transcription. Previous research using HDAC inhibitor compounds have reported neuroprotective effects such as reduction of both inflammation and cell loss. In aims 2 and 3 of this dissertation, we investigated the effects of dietary, broad-spectrum, and narrow-spectrum HDAC inhibitors improve neurological and cognitive outcomes after TBI. Our broad HDAC inhibitor compounds were sodium butyrate and vorinostat (SAHA); we chose entinostat (previously MS-275) as a narrow spectrum inhibitor.

Our results demonstrate that HDAC inhibitor administration normalizes HDAC activity levels to non-injured mice, and results in decreased inflammation, reduced neurodegeneration, and improved quality of life. All HDAC inhibitor compounds reduced seizure burden in a significant fashion. Sodium butyrate reduced frequency and duration of seizures in responding mice, providing a scientific basis of HDAC inhibition as a disease modifier in epileptogenesis. SAHA and entinostat treatments also demonstrated a significant reduction in seizure frequency, but more importantly, we also observed a reduction in the incidence of chronic epilepsy in these cohorts.

Our findings indicate that HDAC inhibition therapy given soon after TBI can be potentially neuroprotective and may be a viable therapeutic to prevent or reduce epileptogenesis after TBI in at-risk patients.

DEDICATION

This dissertation is dedicated to my parents, loving husband, and the two beautiful pups who patiently sat beside me every day as I wrote.

Completing a PhD has been a long and challenging journey, but I certainly did not conquer this feat alone. For every failed experiment, tough question, or celebration, your support guided me.

ACKNOWLEDGEMENTS

First and foremost, I would like to thank my committee chair, Dr. Reddy for his professional mentorship and continuous support of my work. I was fortunate to have the opportunity to work in a lab environment that encourages rigorous scientific work and provided support both inside and outside of the lab. My time working in this lab has helped me grow as a scientist, leader, and teacher. Within the lab, I have gained countless friendships with scholars in every walk of their career. I will forever cherish the opportunities afforded to me, from taking gross anatomy with the medical students to training and mentoring over 40 undergraduate students. Dr. Reddy has always gently pushed me forwards to reach my full potential, even if I didn't know it at the time.

I would also like to thank the members of my committee: Dr. Jane Welsh, Dr. Michelle Hook, and Dr. Gerard Toussaint, for their guidance and feedback on my research and progression through the PhD program. Their input helped shape this project and provided a critical insight to the field. I am sincerely grateful for all the time and energy they invested in my growth.

I would also like to recognize a number of individuals who have provided critical support in the completion of this dissertation—both academic and in the form of friendship, guidance, or support.

The senior graduate students before me: Chase Carver, Bryan Clossen, and Shu-Hui Chuang. They provided the finest example of what it meant to be a diligent and intelligent scientist. Their kindness and personal guidance throughout the years helped

mold me into who I am today. From conferences to lab-fridge leftover pot-lucks to Walmart runs for supplies, these memories will stay with me forever. Even after their graduations, our collaborations remained in the form of Spotify playlists.

I thank Xin Wu and Ramkumar Kuruba for their assistance in technical training in the operation of our EEG systems, histology microscopes, and countless other scientific methods. I also thank Justin McDermott for his assistance with MATLAB seizure detection.

I thank Bhagath Chirra, Dae Chung, Alex Powell and the rest of our Graduate Student Organization for being the best friendship support system anyone could ask for during graduate school, but also for the endless opportunities for professional development and networking. The GSO played a large role in my time here at Texas A&M Health Science Center, and my experience would not have been the same without the student and faculty leadership that shape this program.

I would like to thank the dozens of other students and scientists I worked with during my time as a graduate student. I wish them the very best in their careers as researchers, physicians, pharmacists, and anything in between. It is through these interactions that furthered my love of teaching and mentoring.

Finally, I would like to thank my parents for their encouragement and my husband, Devon, for his endless patience and love.

CONTRIBUTORS AND FUNDING SOURCES

Contributors

This work was supervised by a dissertation committee consisting of Professor Samba Reddy [advisor] and Professors Michelle Hook and Gerard Toussaint of the Department of Neuroscience and Experimental Therapeutics and Professor Jane Welsh of the Department of Veterinary Integrative Biosciences.

All other work conducted for the dissertation was completed by the student independently.

Funding Sources

This work was made possible in part by DOD grant #W81XWH-16-1-0660 to D. Samba Reddy. It is partly supported by the TAMU Presidential X-grant (to Dr. Reddy and team). Its contents are solely the responsibility of the authors and do not necessarily represent the official views of the US Department of Defense or Texas A&M.

Graduate study was supported in part by a fellowship from Texas A&M Health Science Center to Victoria Golub.

NOMENCLATURE

AED	Antiepileptic drug
BBB	Blood-brain barrier
CA1	Cornu Ammonis area 1
CA2	Cornu Ammonis area 2
CA3	Cornu Ammonis area 3
CCI	Controlled cortical impact
CNS	Central nervous system
DG	Dentate gyrus
DH	Dentate hilus
EEG	Electroencephalogram
FDA	Food and Drug Administration
FPI	Fluid percussion injury
GABA	γ-aminobutyric acid
GABA-AR	γ-aminobutyric acid type A receptor
HAT	Histone acetyltransferase
HDAC	Histone deacetylase
HDACi	Histone deacetylase inhibitor
HFO	High-frequency oscillation
PTE	Post-traumatic epilepsy
rTBI	Repetitive traumatic brain injury

SRS	Spontaneous recurrent seizures
TBI	Traumatic brain injury
WT	Wildtype

TABLE OF CONTENTS

Page

ABSTRACT ii

DEDICATION iv

ACKNOWLEDGEMENTS v

CONTRIBUTORS AND FUNDING SOURCES vii

NOMENCLATURE viii

TABLE OF CONTENTS x

LIST OF FIGURES xiv

LIST OF TABLES xvii

CHAPTER I INTRODUCTION AND LITERATURE REVIEW 1

I. 1 Introduction 1
I. 2 Animal Models of PTE 4
I. 2.1 Fluid Percussion Injury (FPI) 10
I. 2.2 Controlled Cortical Impact (CCI) 12
I. 2.3 Impact-acceleration model 14
I. 2.4 Blast Injury Model 15
I. 2.5 Penetrating Ballistic-Like Brain Injury Model 16
I. 2.6 Cortical Undercut Model 18
I. 2.7 Repetitive TBI (rTBI) and Concussion Model 19
I. 2.8 Large Animal Models of PTE 20
I. 3 Neuropathological Mechanisms of Epileptogenesis 23
I. 3.1 Neuroinflammation 26
I. 3.2 Breakdown of the Blood-Brain Barrier (BBB) 29
I. 3.3 Epigenetic Modifications 31
I. 3.4 Reorganization of Neural Circuitry 33
I. 3.5 mTOR Pathway Hyperactivity 38
I. 4 Emerging Biomarkers of PTE 40
I. 4.1 Imaging Biomarkers 41
I. 4.2 Genetic and Genomic Biomarkers 45
I. 4.3 Electrographic Biomarkers 48

I. 4.4 Molecular Biomarkers....52
I. 5 Comorbidities of PTE....55
I. 5.1 Sensorimotor abnormalities....57
I. 5.2 Cognitive dysfunction....58
I. 5.3 Depression, mood disorders, and anxiety....60
I. 5.4 Attention deficit hyperactivity disorder (ADHD)....62
I. 5.5 Sleep disorders....64
I. 6 Pharmacological Interventions for PTE....66
I. 6.1 Anti-epileptic Drugs (AEDs)....68
I. 6.2 Altering the Inhibitory and Excitatory Pathways....70
I. 6.3 Neuroinflammatory Targeting....72
I. 6.4 Disrupting the mTOR Pathway....73
I. 6.5 Neuronal Plasticity....74
I. 6.6 Hypothermia....75
I. 6.7 Electrical Stimulation....76
I. 6.8 Tau Hyperphosphorylation....77
I. 6.9 Cell transplant therapies....78
I. 6.10 Other Potential Therapeutic Strategies....79
I. 6.11 Epigenetic Interventions: A new frontier?....82
I. 7 Future Perspectives of the PTE Field....85

CHAPTER II AIMS AND OBJECTIVES....92

II. 1 Specific Aim 1....92
II. 2 Specific Aim 2....94
II. 3 Specific Aim 3....96

CHAPTER III MATERIALS AND METHODS....98

III. 1 Experimental Animals....98
III. 2 Surgical Techniques and Recovery....98
III. 3 EEG-recording and Seizure Analysis....99
III. 4 6-Hz Seizure Threshold Testing....101
III. 5 Tissue Collection and Immunohistochemistry....102
III. 6 Stereological Quantification of Cell Sub-Types....104
III. 7 Densitometric Analysis of Immunohistochemistry Markers....104
III. 8 Behavioral Examination and Testing....105
III. 8.1 Body Weights and Health Score....105
III. 8.2 Neuroscore....106
III. 8.3 Beam Walk....106
III. 8.4 Rotarod....107
III. 8.5 Elevated Plus Maze....107
III. 8.6 Open Field....108
III. 8.7 Novel object recognition test....109

III. 8.8 Burrowing test 109
III. 8.9 Morris Water-maze test 110
III. 9 Statistical Analysis 111

CHAPTER IV RESULTS 112

IV. 1 Contusion Brain Damage in Mice for Modelling of Post-Traumatic Epilepsy with Contralateral Hippocampus Sclerosis 112
IV. 1.1 Assessment of Severe and Moderate Controlled Cortical Impact Injuries 114
IV. 1.2 Traumatic Brain Injury Leads to Chronic PTE with Spontaneous Seizures 116
IV. 1.3 Reduced Seizure Threshold Coincides with PTE Development 122
IV. 1.4 Epileptiform Discharges Often Precede Generalized Seizures After TBI . 124
IV. 1.5 High-frequency Oscillations as Biomarkers of PTE 127
IV. 1.6 TBI Induces Progressive Brain Tissue Loss and Lesions 130
IV. 1.7 Extensive Neurodegeneration Occurs in PTE Model 132
IV. 1.8 Widespread and Persistent Astrogliosis Occurs in PTE 139
IV. 1.9 Extensive and Long-lasting Microgliosis Arises in PTE 143
IV. 1.10 Aberrant Neurogenesis in PTE 147
IV. 1.11 Mossy Fiber Sprouting in the Hippocampus in PTE 150
IV. 1.12 Progressive Sensorimotor and Behavior Dysfunction in PTE 151
IV. 1.13 PTE is associated with Disrupted Discrimination and Spatial Memory .. 157
IV. 2 Targeting Epigenetic Pathways Reduces Inflammation and Provides Neuroprotection in a Mouse Model of Post-Traumatic Epilepsy 161
IV. 2.1 Systemic Sodium Butyrate Administration Normalizes TBI-induced Increase in HDAC Activity 163
IV. 2.2 Sodium Butyrate Treatment Suppresses Acute Inflammation after TBI ... 165
IV. 2.3 Sodium Butyrate Reduces Progressive Tissue Loss and Lesion Volume .. 170
IV. 2.4 HDACi Therapy Reduces Burden of Post-Traumatic Seizures 172
IV. 2.5 HDACi Therapy Reduces Frequency of Epileptiform Discharges 175
IV. 2.6 Sodium Butyrate Ameliorates Neurodegeneration 177
IV. 2.7 Sodium Butyrate Rescues Rate of Neurogenesis and Reduces Aberrant Mossy Fiber Sprouting 179
IV. 2.8 Sodium Butyrate Reduces Chronic Inflammation 182
IV. 2.9 Sodium Butyrate Treatment Improved Motor Function and Reduced Cognitive Impairment Induced by TBI 185
IV. 3 Broad and Narrow Spectrum HDAC Inhibitors as Potential Antiepileptogenics in a Mouse Model of Post-Traumatic Epileptogenesis 190
IV. 3.1 Effects of SAHA Treatment on Seizure Incidence, Frequency, and Duration Post-TBI 192
IV. 3.2 Effects of Entinostat Treatment on Seizure Incidence, Frequency, and Duration Post-TBI 198
IV. 3.3 Effect of SAHA Treatment on Epileptiform Discharges 200
IV. 3.4 Effect of Entinostat Treatment on Epileptiform Discharges 204

IV. 3.5 Pharmacokinetic Study of SAHA Administration in Blood and Brain.....205
IV. 3.6 SAHA Treatment Reduces TBI-Induce Chronic Neuroinflammation.....207
IV. 3.7 Entinostat Treatment Reduces TBI-Induce Chronic Neuroinflammation .211
IV. 3.8 SAHA Treatment on Long-term Sensorimotor and Behavioral Dysfunction 213
IV. 3.9 Entinostat Treatment on Long-term Sensorimotor and Behavioral Dysfunction 218
IV. 3.10 SAHA Treatment on Cognitive Outcomes following TBI 221
IV. 3.11 Entinostat Treatment on Cognitive Outcomes following TBI 225

CHAPTER V DISCUSSION 227

V. 1 Contusion Brain Damage in Mice for Modelling of Post-Traumatic Epilepsy with Contralateral Hippocampal Sclerosis.....227
V. 2 Targeting Epigenetic Pathways Reduces Inflammation and Provides Neuroprotection in a Mouse Model of Post-Traumatic Epilepsy 234
V. 3 Broad and Narrow Spectrum HDAC Inhibitors as Potential Antiepileptogenics in a Mouse Model of Post-Traumatic Epilepsy.....240

CHAPTER V CONCLUSIONS.....248

REFERENCES.....251

LIST OF FIGURES

Page

Figure 1: Brain injury triggers several acute pathologies. 25

Figure 2: Relationship of Long-term Neurodegeneration and Spontaneous Recurrent Seizures.....37

Figure 3: Evolution of TBI-Induced Hyperexcitability.....51

Figure 4: Characteristics of TBI-Induced Seizures.....118

Figure 5: Traumatic Brain Injury Produces Chronic Spontaneous Recurrent Seizures (SRS) in mice.....121

Figure 6: TBI reduces 6 Hz Seizure Threshold.....123

Figure 7: Epileptiform Discharges in PTE Mice.....126

Figure 8: Increased High-Frequency Oscillations (HFOs) in PTE mice.....129

Figure 9: Acute and Progressive Tissue Loss and Lesion after TBI.....131

Figure 10: Neurodegeneration of Principle Neurons Following TBI.....134

Figure 11: Loss of Inhibitory GABAergic Interneurons after TBI.....137

Figure 12: Histology Trend as a Function of Seizure Occurrence.....138

Figure 13: Immediate and Long-Lasting Astrogliosis following TBI.....141

Figure 14: Time-Course Distributrion of the Extent of TBI-Induced Astrogliosis in Extra-Hippocampal Brain Regions.....142

Figure 15: Extensive and Persistent Microgliosis following TBI.....145

Figure 16: Time-Course Distribution of the Extent of TBI-Induced Microgliosis in Extra-Hippocampal Brain Regions.....146

Figure 17: Fluctuations in Neurogenesis after TBI and Aberrant Mossy Fiber Sprouting in PTE.....148

Figure 18: Sensorimotor and Behavior Functional Deficits after TBI and PTE in mice.....152

Figure 19: Long-term Memory Dysfunction in PTE mice....160

Figure 20: Systemic Sodium Butyrate Administration Normalizes TBI-Induced Hyperactivation of HDAC....164

Figure 21: Sodium Butyrate Treatment Suppresses Acute Astrogliosis after TBI....167

Figure 22: Sodium Butyrate Treatment Suppresses Acute Microgliosis after TBI....169

Figure 23: Sodium Butyrate Reduces Progressive Tissue Loss and Lesion Volume....171

Figure 24: HDACi Therapy Reduces Burden of Post-Traumatic Seizures....174

Figure 25: HDACi Therapy Reduces Frequency of Epileptiform Discharges....176

Figure 26: Sodium Butyrate Ameliorates Neurodegeneration....178

Figure 27: Sodium Butyrate Rescues Rate of Neurogenesis and Reduces Aberrant Mossy Fiber Sprouting....181

Figure 28: Sodium Butyrate Reduces Chronic Inflammation....184

Figure 29: Sodium Butyrate Treatment Improved Motor Function and Reduced Cognitive Impairment Induced by TBI....189

Figure 30: Effect of SAHA Treatment on Moderate TBI-induced Seizures....195

Figure 31: Effect of SAHA Treatment on Severe TBI-induced Seizures....197

Figure 32: Effect of Entinostat Treatment on Severe TBI-induced Seizures....199

Figure 33: Effect of SAHA Treatment on Moderate TBI-induced Epileptiform Discharges....201

Figure 34: Effect of SAHA Treatment on Severe TBI-induced Epileptiform Discharges....203

Figure 35: Effect of Entinostat Treatment on Severe TBI-induced Epileptiform Discharges....205

Figure 36: Pharmacokinetic Study of SAHA Administration for BBB Permeability....207

Figure 37: SAHA Treatment Reduces Chronic Inflammation after Moderate TBI....208

Figure 38: SAHA Treatment Reduces Chronic Inflammation after Severe TBI....210

Figure 39: Entinostat Treatment Reduces Chronic Inflammation after Severe TBI.....212
Figure 40: Effect of SAHA Treatment on Functional Recovery after Moderate TBI ...215
Figure 41: SAHA Treatment Improves Functional Recovery after Severe TBI.....217
Figure 42: Entinostat Treatment Improves Functional Recovery after Severe TBI.....220
Figure 43: Effect of SAHA Treatment on Cognitive Function after Moderate TBI.....222
Figure 44: Effect of SAHA Treatment on Cognitive Function after Severe TBI 224
Figure 45: Effect of Entinostat Treatment on Cognitive Function after Moderate TBI.226
Figure 46: Summary of TBI-induced Pathologies of Epileptogenesis.....228

LIST OF TABLES

Page

Table 1: Advantages and Disadvantages of Current Animal Models of PTE.....8

Table 2: Comorbidities of PTE 56

Table 3: Therapeutic Intervention Studies for PTE.....86

Table 4: List of Primary Antibodies.....103

CHAPTER I

INTRODUCTION AND LITERATURE REVIEW

I. 1 Introduction

Traumatic brain injury (TBI) is a significant cause of death and permanent neurological disability, contributing to nearly one-third of all injury-related deaths in the United States and exacting a profound personal and economic toll. TBI is defined as a disruption in the normal function of the brain that can be caused by a bump, blow, or jolt to the head, or a penetrating head injury. Common causes of TBI include sports-related injuries, falls, car accidents, and military incidents. About 2.87 million Americans experience a TBI each year, with more than 56,000 deaths and 280,000 individuals requiring hospitalization (Taylor et al., 2017). The number of emergency department visits related to TBI increased over 50% between 2007 and 2013; this rise is attributed to an ever-aging population and increased number of fall-related TBIs (DeGrauw et al., 2018).

The extent of damage varies widely based on age, sex, and severity of injury. An individual's physical burden stretches beyond the initial damage, as TBI is often accompanied by a collection of secondary health consequences that negatively affect daily life. These complications include headache, vision impairment, tinnitus, difficulty focusing, imbalance, loss of hand-eye-coordination, cognitive impairment, and affective disorders (Malec et al., 2019). The impact of TBI on close family members and caregivers is also extraordinary, ranging from physical strain and emotional stress of living with a person whose abilities, behavior, and personality have been altered, to

additional demands on the caregivers for on-going monitoring and assistance with daily tasks (Malec et al., 2017). Furthermore, the burden of TBI may unevenly fall on lower income households (Tropeano et al., 2019), shedding light on the inequity of access to critical healthcare both in the USA and abroad. Moreover, TBI puts patients at higher risk of sleep disturbances and post-traumatic seizures (Gilbert et al., 2015). By some estimates, seizures occur in 1 out of every 10 hospitalized persons with moderate or severe TBI. Identified risk factors for post-traumatic seizures include loss of consciousness, intracranial hemorrhage, chronic alcoholism, depressed skull fractures, and cerebral contusions (Englander et al., 2003). Despite the increased resources that have been generated to improve our understanding of TBI and its comorbidities, the development of new diagnostic approaches has been disappointingly slow.

Post-traumatic epilepsy (PTE) is characterized by spontaneous recurrent seizures occurring as a result of TBI. Seizures have been temporally categorized into immediate (within 24 h), early (1-7 days post-injury), and late seizures (>7 days post-injury) (Christensen, 2015). Immediate and early seizures are not considered to be "epileptic" and are thought to be provoked from the injury itself, rather than arising from a multitude of cellular and molecular changes.

The cumulative risk of developing PTE ranges from 2 – 50% depending on the location and severity of injury (Annegers et al., 1998; Tubi et al., 2019). It is well-established that the incidence of PTE increases with severity of initial TBI; however, the mechanism by which these seizures develop is still unclear. Many mechanisms have been identified through studies of status epilepticus and temporal lobe epilepsy (Pitkanen

et al., 2015). Once a TBI patient experiences a single late seizure, their chance of experiencing a subsequent event increases by 80%, and seizure reoccurrence is most likely within two years of the first spontaneous late seizure (Haltiner et al., 1997; Englander et al., 2015). Acute or immediate seizures after TBI are treated with symptomatic anti-seizure medications, but these drugs are ineffective at preventing long-term seizure occurrence (Marion, 1999). Although there are more than 20 anti-seizure medications in clinical use, approximately 30% of epilepsy patients still experience drug-refractory seizures (Kobau et al., 2008).

In a study of 508 patients, it was found that mortality rates were nearly three times higher in TBI patients with seizures compared to TBI alone (Englander et al., 2003). When injury severity and location was accounted for, the most significant difference between PTE and non-PTE patients was the presence of focal cortical contusions. Neuropathology associated with TBI and PTE has recently been identified as a risk factor for developing serious neurological disorders later in life, including Parkinson's disease and dementia (Gardner et al., 2015; Fann et al., 2018). Moderate to severe head injury triggers amyloid plaque buildup in some patients, suggesting a possible link to Alzheimer's disease as well (Barnes et al., 2014). Furthermore, a variety of comorbidities including difficulty focusing, anxiety, learning and memory impairment, motor dysfunction, and sleep disturbances reduce the quality of life for many PTE patients (Hammond et al., 2019).

Prevention of epilepsy and its progression is one of the major U.S. NIH-NINDS research benchmarks. Experimental studies have demonstrated great understanding of

neuropathology and PTE-associated comorbidities including seizures, psychological changes, and motor dysfunction. However, clinical translation of therapeutic strategies is lacking or has been unsuccessful in preventing post-traumatic seizures (Temkin, 2009). Therefore, our current animal models need to be further refined to discover novel biomarkers for PTE and better capture the mechanisms involved in epileptogenesis as related to the human condition. This review describes the present state of animal models used in experimental PTE studies, briefly examines mechanisms and biomarkers of epileptogenesis, then discusses the current progress in prophylactic and preventative therapeutics for PTE. It also covers preclinical trials of new candidate treatments for PTE sequalae and comorbidities.

I. 2 Animal Models of PTE

PTE is a condition characterized by at least one spontaneous recurrent seizure following a head injury. The Department of Defense reports that over 2% of all combat related TBI are penetrating and severe injuries, and it is estimated that over 50% of patients with penetrating TBI will develop PTE (DVBIC, 2019; Chen et al., 2009). Since spontaneous seizures often do not emerge until years following the initial TBI, it is extremely challenging to study the epileptogenic process in the clinical setting. The required studies that would provide insight from immediate injury through to diagnosis of epilepsy are invasive, time consuming, and perhaps not always ethically feasible. Furthermore, longitudinal studies using less invasive procedures, such as MRI and

surface EEG, could take decades of compliance to complete and assumes these patients do eventually develop seizures.

Rodent models of PTE allow for a more extensive investigation into the causal relationship between brain injury and seizures. Here, we can begin to understand the broad and cellular pathophysiology of epileptogenesis, discover and validate new biomarkers for PTE, and assess the efficacy of therapeutics for PTE. Rodent disease models are cost-efficient, more tightly controlled, and consume far less time to complete long-term reports. However, it is important to distinguish models of TBI from those of PTE. PTE requires the occurrence of at least one seizure following brain injury. Therefore, it is important as researchers, we strive to include seizure detection methods within the models. Without the presence of seizures or ability to detect epileptiform abnormalities, the focus of the model becomes brain injury and its comorbidities, rather than posttraumatic epileptogenesis. Presently, a handful of studies report seizure incidences from 0 – 50% after mild to moderate TBI, which can slow progress on therapeutic developments (Kochanek et al., 2006; Hunt et al., 2009; Hunt et al., 2010; Rodgers et al., 2015; Szu et al., 2020). Researchers have attempted to remedy this challenge by including additional electrical or chemical convulsion approaches following injury, to ensure they observe seizures (Kharatishvili et al., 2006; Chrzaszcz et al., 2010; Bolkvadze and Pitkanen, 2012). Though a reduction in seizure threshold to these electrical or chemical stimulations has been observed, these models do not truly depict PTE since the seizures are not naturally generated. Similarly, *in vitro* preparations of slices or cell cultures are an inadequate replacement for the invaluable data that

spontaneously progressing *in vivo* models can provide. Lastly, a crucial benefit of rodent models over the clinical setting is the ability to explore novel targets and investigate efficacy of therapeutics. Even when biomarkers are discovered in humans, it is unethical to test pharmacological agents in patients until the safety and efficacy has been critically evaluated and confirmed.

Three major TBI models which have been adapted to PTE include the fluid percussion injury (FPI), controlled cortical impact (CCI), and impact-acceleration models. Recently, Bugay et al. published the first study demonstrating neuronal excitability and recorded seizure activity following a repetitive blast model of TBI (2019). Additional models such as cortical undercut and penetration injury have also been used to model PTE. However, these models are less widely utilized, and therefore, less data on the translational properties is available. **Table 1** compares the advantages and disadvantages of the animal models of PTE.

Table 1: Advantages and Disadvantages of Current Animal Models of PTE

Model	Advantages	Disadvantages
CCI	(Advantages)	(Disadvantages)
	Produces similar histopathology to the human condition including: concussion, acute subdural hematoma, loss of cortical tissue, axonal injury, inflammation, loss of gray matter, and blood-brain barrier dysfunction	Varied incidence of epilepsy between research groups and cohorts
	Increased seizure susceptibility to chemical convulsants	Prolonged time-course for the development of SRS and some comorbidities
	Decreased seizure threshold to electrical stimulation	Mechanical variation
	Demonstrates persistent sensorifunctional and cognitive deficits	Requires complex technical device to produce injury
	Produces epileptiform EEG activity including discharges, high-frequency oscillations, and seizures in some animals	
	Highly studied and reproducible	
	Can produce varying degrees of severity	

Table 1 Continued

FPI	(Advantages)	(Disadvantages)
	Produces similar histopathology to the human condition including: diffuse or focal injury, contusion, edema, progressive loss of gray matter, inflammation, and blood-brain barrier dysfunction	Varied incidence of epilepsy between research groups and cohorts
	Increased seizure susceptibility to chemical convulsants	Prolonged time-course for the development of SRS and some comorbidities
	Decreased seizure threshold to electrical stimulation	Lacks some translation to therapetutic validity

	Demonstrates persistent sensorifunctional and cognitive deficits	Requires complex technical device to produce injury	
	Produces epileptiform EEG activity including discharges, high-frequency oscillations, and seizures in some animals	Variation in injury can occur because pressure wave is highly sensitive to operational factors	
	Highly studied and reproducible		
	Can produce varying degrees of severity		
Cortical Undercut			
	Simple surgical procedure that produces hyperexcitability	Not widely studied	
	Inexpensive and relatively simple protocol	Failure to consistently produce spontaneous recurrent seizures	
Impact-Acceleration/Weight-Drop Model	(Advantages)	(Disadvantages)	
	Inexpensive and relatively simple protocol	Not widely studied	
	Can produce varying degrees of severity	Difficulty with reliable reproducibility	
	Focal injury with axonal injury and hemorrhage	Failure to consistently produce spontaneous recurrent seizures	
Blast Injury Model	(Advantages)	(Disadvantages)	
	Produces similar histopathology to the human condition including: diffuse or focal injury, intracranial hemorrhage, inflammation, and blood-brain barrier dysfunction	Not widely studied	
	Injury mechanism similar to military TBI	Failure to consistently produce spontaneous recurrent seizures	
Penetrating Ballistic-Like Brain Injury Model	(Advantages)	(Disadvantages)	
	Injury mechanism close to human missile or bullet wound injury	Not widely studied	
	Inexpensive and relatively simple protocol	Needs standardization	
Canine Model	(Advantages)	(Disadvantages)	

	Conducted in a species which naturally develops epilepsy disorders	Not widely studied	
		Needs standardization	
Large Animal (Pig etc.)	(Advantages)	(Disadvantages)	
	Species is an intermediate state between rodent and primates	Not widely studied	
		Needs standardization	
		Requires additional resources and time for surgeries and care	

I. 2.1 Fluid Percussion Injury (FPI)

Fluid percussion injury (FPI) is perhaps the most extensively used and studied model of PTE, largely due to its ability to easily modify the severity of injury, impact site, and species used. FPI can be applied centrally over the sagittal suture between bregma and lambda (midline FPI) or laterally over the parietal cortex (lateral FPI) and has been adapted for mouse, rat, rabbit, cat, and pig animal models. FPI produces a fluid pulse injury directly onto the surface of the dura following a craniectomy. The fluid percussion device consists of an adjustable pendulum that strikes the piston end of a fluid-filled cylinder, generating a fluid pulse that is transmitted along the horizontal axis of the cylinder onto the brain.

The model was initially described by McIntosh et al. in rats with a 4.8 mm craniectomy mid-distance between bregma and lambda and centered between the sagittal suture and lateral ridge (1989). An injury cap is positioned over the craniectomy and secured with dental cement or glue to ensure the fluid bolus remained within the cranial cavity. The injury is produced by a pressure pulse lasting 20 ms and severity of injury can be altered depending on the location and magnitude of pressure used (low 1.5 atm – high 3.5 atm in rats). Parasagittal and lateral FPI are common models for studying PTE.

Following FPI, electrodes can be implanted either immediately, or following a short recovery period.

The FPI model can reproduce neuropathology associated with both diffuse or focal injuries, as well as other aspects of human TBI such as acute hypertension, bradycardia, increased plasma glucose levels, hemorrhages, inflammation, and cognitive deficits (Eakin et al., 2015). The damage of FPI is most severe in the ipsilateral cortex, hippocampus, and thalamus, though mild lesions and cell loss has also been detected contralaterally. Additionally, many labs have demonstrated the development of epileptogenesis including a reduction in seizure threshold, presence of epileptiform discharges, and subgroups with spontaneous recurrent seizures (Kharatishvili et al., 2006; Mukherjee et al., 2013; D'Ambrosio, 2004).

Seizure incidence after FPI has been inconsistent, with ranges from 0% to a cumulative probability of 100% epilepsy. A major limitation in many of the earlier reports is the lack of continuous long-term EEG recording. Random or intermittent epochs of recording do not allow researchers to determine latency to seizure onset, and in many cases, seizure occurrence will be underestimated or over-reported due to missing data. In one of the most highly cited reports of FPI-induced seizures, Kharatishvili et al. found approximately 50% of rats developed PTE over a period of 12 months when monitored with 24/7 video-EEG (2006). Seizures were described as partial or secondarily generalized with a duration between 67 – 159 s; however, seizure frequency was quite low, averaging 0.3 ± 0.2 seizures/day/animal. Neuronal loss was observed within the ipsilateral hippocampus, and aberrant mossy fiber sprouting was

evident within the dentate gyrus. Similar data has now been collected from several laboratories.

I. 2.2 Controlled Cortical Impact (CCI)

Controlled cortical impact (CCI) has also been widely characterized since its first description by Lighthall in 1988. Originating as a model of TBI, CCI has been adapted for studying PTE with the addition of EEG-recording electrodes and measurements of electrophysiological changes. To date, CCI techniques have been replicated in mice, rats, swine, monkeys, and ferrets (Xiong et al., 2013). This method requires general anesthesia of the subject as well as a craniectomy—similar to the FPI model. A computer-controlled impactor is used to deliver a unilateral strike to the intact dura directly at a velocity and depth specified by the researcher. This model can be customized further by choosing the diameter of the impact tip as well as whether the tip is blunt or rounded. Due to the levels of precision involved, CCI can mimic focal injury or widespread degeneration and can remove a potential source of error regarding the position and depth of the impact site. CCI studies have mimicked acute subdural hematoma, axonal injury, cell and tissue loss, blood-brain barrier disruption, and inflammation (Osier and Dixon, 2016). Additionally, many studies have described psychological, functional, and cognitive changes associated with TBI (Kochanek et al., 2002; Yen et al., 2018).

Over time, long-term changes in the organization of neural circuitry due to trauma can lead to significant cell loss as well as an imbalance of excitatory and

inhibitory neurotransmission. Seizures after CCI and FPI have been described in similar terms, both behaviorally and electrographically; however, CCI-induced spontaneous seizures appear to have a swifter onset compared to lateral FPI in rats (Kharatishvili et al., 2006). Previous studies have suggested limbic involvement may not appear for several months after FPI, resulting in a longer latency between initial injury and seizure occurrence (D'Ambrosio et al., 2004; 2005). This shorter, yet clinically relevant timeline, allows for greater flexibility in pharmacological testing.

Both early (within first week post-injury) and late seizures (after first week post-injury) have been successfully reproduced following moderate and severe CCI (Hunt et al., 2009; 2010; Statler et al., 2009; Golub and Reddy, 2021). Similar to FPI studies, seizure incidence after CCI is largely dependent on the severity of impact, ranging between 10-85% of mice exhibiting increased epileptic discharge spiking and seizures in the weeks following CCI (Hunt et al., 2010; Bolkvadze and Pitkanen, 2012; Golub and Reddy, 2021). Additionally, CCI studies have demonstrated progressive hyperexcitability in neocortical circuits within the first two weeks after TBI (Yang et al., 2010). These changes in electroencephalography are often accompanied with mossy fiber sprouting, hippocampal lesions, and changes in neurogenesis—all of which are defined as hallmarks of temporal lobe epilepsy (Hall et al., 2008; Hånell et al., 2010). Like FPI studies, CCI injuries provide consistency, reproducibility, and an overall accepted construct validity. This model also has the added benefit of easily altering injury severity, thereby changing the course of epileptogenesis and hippocampal pathology.

I. 2.3 Impact-acceleration model

The impact-acceleration model, also known as the *weight-drop* model, simulates a diffuse injury to the brain and was first described by Mararmou et al. 1994. Following general anesthesia, rats or mice are placed below the weight-drop device on a foam block or platform intended to provide a consistent placement of the animal's head and body relative to the apparatus. Skull fracture can be prevented by securing a small impact surface onto the location where the force will be applied using cement or another adhesive. The impact-acceleration model can produce graded injuries, based on the heaviness and height at which the weight is dropped.

The clear advantage to this model is the simplicity to induce trauma. The weight-drop apparatus itself can be constructed using inexpensive supplies and does not require a craniotomy within a stereotaxic rig, allowing for low cost and high throughput efficiency. Though this model leads to many known sequelae of human TBI, a critical downside is that weight-drop only produces PTE at extreme intensities, at which most animals do not survive. Furthermore, to identify and analyze abnormalities in EEG activity, such as post-traumatic seizures, typically an electrode is implanted at various focal sites, thereby still requiring access of a stereotaxic apparatus. Though this model is rarely used to identify seizure activity, it has been recently adapted to identify subtle changes in seizure threshold to chemical convulsant compounds, such as pilocarpine, without the need of recording electrode placement (Shimon et al., 2020).

I. 2.4 Blast Injury Model

Blast-related injuries are a frequent outcome of military exposure to explosive detonation. A leading hypothesis for the mechanism by which an explosive blast causes TBI is through the transmission of shock waves across the target tissue causing rapid acceleration and deformation of the brain (Magnuson et al., 2012). These oscillating blast waves have sometimes been referred to as the "bobblehead effect" (Rosenfeld, 2013). Indirect transmission of kinetic energy from blast shock can travel through vasculature, playing a large role in TBI. Several models of blast TBI have been developed, though open-field blast, blast tubes, and shock tubes are the most frequently used (Kovacs et al., 2014).

Open field blast occurs when an explosive detonation occurs within an outdoor open area, either by overhead suspension or placement on the ground. This is one of the most accurate representations of the human blast injury condition since subjects are located a standoff distance away from the blast. However, since debris and clouds from the primary explosion can contribute to the injury, blast tubes provide another method of blast injury in which a combined shock wave and blast wind is initiated by an explosion. In this case, animals are placed at the end of a pressurized blast tube, and the head-on explosion occurs at the opposite end of the tube. The torso and abdomen of the mouse are protected from exposure to prevent confounding injuries of the lungs, heart, and GI tract. This method allows the rodent to be subjected to a "clean" blast without the reflection of shock fronts from the ground or other surfaces. Another advantage of blast tubes versus open field blasts is that an equivalent blast intensity can be achieved with a

much smaller explosive charge. Lastly, shock tubes use compressed gasses such as helium, rather than explosives to achieve injury. Shock tubes are generally safer for the both the subject and researcher to perform, more cost effective, and can be performed indoors—thereby not affected by weather conditions. However, the physics of shock tubes differs from that of explosive shock waves, which may not be as comparable to the human condition.

Blast injuries recreate several pathophysiological processes that likely play a role in the development of PTE including intracranial hemorrhages, vasospasm, neuronal damage and degeneration, focal or diffuse axonal injury, and inflammatory reactions (Nakagawa et al., 2011). Though blast models have revealed neurofunctional changes, only one study has reported posttraumatic seizures and reduction in seizure threshold. Bugay et al. observed 46% incidence of spontaneous seizures in mice within a long-term study following up to three consecutive days of repetitive blast injury (2019). Most seizures were electrograph, with little to no behavioral component observed. They also reported a shortened latency to spiking and hyperpolarization of action potential threshold in patch clamp recording of the hippocampus. These results produced a graded response to the number of blasts each mouse received (i.e., one, two, or three consecutive blasts). Though this is the first study to investigate TBI effects on neuronal excitability, the data clearly demonstrates increased risk of posttraumatic seizures as a measure of severity and repetitive injury.

I. 2.5 Penetrating Ballistic-Like Brain Injury Model

The penetrating ballistic-like brain injury (PBBI) was designed to model two aspects of high-energy bullet wounds to the head: a large temporary cavity produced from energy dissipation, and a permanent injury tract created by the path of the bullet (Williams et al., 2005). The PBBI itself is generated by inserting a custom probe into the brain at the desired location, creating the permanent injury tract, followed by the sudden inflation of an attached balloon to mimic the temporary cavity. The rodent is first placed into a stereotaxic device under anesthesia, scalp incised along the midline, and a small cranial window is created to allow the insertion of the PBBI probe. The probe can be constructed from a thin, 20-gauge stainless steel tube with spatially fixed perforations at one end. The perforations are sealed with airtight elastic tubing, which forms an inflatable balloon when an air pulse is delivered through the steel tube. The probe is then retracted and the craniectomy is sealed with sterile bone wax or dental cement. Screw or depth electrodes can also be placed either before or after PBBI to obtain EEG recording. Since the relationship between the bullet's impact velocity and the diameter of the cavity is liner, the parameters of this model can be altered to generate varied injury types or severities. However, this model of TBI mimics a specific and severe form of injury generally seen only in military populations.

One of the most notable consequences of PBBI is intracerebral hemorrhage, which are most common along the route of the probe entry. Additionally, PBBI recreates pathologies found in the human condition of missile injury such as extensive zones of radiating neurodegeneration, inflammation, neurological impairments, edema, and post-traumatic seizures (Wei et al., 2010).

I. 2.6 Cortical Undercut Model

The cortical undercut model of PTE was developed to mimic penetrating cortical injuries and has been utilized in both *in vivo* and *ex vivo* studies. Cortical undercut has been performed on rats, mice, and cats of varying age (Graber and Prince, 1999; 2006; Chauvette et al., 2017). Typically, rats are anesthetized and placed into a stereotaxic frame before unilateral exposure of the area of interest, typically the sensorimotor cortex. The dura mater and blood supply should be left intact following the craniotomy. A custom-made surgical knife or thin gauge needle, bent at a 90° angle 2mm from the tip is lowered to the white matter below cortical layer VI and rotated 180°, raised, then rotated back to its original position before being withdrawn to transect the underlying white matter. Attention should be paid to avoid any damage to major blood supplies. When a more complete undercut is needed, a second transcortical cut can be made with the needle without rotation (Graber and Prince, 1999; 2006). Following a maturation period, animals are sacrificed, and coronal slices are obtained for electrophysiologic recordings and histology.

When preparing for an *in vivo* EEG study, depth electrodes can be placed in the surrounding or contralateral cortex, hippocampus, or other regions of interest. Array placement of electrodes is common in larger species, such as cats (Nita et al., 2006; Timofeev et al., 2013). Previous experiments demonstrate an immediate reaction to partial cortical deafferentation, resulting in significant reduction of local field potential (LFP) amplitudes in regions above the transected white matter. Furthermore, 70% of

animals experienced a shift in slow oscillatory activity to paroxysmal discharges (Topolnik et al., 2003a; 2003b). Seizure onset in this model evolves from slow oscillation and is characterized by the shortening of silence periods and increased amplitude of depolarization during active periods. Within a month following cortical undercut, electrographic paroxysmal activity spreads to regions distal to the initial transection and can be detected from corresponding electrodes. In mice, generalized seizures can be detected from the leading electrode, located just proximal to the undercut, within hours or days post-injury (Chauvette et al., 2016).

Cortical undercut is a valuable model for investigating the details of functional and structural alteration of neocortical GABAergic interneurons and pyramidal neurons occurring at the site of a focal injury without the spread of widespread damage and inflammation. However, this model is rarely used for pharmacological research due to its lack of translatability to the human condition. Clean transection of the white matter is rarely seen in human TBI without more extensive injury. Furthermore, there are few behavioral studies with this model, though available data indicates no significant motor deficits or cognitive impairment (Graber and Prince, 1999).

I. 2.7 Repetitive TBI (rTBI) and Concussion Model

The majority of TBIs are mild in severity and are often underreported, and therefore undertreated. Close-head impact injuries are a common cause of concussion and TBI. The consequences of repetitive TBI (rTBI) and/or concussions have gained increasing attention with emerging reports of altered mood, behavior, and neurological

function. Concussions are extremely common in sports-related injuries, especially in contact-collision sports such as boxing or American football, putting athletes at a higher risk for neurological injuries such as chronic traumatic encephalopathy and PTE (Mez et al., 2017).

The rTBI model mimics cellular and molecular changes induced by diffuse TBI, representing mild, concussive TBIs. Shandra and Robel recently published a detailed protocol for reproducing rTBI using a modified weight-drop model in mice (2020). Briefly, an anesthetized mouse is placed in an induction chamber with its head positioned under the weight-drop tube on a foam pad. The pin on the weight-drop tube is released so that a 100 g weight is dropped from a height of 50 cm directly onto the scalp. A total of 2-4 weight drops are induced, with a 45 min recovery period in between. EEG electrode implants can be placed via stereotaxic surgery either on the same day, or the following day.

The rTBI model is characterized by a lack of focal lesion to the brain, loss of consciousness, high survivability, and late seizure onset (Shandra and Roebel, 2020). Progressive tauopathy has also been observed in both experimental rTBI models and after repeated sports-related injuries (McKee et al., 2009; Tagge et al., 2018). Contrary to FPI or CCI models, the rTBI model does not require a scalp or cranial opening, reducing the risk of increased inflammation or infection.

I. 2.8 Large Animal Models of PTE

Large animal species, such as pigs, are used in translational research because of their gyrencephalic neuroanatomy and significant white matter composition. However, one limitation of using these animals is that the laminar structure of the pig hippocampus has not been well characterized compared to that of a rat or mouse. Nevertheless, the Wolf group has described a porcine model of brain injury-related hyperexcitability and PTE and has been working towards elucidating the structure and characterization of the pig hippocampus (Ulyanova et al., 2018).

In the pig model of TBI, the primary neuropathological finding is diffuse axonal injury; however hippocampal axonal and synaptic dysfunction as well as regional hyperexcitability have been observed, suggesting this model can be adapted for PTE (Meaney et al., 1995; Johnson et al., 2016; Wolf et al., 2017). Closed-head rotation induces a diffuse brain injury using a HYGE pneumatic actuator at controlled rotational acceleration levels to obtain the intended injury severity (Cullen et al., 2016). Briefly, the animal's head is secured to a custom large-animal stereotaxic rig equipped with a padded snout clamp. The HYGE pneumatic actuator is mounted to the surgical rig using a custom linkage assembly which converts the linear motion to an angular motion. Rapid head rotation is performed within the coronal plane at velocities between 131-195 radians/sec. Pathologies observed in the pig model of TBI include axonal shearing, tau accumulation, inflammation, and increased network excitability in the hippocampus (Smith et al., 1999; Johnson et al., 2016; Wolf et al., 2017; Grovola et al., 2020). Furthermore, motor and cognitive dysfunction has been documented in pigs following TBI (Friess et al., 2007).

A major downfall of larger animal models is the additional resources and time required to perform the appropriate surgical procedures and care. Therefore, pig studies have been inconsistently used due to their difficulty to implement and increased cost (Saito et al., 1998). Furthermore, induction of TBI in cats and dogs have been established but have not been widely used for studying PTE (Morganti-Kossmann et al., 2010). More recently, however, naturally occurring canine epilepsy has been proposed as a translational platform for novel therapeutics for epilepsy disorders (Davis et al., 2011). The prevalence and pathology of naturally occurring canine epilepsy are similar to the human condition (Löscher et al., 1985). In a study evaluating risk of seizures in dogs after head injury, patient records from 1343 diverse breeds were reviewed for previous head injury and recurrent seizures (Steinmetz et al., 2013). Of the 236 dogs with previous head injury, 18.6% exhibited early and/or late post-traumatic seizures. Observed seizure types included convulsive status epilepticus, partial and generalized tonic-clonic seizures, and cluster seizures. Though this data seems promising, the study has a few shortcomings including difficulty obtaining enough questionnaires or telephone interviews to obtain statistical power. Retrospective studies such as these are not as feasible for the testing of therapeutic interventions.

The broad etiology following TBI presents a challenge for a singular paradigm to recreate all pathologies associated with PTE. The most common causes of human brain injury are car accidents, falls, recreational or sports injuries, and military incidents—all of which present differently within the clinic. Furthermore, acceleration-deceleration injuries differ from blunt force closed-head injuries or penetrating trauma in tearing, scar

formation, and contusion (Dixon, 2017). Desirable features in animal models include a high frequency of epilepsy with an absence of extreme seizure clustering, low inter-subject variability in seizure presentation, and a rapid and defined evolution of epileptogenesis. Ideally, this model would also be high throughput and low cost. Although the current animal models of PTE have provided much needed insight, no current model can fully recapitulate the full experience of human TBI. Therefore, it is important to understand the strengths and shortcomings of each model to determine which has the optimum conditions to evaluate specific research questions.

I. 3 Neuropathological Mechanisms of Epileptogenesis

TBI sets into motion a multifaceted cascade of temporally overlapping cellular and molecular events. Primary injury refers to the immediate trauma and tissue deformation that occurs within seconds to minutes after insult. Within this timeline, a flood of neurotransmitters is released, followed by ion channel activation and calcium influx. Immediate and early seizures are thought to occur as a direct result of the excitotoxic environment, mitochondrial damage, inflammation, and tissue injury. Though these seizures are not considered to be “epileptic”, they can exacerbate initial damage (Temkin, 2009). Secondary injury involves several physiological mechanisms associated with progressive damage (Pitkanen et al., 2002). Chronic activation of inflammatory cascades, oxidative stress, and edema causes build-up of free radicals and reactive oxygen species. These factors become compounded by neurodegeneration, mitochondrial dysfunction, and the extended disruption of homeostasis. Furthermore,

self-repair mechanisms occur concurrently and include plastic processes such as structural axonal remodeling, neurogenesis, gliosis, and angiogenesis (Lucke-Wold et al., 2015).

Classically, epileptogenesis was defined as the period of time in which a normal brain is functionally altered, resulting in increased seizure susceptibility and risk of spontaneous recurrent seizures (SRS). Within the framework of acquired epilepsy, researchers relied on the context of a "latent period" in which an epileptogenic insult (mechanical, chemical, or otherwise) triggered a series of changes, and ultimately ended with occurrence of seizure output. However, certain processes, such as molecular and cellular plasticity, inflammatory cascades, and neurodegeneration can continue indefinitely beyond the occurrence of the first seizure (Pitkanen et al., 2002; Dudek and Staley, 2012). Recently, the International League Against Epilepsy (ILAE) revised the definition of epileptogenesis to include disease modification and the concept of continuous epilepsy progression. Thus, the term "disease modification" has two main components: a) alleviation or prevention of seizure development, termed "antiepileptogenesis", and b) modification of PTE-associated comorbidities. In this next section, we discuss some of the major mechanisms associated with the progression of epileptogenesis including changes in neuroinflammation, blood-brain barrier (BBB) breakdown, alteration of the epigenetic landscape, and reorganization of neural circuitry (**Figure 1**).

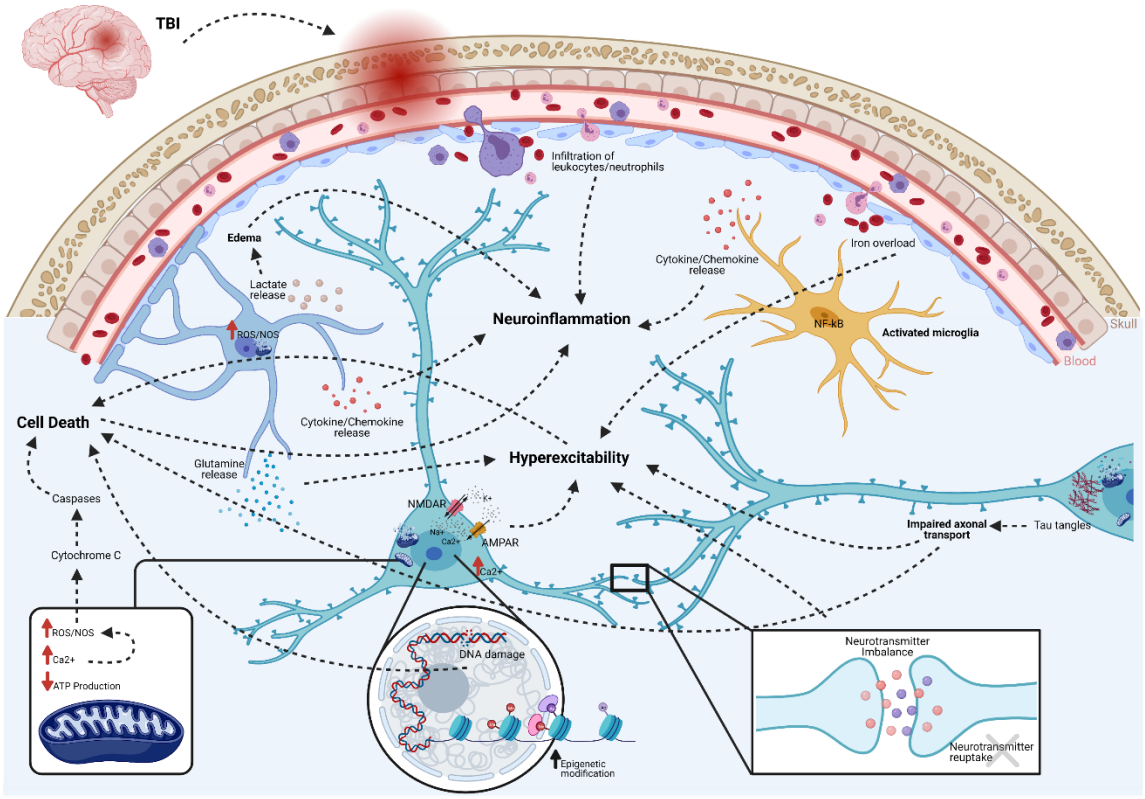

Figure 1: Brain injury triggers several acute pathologies.

Brain injury triggers several acute pathologies. Direct insult compromises the blood-brain barrier, allowing infiltration of peripherally circulating immune cells such as leukocytes, macrophages, and neutrophils. NF-κB translocates to the nuclei of microglia, transforming them to an activated phenotype. This induces cellular proliferation and the release of inflammatory amplifiers such as chemokines, cytokines, ROS, and NOS. Macrophages participate in the cleanup of damaged cells and debris, but based on their functional activation state, may either exacerbate damage or initiate repair mechanisms. Lactate release from astrocytes contributes to water retention and edema. Excess iron from a leaky BBB can contribute to hyperexcitability. Excessive accumulation of glutamate and aspartate neurotransmitters due to spillage from damaged neurons or impaired reuptake by astrocytes activates NMDA and AMPA receptors located on post-synaptic membranes, allowing for influx of calcium ions. Together with the release of Ca2+ stores from the endoplasmic reticulum, increases in Ca2+ leads to production of ROS and activation of calpains. Damaged or dysfunctional mitochondria create a deficit of available ATP, leading to Na+/K+ pump failure, activation of Ca2+ channels, and further production of ROS/NOS. Cytochrome C released into the cytosol activates cell death pathways via caspase proteins. Epigenetic modifications, in the form of increased HDAC activity and altered DNA/histone methylation changes transcriptionally active

sites, including many genes associated with hyperexcitability and serotonin-to-melatonin conversion. Furthermore, DNA damage leads to apoptosis and cell loss. Progressive axonal damage and tau tangles leads to impaired axonal transport and results in both neurodegeneration and hyperexcitability. Together, these acute pathologies are both adaptive and maladaptive. The former contributes to functional and beneficial recovery, whereas the latter exacerbates epileptogenesis and the progression of abnormal electrographic activity. Created with BioRender.com.

I. 3.1 Neuroinflammation

Local inflammation is intended as a beneficial protective measure after tissue insult; however, aberrant inflammatory responses can alter neuronal function and lead to serious consequences such as BBB disruption and seizure development (Vezzani et al., 2013). Activated microglia and astrocytes play a large role in inflammation by releasing pro-inflammatory cytokines into the neuronal environment and promoting scar formation around tissue injury. Cytokine cascades in the brain regulate important pathways such as neuroendocrine function, synaptic plasticity, metabolism of neurotransmitters, neurogenesis, and the kynurenine pathway (Paudel et al., 2018). These innate processes play significant roles in cell excitability and survival, thereby promoting network hyperexcitability. In particular, the IL-1/TLR signaling pathway is disrupted and the associated receptors IL-1R1, TLR2, TLR3, and TLR4 are rapidly upregulated after both cell injury and seizures (Ravizza and Vezzani, 2006). The excitatory effects of IL-1β have been reported in several brain regions (Vezzani et al., 2011). IL-1β reduces GABA inhibition within the CA3 of the hippocampus and increases neuronal excitability in the CA1 by reducing NMDA and voltage-gated calcium channel efflux (Zhang et al, 2010).

Furthermore, LPS-induced inflammation is associated with reduction in seizure threshold in both postnatal and adult rodent models (Galic et al., 2009). This effect on seizure threshold can be reversed by blocking cytokine induction in activated microglia (Galic et al., 2009).

Induction of COX-2 has also been shown to promote epileptogenesis and contribute to neuronal damage in several animal models of epilepsy (Kulkarni and Dhir, 2009). Overexpression of COX-2 intensifies kainic-acid induced seizures and mortality in mice (Kelley et al., 1999). Wei et al. confirmed COX-2 mRNA expression was significantly elevated after maximal electroshock (2018). Though the modulation of the COX-2/PGE2 pathway has been pursued as an alternative therapeutic strategy for controlling seizures, careful study of COX-2 inhibitors could not fully prevent the appearance and development of spontaneous seizures in a rat model of status epilepticus (Holtman et al., 2010). Furthermore, inhibition of COX-2 has been found to either exacerbate or attenuate epilepsy-induced neurodegeneration, depending on the strategies used to interfere with the COX-2 pathway (Baik et al., 1999; Polascheck et al., 2010). These data highlight the ways in which the COX-2 pathway affects epileptogenesis, but mediation of this pathway alone is not sufficient for preventing seizure development. An important consideration of inflammation in post-traumatic epilepsy is its contribution to progressive cell loss after injury. Free radicals and proteases accumulate during periods of inflammation, supporting lipid and protein peroxidation, DNA damage, mitochondrial dysfunction, and induction of apoptosis (Vezzani et al., 2013). Tissue damage, stress, and their subsequent cytokine release also adversely interfere with

neurogenesis and neuroplasticity through their interactions with brain-derived neurotrophic factor (BDNF) and TrkB receptor signaling (Goshen and Yirmiya, 2007). In a healthy brain, BDNF plays a crucial role in neuron maturation by regulating chloride levels and modifying inhibitory GABAergic signaling from depolarizing to hyperpolarizing (Rivera et al., 2002). However, within the context of injury, the upregulation of BDNF and its receptor TrkB are believed to promote aberrant mossy fiber sprouting (Dinocourt et al., 2006). Furthermore, brain injury causes a selective CD74-dependent peripheral lymphocyte activation which may exacerbate neurodegeneration (Tobin et al., 2014).

Prolonged neuroinflammation also greatly affects quality of life and complicates comorbidities, giving cause for identifying therapeutics which explore the mechanistic association between PTE and neurobehavior dysfunction (Paudel et al., 2018). INF-α can decrease BDNF levels, thereby slowing the rate of cell proliferation in the hippocampus and negatively affecting learning and memory consolidation (Lotrich et al., 2013). Additionally, increased cytokine production causes an imbalance of neurotransmitters, such as serotonin and dopamine, by deregulating the kynurenine pathway and disrupting neurotransmitter transport function (De la Garza and Asnis, 2003). Meta-analyses of existing research have concluded the most reliable biomarkers of inflammation in patients with depression are heightened levels of IL-6, TNF-α, IL-1β, and C-reactive protein—all of which are significantly increased with TBI (Miller et al., 2009). Together, these inflammatory processes work in concert to promote depression, anxiety, cognitive impairment, and disturb sleep (Dantzer et al., 2008).

I. 3.2 Breakdown of the Blood-Brain Barrier (BBB)

The blood-brain barrier (BBB) is a particularly important structure for CNS homeostasis. There is increasing evidence demonstrating the BBB as a multifactorial pathophysiologic process involving faulty angiogenesis, neuroinflammation, altered glial physiology, leukocyte-endothelial interactions, and hemodynamic changes resulting in hyperexcitability (Marchi et al., 2012). Epilepsy disorders and TBI manifest with variable extent of BBB dysfunction; however, the link between BBB permeability and seizures has been posed as "the puzzle of the chicken and the egg" (Friedman, 2011). Acute vascular failure with BBB damage is sufficient to cause seizures in the absence of CNS pathologies or concomitant chemical convulsants (Marchi et al., 2007). Additionally, focal chronic seizures are frequent in patients with vascular malformations such as cavernous angiomas (Kraemer and Awad, 1994). Magnetic resonance images of cavernous angiomas often present with BBB dysfunction, intracerebral deposits of iron, and albumin accumulation—all three of these factors have been identified as common features of TBI and temporal lobe epilepsy (Raabe et al., 2012; van Vliet et al., 2007).

BBB damage has been demonstrated to both trigger and sustain seizures in animal models and the human experience (Marchi et al., 2007; Raabe et al., 2012; van Vliet et al., 2007). Tomkins et al. observed greater association of BBB pathology in PTE patients compared seizure-free TBI patients, suggesting a correlation between BBB breakdown and hyperexcitability (2008). Areas of BBB disruption were linked to decreased brain glucose uptake, hypometabolism, and abnormal neuronal activity. After

exposure of the cerebral cortex in rats, hypersynchronous epileptiform activity involving glutamatergic and GABAergic neurotransmission as well as significant endothelial tight junction impairment was observed (Seiffert et al., 2004). Accumulated albumin within the parenchyma is associated with down-regulation of inward-rectifying potassium channels in astrocytes, affecting buffering capacity and contributing to hyperexcitability (Ivens et al., 2007). Additionally, loss of aquaporins expressed in the end feet of astrocytes affects water flux and potassium regulation, further disrupting the homeostatic environment of the brain (Binder and Steinhauser, 2006).

Neuroinflammation also plays a critical role in BBB permeability. Elevated levels of IL-1β, IL-6, and TNF-α can increase the permeability of the BBB and facilitate the movement of peripherally located cytokines into the CNS. These cytokines bind to receptors in the brain vasculature, producing secondary messengers and toxic by-products which further compromise its integrity (Fabene et al., 2010; Yarlagadda et al., 2009). Furthermore, these factors can trigger the activation of astrocytes and resident microglia, contributing to their dysfunction of neurotransmitter clearance and subsequent secretion of immunoregulatory markers. Systemic injection of LPS has been shown to lower seizure threshold to pentylenetetrazol, suggesting peripheral inflammation leads to a leaky BBB and possible infiltration of peripherally circulating leukocytes (Marchi et al., 2012). BBB dysfunction represents a convergence of pathogenic aspects which often create a positive feedback loops for further exacerbation of inflammation, functional impairment, and BBB permeability. For full review on how the breakdown of BBB affects PTE development see: Dadas and Janigro, 2019.

I. 3.3 Epigenetic Modifications

Epigenetics refers to the plastic changes in gene expression that occur without alteration of the DNA sequence itself. Under normal conditions, epigenetic modifications are essential for growth, development, learning and memory, and the immune response (Hwang et al., 2017). Epigenetic modifications such as DNA/Histone methylation, acetylation, and phosphorylation etc. have been implicated in a vast number of diseases, most notably cancer (Weber, 2010). Evidence suggests epigenetic regulation of gene expression may play a critical role in the physiology of both epilepsy and TBI (Younus and Reddy, 2017; Nagalakshmi et al., 2018). Reddy et al. demonstrated the HDAC inhibitor, sodium butyrate, significantly slowed the kindling process in a mouse model of temporal lobe epilepsy when administered prior to electrical stimulation (2017). This study suggests HDAC inhibitor compounds may possess antiseizure effects with an ability to curtail the process of epileptogenesis. Moreover, valproate has been administered as an antiseizure medication for decades, though its inhibitory effect on HDACs was unknown until 2001 (Gottlicher et al., 2001).

Histone modification is perhaps the most widely studied epigenetic modification in both epilepsy and TBI. Reduced H4 acetylation has been observed after pilocarpine administration at GluR/Gria2 promoter loci, a region which encodes for AMPA receptor subunits and limits calcium permeability (Huang et al., 2002). Downregulation of GluR/Gria2 is associated with hyperexcitability and initiating epileptogenesis. The same study also noted H4 acetylation at the BDNF promoter, increasing after seizure activity.

H3 phosphorylation is thought to promote acetylation of histone proteins, and multiple studies have found striking evidence of H3 phosphorylation after pilocarpine and kainic-acid induced seizures (Sng et al., 2006; Crosio et al., 2003). Furthermore, hyperactivity of HDAC proteins occurs at early timepoints after lateral FPI (Zhang et al., 2008). This increased H3/H4 acetylation can be found throughout the hippocampus but is particularly visible in the CA3 (Gao et al., 2006). Increased HDAC activity leads to seizure susceptibility and post-traumatic epilepsy in both experimental models and in the clinical setting (Huang et al., 2012; Dash et al., 2009).

Changes in cell-specific global DNA/histone methylation have been shown to persist for up to 8 months post-TBI (Haghighi et al., 2015). Many of the affected genes have been associated with hyperexcitability, disruption of the sleep cycle, and neuropsychiatric disorders, such as Nos1, Il1r1, Homer1, Per3, and the *Aanat* gene which encodes the enzyme responsible for catalyzing the serotonin to melatonin conversion (Haghighi et al., 2015). DNA methylation also plays a role in the inflammatory response to injury. Within 24 hr post-TBI hypomethylation of microglia promotes active gene transcription in areas of widespread necrosis (Zhang et al., 2007). Furthermore, a study of patients with intractable temporal lobe epilepsy found expression of Dnmt1 and Dnmt3a were significantly higher in epileptic versus healthy controls, suggesting aberrant DNMTs may contribute to the pathogenesis of seizures (Zhu et al., 2011). DNMT inhibitors have shown some promise for suppressing neuronal excitability in hippocampal neurons (Nelson et al., 2008; Levenson et al., 2006).

I. 3.4 Reorganization of Neural Circuitry

The culmination of neuroinflammatory cascades, weakened BBB integrity, and epigenetic modification leads to consequent reorganization of neural circuitry through progressive cell loss, aberrant axonal sprouting, and neurogenesis. Several experimental models have highlighted the loss of inhibitory interneurons coupled with recurrent excitatory circuits as a basis for hypersynchronous epileptiform activity (Dudek and Spitz, 1997; McCormick and Contreras, 2001; Golub and Reddy, 2021). The hippocampus is a model system to study circuitry changes since it is particularly susceptible to injury and undergoes structural reorganization after TBI and in epilepsy disorders (Hunt et al., 2009; Kharatishvili et al., 2006).

$GABA_A$ receptors are responsible for the majority of inhibitory signaling in the brain. GABAergic interneurons form robust local synaptic connections with excitatory principal cells to control activity in two primary ways: phasic (synaptic) and tonic (extrasynaptic) inhibition (Farrant and Nusser, 2005). Phasic inhibition refers to the rapid transmission of information and activation of receptors at the synaptic junction following exposure to high concentrations of GABA released from presynaptic vesicles. Tonic inhibition, on the other hand, is mediated by extrasynaptic $GABA_A$ receptors, persistently activated by low concentrations of ambient GABA. A common histopathologic feature of PTE is the drastic loss of inhibitory interneurons in the dentate gyrus and hilar regions (Lowenstein et al., 1992). Loss of these cells is correlated to an increase in tonic current amplitude in the dentate gyrus contralateral to TBI (Mtchedlishvili et al., 2010). Additional studies have reported changes in the subunit

configuration of $GABA_A$ receptors after CCI injury, which may also affect inhibitory control (Gupta et al., 2012; Raible et al., 2012).

Neurodegeneration after TBI affects both principal neurons and interneurons, though it was unclear whether one population is preferentially lost. Carron et al. examined how TBI affects different populations of interneurons, observing heterogenous changes of calbindin, parvalbumin, calretinin, neuropeptide Y, and somatostatin expressing interneurons in the hippocampus (2019). Their findings suggest a differential vulnerability of interneurons across various brain regions and function after TBI. In a recent study, we performed a time-course of stereological neuroquantification in the hippocampus contralateral to CCI at days 1, 3, 7, 30, 60, and 120. Populations of principal neurons and inhibitory PV+ GABAergic interneurons had decreased by roughly 30% and 45%, respectively, at 4 months post-injury; however, the degeneration in interneurons was accelerated to that of excitatory cells. Furthermore, the steep decline in interneurons coincided with the onset of spontaneous seizures (Golub and Reddy, 2021). **Figure 2** highlights the linear regressions of cell loss during epileptogenesis and their temporal association to seizure onset. Our data agrees with a previous study by the Hunt group that found a dramatic shift of interneuron diversity and loss following contusion injury (Frankowski et al., 2019). As previous studies have pointed to, the dentate gyrus and hilar regions showed the greatest loss of inhibitory interneurons (Hunt et al., 2011; Gupta et al., 2012). Loss of cells, whether excitatory or inhibitory, forces reorganization of these neural circuits, contributing the ongoing pathology of epileptogenesis. Restoration of the excitatory and inhibitory balance may be possible

with transplantation of neuronal stem cells (Ngwenya et al., 2018). These animals also exhibited improved recovery and novel object recognition compared to non-transplant FPI animals.

Excitatory dentate granule cells are not typically connected to each other. However, several laboratories have demonstrated the reactive plasticity of these circuits in TBI and epilepsy models (Hunt et al., 2009; 2010; Kharatishvili et al., 2006; Bolkvadze and Pitkanen, 2012). Aberrant mossy fiber sprouting refers to the germination of axon collaterals from dentate granule cells into the inner molecular layer, forming functionally recurrent excitatory circuits. These local circuit changes are easy to detect with Timm's immunohistochemistry and have been consistently reproduced in human and rodent tissues (Sutula et al., 1989; Hunt et al., 2010). Mossy fiber sprouting is generally more robust after severe versus mild TBI, suggesting degree of sprouting is correlated to both severity of injury and seizure risk (Hunt et al., 2012). Sprouting is most often noted in the hippocampus ipsilateral to TBI; however, damage is not constrained to the injured hemisphere and may influence circuitry reorganization with increased mossy fiber density (Pischiutta et al., 2018). Aberrant sprouting may provide a means for regional network synchronization which is particularly vulnerable if basal inhibition is lost or impaired by cell loss or dysfunction.

Neural precursors proliferate in areas both proximal and distal to TBI impact. Much of this proliferation makes up the astrogliotic scar that forms around the injury site (Kernie et al., 2001). Changes in the rate of neurogenesis have also been found after TBI and ectopic migration of these newborn cells may affect the excitability of the neural

circuitry. TBI-induced newborn cells have increased dendritic branching proximal to the soma and wider dendritic reach which persists through cell maturity (Villasana et al., 2015). Neurogenesis has been a point of controversy in epileptogenesis, with some reports suggesting increased cell proliferation after TBI (Gao et al., 2009; Dash et al., 2001), while others observe reduced neurogenesis (Rola et al., 2006). However, differences in the rate of neurogenesis may be in part due to proximity to injury, timepoint of tissue sampling following TBI, or even the possibility selective death of vulnerable newborn cells (Gao et al., 2008). Yu et al., observed both upregulation of type-1 quiescent progenitor cell activation in the injured hippocampus as well as progressive elimination of type-2 doublecortin-expressing progenitors (2008). At the same time, the contralateral hippocampus also saw upregulation of type-1 progenitors, suggesting TBI may differentially impact damage vs compensatory signaling. Furthermore, severity of injury affects neurogenesis at different stages (Wang et al., 2016a). Regardless of location, severity, or timing after injury, fluctuation of cells born into the hilar and molecular layers of the dentate gyrus have been suggested to play a role in epileptogenesis (Danzer et al., 2019). Villasana et al. found TBI-induced newborn granule cells receive a normal balance of excitatory and inhibitory inputs and are involved in information processing, but suggested TBI-induced anatomic changes and dendritic projection patterns may be the root cause of maladaptive neurogenesis network properties (2015). Insulin-like growth factor-1 overexpression has been found to increase the survival of newly born granule cells while inhibiting ectopic migration, the main implication of neurogenesis-associated circuitry changes (Carlson et al., 2014; Littlejohn

et al., 2020). Therefore, conditional expression of astrocytic insulin-like growth factor-1 may be beneficial in reducing reactivity of astrocytes and preserve cognition after TBI.

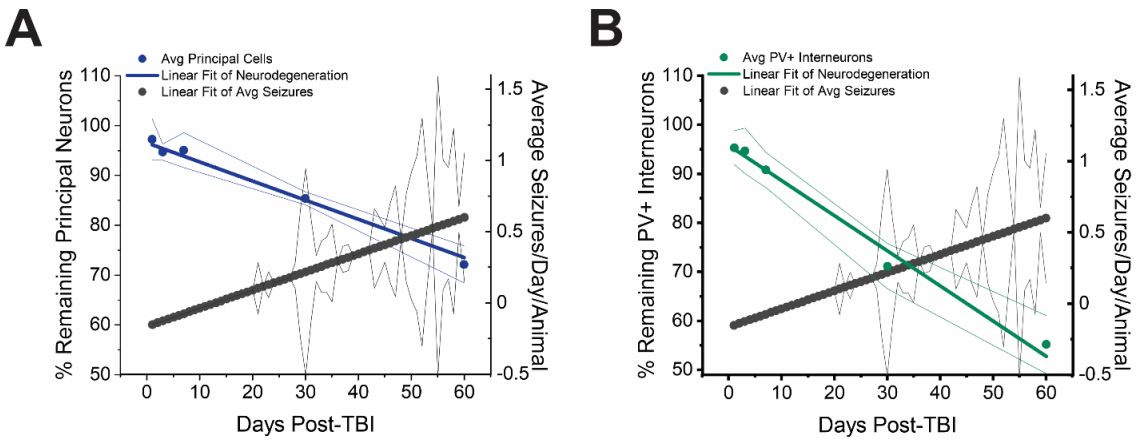

Figure 2: Relationship of Long-term Neurodegeneration and Spontaneous Recurrent Seizures

TBI induces a state of immediate inflammation and hyperexcitation in the brain which exacerbate cell loss both ipsilateral and contralateral to the lesion. PTE was induced via a severe 2.0 mm depth CCI model of TBI. Following injury, mice were tethered to 24/7-videoEEG for up to 4 months and seizures were identified by a customized MATLAB script and validated by unbiased researchers. Stereological quantification of two cell populations in the contralateral hippocampus was performed at days 1, 3, 7, 30, 60, and 120 post-TBI in subsets of these recorded mice. **A)** Linear fit of remaining NeuN+ principal neurons overlayed the linear regression of average seizure output from responding mice to highlight the temporal relationship between cell loss and seizure occurrence. **B)** Linear fit of remaining PV+ GABAergic interneurons overlayed the linear regression of average seizure output from responding mice to highlight the temporal relationship between cell loss and seizure occurrence.

I. 3.5 mTOR Pathway Hyperactivity

The mammalian target of rapamycin (mTOR) pathway regulates several physiological functions, and, in the brain, it is involved in cell proliferation and survival, neuronal morphology, and protein synthesis (Bockaert and Marin, 2015). Dysregulation of this pathway has been implicated in a number of brain disorders including tuberous sclerosis complex, gangliоglioma, and focal cortical dysplasia—all of which may potentially or certainly lead to epilepsy (Liu et al., 2014). Hyperactivation of the mTOR seems to play a critical role in the pathogenesis of animal models of acquired epilepsy, and mTOR inhibitors, such as rapamycin, have prevented epileptogenic mechanisms and reduced seizure burden. In the clinical setting, rapamycin and its derivatives have been tested mainly on severe, refractory epilepsy disorders such as tuberous sclerosis complex. Rapamycin and everolimus treatments improved seizure control in phase I/II studies (Krueger et al., 2013), and in some cases, patients experienced complete cessation from previously intractable seizures (Perek-Polnik et al., 2012).

The mechanisms by which mTOR inhibition reduces seizure activity in experimental models is still largely unclear but seem to point towards neurocircuitry reorganization. Inactivation of PTEN induces aberrant mossy fiber sprouting in animal and human hippocampal granule cells. Sutula and Dudek demonstrated that PTEN deletion was sufficient to trigger spontaneous seizures, and that mTOR hyperactivation played a central role in this process (Sutula and Dudek, 2007). Furthermore, rapamycin inhibition of mTOR signaling reduces abnormal axonal sprouting and other pathologies associated with epileptogenesis, including neuronal excitability (Zeng et al., 2009).

Though these data are positive, other studies have found rapamycin treatment reduces mossy fiber sprouting but has little effect on decreasing seizure frequency or duration (Buckmaster et al., 2009). In addition to aberrant sprouting, studies have shown inhibition of mTOR signaling rescues neurodegeneration and stabilized neurogenesis after kainic-acid status epilepticus (Zeng et al., 2009). The authors claimed the disruption of mTOR pathway could have anti-epileptogenic effects, since they also observed reduced spontaneous epilepsy in treated mice. Paradoxically, mTOR activation has been shown to possess both anti-apoptotic and pro-apoptotic effects, depending on the phase of the cell cycle. (Asnaghi et al., 2004). Early administration of rapamycin (within 1 hr of kainite injection) enhanced mTOR signaling even higher than kainate alone, whereas administration of rapamycin greater than 1-hour post-kainate resulted in the expected inhibitory effects (Zeng et al., 2010). Therefore, it is important to consider both therapeutic dose and timing after insult. Inhibitors of mTOR possess low efficacy in halting seizures within the preclinical models since multiple days of treatment are needed to achieve an anti-seizure impact and beneficial effects typically cease after drug discontinuation.

When considering the mechanisms of epileptogenesis for prophylactic approaches, it is important to consider that both adaptive and maladaptive processes are activated by brain injury. The former can contribute to functional and beneficial recovery, whereas the latter may contribute to epileptogenesis. Questions emerge to determine whether these processes are separate or concurrent, if they are distinctly different forms of plasticity involved in either functional recovery or epileptogenesis,

and if these processes are not distinct, do they differ quantitatively in their timing or intensity? Preventative or curative treatments may interfere with both epileptogenesis and development of comorbidities. It is likely that multiple agents will be needed to provide full spectrum symptomatic relief to patients. The answers to these questions are critical to pharmacological progress in epilepsy and head trauma.

I. 4 Emerging Biomarkers of PTE

In 2015, the Food and Drug Administration (FDA) developed the Biomarkers, EndpointS, and other Tools (BEST) effort to promote consistent use of biomarker terms and concepts. The use of the BEST resource has evolved the term "biomarker" to be labeled as "a defined characteristic that is measured as an indicator of normal biological processes, pathogenic processes, or responses to an exposure or intervention, including therapeutic interventions". This definition includes characteristics such as changes in a patient's molecular, radiographic, genetic or genomic, electrographic, physiologic, and histologic traits. Biomarkers are objectively measured and quantifiable and should ideally be cost-effective and non-invasive for both the patient and healthcare provider. Furthermore, an effective biomarker should have limited variability among the general population. Within the context of disease or environmental exposure, the presence of biomarkers can indicate change in a biological condition, predict risk or development of comorbidities, and measure progression of a disease state. In this section, we review the current state of PTE biomarker discovery and use, both in the clinical state as well as experimental animal model research.

I. 4.1 Imaging Biomarkers

Imaging within the context of TBI has thus far focused largely on primary lesion formation and the evolution of gliosis; however, imaging techniques have the potential to capture progression of pathologies of PTE. Neuroimaging biomarkers are incredibly appealing not only due to their non-invasive procedures but also because they are routinely performed as part of a patient's typical medical care. Furthermore, imaging can detect patterns across specific structures or within the whole brain.

Computed tomography (CT) scans have been used for decades to assess global structural damage after TBI (D'Alessandro et al., 1988). Characterization of early CT scans have identified an increased risk of PTE development in patients with depressed skull fracture, dural penetration, and intraparenchymal, subdural, or epidural hemorrhage. Additionally, patients with cortical/subcortical contusions or large lesions in the temporal lobe have shown higher rates of PTE incidence, regardless of injury severity (Englander et al., 2003; Tubi et al., 2019).

Positron emission tomography (PET) allows researchers to visualize inflammatory responses and the metabolic impact of neuronal injury after TBI. 18F-Fluorodeoxyglucose (FDG) is a radioactive tracer of cerebral metabolism often used in PET experiments. Hypometabolism has been observed within the first 24 hr following kainic acid-induced status epilepticus, suggesting abnormal metabolism may play a role in epileptogenesis (Jupp et al., 2012). Conversely, FDG-PET scans of severe TBI patients demonstrate hyperglycolysis occurs up to 2 weeks following initial damage

(Bergsneider et al., 1997). This increase in glucose consumption may be due to the rise in inflammatory cell populations surrounding the impact site.

Gliosis appears bright on T2-weighted magnetic resonance imaging (MRI) and fluid attenuated inversion recovery (FLAIR) techniques. Inflammation and glial scarring are extremely common around the impact site after TBI in both rodent models and in the clinical setting (Dixon, 2017). Activation of astrocytes and microglia through maladaptive inflammatory cascades have been correlated to excitotoxicity, mitochondria dysfunction, and cell loss—all of which have also been indicated as epileptogenic factors (Oleksii et al., 2019; Alyu and Dikmen, 2017). Magnetic resonance spectroscopy (MRS) is also a useful tool for providing quantitative data on altered metabolite profiles related to inflammation, and hyperexcitability. Reductions in glucose and GABA neurotransmitter, as well as increased glutamate have been observed after TBI using MRS (Friedman et al., 1999). To further assess metabolite profiles as a function of epileptogenesis, Filibian et al. investigated glutathione levels, an antioxidant produced by activated astrocytes, in rats with pilocarpine-induced status epilepticus (2012). Glutathione was negatively correlated with seizure frequency, providing strong evidence of astrocytic involvement in seizure generation.

MRI has excellent resolution and tissue classification, using strong magnetic fields to form images of the anatomical and physiological processes of given organs. Structural MRI studies have revealed minor, but significant changes in the ipsilateral hippocampus relative to baseline in rats experiencing posttraumatic seizures vs nonepileptic rats one week following lateral FPI (Shultz et al., 2014). The same study

boasted high predictability of PTE incidence using a multivariate logistic regression model of serial FDG-PET parameters amongst all injured and non-injured cohorts. Similarly, hyperexcitability in the hippocampus has been correlated to early 3 h post-injury decreases and later 1–12-month post-injury increases in hippocampus diffusion (Kharatishvili et al., 2007). Furthermore, mossy fiber sprouting scores, which have been long considered a hallmark of epilepsy, were correlated with diffusion values after lateral FPI, providing greater evidence that quantitative diffusion MRI is a potential tool for facilitating the prediction of increased seizure risk after TBI. In a follow-up study, the same group accurately predicted seizure susceptibility to PTZ-administration using similar MRI diffusion patterns, with the greatest accuracy to be found with a combinational biomarker calculated from diffusion in the ipsilateral somatosensory cortex and thalamic regions at 2 months post-TBI (Immonen et al., 2013).

Functional MRI (fMRI) can be used to analyze connectivity, plasticity, and remodeling within the brain following injury. There is extensive reporting on functional changes after TBI and clinical outcome, but studies focusing on epileptogenesis and PTE are scarce and inconsistent. Evidence of both hypoconnectivity and hyperconnectivity have been observed in several networks after TBI, and these abnormalities have been linked to changes in behavior, cognitive impairment, and motor control (Hillary et al., 2011; Stevens et al., 2012; Tang et al., 2011). For example, abnormal frontoparietal network connectivity after mild TBI affected performance in working memory tasks, suggesting interhemispheric connectivity between left and right inferior frontal gyri may contribute to learning and memory impairments seen in the clinical setting (Kasahara et

al., 2010). A single experimental study has investigated fMRI biomarkers in relation to epileptogenesis using lateral FPI and PTZ susceptibility as a model. Mishra et al observed decreased connectivity between the ipsilateral and contralateral parietal cortex and between the hippocampus and parietal cortex in the injured hemisphere compared to sham-operated rats (2014). However, no significant relationship was found between functional connectivity and seizure susceptibility during the PTZ test.

Blood-brain barrier (BBB) dysfunction has long been suggested to play a key role in seizure susceptibility after TBI and in epilepsy disorders (Cornford and Oldendorf, 1986). Recent studies demonstrate that abnormalities in the BBB can be visualized using dynamic contrast-enhanced MRI and FLAIR techniques. Disrupted BBB function has been found with increased frequency and to a larger extent in patients with posttraumatic seizures versus non-epileptic TBI patients (Tomkins et al., 2011). Furthermore, reduced BBB integrity within the cortical regions surrounding the impact site or within the piriform network have been suggested as sensitive predictors of epilepsy (Bar-Klein et al., 2017). There are several hypotheses which associate cerebrovascular permeability with epileptogenesis, including imbalance of ion and molecule distribution and disturbance of neuronal homeostasis (Dadas et al., 2019).

Two of the biggest challenges regarding imaging biomarkers is the heterogeneity of PTE-related injuries and the rarity of longitudinal studies. Thus, a consistent and validated imaging biomarker for PTE has yet to be discovered. For a full review over imaging biomarkers in PTE see Garner et al., 2019 and Immonen et al., 2019.

I. 4.2 Genetic and Genomic Biomarkers

A genetic biomarker is a sequence of DNA which causes or is associated with susceptibility of a disease. Genetic biomarkers typically present as a genetic variant such as a copy number variant or single-nucleotide polymorphism (SNP) in the clinical setting. Likewise, genomic biomarkers reflect the expression, function, and regulation of a gene and its interrelationships to identify a combined influence within a biological state or within the context of disease progression (WHO, 2002). Genomic biomarkers include both DNA and RNA characteristics. DNA characteristics include single nucleotide polymorphisms (SNPs), DNA modifications (e.g., methylation or acetylation), variability within short sequence repeats, insertions, deletions, copy number variations, or cytogenetic rearrangements (e.g. duplications, deletions, inversions, translocations). Characteristics of potential RNA biomarkers include changes in RNA expression levels and sequence, alteration of RNA processes such as splicing or editing, and variation of microRNA levels. These two terms “genetic” and “genomic” biomarkers are similar in that they represent a change at the level of DNA or RNA but should not be used interchangeably. The main difference between genetic and genomic biomarkers is their respective focus on a specific gene and heredity vs an organism’s entire genetic make-up including coding and non-coding DNA and their interactions. For example, Huntington’s disease is caused by a genetic mutation in the HTT gene, representing a genetic biomarker; whereas significantly altered mRNAs found in the peripheral blood of Huntington’s patients serve as a genomic biomarker (Borovecki et al., 2005). Genomic biomarkers could be a useful prognostic marker for PTE by

identifying individuals with a higher risk of epileptogenesis and enriching the population of antiepileptogenesis trials.

Preclinical rodent trials have included genetically modified mice and/or animals with varying genetic backgrounds to help identify genomic influence on epileptogenesis and TBI. Adenosine is known to exhibit some anticonvulsant effects within epilepsy (Knutsen and Murray, 1997; Avsar and Empson, 2004). Knockout of the *Adora1* gene, affecting the adenosine receptor A1, was found to increase the incidence of acute postimpact status epilepticus (Kochanek et al., 2006). Adenosine receptor deficiency also exacerbated the microglial and neuronal damage response after TBI (Haselkorn et al., 2010). In the clinical setting, variants of adenosine kinase influenced the rate of epileptogenesis after TBI (Diamond et al., 2015). This same study also identified the genotype *rs1143634*, a variation in the IL1 proinflammatory cytokine profile, increased risk for developing seizures.

Several studies have focused on genes related to plasticity of the extracellular matrix. Pijet et al. used MMP-9 knockout and overexpression mice to determine the role extracellular matrix restructuring in posttraumatic epileptogenesis. Two peaks of MMP-9 expression were found at 30 min and 6 hr post-injury. Their results demonstrate overexpression of MMP-9 resulted in greater seizure frequency and lowered PTZ seizure threshold after TBI (2018). Prevalence of posttraumatic seizures was also correlated to increased lesion volume in these mice. APP/PS1 mice, which are predisposed to plaque deposition and gliosis, were found to have more pronounced epileptogenesis and robust comorbidities, such as cognitive impairment, following TBI (Miszczuk et al., 2016). A

series of studies investigated the role of the extracellular matrix proteinase urokinase-type plasminogen activator (uPA) and its receptor (uPAR) on PTE. Neither mutations of the *Plua* or *Pluar* gene, resulting in the deficiency of urokinase or its receptor, affected the progression of PTE after TBI. The authors concluded that epileptogenesis and seizure susceptibility was not worsened with uPA or uPAR deficiency, though comorbidities such as cognitive impairment and motor function were exacerbated (Bolkvadze et al., 2016; Bolkvadze et al., 2016). However, a recent follow-up study using a double knockout of both *Plau* and *Plaur* genes found significantly increased susceptibility to PTZ without brain injury (Kyyriäinen et al., 2019).

In the clinical setting, mutations affecting the balance of inhibitory-excitatory circuitry have been linked with an increased risk of PTE. Variations in the *GAD1* gene, responsible for producing the enzyme which catalyzes the production of inhibitory GABA from glutamate, increases a patient's risk for exhibiting post-traumatic seizures. Three high-risk genotypes have been identified for higher risk thus far: *rs769391*, *rs3791878*, and *rs3828275* (Darrah et al., 2013). Furthermore, a military-cohort study found a common variant in the methylenetetrahydrofolate enzyme (MTHFR C677T) may predispose an individual to PTE and other epilepsy disorders (Scher et al., 2011). Lastly, the role of *APOPE* gene has also been studied within the context of clinical PTE. Though no statistically significant associations were found, Miller et al. found half of the individuals with the E4/E4 genotype of *APOPE* had exhibited chronic post-traumatic seizures suggesting this variant may be at greater risk for delayed PTE (2010). The lack of studies reporting the effect of genetic and genomic factors on epileptogenesis after

TBI limits the progress to be made in determining targeted measures for therapeutics and clinical trials. There is a great need to continue research on these mechanisms to contribute to the progress in preventative therapies for PTE.

I. 4.3 Electrographic Biomarkers

Electrographic biomarkers may predict the onset of seizures and epileptogenesis, allowing for development of targeted preventative therapies. Currently, there are no validated electrophysiological biomarkers for post-traumatic epilepsy; however, experimental EEG studies using lateral FPI and CCI in rodents have identified potential candidates including: pathological high-frequency oscillations (HFOs), reduction in sleep spindle duration and dominant frequency at the stage III to rapid eye movement sleep, and epileptiform spiking/discharges preceding seizure onset.

HFOs are commonly classified into ripples (80-250 Hz) and fast ripples (250-500 Hz) and are believed to be a naturally occurring phenomena involved in both physiological and pathological processes (Zijlmans et al., 2012). Though ‘physiological’ and ‘pathological’ HFOs cannot be differentiated on spectral frequency alone, increased rhythmic patterns and power of HFOs have been correlated to epileptic foci (Jirsch et al., 2006; Staba, 2012). Early investigators of HFOs questioned whether HFOs could be evaluated by standard invasive macroelectrodes, but recent reports have shown that HFOs can be detected for long periods of time by a wide variety of methods including the standardized scalp EEG (Andrade-Valenca et al., 2011).

The theory that HFOs may play a role in epileptogenesis was first hypothesized by Bragin et al. who observed fast ripple occurrence preceded spontaneous seizures by weeks in a kainic acid model of status epilepticus (2000). A follow-up study found 19/26 rats developed pathological HFOs in the first month post-kainic acid injection, and that all 19 rats later developed epilepsy, whereas the remaining 7 rats did not exhibit pathological HFOs or seizures (Bragin et al., 2004). In a lateral FPI study, repetitive HFOs occurred at a significantly higher rate after moderate or severe injury, compared to mild or sham injured animals, providing additional evidence that injury severity correlates to epilepsy (Reid et al., 2016). Among these FPI rats, HFOs tended to occur more frequently in the early stages of the study before seizure onset. These studies suggest a pattern of intense and increasing abnormal epileptic activity during the epileptogenic period, starting with increased HFOs and ending the latency period with spontaneous seizures (**Figure 3**). For full review of HFOs as biomarkers for epilepsy see Perucca et al., 2019 and Jacobs and Zijlmans, 2020.

Sleep spindles occur at a frequency between 10-20 Hz (typically 12-14 Hz) with a duration of 500-2000 ms. Spindle generation involves interaction between inhibitory neurons in the thalamic regions to function as pacemakers. An increase in spindle frequency is known to occur immediately preceding REM sleep in both rodents and humans (Vyazovskiy et al., 2004; Purcell et al., 2017). Sleep disturbances are well documented after TBI, and disruption of normal spindle activity may contribute to epileptogenesis (Duclos et al., 2014). A recent study by Andrade and colleagues discovered 92% of detected seizures occurred during the transition period between stage

3 and REM sleep after lateral FPI in rats (Andrade et al., 2017). Sleep spindles in these epileptic rats were significantly shorter and slower during the transition from slow-wave N3 to REM sleep, compared to non-epileptic rats. These changes were identified at 9 weeks post-injury but were not observed within the first 2-3 weeks (Bragin et al., 2016), providing greater evidence of the progression of abnormal EEG over time.

EEG spikes, sometimes called interictal spiking, have been observed in both rats and mice after brain injury (Statler et al., 2009; Bolkvadze and Pitkanen, 2012). These spikes represent abnormal fluctuations in brain waves but have yet to be correlated with the onset of late spontaneous seizures. Furthermore, stimulation-evoked hyperexcitability in the hippocampus has been demonstrated after weight-drop and in neocortical brain slices after CCI (Golarai et al., 2001; Yang et al., 2010). It is unclear whether these electrophysiological disturbances are associated directly with the injury state or with epileptogenesis. Recently, Golub and Reddy observed short bursts of high-energy activity lasting between 3-9s after CCI injury in mice (2021). Though this definition of epileptiform discharges is intermediary to interictal spikes and seizures, it does provide further evidence of the evolution of abnormal EEG activity to seizure development.

Although there are currently no validated electrophysiological biomarkers for PTE, experimental studies continue to identify potential candidates which may be instrumental in predicting, and therefore preventing epilepsy with targeted therapeutic approached. These EEG abnormalities include pathological or repetitive HFOs, sleep spindle disturbances, and abnormal interictal spiking. Further experimental studies using

a controlled means of EEG analytics are needed to determine which features may be reliable biomarkers of PTE in the clinical setting. Machine learning, which has been recently instituted for seizure detection (Abbasi and Goldenholz, 2019), may also help to classify these abnormal EEG patterns in more meaningful ways. Furthermore, standardization of detection protocols, analysis algorithms, and sampling of EEG recordings will aid the progress of neurophysiologic biomarker discovery.

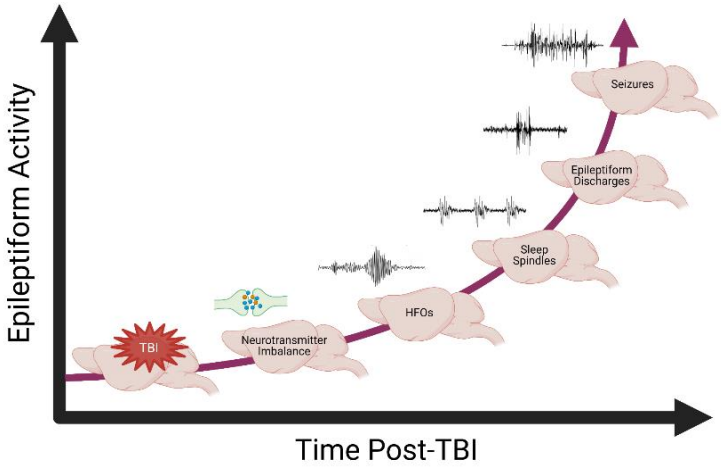

Figure 3: Evolution of TBI-Induced Hyperexcitability

Electrographic biomarkers may predict onset of seizures, as hyperactivity in the brain progresses overtime to the culmination of spontaneous recurrent seizures. TBI induces a state of heavy inflammation, disrupting both neurotransmitter and metabolic homeostasis. The emergence of these abnormal electrographic activities may reflect different stages of the epileptogenic process post-injury. Pathological HFOs often precede seizures by weeks, followed by reduced frequency and duration of sleep spindles during the transition between stage 3 and REM sleep. Disruption of normal sleep spindles contribute to several sleep-wake disorders reported by TBI patients. EEG spiking and discharges represent an advanced hyperactive disturbance have been described as epileptiform abnormalities in animal brain slices and *in vivo* at various time-points post-injury. The final stage is the end of latency indicated by the occurrence of spontaneous seizures; however, epileptogenesis can continue to progress even after the first seizure. Figure adapted from Perucca et al., 2019. Created with BioRender.com.

I. 4.4 Molecular Biomarkers

Biofluid markers are useful for determining TBI severity and play a critical role in monitoring disease progression and clinical prognosis (Sharm and Laskowitz, 2012). Molecular biomarkers refer to non-imaging factors that have biophysical properties allowing for measurement in biological samples such as blood, plasma, cerebrospinal fluid (CSF), saliva, or biopsy. Circulating biofluid markers such as miRNAs, proteins, extracellular vesicles, and cytokines have been widely studied in both TBI and epilepsy conditions (see reviews Agoston et al., 2017; Engel et al., 2013), but few studies have combined their efforts to identify biomarkers for epileptogenesis and PTE. Furthermore, there is little evidence to suggest biomarkers for TBI overlap with those for epileptogenesis; therefore, this subsection will briefly cover molecular biomarkers of TBI which have been indicated as potential risk factors for seizures.

Severe and penetrating TBI represent the highest risk of PTE development due to the extent of tissue damage, bleeding, inflammation, and bone fracture. These processes produce a graded increase in circulating levels of inflammatory chemo- and cytokines, regulators, and bone morphogenic proteins, providing a molecular basis for classifying injury severity (Heggeness et al., 2017). Deposition of bone particles and other foreign bodies in the brain parenchyma are among the most important risk factors for developing seizures after TBI (Salazar and Grafman, 2015). Likewise, increased serum and/or CSF levels of claudin-5, VEGF, occludin, aquaporin-4, and von Willebrand factor (vWF) may indicate a breakdown of the BBB and/or vascular injury (Jiao et al., 2011; Thrane et al., 2011; Ahmed et al., 2015; De Oliveira et al., 2007; Croll et al., 2004).

Iron levels, due to excessive bleeding, increases risk of PTE (Ding et al., 2016). Accumulation of iron in the blood can be cytotoxic, resulting in mitochondrial dysfunction and oxidative stress through the generation of free radical particles. In the clinical setting, TBI patients with low ceruloplasmin, an important protein involved in iron metabolism and injury repair, develop increased intracranial pressure that can lead to posttraumatic seizures (Dash et al., 2010). Neuroinflammation around the impact site also contributes to the rise in intracranial pressure. Increased cytokines and inflammatory proteins such as IL-1, IL-6, TNFα, CD53, fibrinogen, and MIP1α have been implemented in prolonged inflammation in human and animal studies (McManus et al, 1998; Katayama et al., 2009; Woodcock and Morganti-Kossmann, 2013). A genetic biomarker study demonstrated higher CSF:serum IL-1β ratios were associated with increased PTE incidence (Diamond et al., 2015). Furthermore, due to the astrocytic roles in both inflammation and glucose metabolism, CSF and/or serum levels of GFAP can provide insight into more than one pathology associated with PTE. It is likely that a combination of disrupted neural connectivity due to cell loss, metabolic dysregulation, and inflammation are critical components of immediate and early seizure onset after TBI (Tubi et al., 2019).

In plasma, miRNA can be either bound to argonaute2 protein or held within extracellular vesicles. Extracellular vesicles are involved in intercellular communication and can carry biomolecules such as DNA, mRNA, miRNA, proteins, and lipids. Raoof et al. conducted a study including temporal lobe epilepsy and status epilepticus patients which identified miR-19-3p was largely argonaute2-bound in both epileptic conditions,

and miR-21-5p was mostly carried within extracellular vesicles in status (2017). A follow-up study discovered the proportion of argoaute2-bound miR-328-3p increases after a spontaneous seizure in temporal lobe epilepsy (Raoof et al., 2018). Lastly, patient levels of transfer RNA fragments 5'GluCTC, 5'AlaTGC, and 5'GlyGCC have been found to be upregulated in pre-seizure vs post-seizure samples (Hogg et al., 2019). Since extracellular vesicles can be extracted from all biologic fluids, they have exciting potential for identifying biomarkers of PTEgenesis.

Discovery for PTE biomarkers is at an early stage. Each potential biomarker discussed as both advantages and disadvantages, therefore, it is unreasonable to expect a single biomarker to measure the progression of a heterogenous disease such as PTE. It is more likely that a combination of multimodal biomarkers will be needed to accurately identify epileptogenesis after brain injury. Relatively noninvasive biomarkers, such as imagining, surface EEG, and blood/plasma samples, are promising for TBI patients in which the likelihood for seizures is uncertain. However, there is little evidence to suggest that biomarkers for epileptogenesis following brain injury overlap with those of TBI in general. These differences may be exaggerated by variance in models, detecting methods, analysis platforms used, and stage of epileptogenesis. Furthermore, translating preclinical studies into clinical biomarkers is challenging. The timeline of molecular and cellular changes which occur in the development of epilepsy is much shorter in rodents than in humans, explaining why dozens of successful experimental pharmacotherapies have failed in clinical trials (Agoston et al., 2019). Longitudinal data in both rodent and clinical studies is lacking, therefore no standard temporal window comparing imaging

pathology or sampling has been followed. A concerted effort to standardize biomarker efforts for TBI, PTE, and other epilepsies may be an optimal strategy for discovery of novel biomarkers which are translatable throughout these related disorders.

I. 5 Comorbidities of PTE

Apart from seizures, traumatic insults are well-known to be associated with an assortment of behavioral and psychiatric dysfunctions including depressive symptoms, learning and memory deficits, personality changes, anxiety-like behavior, difficulty with social interactions, balance, motor impairment, as well as sleep disturbances. These features can have a profoundly negative effects on an individual's quality of life, perhaps more so than even the seizures themselves (Boylan et al., 2004). A population-based cohort study found patients with PTE have 7.85 times as many medical visits per year compared to non-epileptic TBI patients, suggesting a significantly increased medical burden (Lin et al., 2019). Pre-injury behavior and functioning are also strong indicators of long-term behavioral and recovery outcomes, including development of psychiatric disorders after TBI. Children who experience high-stress or significant life changes were found to be at greater risk for persistent post-concussion symptoms after brain injury (Smyth et al., 2014). The relationship between behavioral functions and seizures is extraordinarily complex, likely influenced by both recurrent seizure activity but also the therapeutic regimens used to control seizures (Szemere and Jokeit, 2015). A retrospective clinical study on rehabilitation after TBI found patients given prophylactic anti-seizure medications predicted poorer recovery, independent of whether these

patients experienced post-traumatic seizures (Pingue et al., 2021). Despite the well-established overlap of comorbidities between TBI and epilepsy patients, there is little research looking into the prevalence, presentation, or mechanisms associated with these impaired recovery outcomes in PTE.

Table 2: Comorbidities of PTE

	Conditions/Diagnoses	Symptoms
Sensorimotor Deficits	Vision disturbances	Difficulty recognizing or processing objects, blurry or lost vision, double vision, loss of depth perception
	Tinnitus	High-pitched ringing or buzzing in one or both ears, often associated with hearing loss
	Neuropathic itch	Skin tingling or pain resulting from nervous system damage
	Vestibular agnosia	Loss of vertigo perception and imbalance
	Motor deficits	Imbalance, changes in ambulatory gait, loss of fine motor skills
Cognitive Impairments	Mental fatigue and Attention impairment	Inability to concentrate or focus, even on simple tasks
	Short-term memory impairment	Inability to recall or remember information to which the subject was recently exposed
	Difficulty with critical thinking or problem solving	Difficulty processing, analyzing, evaluating, or synthesizing information in order to reflect, reason, communicate, or solve problems
Psychiatric Disorders	Depression/Affective Disorders	Constant feeling of sadness, loss or interest, and irritability; often associated with fatigue, lack of motivation, difficulty with recall, or suicidal thoughts
	Anxiety	Intense, excessive, and persistent worry or fear about everyday situations; avoidance; phobias; obsessive compulsive symptoms
	PTSD	Difficulty recovering after a traumatic event which triggers moments of intense emotional and physical reactions such as headache, nightmares, pain, flashbacks, amnesia, or difficulty concentrating
	ADHD	Hyperactivity, impaired attention, reduced work speed, and difficulty with working or short-term memory
Sleep Disorders	Insomnia	Difficulty falling or staying asleep, insufficient number of hours or sleep despite adequate opportunity
	Parasomnia	Night terrors, sleep walking/talking, confusion arousals, REM sleep behavior disorder
	Idiopathic Hypersomnia	Excessive daytime sleepiness
	Narcolepsy	Overwhelming daytime sleepiness and sudden attacks of sleep, cataplexy, sleep paralysis, sleep related hallucinations
	Sleep Apnea	Snoring, restlessness, apnea, open mouth breathing, sleep fragmentation
	Circadian Rhythm Disorder	Sleep-wake cycle is not aligned with environment/schedule and interferes with daily activities; difficulty falling asleep or staying asleep

I. 5.1 Sensorimotor abnormalities

Risk of complications increases with the severity of trauma, though mild TBI can also result in disabilities that interfere with daily life (van der Naalt, 2001). Patients may experience sensory problems, especially complications with vision (Ripley and Plitzer, 2010). One of the brain's primary functions is to integrate information from the outside environment, process it, and determine an appropriate reaction or response. Disturbances in vision, either in recognition or registration of objects, can lead to clumsiness and poor hand-eye coordination. Double vision also affects depth perception and ambulatory balance. Other sensory deficits, such as those affecting hearing, taste, smell, or touch are less common but not unlikely. Damage to regions of the brain which process taste or smell may cause the perception of bitter and/or noxious smell. Likewise, injury to sensory pathways can trigger neuropathic itch, skin tingling, or pain (Oaklander, 2011).

The motor and somatosensory cortices are among the most vulnerable brain regions affected by TBI and diffuse axonal injury due to their superficial position. Damage to these regions is associated with impaired motor control and function. TBI patients often report difficulty with balance, changes in ambulatory stride, and loss of fine motor control. Recently, a first-of-its-kind study characterized the presence of a newly defined neurological disorder called vestibular agnosia in TBI patients (Calzolari et al., 2021). This condition results in the loss of vertigo perception and imbalance. The Seemungal group found TBI patients exhibiting vestibular agnosia have worse balance problems and are unlikely to experience dizziness. Therefore, these patients are at higher risk of subsequent falls or TBI.

In preclinical studies, researchers have focused on changes in motor functionality as a parameter of recovery outcomes. These changes in motor function have been measured with numerous behavioral tests including comprehensive neurological scoring, beam walk, and rotarod testing. Furthermore, tasks such as open field and water maze can also provide insight on functional recovery by evaluating walking and swim speed between injured and non-injured cohorts. Rodents with TBI and/or PTE demonstrate significantly worsened sensorimotor complications compared to sham-injured controls (Nissinen et al., 2017; Golub and Reddy, 2021; Gold et al., 2013). Insulin-like growth factor-1 overexpression attenuates posttraumatic motor dysfunction, suggesting sensorimotor recovery may be influenced by overactive inflammatory signals or reactive astrocytes (Madathil et al., 2013). While locomotive ability progressively recovers overtime, sensory and cognitive deficits often persist for months or years after injury. Therefore, it is critical to assess sensorimotor outcomes as an indicator of rehabilitation in both preclinical and clinical trials.

I. 5.2 Cognitive dysfunction

There are many forms of cognitive dysfunction, whether it be difficulty retaining or recalling information, disrupted focus, or higher order impairments such as inability to plan, lack of motivation, or psychosocial disability. Psychometric tests found patients with PTE exhibited a significantly reduced ability to plan, showed a lack of initiative, and had a higher incidence of disinhibited behaviors compared to TBI patients without seizures (Mazzini et al., 2003). Furthermore, clinical studies have found evidence for

impairments in attention (Fenwick and Anderson, 1999), problem solving (Cazalis et al., 2006), short-term and working memory (Vallat-Azouvi et al., 2007), and mental fatigue (Ziino and Ponsford, 2005).

Preclinical research has hypothesized altered synaptic plasticity and neurodegeneration induced by TBI may play a critical role in cognitive impairment. Mild to moderate TBI is associated with altered hippocampal bursts, with longer duration and lower inter-burst spike frequency (Muyon et al., 2014). Shorter interval bursts in CA1 hippocampal neurons provoke LTP and plays a role in synaptic plasticity, thus affecting information coding after TBI and resulting in hippocampal-associated cognitive impairments (Thomas et al., 1998; Ouyang et al., 2017).

TBI is known to affect both short and long-term memory (Enomoto et al., 2005; Carron et al., 2019). Preclinical *in vivo* studies often utilize behavioral tests such as the Morris water maze or Barnes maze to evaluate spatial learning and memory (Morris, 1984; Barnes, 1979). Both tests involve training rodents to use visual spatial cues to escape the arena. Over a series of trials, rodents remember the location of the hidden platform or escape box and complete the task progressively faster. Another common task is the Novel Object Recognition Test (NORT), which was initially described in 1988 (Ennaceur and Delacour, 1988). NORT examines recognition memory by first exposing rodents to two identical objects during a familiarization phase, followed by the replacement of one of those objects with a novel object. Healthy rodents recognize the new object, spending more time investigating it, using hippocampal-dependent recognition memory (Bevins and Besheer, 2006). Several research groups have

evaluated short- and long-term cognitive deficits within the context of PTE, finding PTE cohorts perform poorly at these tasks compared to uninjured controls (Scheff et al., 1997; Lu et al., 2015; Golub and Reddy, 2021; Nissinen et al., 2017). These studies reflect similar cognitive deficits found after TBI along (Paterno et al., 2017). Due to the extent of cognitive impairment often seen after TBI and how this relates to poorer quality of life in the human condition, it is our opinion that the success of future clinical trials of PTE depends on preclinical models which incorporate both the measurement of cellular and molecular pathologies associated with hyperexcitability as well as memory and behavior tasks.

I. 5.3 Depression, mood disorders, and anxiety

Cognitive deficits resulting from brain injury can also overlap with development of affective disorders. For example, emotion-recognition difficulties, such as facial affect recognition disorder, contribute to a suite of social functional impairments in patients with TBI (Babbage et al., 2011). Social dysfunction in TBI is well-documented and can negatively affect a person's ability to form relationships, impairs empathy, and results in low social participation and stress (Hammond et al., 2004).

Among the general population, anxiety and depression have the highest prevalence of any other group of psychiatric disorders, with a lifetime occurrence reported at approximately 30% (Barlow, 2004). A growing body of research indicates that mood and anxiety disorders are even more prevalent in TBI patients. Approximately 70% of TBI patients experience a psychiatric illness within the first year following initial

injury (Tao and Lyketsos, 2002; Bombardier et al., 2010; Ponsford, 2017). The most common manifestations of psychiatric disorders among adolescents and adults with TBI are generalized anxiety, depression, phobias, post-traumatic stress disorder, and obsessive-compulsive disorder. A long-term neuropsychiatric study found that patients with PTE showed higher incidence of irritability and agitated behaviors, aggression, and personality disorders compared to non-epileptic TBI patients (Mazzini et al., 2003). Aggressive behaviors may limit access to rehabilitation treatment, participation in employment and social activities, as well as contribute to drifting friendships and romantic relationships.

Decreased functional connectivity between the amygdala and prefrontal cortex has been proposed to be a core neurobiological feature of psychiatric disorders (Makovac et al., 2016). The prefrontal cortex is a critical structure for effective regulation of emotions, particularly when controlling negative emotion (Diekhof et al., 2011). The amygdala plays an essential role in bottom-up and top-down emotional processing as well, with connections to the cortical-striatal-pallidal-thalamic circuit. Due to its widespread network, the amygdala is a core mediator in mood regulation and disorders (Price and Drevets, 2012). Neuropathological changes associated with TBI can lead to dysfunction of the lateral and dorsal prefrontal cortices and increased activation of the limbic and paralimbic structures, including the amygdala. Altered amygdala connectivity has been identified as a possible biomarker of both comorbid depression and anxiety in TBI patients. Relative increases in amygdala connectivity were found in the left dorsomedial and right dorsolateral prefrontal cortices and thalamus as well as the

brainstem with spatially dissociable patterns of correlation between this increased connectivity and symptom severity (Han et al., 2015). Another study investigating psychiatric symptoms associated with TBI found that patients with history of major depression often exhibit comorbid anxiety (77%) and aggressive behavior (57%) (Jorge et al., 2004). These patients had significantly worse executive functionality compared to their non-depressed counterparts. Furthermore, neurotransmitters such as norepinephrine, serotonin, dopamine, and GABA are mediators of anxiety and depression symptoms. Disruption of these systems, by either direct impact of TBI or indirect pathologies such as chronic stress or inflammation can negatively influence comorbid development of psychiatric disorders.

I. 5.4 Attention deficit hyperactivity disorder (ADHD)

A meta-analysis documented a significant association between mild TBI and attention deficit hyperactivity disorder (ADHD) (Adeyemo et al., 2014). ADHD is a neurodevelopmental, childhood onset and persistent disorder characterized by increased impulsivity and risk-taking behavior in individuals. Not only has ADHD been shown to heighten risk of experiencing a TBI, but preexisting diagnosis of ADHD may also result in worsened recovery outcomes after injury (Bonfield et al., 2013). Compared to TBI patients without ADHD, individuals with both diagnoses were significantly more impaired on individual scores of working memory, planning/organization, metacognition indices, and behavioral regulation (Biederman et al., 2015).

ADHD that develops as a comorbidity of TBI is referred to as secondary ADHD and has been shown to occur in 10-20% of patients post-TBI (Gerring et al., 1998). Many studies support the hypothesis that dysfunction in the prefrontal cortex, basal ganglia, and their related neurotransmitter systems underlie deficits in inhibitory regulation found in ADHD patients (Dickstein et al., 2006). Therefore, damage to these areas have the potential to manifest as secondary ADHD or other psychiatric disorders in children and adults. Secondary ADHD may be more prevalent in children and adolescents due to the underdevelopment of brain regions linked to inattention and hyperactivity. Anatomic studies of youth with developmental ADHD demonstrate a loss of volume of frontal and striatal structures without lesions. One case study describes secondary ADHD development in a 10-year-old boy who suffered head trauma and early post-traumatic seizures (Ceylan and Akca, 2013). Cranial CT scans demonstrated decreased density of the right basal ganglia and loss of corticomedullar differentiation in the right frontal area. Six months following the accident, reports from the patient's parents and teachers describe a change in the child's behavior of overactivity, boredom at class and home, difficulty maintaining concentration, and depressive-like symptoms. Social disinhibition, hyperactivity, poor impulse control, forgetfulness, and lack of judgement/foresight are among the chronic sequelae of closed head injuries (Kaitaro et al., 1995).

I. 5.5 Sleep disorders

Sleep-wake dysfunction after brain injury is common, affecting up to 70% of patients (Viola-Saltzman and Watson, 2012). Common diagnoses after TBI include insomnia, parasomnia, idiopathic hypersomnia, narcolepsy, sleep apnea, and circadian rhythm disorder (Morse and Garner, 2018). This sleep-wake cycle is regulated by a concerted effort between circadian rhythms, sleep-wake homeostasis, metabolism, external environmental factors such as diet, stress, medication, and surroundings. Pre-existing sleep conditions can increase the likelihood of post-TBI sleep-wake disturbances. Additionally, comorbid sleep disorders contribute to psychologic instability, resulting in behavioral problems, mood or emotional lability, and worsened daily functioning (Shay et al., 2014).

Alertness and cortical arousal are mediated by several pathways which project from the brainstem near the junction of the midbrain and pons to innervate the thalamus, posterior hypothalamus, and forebrain (Fuller et al., 2006). These ascending pathways are populated by key cell types including cholinergic, histaminergic, noradrenergic, dopaminergic, and serotoninergic neurons which fire in a distinct pattern to promote wakefulness. Orexin peptides produced in the lateral hypothalamus reinforce the arousal state. However, this system is inhibited roughly every 24-hr by sleep-active GABAergic and galaninergic neurons of the ventrolateral preoptic nucleus (VLPO) to promote sleep onset (Schwartz and Roth, 2008). The VLPO is a known sleep center influenced by the suprachiasmatic nucleus (SCN) and activated by endogenous sleep-promoting

substances such as adenosine and prostaglandin D2. Melatonin production from the pineal gland plays a role in REM sleep and aids in synchronizing circadian rhythms.

The pathophysiology of post-traumatic sleep disorders has not been fully explored, however decreased levels of wake-promoting neurotransmitters such as hypocretin (orexin) and histamine are believed to play a contributing role. Post-mortem assessments of brains from TBI patients demonstrate significant reductions in hypocretin neurons (Shekleton et al., 2010). Even after 6 months of recovery, many TBI patients exhibit persistently low hypocretin-1 levels, suggesting sleep disorders as a chronic consequence of TBI (Baumann et al., 2007). Disturbed orexin signaling contributes to sleep-wake disorders by causing excessive daytime sleepiness and circadian rhythm disruption (Nishino et al., 2000; Baumann et al., 2005). Moreover, decreased CSF levels of orexin have been associated with poorer clinical outcomes and higher risk of depression and sleep disorders (Brundin et al., 2007). Low CSF histamine levels have also been reported in patients with narcolepsy and after TBI (Kanbayashi et al., 2009). Injury may cause lifestyle changes which can affect sleep and arousal, including changes to diet or medication, exercise routines, or environmental factors. Furthermore, insomnia may develop as a result of psychological trauma, resulting from personal assaults or accidents which resulted in TBI. Lastly, direct injury to sleep-wake brain centers, such as the VLPO or SCN, may also explain development of circadian rhythm disorders.

Once the prevalence of PTE associated comorbidities is established, the search for biomarkers for PTE and recovery may benefit from the neurocognitive network model of affective and/or sleep disorders currently applied to primary epilepsy. Since

sensorimotor, cognitive, psychiatric, and sleep-wake comorbidities are so common after TBI, it is important for future work to incorporate quality of life measurements as indicators of recovery outcomes when assessing new therapeutic targets. By examining cellular and synaptic changes in the affected neural circuitry, we can better understand how learning and memory deficits occur. Using newer technologies, such as chemogenetics or optogenetics, could substantiate the relationship between behavior and physiology in a meaningful way.

I. 6 Pharmacological Interventions for PTE

Epilepsy and epileptogenesis are both associated with a wide range of comorbidities, ranging from mild to severe, and often originating from overlapping processes. Therefore, disease modification has two major components: antiepileptogenesis and/or the reduction of its associated comorbidities. Antiepileptogenesis includes the prospect of the prevention of epilepsy, seizure modification, or cure. Prevention can be either partial or complete. Partial prevention consists of delayed epilepsy development or reduced severity, whereas complete prevention is the cancellation of the development of epilepsy. Modification of seizures is considered a form of partial protection and can come in many forms: reduced frequency, milder seizure type, and shorter duration (Cross and Lagae, 2020). Antiepileptogenic treatments can be administered before or after the onset of seizures to prevent or delay the development of epilepsy. This contrasts modification of the epileptogenic insult in which a treatment is given before the onset of seizures and alters epileptogenesis by

modifying the injury or insult directly. Modification of seizures, if they occur in either case, can be milder in their progression, severity, frequency, or duration. On the other hand, a cure, refers to the absolute and permanent reversal of the epileptic state such that no seizures occur after withdrawal of treatment. Treatments that treat or modify comorbidities of PTE may alleviate or reverse the progression of somatosensory or functional impairment, cognitive decline, anxiety, depression, or any other epilepsy-associated comorbidity. Treatments of comorbidities may be singular or broad with their ability to affect a range of symptoms.

To date, the current management of clinical PTE remains as prophylactic treatment with first-line therapies such as levetiracetam or phenytoin for the first seven days following initial injury (Temkin et al., 2001). These antiseizure medications have shown efficacy in focal epilepsies, but have limited effectiveness in PTE. Many studies have reported evidence that there is currently no pharmacological prevention or treatment for posttraumatic seizures, and PTE is often refractory to medical management (Zimmerman et al., 2017; Piccenna et al., 2017). Novel drug discovery requires reliable animal models to elucidate the complex pathophysiology of epileptogenesis, validate targets, and test agents for efficacy and safety.

Rodent studies have been particularly useful for discovering novel therapeutic targets, though there are limited studies which have specifically investigated interventions for PTE. This next section reviews research which has focused on pharmacological prevention of PTE. **Table 3** details the available data on experimental and clinical trials of therapeutic interventions for PTE.

I. 6.1 Anti-epileptic Drugs (AEDs)

Perhaps the most accessible experiments for PTE are those which evaluate the effect of clinically available anti-epileptic drugs for beneficial effects on disease modification or recovery outcomes. Early studies with positive but uncontrolled results led to widespread use of phenobarbital and/or phenytoin for prophylaxis against immediate and long-term post-traumatic seizures. One survey, conducted in 1973, reported over 60% of clinicians supported immediate pharmacological prophylaxis for head injuries, with 40.3% of respondents prescribing treatment for 1 or more years following injury (Rapport II and Penry, 1973). Current evidence suggests treatment of early seizures does not influence the incidence of PTE (Agrawal et al., 2006). Within the clinical setting, carbamazepine, phenytoin, phenobarbital, and valproate all failed to prevent long-term PTE after head injury (Temkin, 2009). In a recent clinical trial, Hazama et al. evaluated the benefit of levetiracetam after head trauma (2018). The study consisted of 403 patients, 227 of whom were treated with levetiracetam for early post-traumatic seizure prophylaxis. Though patients receiving levetiracetam treatment trended with lower seizure incidence, this trend never reached statistical significance. These AEDs have shown successful seizure control in other epilepsy disorders but have little effect on preventing or modifying epileptogenesis.

Preclinical research has demonstrated a similar lack of efficacy in reducing PTE incidence with AEDs. Eastman et al. utilized the FPI model to systematically detect potential anti-epileptic effects of carbamazepine and valproate 1-month post-injury (2010). Carbamazepine (up to 12mg/kg/day for 4.5 days) treatment did not reduce

seizure frequency or duration, nor did it reduce incidence of PTE. However, valproate (480 mg/kg/day for 7 days) reduced seizure frequency and cumulative seizure duration. Comorbidities were not evaluated as part of these investigations. In a follow-up study, carisbamate administration was also found to be ineffective at reducing seizure burden or preventing PTE (Eastman et al., 2011) Recently, retigabine, an AED that was removed from the commercial market in 2017, has shown some promise in reducing seizure burden after CCI in mice. Not only did retigabine administration reduce inflammation, BBB breakdown, and neurodegeneration at the impact site, but also significantly reduced frequency of spontaneous seizures and enhanced susceptibility to chemoconvulsants (Vigil et al., 2019). Gabapentin administration inhibited synapse formation and decreased excitatory synaptic activity after cortical injury (Li et al., 2012). Gabapentin treatment also reduced the expression of astrocytic GFAP expression and TSP1 protein, as well as the number of FJB+ stained cells. These results suggest gabapentin may modify pathways associated with plastic changes in brain excitability, but a controlled *in vivo* study with continuous EEG recording has yet to confirm an antiepileptogenic effect.

Lastly, Mountney et al. demonstrated administration of ethosuximide, or phenytoin dose-dependently attenuates in the incidence, frequency, and duration of nonconvulsive seizures following a penetrating blast-like brain injury (2013). In this study, a loading dose of either ethosuximide or phenytoin was given 30-min post-TBI, followed by a maintenance dose 8hr later. Four doses of each drug were used to provide a full dose-response curve, with the two highest doses of each drug showing significance

in reducing seizure burden. Though this data is promising, this study only follows the rats for up to 72 hr post-injury and identifies immediate and early nonconvulsive seizures, which are considered to be caused by direct impact rather than epileptogenesis. Furthermore, there is little evidence that suggests early seizure prophylaxis to reduce incidence of long-term spontaneous seizures.

I. 6.2 Altering the Inhibitory and Excitatory Pathways

The balance of inhibition and excitation in the brain is very delicate. TBI triggers changes which ultimately result in the disruption of this harmony, leading to increased risk of seizures and epileptogenesis. One approach aimed at minimizing excitotoxicity and preserving cortical inhibition after TBI is the administration of ceftriaxone, a common β-lactam antibiotic with BBB permeability. Ceftriaxone is also a known potent stimulator of GLT-1 expression, a critical protein responsible for 95% of total glutamate clearance in the rat brain (Lehre and Danbolt, 1998). Ceftriaxone (200 mg/kg) rescues TBI-induced downregulation of GLT-1 expression within the first week following injury (Goodrich et al., 2013). Authors also report a reduction in regional GFAP expression relative to untreated rats. A follow-up study reported ceftriaxone significantly suppressed both the frequency and duration of post-traumatic seizures weeks after injury (Hameed et al., 2018).

Enhancing GABAergic inhibitory tone is a well-established mechanism for seizure prophylaxis, as many AEDs are approved in this class. $GABA_A$ receptors are also targets of general anesthetics, such as halothane, which can completely suspend

seizure activity after FPI, though it leaves the subjects immobile (Eastman et al., 2010). Recent attention has been directed towards selective, rather than nonselective (e.g., diazepam) positive allosteric modulators of GABA due to a lower risk for somnolence, motor impairment, and drug abuse (Witkin et al., 2018). KRM-II-81 is an orally bioavailable compound selective for α2/3-containing $GABA_A$ receptors. Witkin et al. used several models of pharmaco-resistant epilepsy, including kainate-induced mesial temporal lobe seizures, CCI-induced focal injury, and corneal-kindling, to investigate the antiepileptogenic properties of KRM-II-81 (2020). They report complete suppression of corneal-kindling seizures in treated mice as well as reduced paroxysmal discharges after kainate injection. Furthermore, repeated injection of KRM-II-81 administration immediately reduced neural hyperactivity for weeks after CCI, suggesting drug-resistance or tolerance was negligible. Many AEDs have little therapeutic impact after TBI for controlling post-traumatic seizures, therefore, the cortical excitatory reductions by KRM-II-81 encourage future preclinical and clinical studies.

Lastly, 2-Deoxyglucose (2-DG), a competitive inhibitor of hexokinase, the rate-limiting enzyme in glycolysis has also shown anticonvulsive properties both *in vivo* and *in vitro*. Recently, Koenig et al. explored the compound as a disease modifying agent to prevent epileptogenesis after TBI (2019). Using the CCI model of brain contusion, they report acute 2-DG treatment attenuated hyperexcitability in the brain and prevented development of epileptiform activity in slices taken 3-5 weeks after injury. Additionally, 2-DG treatment reduced the loss of parvalbumin-expressing interneurons, thereby showing neuroprotection against TBI-induced cell loss.

I. 6.3 Neuroinflammatory Targeting

Targeting neuroinflammation has been a therapeutic strategy in epilepsy disorders for decades, for good reason. Neuroinflammation involves both resident microglia and astrocytes, as well as peripheral immune signaling when the BBB integrity becomes compromised. Furthermore, reactive glial cells can be the drivers of abnormal neuronal activity by impairing the inhibitory action of GABA receptors, reduced neurotransmitter clearance, and disrupted homeostasis (Robel and Sontheimer, 2016). To this end, a handful of compounds have been tested as potential anti-epileptogenics for PTE. While glycyrrhizin, a HMGBI1 inhibitor, was recently found to be ineffective at preventing seizures or reducing susceptibility after TBI, its administration did reduce edema and microglial activation following CCI in pediatric mice (Webster et al., 2019). Toll-like receptor agonists, such as monophosphoryl lipid A and Pam3Cys, significantly slowed amygdala kindling after TBI, demonstrating a reduction in seizure susceptibility (Hesam et al., 2018). Treated rats also exhibited a lessened behavioral response to kindled seizures similar non-traumatic rats. Given that monophosphoryl lipid A and Pam3Cys are safe and have clinical use as components in vaccines, they have the potential to be used in combination with other agents as a therapeutic strategy for PTE.

Minozac, a suppressor of pro-inflammatory cytokine upregulation, has been shown to significantly reduce electroconvulsive shock seizures after TBI in mice (Chrzaszcz et al., 2010). This data was coupled with a favorable reduction in TBI-induced metallothionein expression in the CA1, suggesting a reduction in oxidative stress with treatment. Similarly, kineret, an IL-1 receptor antagonist, reduces seizure

susceptibility and improved neuropathology associated with epileptogenesis two weeks following CCI (Semple et al., 2017). Moreover, mice treated with kineret showed significantly lower seizure frequency compared to vehicle-treated controls at 5 months post-injury. Combined with improved neurobehavioral function, these data provide evidence of IL-1 signaling as a mediator of injury-associated epileptogenesis.

I. 6.4 Disrupting the mTOR Pathway

As discussed above, the mTOR signaling pathway is implicated in the regulation of multiple cellular functions which contribute to epileptogenesis. The current hypothesis is such that mTOR signaling is hyperactivated after TBI and triggers multiple downstream mechanisms of PTE. Several studies of mTOR inhibition have demonstrated a beneficial effect of rapamycin, an mTOR inhibitor, treatment for epilepsy disorders and improving recovery outcomes after TBI.

Within PTE models, three studies have shown reduced seizure incidence, frequency, or duration after CCI in mice (Guo et al., 2013; Butler et al., 2015; Butler et al., 2016). Guo et al. observed a significant reduction in seizure incidence, dropping from 50% to 13% in treated versus untreated mice (2013). It was also noted that when rapamycin-treated mice did exhibit seizures, the behavioral component was lessened, suggesting seizure intensity was also reduced by mTOR inhibition. Butler et al., reported a trend of reduced seizure frequency and incidence with continuous rapamycin treatment but indicated mTOR inhibition was not sufficient to prevent epileptogenesis after CCI (2015). Furthermore, a follow-up study confirmed rapamycin treatment can modify

synaptic and tonic $GABA_A$ receptor-mediated currents, hinting towards another mechanism of anti-epileptogenic properties (Butler et al., 2016).

Similar to reports on status epilepticus, rapamycin administration resulted in reduced neurodegeneration and attenuated mossy fiber sprouting. Unfortunately, the beneficial effects of rapamycin appear to cease upon discontinuation of the drug in both animal and clinical trials (Buckmaster et al., 2009). Life-long treatment with mTOR inhibitors is questionable given the known adverse effects such as immunosuppression, risk of cognitive impairment, and negative influences on normal growth and development in children or adolescents (Bissler et al., 2008).

I. 6.5 Neuronal Plasticity

Neurotrophic factors like BDNF, NGF, and FGF promote cell survival, growth, and differentiation through activation of signaling pathways following TBI. Abnormalities of interneurons and cell loss play critical roles in epileptogenesis after TBI; therefore, enhancing the function of remaining parvalbumin+ interneurons may be a novel therapeutic approach to preventing PTE. BDNF is known to have positive influences on interneuron growth and function through activation of its receptor, TrkB (Marty et al., 1997). A recent study tested the hypothesis that supporting TrkB function may decrease epileptogenesis after cortical undercut (Gu et al., 2018). LM22A-4 or PTXBD4-3, both partial agonists of the TrkB receptor, were administered up to two weeks after injury. PTXBD4-3 reduced seizure susceptibility to PTZ but did not affect seizure duration or latency. LM22A-4, however, decreased the incidence of epileptiform

discharges compared to untreated controls. Activation of the TrkB receptor also resulted in increased parvalbumin immunoreactivity, suggesting that partial activation of TrkB may be neuroprotective to interneurons, thereby preserving inhibitory circuity and reducing seizure susceptibility. A different approach explored the use of BDNF blockers in *ex vivo* organotypic hippocampal slice cultures with collateral lesions and observed reduced hyperexcitability of CA3 pyramidal neurons as well as a reduction in aberrant mossy fiber sprouting (Gill et al., 2013). These differing approaches provide supporting evidence for TrkB signaling modification, but further investigations are needed to confirm anti-epileptogenic effects.

I. 6.6 Hypothermia

Focal cooling can be broadly neuroprotective and has suppressed seizures in animal models, providing evidence that therapeutic hypothermia should be investigated within the context of PTE. Blind, randomized studies of FPI found that a graded cooling up to 2°C significantly reduced seizure frequency and duration in rats. Cessation of ictal activity lasted up to 10 weeks after hypothermia treatment ended (D'Ambrosio et al., 2013). Another study reported reduction of seizure threshold to chemical convulsants and reduced mossy fiber sprouting with hypothermia treatment but did not exhibit neuroprotective effects on cell loss (Atkins et al., 2010). Hypothermia appears to be safe with few negative consequences; however, more research is needed to optimize treatments and define its clinical value.

I. 6.7 Electrical Stimulation

Deep brain stimulation (DBS) has shown to be remarkably effective, safe, and practical for the treatment of movement disorders such as tremor, dystonia, and Parkinson's disease (Deuschl et al., 2006). These successes inspired the application of DBS for other neurological disorders, including epilepsy. The action of DBS is multifaceted and complex, with high frequency stimulation (>50 Hz) mimicking the effects of ablative procedures by inducing a reversible functional lesion (Benabid et al., 2002). Lower frequency stimulation has been associated with anticonvulsant effects, changes in adenosine receptor expression, and altered levels of neurotransmitters and hormones in cerebrospinal fluid. The basis of DBS is to improve abnormal synchrony between different brain regions. One case study was found using DBS as a potential therapeutic intervention for PTE. The patient reported a post-traumatic episode during childhood which resulted in subsequent seizures throughout adulthood. AED treatments, such as carbamazepine, phenobarbital, and clonzapam had all been unsuccessful in providing adequate symptomatic control of seizures. Bilateral DBS hippocampal stimulation resulted in a progressive decrease in seizure frequency over the 8 years of follow-up; though the clinicians postulate whether the surgical placement of the DBS system may have contributed to the disruption of the epileptic foci in this case (Piacentino et al., 2018). Other studies have found behavioral improvements and functionality using DBS after TBI, though seizure outcomes were not applicable in these cases (Schiff et al., 2013; Shin et al., 2014; Rezai et al., 2016).

I. 6.8 Tau Hyperphosphorylation

Tau is a microtubule-associated protein that has roles in maintaining neuronal health, axonal transport, and microtubule stabilization. Tau phosphorylation is a normal metabolic process critical to tau's ability to bind to microtubules. Hyperphosphorylation of tau can cause aggregation and form insoluble fibrillar deposits in tissues. Hyperphosphorylated tau is a long-known hallmark of neurodegenerative diseases such as Alzheimer's disease and dementia; however, the causal role of TBI-induced tauopathy has been debated for decades (Castellani and Perry, 2019). Recent studies have confirmed moderate and severe brain injury can trigger the formation of pathological tau aggregates, linking TBI to increased risk of Alzheimer's disease (Edwards III et al., 2020; Wu et al., 2020).

Sodium selenate mitigates hyperphosphorylated tau by antagonizing PP2A activity and can improve TBI outcomes. Liu et al. administered sodium selenate (1mg/kg/day), a less toxic form of selenium, via osmotic pumps for 12 weeks following FPI (2016). Treatment with sodium selenate ameliorated the enlargement of ventricles and hippocampal atrophy which often accompanies brain injury. Additionally, the latency period to spontaneous epileptiform activity, such as seizures or discharges, was extended compared to vehicle-treated rats, suggesting possible interruption of the epileptogenic process. Though this is the only study to specifically investigate the effects of sodium selenate on PTE, sodium selenate has been demonstrated to suppress seizures, improve comorbidities, and reduce seizure susceptibility in experimental models of

Lafora disease and temporal lobe epilepsy (Jones et al., 2012; Sanchez-Elexpuru et al., 2017).

I. 6.9 Cell transplant therapies

Cell transplantation including genetically modified cell types have been tested as a recovery-enhancing treatment after TBI. Outcome measures include the effects of treatment on lesion volume, severity of neurodegeneration, axonal injury, edema, motor ability, and cognitive function (Jackson et al., 2017). Although positive data has emerged from these studies, most reports have not measured development of spontaneous seizures as an outcome. One recent study, however, found the transplantation of GABAergic progenitors derived from the embryonic medial ganglionic eminence (MGE) migrated, integrated, and restored post-traumatic decreases in synaptic inhibition (Zhu et al., 2019). Using a CCI model of PTE, mice were recorded using continuous 24/7 video-EEG for between 7 and 20 days at 4 months post-injury. Since most models of PTE find the onset of seizures to be between 20-90 days, this timeline was assumed to be after onset of spontaneous epileptiform activity. Incredibly, no electrographic seizures were observed in TBI mice that were implanted with MGE cells, whereas 5 of 8 untreated mice exhibited repeated ictal events. Cell transplantation therapy also resulted in improved memory precision in transplant mice using the novel object location test. Together, these results provide powerful evidence of antiepileptogenesis using cell-based therapies by restoring long-term deficits in both synaptic inhibition and neurobehavioral impairments. However, this study was limited

by the relatively small cohort sizes and shortened length of EEG recording. Follow-up studies could easily address these limitations. This work establishes a promising framework for future studies to evaluate other populations of neurons for cell transplantation therapies for PTE.

I. 6.10 Other Potential Therapeutic Strategies

Studies dating back to the 1920s have shown that diet and exercise can improve seizure control for patients with epilepsy, with a special emphasis on the ketogenic diet (Wilder, 1921). The ketogenic diet is a high-fat, adequate-protein, and low-carbohydrate diet that has been shown to reduce seizure frequency by over 50% in children and adolescents but has not demonstrated evidence of disrupting the epileptogenic process (Neal et al., 2008). Similar to clinical indications, the ketogenic diet was found to not be effective in preventing PTE after brain injury (Schwartzkroin et al., 2010). However, regular treadmill exercise not only lengthen the latency to seizure onset, but also reduced ictal duration and susceptibility to PTZ-induced seizures in rats (Silva et al., 2013). Creatine supplementation to the diet, on the other hand, has produced contradicting results. Gerbatin et al. report decreased duration of tonic-clonic seizures and reduced PTZ-induced epileptiform discharges (2019). Creatine supplementation was also found to reduce neurodegeneration of parvalbumin+ interneurons in the hippocampus at 1-month post-injury. These results required long-term administration of daily creatine. Saraiva et al., however, found no reduction on convulsive parameters induced by PTZ in the first week following TBI, but did reduce oxidative damage at the impact site (2012).

Together, these studies suggest creatine supplementation may not be a sufficient prophylactic for early post-traumatic seizures but may possess long-term downstream effects which stabilize epileptogenesis.

Cannabis and related compounds have recently broke foreground in epilepsy disorders with the USA FDA-approval of Epidiolex for Lennox-Gastaut and Dravet syndromes in 2018. Cannabidiol has yet to be evaluated for post-traumatic epilepsy, but Rimonabant (SR141716A), a CB1 receptor antagonist may modify disease progression. CB1 receptors are present on both excitatory and inhibitory nerve terminals, where they inhibit glutamate and GABA release, respectively. Therefore, agents which act at this receptor may have multiple effects on neurotransmission. Interestingly, rimonabant is a proconvulsant that has been demonstrated to lower threshold to kainate-induced seizures. Blocking CB1 receptors prevented increased seizure susceptibility in an experimental model of febrile seizures (Chen et al., 2007). Similar results were found in a rat model of PTE in which a single injection of rimonabant reduced long-term hyperexcitability and susceptibility to kainic acid (Echegoyen et al., 2009). Rimonabant administration after LFPI reversed the overexpression of mGluR5 in late-stage brain injury, thereby lengthening latency to PTZ-induced seizures (Wang et al., 2016b). However, these studies are limited by their use of secondary convulsants, such as PTZ and kainic acid, and did not utilize continuous EEG recording. Moreover, a recent report found investigated the therapeutic effects of Δ9-tetrahydrocannabinol on repetitive mild traumatic brain injury and found post-injury administration reduced anxiety, depressive-like behaviors, and mitigated injury-induced deficits in short-term working memory

(Bhatt et al., 2020). More research is needed in this field to fully understand how these compounds may positively or negatively affect recovery outcomes.

Atipamezole, a synthetic α2 adrenergic receptor antagonist, is used mainly in veterinary medicine as it is indicated for the reversal of sedative and analgesic effects of dexmedetomidine and medetomidine in dogs. Treatment with atipamezole reduced PTZ seizure susceptibility at 14 weeks following TBI and improved motor performance but did not prevent the development in spontaneous seizures (Nissinen et al., 2017). Dextromethorphan, typically used as an over-the-counter cough suppressant, has multiple mechanisms of action including acting as a nonselective serotonin reuptake inhibitor, sigma-1 receptor agonist, and also blocks NMDA glutamate receptors at high doses. The dextromethorphan derivative, C-10068, was found to reduce non-convulsive seizure frequency and cumulative seizure duration in a penetrating ballistic-like brain injury model of PTE (Lu et al., 2015). The most efficacious dose of C-10068 also reduced inflammation and reactive microglia accumulation around the lesion site. However, this study saw no improvement in neurobehavioral function and continuous EEG recording was only performed for up to 72 hr post-injury.

Lastly, steroid hormones have been proven to be neuroactive and protective in a variety of CNS disorders (for review see Reddy and Estes, 2016). Neurosteroids regulate the plasticity of synaptic and extrasynaptic $GABA_A$ receptors involved in the pathology of epilepsy. Progesterone is the precursor to allopregnanolone, which acts as a positive allosteric modulator and direct activator of $GABA_A$ receptors to enhance inhibition in the brain. A recent study utilizing the weight-drop model of PTE reported a reduced

duration of PTZ-induced seizures after progesterone treatment (Ghadiri et al., 2019). The behavioral component of seizures was also reduced, suggesting decreased seizure intensity and neuroprotection.

I. 6.11 Epigenetic Interventions: A new frontier?

Epigenetic interventions, such as histone modifiers, represent a novel therapeutic pathway that remains to be fully explored. Global and regional changes in gene expression due to epigenetic modification have been observed after TBI and in epilepsy disorders. TBI is known to increase HDAC activity in the brain, resulting in reduced H4 acetylation and increased seizure susceptibility (Dash et al., 2010; Huang et al., 2012). Reversing hyperacetylation improves motor function and reduces the inflammatory response (Zhang et al., 2008). Furthermore, posttranslational histone modifications, such as histone methylation and acetylation, have also strongly implicated in TBI-induced neuropsychiatric disorders (Sagarkar et al., 2017).

Epigenetic HDAC inhibitor treatments, such as valproic acid, sodium butyrate, and SAHA, have been recently identified as potential disease modifying agents. Valproate has been administered as an anticonvulsant drug for decades, yet its inhibitory effect on HDAC activity was not discovered until 2001 (Gottlicher et al., 2011). Valproate administration reduced neuronal damage, improved cognitive outcomes, and decreased BBB permeability in a CCI model of TBI (Dash et al., 2010). Though experimental and clinical trials using valproate for PTE have not been effective, some of

the observed neuroprotective properties may be linked to this mode of action (Temkin, 2009; Eastman et al., 2010).

Recently, Reddy et al. discovered inhibiting HDAC hyperactivity via sodium butyrate treatment retarded the rate of hippocampal kindling in a model of temporal lobe epilepsy (Reddy et al., 2017). Sodium butyrate treatment also reduced aberrant mossy fiber sprouting in the hilar region of the hippocampus. In addition to blocking a broad spectrum of HDAC enzymes, sodium butyrate is also a known anti-inflammatory agent and shows neuroprotection after stroke (Park and Sohrabji et al., 2016). These data point towards the potential of sodium butyrate as a multifunctional approach to reducing several pathologies associated with epileptogenesis.

In a drug screening study with 870 unique compounds, SAHA was identified as a potential anti-seizure drug with selective inhibition of HDAC1 and HDAC3 proteins (Ibhazehiebo et al., 2018). Downstream activity of SAHA results in increased transcription factors crucial to expression of genes needed to induce cell differentiation. Additionally, recent study concluded that SAHA administration after TBI protected against neuronal injury by reducing oxidative stress and inflammation by inducing the iNOS/Nrf2/ARE pathway (Xu et al., 2018). Mice treated with SAHA exhibited significantly improved grip test scores and reduced water content in the brain compared to untreated mice. SAHA (Vorinostat) is FDA-approved in patients with cutaneous T cell lymphoma, therefore, validating additional indications in the clinical setting will be a much faster and cost-effective process. Currently, an ongoing phase 2 clinical trial is

evaluating the safety and efficacy of SAHA in pediatric patients with drug resistant epilepsy (NCT03894826). Results from this study are forthcoming.

There are many studies which highlight disease modifying effects of experimental treatments on TBI and functional comorbidities (Yun Ng and Lee, 2019), but evidence of an antiepileptogenic effect is rare. Furthermore, many studies investigating epileptogenesis have done so by measuring seizure threshold to chemical convulsant administration after injury. Though this data is valuable, it does not speak towards the agent's effect on development of spontaneous seizures and prevalence of long-term epilepsy.

Traditional management of epilepsies has involved the evaluation of the electroclinical phenotype; however, seizures are a symptom of many different causes. Interventions for PTE require alleviation of seizures through the disruption of underlying maladaptive processes as well as protection against functional and cognitive impairment. Anti-seizure medications are often used for prophylaxis against early TBI-induced seizures but are ineffective at preventing long-term PTE (Wat et al., 2019). Though progress in the field continues to be made, the issue remains as to whether more effective agents will be discovered once the distinct causal processes of PTE are determined, and whether these more precise therapeutics will have a stronger beneficial impact when used earlier in the epileptogenic process.

I. 7 Future Perspectives of the PTE Field

Treating TBI and preventing PTE is a complex and daunting challenge. Heterogenous injury categories, variances in pathologic responses, and difficulty powering both clinical and preclinical trials make this task even more complex. The ultimate goal of epilepsy research is to identify therapeutics that can prevent, interrupt, or reverse the epileptogenic process. Ideally, therapeutic strategies should also relieve PTE-associated comorbidities and improve quality of life. As discussed in this review, such an intervention has yet to be identified; however, the last decade has provided promising data demonstrating disease modifying, anti-inflammatory, and neuroprotective effects suggesting this goal is not unrealistic.

Our understanding of epileptogenesis is continuously evolving as animal models are improved to simulate the human condition. Fluid percussion injury and controlled-cortical impact are the leading models of PTE, and several research groups have implemented continuous EEG recording as the gold standard of epileptiform brain activity. These models represent an excellent paradigm for further elucidating the mechanisms of epileptogenesis and testing novel therapeutic interventions. Furthermore, a new line of imaging and protein biomarkers is emerging, and advances in machine learning EEG analysis will aid in seizure prediction and patient diagnoses.

Table 3: Therapeutic Intervention Studies for PTE.

System/Focus	*Model*	*Species*	*Effect on Epileptiform Activity*	*Disease Modification*	*Ref.*
AEDs					
Carbamazepine	Human condition	Clinical	Not effective for prevention of PTE	N/A	Temkin, 2009
Phenytoin	Human condition	Clinical	Not effective for prevention of PTE	N/A	Temkin, 2009
Phenobarbital	Human condition	Clinical	Not effective for prevention of PTE	N/A	Temkin, 2009
Valproate	Human condition	Clinical	Not effective for prevention of PTE	N/A	Temkin, 2009
Carbamazepine	FPI	Rat	Not effective for prevention of PTE	N/A	Eastman et al., 2010
Valproate	FPI	Rat	Reduced seizure frequency; Reduced cumulative seizure duration	N/A	Eastman et al., 2010
Carisbamate	FPI	Rat	Not effective for prevention of PTE	N/A	Eastman et al., 2011
Gabapentin	Cortical Undercut	Rat	Evoked epileptiform discharges in cortical slices 1d and 14d post-gabapentin	Reduced GFAP expression	Li et al., 2012
Phenytoin	Penetrating Brain Injury	Rat	Reduced incidence, frequency, and duration of nonconvulsive seizures in a dose-dependent manner	No effect on lesion volume or body weight with treatment	Mountney et al., 2013
Ethosuximide	Penetrating Brain Injury	Rat	Reduced incidence, frequency, and duration of nonconvulsive seizures in a dose-dependent manner	No effect on lesion volume or body weight with treatment	Mountney et al., 2013

Table 3
Continued

Levetiracetam	Human condition	Clinical	Trended with lower seizure incidence in clinical patients but never reached significance	N/A	Hazama et al., 2018
Retigabine	CCI	Mouse	Reduced seizure susceptibility; Reduced seizure frequency	Reduced inflammation; Lessened BBB breakdown; Reduced neuro-degeneration	Vigil et al., 2020
Inhibitory/ Excitatory Pathways					
Halothane (anesthetic, GABAA agonist)	FPI	Rat	No seizures occurred while subjects were under anesthesia	N/A	Eastman et al., 2010
Ceftriaxone (Beta-lactam antibiotic and stimulator of GLT1 expression)	FPI	Rat	Reduced cumulative seizure duration	Preserved GLT1 expression	Goodrich et al., 2013
Ceftriaxone (Beta-lactam antibiotic and stimulator of GLT1 expression)	FPI	Rat	Reduced cumulative seizure duration	Preserved cortical inhibitory interneuron function with continuous treatment	Hameed et al., 2018
2-deoxyglucose (glycoylsis inhibitor)	CCI	Mouse	Restored excitatory and inhibitory synaptic activity; Reduced epileptiform activity	Reduced neuro-degeneration of PV+ interneurons	Koenig et al., 2019
Imidizodiazepine KRM-II-81 (selective for alpha2/3 containing GABAAR)	CCI	Mouse	Reduced hyperactivity	N/A	Witkin et al., 2020

Table 3
Continued

Inflammation					
Minozac	CCI	CD1 mice	Reduced seizure susceptbility	Reduced inflammation; Improved cognitive impairments	Chrzaszcz et al., 2010
Kineret (IL-1R antagonist)	CCI	Pediatric mouse	Reduced seizure susceptibility	Improved neuropathology; Improved cognitive impairments	Semple et al., 2017
Monophosphoryl lipid A and Pam3Cys	CCI; Kindling	Rat	Reduced seizure susceptibility; Slowed kindling rate	Reduced TNF-alpha brain levels	Hesam et al., 2018
Glycyrrhizin (HMGB1 inhibitor)	CCI	Pediatric mouse	Not effective for prevention of PTE	Reduced HMGB1 brain levels, edema, and microglial activation	Webster et al., 2019
mTOR pathway					
Rapamycin	CCI	CD1 mouse	Reduced seizure incidence (13% vs 50%); Reduced seizure frequency; Lessened behavioral component of seizures	Reduced neuro-degeneration; Attenuated mossy fiber sprouting	Guo et al., 2013

Table 3
Continued

Rapamycin	CCI	Mouse	Reduced seizure frequency	Reduced neuro-degeneration; Attenuated mossy fiber sprouting; Stabilized neurogenesis	Butler et al., 2015
Rapamycin	CCI	Mouse	Modified synaptic and tonic GABAAR-mediated currents.	N/A	Butler et al., 2016
Plasticity					
BDNF blocker (TrkB-Fc)	Ex vivo Schaffer collateral lesions in organotypic hippocampal slice cultures	Pediatric mouse	Reduced hyper-excitability of CA3 neurons	Attenuate mossy fiber sprouting	Gill et al., 2013
LM22A-4 (partial agonist of TrkB)	Cortical Undercut	Rat	Decreased incidence of epileptiform discharges	Increased parvalbumin immunoreactivity	Gu et al., 2018
PTX BD4-3 (partial agonist of TrkB)	Cortical Undercut	Rat	Reduced PTZ susceptibility.	N/A	Gu et al., 2018
Hypothermia					
Hypothermia	FPI	Rat	Reduced PTZ susceptibility	Attenuate mossy fiber sprouting; Did not exhibit neuroprotective effects on cell loss	Atkins et al., 2010
Hypothermia	FPI	Rat	Abolished ictal activity up to 10 weeks after hypothermia treatment	N/A	D'Ambrosio et al., 2013

Table 3
Continued

Electrical Stimulation					
Deep Brain Stimulation	Human Condition	Clinical	Reduced seizure frequency	N/A	Piacentino et al., 2018
Hyper-phosphorylation of Tau					
Sodium Selenate	FPI	Rat	Increased latency to seizures/epileptiform activity	Ameliorated enlargement of ventricles and hippocampal atrophy	Liu et al., 2016.
Cell Transplant Therapy					
Cell transplantation therapy (GABAergic progenitors from medial gaglionic eminence)	CCI	Mouse	Reduced incidence of PTE	Improved cognitive impairments;	Zhu et al., 2019
Other					
rimonabant CB1R antagonist 1 or 10 mg/kg immediately or 20min after TBI	FPI	Rat	Reduced KA susceptiblity	N/A	Echegoyen et al., 2009
Ketogenic Diet	FPI	Rat	Not effective for prevention of PTE	N/A	Schwartzkroin et al., 2010
Creatine	FPI	Rat	Not effective for prevention of PTE	Reduced oxidative stress markers	Saraiva et al., 2012
Exercise (treadmill)	FPI	Rat	Lengthened latency to seizures; Reduced seizure duration; Reduced PTZ susceptibility	N/A	Silva et al., 2013
C-10068 (Dextromethorphan derivative)	PBBI	Rat	Lengthen latency to seizures; Reduced seizure frequency, Reduced cumulative seizure duration	Reduced inflammation	Lu et al., 2015

Table 3
Continued

Atipamezole, alpha2 adrenergic receptor antagonist	FPI	Rat	Reduced PTZ susceptibility	Improved functional recovery	Nissinen et al., 2017
Creatine supplementation, may be needed longterm; 300mg/kg P.O. 4wks	FPI	Rat	Lengthened latency to seizures; Decreased duration of tonic-clonic seizures; Reduced PTZ-induced epileptiform discharges	Reduced neurodegeneration	Gerbatin et al., 2019

CHAPTER II

AIMS AND OBJECTIVES

The main objective of this dissertation research is to develop an experimental model of PTE that exhibits spontaneous seizures and to utilize this robust model for testing novel epigenetic therapeutic interventions and profiling neuropathological and behavioral indicators associated with TBI and PTE. Since current animal models of posttraumatic epilepsy have largely relied on the induction of seizures using chemoconvulsants, we propose to develop a more translationally relevant mouse model that produces spontaneous recurrent seizures (SRS). Emerging evidence suggests that epigenetic interventions such as HDAC inhibitors may help to retard or prevent epileptogenesis in models of temporal lobe epilepsy. Therefore, this study proposes to investigate alterations in the epigenetic landscape and the role that epigenetic HDAC-based interventions may have on seizure amelioration and recovery outcomes in both young and aged mouse models.

II. 1 Specific Aim 1

The first specific aim of this dissertation is to develop and characterize an experimental model of post-traumatic epilepsy (PTE) with spontaneous seizures in mice.

PTE is one of the few forms of epilepsy that is truly preventable. Therefore, it is imperative that we understand the underlying process of epileptogenesis, or the combination of the secondary restructuring processes and immune responses that transform a normal brain into a hyperexcitable epileptic brain (McNamara et al., 2006).

Epileptogenesis has also been used to refer to the latent period which begins with precipitating event (i.e., TBI), and ends at the occurrence of the first spontaneous seizure (Reddy, 2013). The secondary neurologic damages are often produced by cascades of pathological events including damage to the blood-brain barrier, hypoxia/ischemia, cerebral edema, excitotoxity, free radical oxidative damage, aberrant epigenetic activity, neuroinflammation, and neuronal death (Bullock et al., 1998; Merlo et al., 2014; Raghupathi, 2004). Many of these processes are triggered by the initial injury of a TBI and continue to progress even after the appearance of spontaneous seizures; however, these secondary injuries are thought to be therapeutically reversible and may offer novel targets for improving recovery and preventing PTE. Furthermore, current drug therapies are aimed at symptomatic relief, in that they attempt to inhibit seizures; however, neither effective prophylaxis nor a cure for acquired epilepsy is currently available. With the high prevalence refractory epilepsy, the development of more effective treatments and interventions aimed at stopping the epileptogenic processes are of critical concern.

PTE is a major source of disability following TBI. Many of these seizures are intractable, and therefore, cannot be medically treated with currently available anticonvulsants (Temkin, 2009). Though models of PTE exist, many rely on the induction of seizures through a chemical convulsant agent, rather than through the natural progression of changes that occur during the latent period. In order to truly study this complex phenomena, spontaneous recurrent seizures need to occur. Therefore, we suggest some modifications to the current models of PTE to ensure spontaneous seizures

occur over time; additionally, this study will characterize the acute and chronic behavioral and biometric changes that occur after a TBI.

II. 2 Specific Aim 2

The second specific aim investigates the therapeutic potential of dietary epigenetic HDAC inhibition on the development of PTE and associated comorbidities in mice, using sodium butyrate as the compound of choice.

Epigenetics refers to the study of cell specific, plastic changes caused by an alteration in gene expression through modifications such as DNA or histone acetylation, methylation, and phosphorylation. These epigenetic changes lead to chromatin remodeling and play a role in regulating a number of DNA/RNA-mediated processes including transcription, translation, repair, and DNA replication without directly altering the genetic code. Aberrant epigenetic processes have been implicated as critical drivers in a number of diseases such as TBI (Zhang et al., 2008; Gao et al., 2006), Huntington's disease (Haiqun et al., 2016; Chopra et al., 2016), neurodevelopmental disorders (Angelova et al., 2018), and a myriad of cancers (Nebbioso et al., 2018). Post-translational acetylation of histones is determined by opposing activities of two classes of enzymes: histone acetyltransferases (HATs), which add acetyl groups to either histone tails or DNA, and histone deacetylases (HDACs) which remove them. Reports have shown a decrease in hippocampal histone H3 acetylation after TBI; these effects were attributed to upstream stress and excitotoxic cascades, which are associated with the induced trauma (Gao et al., 2006). TBI leads to an increase in blood brain barrier

permeability and early inflammatory cytokine responses by resident microglia and peripheral immune cells (Schmidt and Grady, 1993). Preclinical trials investigating dose-response treatments of HDAC inhibitor compounds have demonstrated some relief of inflammation or neuroprotective effects following injury (Kozikowski et al., 2007; Zhang et al, 2008). These studies demonstrate the potential of HDAC inhibitor compounds as therapeutic interventions that may help to reduce negative recovery outcomes and risk of comorbidities.

Plastic changes in the epigenome throughout life are responsible for not only controlling normal development, homeostasis, and aging, but also for regulating responses to injury and environmental stimuli. The role of epigenetics in the pathophysiology of TBI has emerged somewhat recently, providing scientific researchers with novel targets for intervention, including the inhibition of HDAC enzymes. Initial reports show a post-injury decrease in H3 and H4 acetylation within the ipsilateral hippocampus following TBI (Zhang et al., 2008). HDAC inhibition, in both neurological and peripheral disorders, has shown to reduce cell death and demonstrate neuroprotection (Soriano et al., 2009). The main goal of this aim is to determine the therapeutic effect of epigenetic modification in acute and chronic recovery following TBI as well as its effect on epileptogenesis.

II. 3 Specific Aim 3

The final aim seeks to identify whether broad- or narrow-spectrum HDAC inhibitors are optimal in interrupting the epileptogenic consequences of TBI, such as spontaneous seizures, in mice.

To identify the protective potential of HDAC inhibition, various HDAC inhibitor agents (including sodium butyrate, vorinostat, romidepsin, panobinostat, entinostat, SBHA, and givinostat) will be administered in varying dosages 20-min prior to corneal 6-Hz stimulation and/or hippocampus kindling stimulation to produce a drug-response curve. Effectiveness of treatment will be determined by percent inhibition of behavioral seizures and electrographic parameters. These data will provide insight on the pharmacological class actions of broad- and limited-spectrum HDAC inhibitors. Leading drug candidates of broad- or limited-spectrum HDAC inhibitors will be further tested in the context of PTE development for reduction in epilepsy incidence as well as motor recovery. Additionally, we intend to determine the reversal potential of selected HDAC inhibitors on the persistence of SRS in mice with active PTE with spontaneous seizures.

We hope to provide a molecular evidence of epigenetic alteration and mechanism in this process of epileptogenesis. Inflammation and cell death are considered as critical maladaptive processes in epileptogenesis. We will focus on inflammation and cell death, which are hallmark characteristics of secondary injury following TBI, suggesting that risk PTE can be reduced if these processes are interrupted. We anticipate increases in proinflammatory cytokines as well as increased caspase activity following injury. We also test HDAC inhibition by sodium butyrate or vorinostat and confirm the above

mechanistic cascades in PTE development. The proposed PTE model will be useful for uncovering the therapeutic potential of epigenetic targets after TBI.

The main objective of this aim is to identify an optimum (broad- vs limited-spectrum) lead candidate for maximal inhibition of development of PTE, behavior deficits, and long-term neuropathology. One lead drug will be rigorously evaluated in additional PTE models. Finally, molecular mechanistic studies will be performed to determine downstream (e.g., caspase and/or cytokine) targets involved in the protective effect of HDAC inhibition in the brain. The study will focus on the functional role epigenetic modulation in the context of TBI and epileptogenesis. TBI injuries are often characterized into stages: initial and secondary. The initial injury is caused by the direct blow to the head or from extreme acceleration/deceleration. Secondary injury measures include inflammation, oxidative stress, disruption of the blood brain barrier, excitotoxicity, cell death, and mitochondrial dysfunction. Previous studies report that neuronal damage and inflammation caused by initial injury can be further exacerbated by chronic secondary measures and increase risk of PTE. In this aim, we will explore inflammation and cell death cascades in the context of TBI. We will also evaluate the role of HDAC inhibition on these pathways to determine the role of epigenetic modulation after a TBI. Finally, we hope to confirm possible mechanisms of HDAC inhibition therapy using both acute and chronic models of epileptogenesis.

CHAPTER III

MATERIALS AND METHODS

III. 1 Experimental Animals

Wildtype (WT) adult female C57BL/6 mice, 25 to 35g each were used in this study. All strains were maintained on a hybrid C57BL/6-129SV background. All mice were housed 1-4 to a cage with access to food and water *ad libitum*. The mice were housed in an environmentally controlled animal facility with a 12 h light/dark cycle. The animals were cared for in strict compliance with the guidelines outlined in the National Institutes of Health *Guide for the Care and Use of Laboratory Animals*. Animal procedures were performed in a protocol approved by the university's Institutional Animal Care and Use Committee.

III. 2 Surgical Techniques and Recovery

On the day of surgery, animals were weighed then anesthetized with a mixture of ketamine and xylazine (ketamine-100mg/kg; xylazine-10mg/kg) and mounted on a stereotaxic frame. A vertical incision was made between the ears to expose the skull. Sham animals received a 4.5mm cranioplasty over the left hippocampus. TBI animals received a 4.5mm cranioplasty over the left hippocampus followed by a controlled cortical injury at a velocity of 4.0m/s using a 3mm diameter rounded-tip impactor (Hatteras Instruments, Cary, NC). The depth of the TBI injury was either 1 mm or 2 mm, depending on the cohort of animals. The removed skull was replaced with a custom-

made domed polypropylene cap with a base diameter of 5.5 mm. Additionally, animals were implanted with a deep-hippocampal electrode in the contralateral hippocampus for EEG recording (2.9mm posterior, 3.0mm lateral, and 3.0mm below dura) which was secured to the skull with dental acrylic and small anchor screws (P1 Technologies, Roanoke, VA). Two wired anchor screws also served additional purposes, one as a surface electrode in the ipsilateral cortex (anterior to impact), and the second as an electrical ground (placed posterior to lambda). We determined a mandatory recovery period of 10 days was required to increase survivability after severe TBI impacts. Therefore, following the 10-day recovery, mice were single-housed in the vivarium for tethered 24/7 EEG-video recording and could still freely move about their cage.

It should be noted that additional cohorts of non-implanted animals were generated to observe the changes in seizure threshold using the 6-Hz model of seizure threshold testing or increase sample sizes for behavioral testing. The surgeries were identical to their implanted counterparts, except for the lack of electrode in the contralateral hippocampus.

III. 3 EEG-recording and Seizure Analysis

After the mandatory recovery period, animals were single-housed and freely moving with 24/7 EEG-video monitoring for up to 120 days (Grass-Astromed, Warwick, RI; Plastics One, Roanoke, VA). EEG signals were recorded using Axoscope/pCLAMP software connected to Grass Technologies P511 AC Preamplifiers and filtered through Digidata 1322A for noise reduction. Sampling was set to 2 KHz. Identification of seizure

events was performed using a customized Matlab analysis program designed to detect rapid increases in spike amplitude and specific wave patterns. Seizures were defined as events that lasted between 10 and 90 seconds, where the amplitude and frequency of the spikes were at least doubled from each animal's respective baseline. Discharge events were defined as a minimum of 200% increase in spike amplitude and frequency over baseline for 3–9 seconds. Further confirmation of seizure events was performed manually. Our MATLAB code consistently produced a false positive and false negative score of approximately 5% (FP = 4.57%, FN = 4.86%). Both seizure and discharge events were also confirmed by power spectral analysis in which the power threshold exceeded 5 dB.

Throughout this manuscript, we describe discharges as non-convulsive non-motor epileptiform activity since the likelihood of a motor component during this short time is low. Recordings began on day 10 post-TBI to allow animals to fully recover, as we observed animals would have a greater risk of premature death if EEG recordings were started any earlier. Discharges were accounted for starting with the first days of EEG monitoring. Incidence of epilepsy was determined only if the recorded mouse exhibited both spontaneous seizures and epileptiform discharges; discharge activity alone suggests hyperactivity of circuitry, but it was not considered sufficient to diagnose subjects with PTE. The video component of our EEG analysis protocol was recorded using security cameras with 1080p HD digital security cameras with infrared LEDs for night vision.

To evaluate high-frequency oscillations (HFOs) such as ripples (HFO-R) and fast ripples (HFO-FR), raw EEG files were bandpass-filtered through the 80-200 Hz for HFO-R and 250-500 Hz (HFO-FR) ranges using a finite impulse response filter. Filtered EEG recordings were normalized using their own average mean values. A minimum of three consecutive cycles three standard deviations from the mean in the frequency band was selected as the *a* priori criteria required to be considered a viable HFO candidate. Potential events that overlapped in time were removed to avoid false detections from using bandpass filtering in higher frequency ranges, as cited in previous publications (Benar et al., 2010). Since mice are nocturnal organisms, we evaluated the average frequency of ripples and fast ripples of TBI mice against Sham mice in 10 min epochs during each animals' respective high points in activity, which typically occurred around 8:00am and 8:00pm. This analysis was extended through the 120D observation period.

III. 4 6-Hz Seizure Threshold Testing

The 6-Hz model of partial seizures was used to determine seizure thresholds following CCI-induced TBI according to a previously described protocol (Barton et al., 2001; Reddy et al., 2015). Mice were stimulated with a constant-current device delivered via corneal stimulation for 0.2 ms-duration monopolar rectangular pulses at 6-Hz for 3 seconds (World Precision Instruments, Sarasota, FL). 1 week before TBI or sham injury, baseline seizure threshold was determined by administering different current intensities in the range of 5 to 45 mA to groups of animals. Current intensity at 35 mA was determined to elicit seizures in 100% of selected mice, similar to our previous reports

(Reddy et al., 2015). Selected mice were randomly placed into either TBI or sham groups and respective surgeries were induced. Following sham or injury operations, seizure thresholds were assessed at various time points by eliciting different current intensities in the range of 5 to 45 mA until seizure behavior was evoked. Ocular anesthetic (0.5% tetracaine) was administered as an anti-pruritic to the corneas 10 min before stimulations. Immediately prior to stimulation, the corneal electrodes were wetted with 0.9% saline solution. Mice were manually restrained during the 6 Hz stimulation, and they were then immediately released into an observation chamber. Seizures were scored immediately by direct observation by a blinded investigator. Signs of seizures include stunned posture and eye blinking, head nodding, straub tail as well as repetitive rhythmic movements such as chewing, forelimb clonus, running, and cage jumping. At least 15 min were given between stimulations of increasing current intensities if seizure behavior was not elicited. Seizures elicited by 6-Hz typically last between 8 – 90 s, and normal exploratory behavior is resumed within seconds of seizure end.

III. 5 Tissue Collection and Immunohistochemistry

For immunohistochemistry, mice were anesthetized with ketamine-xylazine mixture and transcardially perfused at either 1 day, 3 days, 7 days, 30 days, 60 days, or 120 days post-TBI with 4% paraformaldehyde solution (Fischer Scientific) in sodium phosphate buffer (pH 7.4). Brains were carefully removed from each animal and post-fixed in 4% paraformaldehyde for 16 h at 4° then treated with sodium phosphate buffer for 24 h. Brain tissues were next treated with 10, 20, and 30% sucrose solution for 72 h

each and then rapidly frozen with O.C.T. compound (Sakura Finetek, CA, USA) on dry ice (Kuruba et al., 2011). Serial sections (20μm thick) were cut coronally through the mouse forebrain containing the hippocampus and amygdala, approximately from bregma -1.15 mm to -3.75 mm (Paxinos and Watson, 2007). Serial sections were saved in 24-well plates filled with sodium phosphate buffer.

Sections were taken every 300-μm and processed for Nissl bodies (cresyl violet; CV), neuronal nuclei antigen (NeuN), parvalbumin (PV), glial fibrillary acidic protein (GFAP), ionized calcium binding adapter molecule-1 (IBA-1), and doublecortin (DCX)-immunoreactivity. Post-sectioning measurements revealed little variability in slice thickness. For mossy fiber sprouting, Timm staining was conducted as described previously using a sub-set of the corresponding TBI and sham cohorts (Cavazos et al., 1991; Rao et al., 2006).

Table 4: List of Primary Antibodies.

Antigen	Host	Clonality	Dilution	Supplier	Cat No.
NeuN	guinea pig	polyclonal	1:1000	Millipore	ABN90P
PV	mouse	polyclonal	1:2000	Sigma-Aldrich	P3088
DCX	mouse	monoclonal	1:250	Santa Cruz	SC390645
GFAP	rabbit	polyclonal	1:1000	Dako	GA524
IBA1	rabbit	polyclonal	1:400	Wako Chemicals	01919741
FJB	mouse	cytochemical	0.001%	Histochem, AR	#1FJB
Timm	mouse	cytochemical	see manual	FD Neurotech	PK701

III. 6 Stereological Quantification of Cell Sub-Types

To determine the extent of neurodegeneration after severe TBI, we used an optimized neurostereology protocol, which has been previously described in detail (Golub et al., 2015). Briefly, our stereology system consists of an Olympus BX53 microscope fixed with a DP73 digital color camera (Model: DP73-1-51-, Olympus, Tokyo, Japan), a motorized stage (Model: H101ANNI, Prior Scientific, Rockland, MA, USA) and a universal microscope automation controller with encoder (Model: 500-H3XYZEF, ProScan III, Prior Scientific, Rockland, MA, USA). High resolution images of the whole brain slices were taken using a 1.25x lens objective. Regions of the hippocampus (CA1, CA2, CA3, DG, DH) were delineated separately using the newCAST software (Version: VIS4.6.1.630, Visiopharm, Denmark). Volume of each region of interest was calculated first using the 10x objective, then cell density was counted using a 60x oil immersion objective. Additionally, ipsilateral lesion volume was calculated using the same volume estimation technique. Images for manuscript figures were captured using the same bright field microscopy techniques.

III. 7 Densitometric Analysis of Immunohistochemistry Markers

To determine the extent of inflammation, an area fractionation method was used to quantify the ratio of cells to background in hippocampal regions of the dentate gyrus (DG), CA1, CA3, as well as the amygdala (AMY). Images of the regions of interest were acquired using the Olympus microscope system and 20x objective. All images were captured using uniform settings and no alteration was performed on the images

before analysis. Densitometry of astrocytes and microglia was quantified using NIH ImageJ software to calculate the percentage area of GFAP or IBA-1 stained cells in relation to the total area for the entire slice. Color threshold settings were kept constant for all sections and background interference was eliminated by only counting cells larger than 300 pixels. Neuroinflammation was compared between naïve control and TBI cohorts. Mossy Fiber density was measured using the same Densitometric methodology described as above. Images were acquired using the Olympus BX51 microscope and camera with a 10x objective. A total of 6 images containing the hippocampal regions of the DG and DH were acquired from each animal with uniform settings. The averages were calculated for each animal before statistical analysis was performed between groups.

III. 8 Behavioral Examination and Testing

Mice were placed in the testing room for 1-2 h prior to the initiation of each training or testing session. All behavior tests were performed in a quiet room under normal fluorescent lighting. Between each subsequent mouse, the equipment was cleaned with 75% ethanol and allowed to dry.

III. 8.1 Body Weights and Health Score

Records of individual body weights for all mice were taken throughout the length of the study. Body weight is a sensitive indicator of overall health and disease

progression. Since body weights can vary throughout the course of a day, body weights were taken around the same time at each time point.

To better evaluate initial recovery from injury as well as disease progression, we incorporated a health scale evaluation. Mice were scored for the following out a total of 16 points: alertness and normal activity (0-1), grooming behavior (0-1), skin/coat condition (0-3), cleanliness and health of eyes (0-2 for each eye), lack of kyphosis (0-2), weight support (0-3), posture while sitting or walking (0-2). Lower scores were considered abnormal or severely impaired. Typical impairments seen throughout recovery were lack of grooming, milky-white discharge or swelling of the eyes, kyphosis, inability to support weight, and a strong lean toward the uninjured side.

III. 8.2 Neuroscore

Neurological motor function was assessed using a composite of seven 4-point tests for a maximum score of 28 points. Mice were scored from 4 (normal) to 0 (severely impaired) for: resistance to left or right propulsion by push, forelimb and hind limb flexion during tail suspension, hind limb flexion with front paws touching a surface, observation of gait and weight support while walking on a flat surface, and a 60 sec grip test on inverted grid.

III. 8.3 Beam Walk

Performance on a narrow balance beam is a useful measurement for detecting impairments in fine motor coordination and balance. The elevated beam apparatus measures 1 meter in length with a flat surface width of 3 cm standing 60 cm from the

floor. Mice were placed on one end of the beam and given a total of 60 sec to reach their home cage at the opposite goal. At the start position, a bright lamp was used as an aversion stimulus. Performance on the beam walk was measured as the amount of time (sec) taken to traverse the beam as well as the number of foot faults while walking. In this study, calculations are based off of an average of 3 tests per time-point.

III. 8.4 Rotarod

As an additional assessment of motor function and coordination, mice were evaluated using a rotarod apparatus (IITC Life Science Instrument) for 60 sec at a fixed speed of 5 rpm. The latency to fall from the rotating rod was recorded. Calculations are based off an average of 3 tests per time-point. Naïve mice are typically able to complete the rotarod assessment for the full-time allotment without falling; therefore, falling from the rotating rod before 60 s is interpreted as motor coordination or balance impairment.

III. 8.5 Elevated Plus Maze

Mice were evaluated for anxiety-like behaviors using the elevated plus maze (EPM) test, a sensitive behavioral assay that exploits the natural conflict between exploration of a novel area versus rodent aversion to open areas and height (Lister, 1987; Kulkarni and Reddy, 1996). The EPM apparatus was constructed of two closed arms (32.5 x 10 cm) and two open arms (32.5 x 10cm) elevated to a height of 25cm from the floor. The testing period was 5 minutes long and began when each mouse was placed in the center of the plus maze facing an open arm. Arm entry was recorded when the entire

head and two front paws entered into an arm. In the present study, we calculated the percent of open arm entries with respect to the total number of arm entries within the 5 min testing period. We also measured the percentage of time mice spent on open arms compared to closed arms. Decreased number of open arm entries as well as a decreased percent of time spent on open arms is interpreted as an anxiogenic behavior.

III. 8.6 Open Field

Open field exploits the natural conflict exhibited by rodents between their natural tendency to explore novel areas and their aversion to open spaces where they would be vulnerable to predation and danger. The open field arena is constructed of a 60 cm x 60 cm wooden square base surrounded by clear plexiglass measured 50 cm in height. The central area of the arena consisted of a 30 cm x 30 cm square, lightly outlined on the base. The area of the maze within 15 cm from the walls was considered as “peripheral”. Mice were placed in the center of the arena and observed for 5 min. Mice were allowed to freely explore the arena and were measured for entries to the center area as well as time spent in the center. Total center entries provide estimates of overall locomotor activity. Animals will typically spend more time in the perimeter, rather than the central area. Decreased locomotor activity and entries/exits from the center are interpreted as more anxiogenic behaviors.

III. 8.7 Novel object recognition test

The novel object recognition test (NORT) was used to evaluate recognition memory and assess cognitive functionality after sham or TBI injury. The same open field arena (described above) was used as the testing apparatus. NORT consists of three phases: habituation, training, and retention. During the habituation phase, animals are placed in the open field arena and allowed to freely explore for 5 min without any objects present. The next day, animals are placed back into the open field arena with two identical objects located in opposite corners of the open field space for 10 min (training phase). During the retention phase, one of the identical objects is switched with a novel object and mice are again placed in the middle of the open field to explore for 5 min. The time spent investigating the old and novel objects are recorded during this time, and a discrimination index (DI) is calculated (DI = [(time spent exploring novel object – time spent exploring old object)/total time spent exploring both objects] x 100).

III. 8.8 Burrowing test

The burrowing test was conducted at 4-months post-injury in the mouse's home cage. Each burrowing tube (dimensions) was placed in the corner opposite the nest in the cage. Burrowing tubes were filled with 50 g of novel wood chips for 2 hours. The weight of displaced wood chips was measured at the end of the session.

III. 8.9 Morris Water-maze test

The Morris water-maze (MWM) was used to detect spatial learning impairments in all animal groups at 4 months post-TBI or post-sham. The swimming pool was located in a large room with cues visible to the mice around the walls of the pool or room, presumably to be used by the mice for spatial orientation. The position of the cues remained unchanged throughout the experiments. Data collection was automated by the Noldus Ethovision XT system. The pool consisted of a circular apparatus of 76 cm diameter, which was subdivided into four equal quadrants. Mice were given four learning days with six trials each day. At the start of each trial, the mouse was placed at one of the six fixed starting points, facing a wall (designated as North, West, East, South, Northwest, Northeast, or Southwest). The mice had 60 seconds to swim and find the platform, which was located in the southeastern quadrant 2mm below the surface of the water. If the animal found the platform, it remained on the platform for 15 seconds. If the mouse failed to find the platform within the 60 second timeframe, the trial was terminated and a maximum score of 60 was assigned to the trial. The mouse would be then guided to the platform location and allowed to remain on the platform for 15 seconds before exiting the pool. Twenty-four hours following the final learning trial, the platform was removed from the pool and the mice were given 60 seconds to swim. Time spent searching in the target quadrant was calculated. A second probe trial was conducted 5 days following the last learning trial to determine long-term memory retrieval.

III. 9 Statistical Analysis

All experiments were randomized and performed by blinded investigators. All data are presented as mean ± SEM. Statistical tests were performed using the Macrocal Origin 8 software (OriginLab Corporation, Northamptom, MA). One-way ANOVA was performed to determine if any significances could be seen between groups. Independent t-tests were used to determine which groups were significantly different. Nonparametric outcomes, such as mortality rate, incidence of epilepsy, and completion of the beam walk behavioral test, were compared between groups using the Kruskal-Wallis U-test or the two-proportion z-test. Post hoc analysis was also conducted using Macrocal Origin 8 software, including Bonferroni and Tukey Honestly Significant Difference when appropriate. No data were excluded from analysis. Sample sizes were determined based on a priori power analyses and previous TBI studies (Reddy et al., 2018; Zhu et al., 2019). In all statistical tests, statistically significant differences were set at $*p < 0.05$.

CHAPTER IV

RESULTS

IV. 1 Contusion Brain Damage in Mice for Modelling of Post-Traumatic Epilepsy with Contralateral Hippocampus Sclerosis

Traumatic brain injury (TBI) is a complex condition that includes varying degrees of contusion, hemorrhage, and tissue damage, as well as an increased risk of developing post-traumatic epilepsy (PTE), a chronic brain condition with spontaneous recurrent seizures (SRS). An estimated 2.87 million people experience a TBI each year and over 280,000 victims are hospitalized due to a TBI in USA (Faul et al., 2010). About 5 million people in the US are living with a TBI-related disability (Finkelstein et al., 2006); however, that number may be grossly underestimated since many mild TBI cases go unreported or untreated in the clinic. PTE accounts for 10-20% of symptomatic epilepsy and a common cause of disability from intractable seizures in military members and civilians (Christensen et al., 2009; Raymont et al., 2010). Severity of injury is the main risk factor in determining development of long-term seizures, though occurrence of early seizures can greatly increase a patient's risk of PTE. Incidence of PTE ranges from 2-17% following TBI (Mahler et al., 2015; Annegers et al., 1998), however, studies in military populations have reported consistently higher rates over civilian studies. About 50% of Vietnam veterans who experienced TBI developed epilepsy within one year (Salazar et al., 1985). In a recent longitudinal analysis of patients with moderate-severe TBI, 46% of patients developed PTE within 2 years post-injury (Tubi et al., 2019). There

is currently no effective drug therapy for protecting or preventing PTE. Cases of PTE are of particular concern, since these chronic seizures are often refractory to currently available antiepileptic drugs. Acute or immediate seizures following initial injury are treated with symptomatic anti-epileptics, but these drugs are ineffective at preventing development of long-term PTE (Marion et al., 1999; Schierhout and Roberts, 2001; Clossen and Reddy, 2017).

The molecular mechanisms underlying the development of PTE are unclear. Animal models of TBI have been used for decades to better understand how the underlying mechanisms of brain injury can trigger PTE. The controlled cortical injury (CCI), fluid percussion injury (FPI), and weight-drop models are the most used rodent models of TBI (Ostergard et al., 2016). There are advantages to each of these models. The commonly used CCI probes at the complex pathophysiology of the disease and attempts to mimic the conditions of blunt-force human injury. Even with use of these models, few studies have been able to demonstrate the occurrence of SRS, and the incidence of seizures is extremely low and highly variable, ranging from 0-50% (Kharatishvili et al., 2006; Bolkvadze and Pitkanen, 2012; Shandra and Robel, 2020). One of the hallmark features of PTE is the presence of a latent period between the initial injury and onset of SRS. This window of time is a natural plasticity−recovery period and it represents the opportunity to prevent or mitigate epileptogenesis from occurring. The secondary neurological damages are often produced by cascades of pathological events including neuroinflammation, neurodegeneration, excitotoxicity, hyperexcitability, damage to the blood-brain barrier, and reduced neurogenesis (Pitkanen et al., 2012).

Previous research on PTE models has shown limited aspect of epileptogenesis after injury, especially how it relates to the extending damage to the contralateral hemisphere and functional circuitry. Small animal models that recapitulate consistent SRS, an essential feature of PTE, are urgently needed.

Here we demonstrate an advanced mouse PTE model with consistent long-term SRS and neuropathology reminiscent of human TBI. We conducted a vast array of studies to fully characterize: (a) the latency, frequency, and duration of epileptic seizure activity after an impact TBI; (b) progressive motor, behavior and cognitive comorbidity; and (c) progressive neuropathological changes associated with PTE. These studies were done with a moderate (1mm) and severe (2mm) brain injury using the gold-standard 24/7 video-EEG technique for 4 months. Furthermore, this study focuses both on comparisons of depth, but also on non-injured vs injured tissues, thereby providing a more inclusive perspective of the whole brain.

IV. 1.1 Assessment of Severe and Moderate Controlled Cortical Impact Injuries

To study the impact of injury severity on the development of spontaneous seizures, we assessed two different impact depths –1mm (moderate) and 2mm (severe) in adult male mice. To deliver the brain injury, we used the CCI model, a widely used model of human TBI (Nilsson et al., 1994; Guo et al., 2013; Hunt et al., 2009, 2010). We have set up a computer-controlled Precision Cortical Impact Device for CCI, in which the impact is delivered through a small craniotomy. This model simulates the TBI experienced during blunt-head injuries on the battlefield, or in vehicular accidents or

falls. A 1 mm impact depth is the most frequently used protocol to study PTE; however, this model often results in low incidence of spontaneous seizures (Hunt et al., 2009, 2010; Kochanek et al., 2006). Therefore, we also used a 2 mm impact depth to increase the robustness of spontaneous recurrent seizure (SRS) development, as an end-goal of the PTE model. A 2 mm impact in a mouse would land at the dentate hilus at the dorsal portion of the hippocampus and hit the most superior portion of CA1 in the ventral hippocampus, generating a severe TBI.

Mice underwent either a 1 mm or 2 mm impact depth by CCI, designated as a moderate and severe injury model. Within the 1 mm cohort, acute mortality (immediate to 14 days post-injury) was 0%, whereas the severe 2 mm TBI cohort mortality was 28%. One additional mortality occurred in the 2 mm cohort at day 100 post-injury (100d). Upon post-mortem assessment of video-EEG on 100d, the mouse was determined to have experienced a fatal seizure. Previous behavioral evaluations of this subject were within the average range of its cohort for all time-points leading up to the seizure event. A sham cohort underwent identical surgical procedures, receiving a cranioplasty but no impact; these mice were used as controls for this experiment. All mice were recorded by 24/7 video-EEG analysis for up to 4 months, starting after the recovery period of 10 days. During the study, animals would be periodically removed from EEG recording to gather sensory-motor and functional data. At 4 months post-injury, animals were perfused for chronic histology assessment. Sham animals did not exhibit any seizure-like behaviors or altered EEG activity. Additional sub-sets of non-

EEG implanted sham and TBI mice were created for 6 Hz corneal seizure threshold testing as well as for histology assessment at 1d, 3d, 7d, 30d, and 60d post-TBI.

IV. 1.2 Traumatic Brain Injury Leads to Chronic PTE with Spontaneous Seizures

We first tested whether TBI leads to long-term epileptic state with spontaneous recurrent motor seizures. It is well-known that severity of initial injury correlates with the risk of seizure development after TBI (Annegers et al., 1998). Previous studies of brain contusion and concussion have recapitulated much of the biomechanics, pathology, and neurological deficits often seen with TBI (Hall et al., 2005, 2008; Yang et al., 2010); however, many of these models are lacking the SRS necessary for investigating the development of PTE. One of the favored protocols of PTE in mice is a CCI-induced TBI with an impact depth of 1 mm, which has been performed as both open and closed skull models. These studies have recorded seizure incidences between 0-40%, with most studies showing 25-35% epilepsy in mice (Kochanek et al., 2006; Hunt et al., 2009, 2010; Szu et al., 2020). To increase our understanding of epileptogenesis, the animal models we use require the occurrence of at least one unprovoked seizure with increased risk of consequent ictal events. However, to generate statistically high-powered cohorts for therapeutic studies, higher baseline incidence of SRS is needed.

To characterize TBI-induced PTE development, animals were recorded through 24/7 video-EEG system for 4 months by a depth electrode placed within the contralateral hippocampus. Seizures were defined as hyperactive ictal states lasting between 10-90 s in which the amplitude and frequency of the spiking activity was at least 200% the

animal's respective baseline. We observed both generalized motor seizures and non-convulsive seizure activity as early as 21-days post-injury. Seizures sometimes occurred within clusters and were followed by a postictal depressive state. Behavioral responses, when present, included twitching, shaking, forelimb clonus, straub tail, and rearing. **Fig. 4** presents a high-quality example of seizure activity as a raw EEG, power spectral analysis, and raster plot. Seizures developed in both TBI cohorts, with an incidence of epilepsy in 33.33% of 1 mm depth mice and 86.67% of 2 mm depth mice.

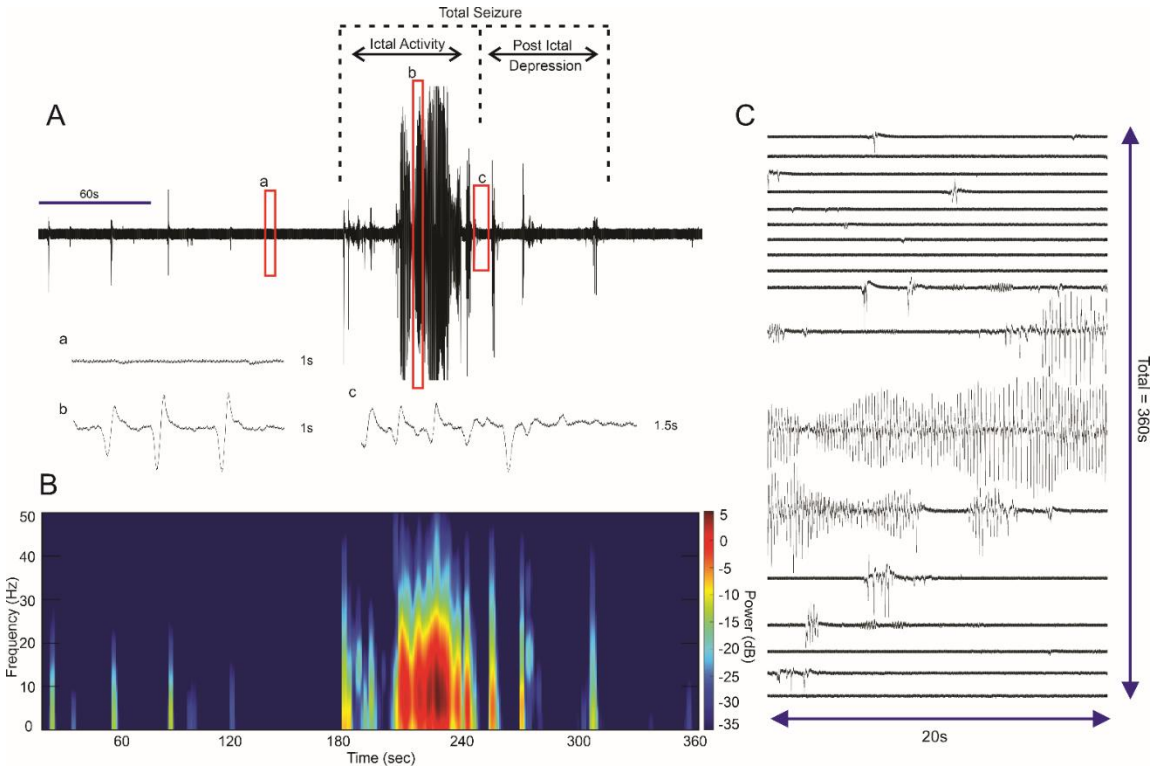

Figure 4: Characteristics of TBI-Induced Seizures.

A, Spontaneous seizure observed in chronically epileptic mouse following severe 2 mm CCI. EEG was recorded from deep electrode placed in the contralateral hippocampus. Sections of this seizure (either 1 s or 1.5 s) have been expanded to demonstrate the quiet baseline (a), ictal activity (b), and termination (c) of the seizure event. The seizure was followed by a postictal depression and return to baseline, as expected. Total trace equals 360 seconds, whereas the seizure and postictal depression lasted approximately 70 s. **B,** Power spectral analysis of full EEG trace represented in *A*. Greater power (db) implicates higher activity levels, which are concentrated towards the center of ictus. **C,** Raster plot of the EEG depicted in *A*. Each line = 20 s of EEG, for a total of 360 s.

SRS peaked within the first two months for the 1 mm cohort but continued well into the 4-month analysis period. Seizures in the 2 mm cohort developed progressively, with a noted increase in frequency of seizures during weeks 11-14 (77-98 days post-injury). This increase in seizure frequency is most likely due to a longer latency period in a few responders who did not show SRS output until 84d-112d. Average seizures per day per animal ranged in both cohorts for all responding animals, though average seizure frequency was lower in the lesser impact group (1 mm seizures/day = 0 - 2.74; 2 mm seizures/day = 0 – 4.17) (**Fig. 5A-D)**. Representative EEG traces with power spectra analysis from Sham, 1 mm, and 2 mm cohorts showing significant differences in spiking amplitude and frequency can be found in **Fig. 5C.** Since this study was conducted in two consecutive cohorts, take note that some animals were recorded for up to 90 days post-injury and others up to 120 days post-injury. Both 2mm TBI cohorts are presented together in **Fig. 5** as no significant differences were found between their EEG output, histology, or behavioral data. Interestingly, mice with a lesser impact showed a shorter latency period and more frequent seizures compared the more severe impact group (1 mm latency = 19.5 ± 2.96 days, 2 mm latency = 52.9 ± 7.66 days; 1 mm cumulative seizures/animal = 84 ± 15.9, 2 mm cumulative seizures/animal = 46.77 ± 12.03) (**Fig. 5E and F**). The overall average duration of seizures was very similar between cohorts, though we observed higher variation in both seizure duration and severity within the 2 mm cohort, as determined through quality checks from EEG traces (1 mm = 39 ± 2 s; 2 mm = 40.5 ± 6 s) (**Fig. 5G)**. Together, our data show a graded response to TBI injury severity. Though both groups developed spontaneous seizures, the 2mm cohort

displayed a more progressive response and higher incidence of chronic epilepsy. These changes in seizure susceptibility address the latent period of epileptogenesis seen in the human response to TBI. With the current definition of epileptogenesis as a continuous and prolonged response that includes mechanisms of generating SRS even after the diagnosis of epilepsy, we expect this model fulfills the requirements of a practical PTE model in mice. Thus, induction of moderate or severe TBI in mice is associated with chronic PTE state with robust occurrence of SRS for at least 4 months post-injury.

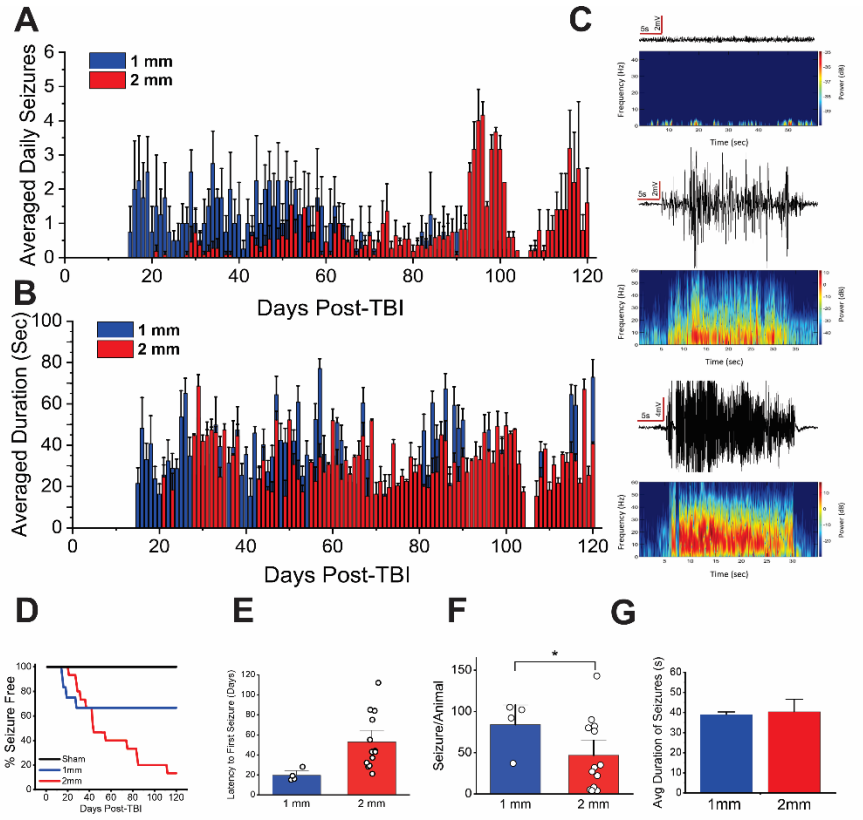

Figure 5: Traumatic Brain Injury Produces Chronic Spontaneous Recurrent Seizures (SRS) in mice.

A, Average seizures per day per animal over 120-day observation period for both moderate (1mm) and severe (2mm) TBI cohorts. Following two-week recovery period from CCI, mice were hooked to 24/7 Video-EEG recording. Seizures were identified through a custom MatLab algorithm. Only responding animals were used for calculations (2mm-TBI: n=13, 1mm-TBI: n = 4). **B,** Average duration of seizures per day over 120 days. All seizure events on each day from responding mice (2mm-TBI: n=13, 1mm-TBI: n = 4) were used in calculations. **C,** Representative seizure, or baseline EEG traces (above) and corresponding power spectral analysis (below) for Sham, 1mm, and 2mm TBI cohorts. **D,** Incidence curve of epileptic animals over time, showing latency to first spontaneous recurrent seizure (SRS) (Sample sizes: Sham = 10; 2mm-TBI = 15; 1mm-TBI = 12) **E,** Average latency to first SRS in 1mm and 2mm TBI cohorts. (Sample sizes: 2mm-TBI = 13; 1mm-TBI = 4). **F,** Average cumulative number of seizures per animal. (Sample sizes: 2mm-TBI = 13; 1mm-TBI = 4). **G,** Average duration of seizures. All seizure events from responding mice (2mm-TBI: n=13, 1mm-TBI: n = 4) were used in calculations.

IV. 1.3 Reduced Seizure Threshold Coincides with PTE Development

To examine the seizure threshold properties, we investigated the progressive changes in seizure threshold in PTE mice. Since we observed spontaneous seizure development in both cohorts of mice, we expected to find decreased seizure thresholds in the 6-Hz corneal stimulation test (Barton et al., 2001). A new cohort of CCI and sham mice without electrode implantation was generated to determine seizure threshold following TBI. Only mice which pretested for a seizure threshold of 35 mA, the average 6-Hz threshold for this strain of mice, before operation were selected for this study. At 14d post-injury, TBI animals exhibited significant reduction in seizure threshold, showing a threshold of 75.5% of their 0d threshold ($p > 0.0001$). This difference in seizure threshold level continued to decrease over time and by 120d, 2mm-TBI animals exhibited more than a 50% reduction of their original threshold ($p < 0.0001$) (**Fig. 6A**). These long-term changes reveal evidence of epileptogenesis in the non-implanted cohort which coincides with the onset of seizure activity and progression of spontaneous seizures in our implanted cohorts.

At 120-day post-injury, we observed a graded injury response to 6-Hz seizure threshold testing. The 1 mm impact group demonstrated a significant reduction in seizure threshold compared to sham animals ($p = 0.0096$), and to the 2 mm cohort ($p = 0.0193$) (sham threshold = 35 ± .44 mA, 1mm threshold = 27.75 ± 2.92 mA, 2mm threshold = 18.54 ± 1.48 mA) (**Fig. 6B**). Seizures induced by the 6-Hz model display behavioral responses such as stun often followed by rearing, forelimb and/or hindlimb

clonus, twitching of the vibrissae, and straub tail lasting between 8 – 90 s. Of note, some of our TBI mice in both cohorts displayed a novel behavioral response after stimulation in which they showed twitching and forelimb clonus only on the contralateral side of their body from TBI impact. This asymmetric forelimb clonus (AFLC) was observed in 25% of 1 mm mice and 30% of 2 mm mice (**Fig. 6C**). Generalized seizures with a motor component typically exhibit bilateral movements influenced by the motor cortex of each hemisphere. However, the large lesions around the site of injury in TBI cohorts extended into the motor cortex, suggesting that this AFCL was caused by ipsilesional deficits, such as that also occur in stroke survivors (Schaefer et al., 2012). Thus, brain injury produces a long-lasting reduction in threshold to generalized seizures that is highly consistent with the development of PTE with SRS.

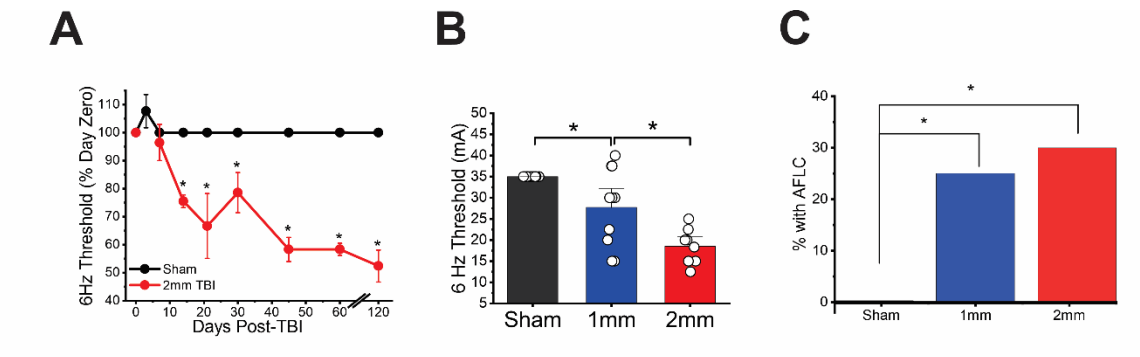

Figure 6: TBI reduces 6 Hz Seizure Threshold.

A, Seizure threshold in 2mm-TBI animals over time. An additional cohort of 2mm-TBI animals was generate with no EEG implant, seizure thresholds were tested through 6 Hz model. (Sample sizes: Sham = 10; 2mm-TBI = 8; 1mm-TBI = 10). **B,** 6 Hz seizure threshold of Sham, 1mm, and 2mm at 120 days post-injury. (Sample sizes: Sham = 10; 2mm-TBI = 8; 1mm-TBI = 10). **C,** Percent of animals exhibiting asymmetric forelimb clonus (AFCL) as a behavioral seizure component after 6 Hz. (Sample sizes: Sham = 10; 2mm-TBI = 8; 1mm-TBI = 10).

IV. 1.4 Epileptiform Discharges Often Precede Generalized Seizures After TBI

To identify non-motor seizures that occur after TBI, we determined the epileptiform discharges (non-convulsive) from the 120-day EEG recordings. In human studies of PTE, over 50% of seizures identified during ICU continuous EEG monitoring have been non-convulsive and appear to be associated with long-term ipsilateral hippocampal atrophy (Vespa et al., 2010). Some epilepsy syndromes, especially those with hippocampal sclerosis or due to injury, are thought to be progressive in nature, with earlier seizures being less intense in both amplitude and duration than late seizures (Coan et al., 2009; Reid et al., 2016). The complexity and heterogeneity of PTE makes the task of identifying early biomarkers or risk factors for epileptogenesis difficult. To further investigate the TBI-induced epileptiform activity, we analyzed the EEG output for non-convulsive seizure discharges. Electrographic discharges lasting between 3-9 s were observed following TBI, and in many cases preceded the archetypal seizures described above in **Fig. 7**. These non-convulsive epileptiform discharges consisted of a rapid increase in EEG spiking with an amplitude and frequency at least twice each animal's respective baseline. Sham animals did not display any epileptiform discharge activity. Epileptiform discharges were seen in 41.67% of the 1mm cohort and 86.67% of the 2mm cohort, showing a similar pattern of frequency to seizure output (**Fig. 7A and B**). Duration was limited between 3 to 9s as to not double count any potential seizure occurrence. Therefore, duration of epileptiform discharges was reasonably stable throughout the observation period, averaging 5.67 ± 0.05 s and 5.66 ± 0.07 s in the 1mm and 2mm cohort, respectively (**Fig. 7C and D**). Discharges began approximately 18.6 ±

1.17 days (1mm) and 48.31 ± 6.65 days (2mm) post-injury, often preceding each animals' seizure onset by a few days (**Fig. 7E**). Some animals in the 1mm cohort that did not experience any archetypal seizures exhibited several epileptiform discharges, suggesting even these non-epileptic animals may be experiencing alteration in network signaling.

Discharges occurred more frequently than seizure events with a ratio of discharges to seizures at 2.07 ± 0.43 (1mm) and 2.77 ± 0.40 (2mm) (**Fig. 7F**). Interestingly, even though the 1mm cohort had a much lower incidence of epileptiform activity, they showed significantly higher frequency of discharges compared to 2mm animals (average discharges 1mm = 202.2 ± 42.34; 2mm = 86.54 ± 3.45; $p = 0.04966$) discharges per animal (**Fig. 7G**). Electrographic characteristics of discharges were similar between groups. **Fig. 7H** shows a representative example of 1mm and 2mm epileptiform discharges alongside a sham baseline. Thus, these results show that during the latent period following TBI, epileptiform circuitry changes occur resulting in the reduction of seizure threshold, followed by the increase in hypersynchronous activity, and eventually manifesting in epileptic discharges and generalized seizure output for at least 4 months post-injury.

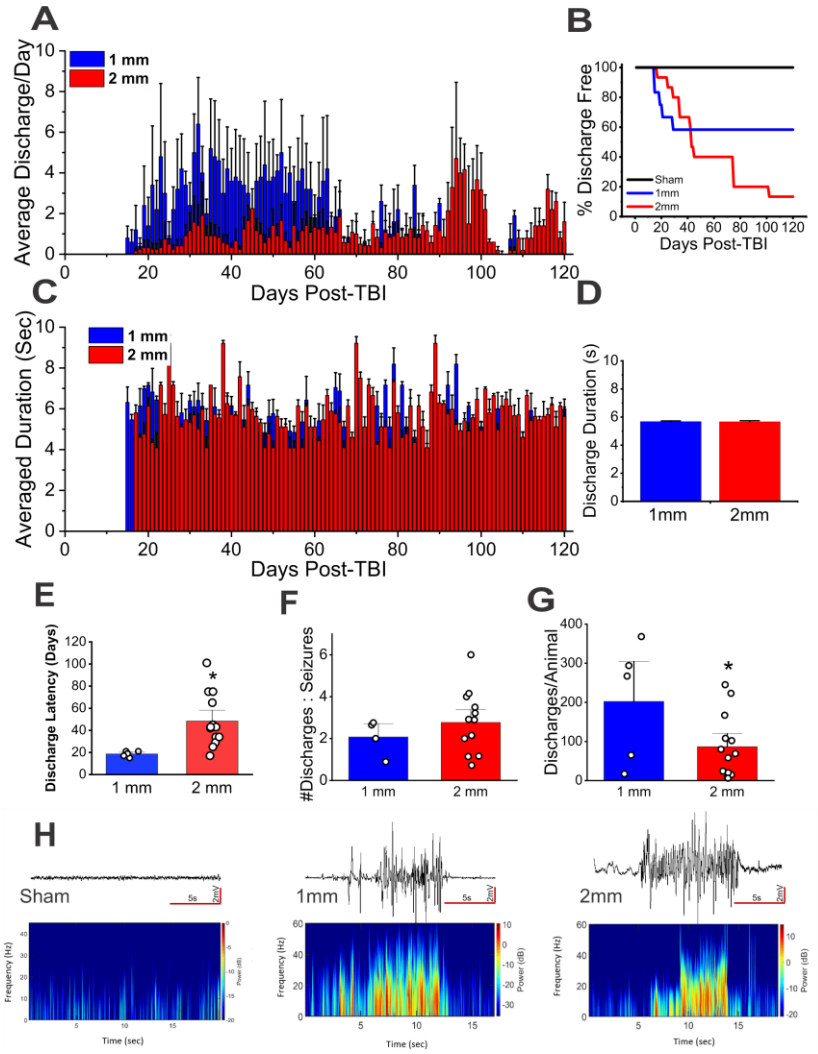

Figure 7: Epileptiform Discharges in PTE Mice.

A, Average epileptiform discharges per day per animal over 120-day observation period for both moderate (1mm) and severe (2mm) TBI cohorts. Epileptiform discharges (3 – 9s) were identified through a custom Matlab script. Only responding animals were used for calculations (2mm-TBI: n=14, 1mm-TBI: n = 6). **B,** Incidence curve showing latency to first epileptiform discharge over time. **C,** Average duration of discharges per day over 120 days. All epileptiform discharge events on each day from responding mice (2mm-TBI: n=14, 1mm-TBI: n = 6) were used in calculations. **D,** Overall average duration of epileptiform discharges in 1mm and 2mm TBI cohorts. **E,** Average latency to first epileptiform discharge. **F,** Ratio of number of discharges to number of seizures for each responding animal. Only animals which experienced both seizures and discharges were used for calculation. **G,** Cumulative number of discharges per animal during 120-day observation period. **H,** Representative discharge or baseline EEG traces (above) and corresponding power spectral analysis (below) for Sham, 1mm, and 2mm TBI cohorts.

IV. 1.5 High-frequency Oscillations as Biomarkers of PTE

Next, we analyzed the high-frequency oscillations (HFO), including 'ripples' (80-200Hz) and 'fast ripples' (250-500 Hz), which are thought to represent biomarkers of the epileptogenesis (Bragin et al., 1999; Behr et al., 2015; Jefferys et al., 2012). There are few studies that correlated changes in HFO activity following TBI, though it is understood that ripples and fast ripples correlate with the onset and spread of ictal activity (Schonberger et al., 2019). In order to identify biomarkers and the epileptogenic zone that guides surgeons in epileptic procedures (Zijlmans et al., 2012), we analyzed our TBI models for HFOs. Using a custom-written script in Matlab (Mathworks, Natic, MA) EEG data were filtered for HFO events (80-500 Hz) (**Fig. 8A and B**). Filtered EEG recordings were normalized using their own mean values. A minimum of three consecutive cycles three standard deviations from the mean in the frequency band were needed to be considered a viable HFO candidate. Potential events that overlapped in time were removed to avoid false detections from using bandpass filtering in higher frequency ranges, as cited in previous publications (Benar et al., 2010). For week 11 post-TBI (77d – 84d), we evaluated the average frequency of ripples and fast ripples of the 2mm cohort against the sham cohort in 10 min epochs during each animals' high points in activity throughout the day. Ripples were present within both cohorts, though significantly increased within the 2mm TBI cohort ($p < 0.0001$) (**Fig. 8C**). As expected, sham mice did not show fast ripple activity, whereas 2mm mice experienced between 49 – 71 fast ripples per 10 min epoch during this week (**Fig. 8D**).

To probe at the progressive HFO activity following TBI, we analyzed the full 120-day observation period for ripples and fast ripples using the same 10 min epoch methodology. Overall, average ripple frequency remained steady throughout the 4 months and ranged between 0–18.67 ripple/10 min (average frequency 8.04 ± 0.33 ripples/10 min). We observed few fast ripples during the first week of recording; however, frequency increased drastically by 20D in TBI mice— before the onset of epileptiform discharges and seizures. Fast ripple frequency ranged between 0 – 85.5 fast ripples/10 min throughout the 4 months with an average of 45.65 ± 1.72 fast ripples/10 min (**Fig. 8E-G**). Representative EEG traces with bandpass filter and power-spectrogram for both ripples and fast ripples can be seen in **Fig. 8H and I**. HFOs occur within a normal brain (Jefferys et al., 2012), but changes in their dynamics and frequency can be associated with pathological excitability states like PTE. These observations suggest significant increase in ripple and fast ripple activity in PTE models, which is consistent with previously reports in experimental epilepsy (Foffani et al., 2007; Ewell et al., 2019).

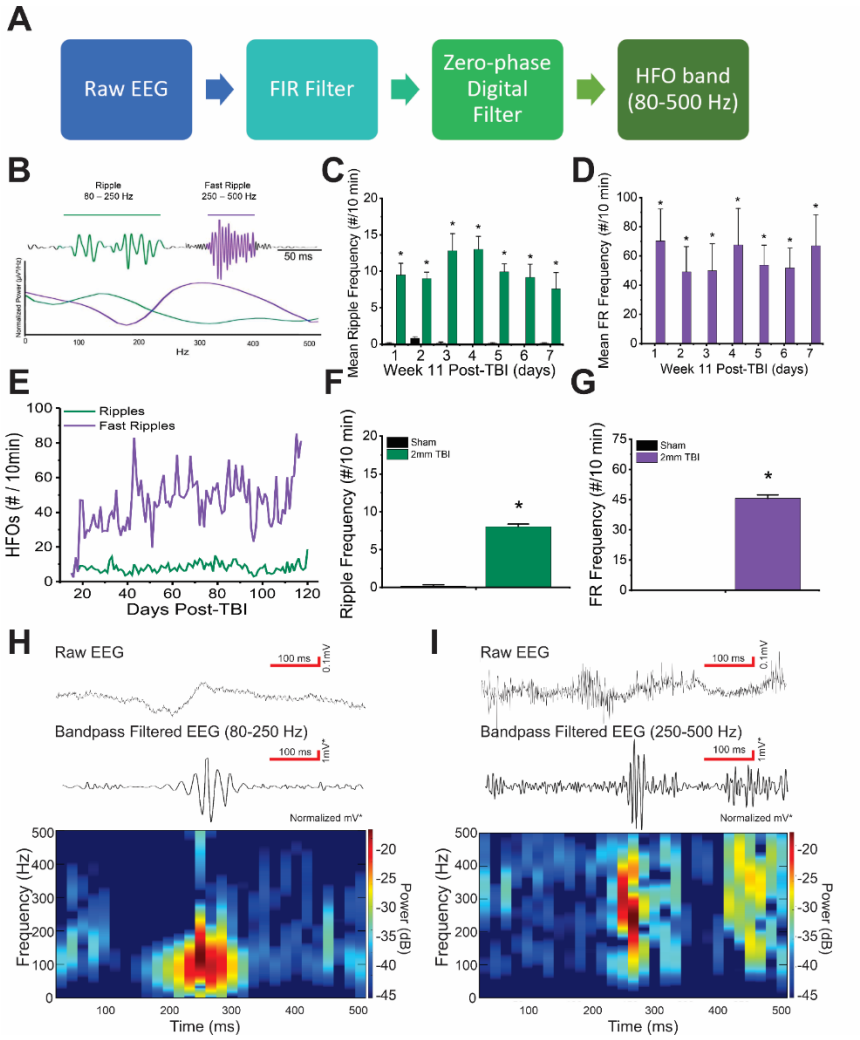

Figure 8: Increased High-Frequency Oscillations (HFOs) in PTE mice.

A, Flow chart showing the preparation and process of identifying HFO events. Following EEG recording, data was analyzed through a custom Matlab script for Ripples (80-250 Hz) and Fast Ripples (250-500 Hz). **B,** Periodogram showing EEG trace example of Ripple and Fast Ripple under normalized power ($\mu V^2/Hz$). **C,** Average Ripple frequency per 10 min epoch over 7-day period in Sham and 2mm-TBI cohorts. Data was extracted from week 11 of recording. **D,** Average Fast Ripple frequency per 10 min epoch over 7-day period in Sham and 2mm-TBI cohorts. Data was extracted from week 11 of recording. **E,** Number of HFO events per 10 min epoch over 120 days post-injury in 2mm-TBI cohort. **F,** Average Ripple frequency per 10 min epoch over 120-day period. **G,** Average Fast Ripple frequency per 10 min epoch over 120-day observation period. **H,** Representative traces of raw EEG, bandpass filtered EEG, and power spectral analysis of Ripple in 2mm-TBI group. **I,** Representative traces of raw EEG, bandpass filtered EEG, and power spectral analysis of Fast Ripple in 2mm-TBI group.

IV. 1.6 TBI Induces Progressive Brain Tissue Loss and Lesions

To examine the extent of tissue loss and lesion following brain injury, we conducted systematic histological analysis of brain sections. Histological examination of serial brain slices (Nissl) at 4 months post-CCI revealed severe focal damage in the ipsilateral hemisphere that extended beyond the dimensions of intended injury (3mm impact tip, 1mm or 2mm depth). Serial slice images showing full brain architecture from Bregma -1.16 mm through – 3.64 mm can be seen in **Fig. 9A** for all cohorts. Vast lesions (1 mm-TBI= 11.51 ± 1.83 mm^3, 2mm-TBI= 22.489 ± 1.482 mm^3 vs Sham= 0.52 ± 0.267 mm^3) with irregular edges spread through the cortical and hippocampal regions (**Fig. 9B**). Lesions protruded into the ipsilateral hippocampus in both TBI cohorts (1mm-TBI = 1.82 ± 0.66 mm^3, 2mm-TBI = 4.767 ± 0.462 mm^3 vs Sham = 0.42 ± 0.113 mm^3) (**Fig. 9C**). At 1d post-injury, 2mm mice showed total and hippocampal lesion volumes of 4.28 ± 1.12 mm^3 and 2.91 ± 1.12 mm^3, respectively. Similarly, the 1mm-TBI cohort a time-dependent response to TBI impact (1mm-TBI total = 2.059 ± 0.879 mm^3; 1mm-TBI hippocampal = 0.814 ± 0.467 mm^3) (**Fig. 9D and E**). This change in lesion volume over time indicates significant tissue loss and necrosis around the injury site in both the moderate and severe TBI cohorts. Due to the dramatic loss of tissue in the injured hemisphere, most of our histological analysis focuses on the contralateral hemisphere, and specifically the contralateral hippocampus. In some cases, we also compared the intact 1mm ipsilateral and contralateral hippocampi. Any differences in contralateral vs ipsilateral hippocampal volume in the sham cohort is thought to be due to inter-animal

variability rather than necrosis and tissue loss since slide images show no signs of tearing or extreme damage.

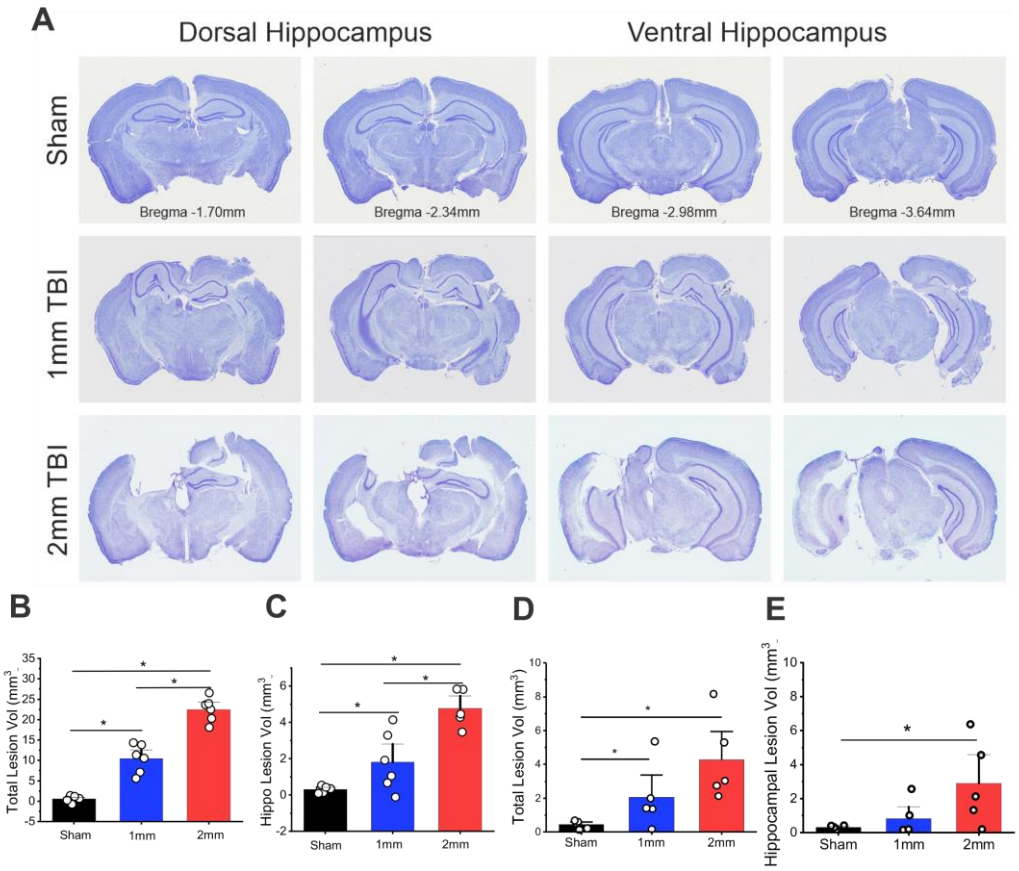

Figure 9: Acute and Progressive Tissue Loss and Lesion after TBI.

A, Coronal slices of whole brain showing dorsal and ventral hippocampus in both moderate (1mm) and severe (2mm) TBI cohorts. **B,** Total lesion volume at 120D post-injury in Sham, 1mm-TBI, and 2mm-TBI cohorts. **C,** Hippocampal lesion volume at 120D post-injury in Sham, 1mm-TBI, and 2mm-TBI cohorts. **D,** Total lesion volume in Sham and 2mm-TBI cohorts at 1D post-injury. **E,** Hippocampal lesion volume in Sham and 2mm-TBI cohorts at 1D post-injury. For all lesion volume calculations, sample sizes: Sham = 8; 2mm-TBI = 5 per time point; 1mm-TBI = 6. *$p<0.05$ vs. Sham group (n = 5-8 per group, as indicated above); one-way ANOVA with Bonferroni or Tukey HSD post hoc test.

IV. 1.7 Extensive Neurodegeneration Occurs in PTE Model

To determine whether our model displayed signs of reciprocal damage to the hemisphere without direct contact over time, we performed stereological analysis on the neuronal nuclear antigen (NeuN+) principal neurons in the contralateral hippocampus at 1d, 3d, 7d, 30d, 60d, and 120d post-injury in the 2mm-TBI cohort (**Fig. 10A**). Neurodegeneration is a well-established hallmark of chronic epilepsy and may have a role in the secondary cascades of epileptogenesis (Tai et al., 2016; Sloviter, 1987). Animal models of TBI have demonstrated a loss of neurons, particularly in the ipsilateral hemisphere where the damage is most prevalent (Bolkvadze and Pitkanen, 2012; Kelly et al., 2015). No significant changes in absolute cell count were found within the contralateral hippocampus during first week after brain injury, though a steep decline began at 30d (**Fig. 10B**). Hippocampal counts were separated into regions of interest (CA1-CA3, DG, DH) to determine if a specific region was more susceptible to damage (**Fig. 10C**). Overall, hippocampal subregions suffered comparable losses in NeuN+ neurons proportionate to their sham or 0d basal levels, suggesting no subregion was more vulnerable to neurodegeneration. Next, we normalized our cell density to age-matched sham mice to determine the extent of neurodegeneration occurring within the hippocampus. Neurodegeneration in the first week post-injury was negligible (1d = 5.1% cell loss, 3d = 5.3% cell loss, 7d = 8.7% cell loss). However, we observed progressive neurodegeneration in the contralateral hippocampus beginning 30d post-injury (30d = 14.6% cell loss, 60d = 27.9% cell loss, 120d = 38.3% cell loss) (**Fig. 10D**).

Within the 1mm-TBI cohort, we observed significant loss of principle neurons in the contralateral hippocampus at 4-months post-injury (**Fig. 10E and F**). After analysis by subregion, we found that the greatest loss of hippocampal neurons in this cohort was found to be in the CA3 (1mm = 65837.1 ± 5389.7 cells vs Sham = 100001.4 ± 4573.8 cells, $p = 0.0005$) and DG (1mm = 36377.2 ± 3276.8 vs Sham = 97763.4 ± 2575.9 cells, $p < 0.0001$), as the other regions were not significantly different from sham mice. When normalized to the sham cohort, we observed 31.16% neurodegeneration in the contralateral hippocampus compared to a 36.5% reduction in NeuN+ cells within the 2mm-TBI cohort (**Fig. 10G**). Overall, our data demonstrates huge chronic loss of principle neurons in both TBI cohorts at 4-months post-injury. Within the 2mm-TBI cohort, these losses emerged at approximately 30d, before the average onset of spontaneous seizures.

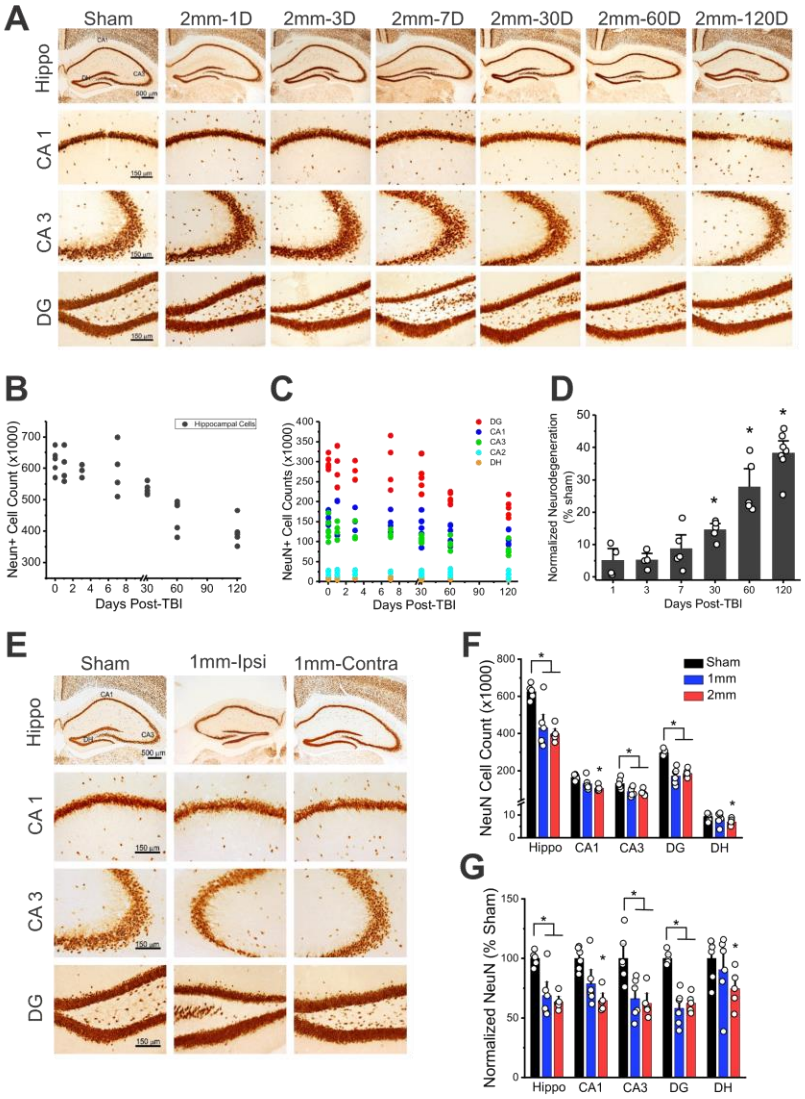

Figure 10: Neurodegeneration of Principle Neurons Following TBI.

A, Time-course of contralateral hippocampal NeuN+ immunohistochemistry in Sham and TBI (2-mm) cohort at 1D, 3D, 7D, 30D, 60D, and 120D post-injury. Hippocampal images taken at 4x. CA1, CA3, and DG images taken at 20x. **B,** Total NeuN+ hippocampal cell count over time. **C,** NeuN+ cell counts divided into regions of interest CA1-CA3, DG & DH. **D,** Percent loss of NeuN+ cells over time, compared to Sham. **E,** Hippocampal and regional NeuN+ immunohistochemistry at 120D post-injury in Sham, 1mm-TBI ipsilateral hippocampus, and 1mm-TBI contralateral hippocampus. Hippocampal images taken at 4x. CA1, CA3, and DG images taken at 20x. **F,** Total NeuN cell count divided by hippocampus and region of interest at 120D post-injury in Sham, 1mm-TBI, and 2mm-TBI cohorts. **G,** NeuN+ cell count at 120D post-injury in Sham, 1mm-TBI, and 2mm-TBI cohorts normalized to Sham to show percent loss in regions of interest.

Inhibitory interneurons provide a crucial GABAergic inhibitory balance within the limbic circuits under normal conditions. Within the context of epilepsy, studies have found preferential loss of parvalbumin+ (PV) interneurons in both human patients and experimental animal models (Dinocourt et al., 2003; Andrioli et al., 2007). Sudden loss of these interneurons may give rise to the formation of an epileptic focus (Guyás and Freund, 2015). Therefore, we also performed stereological analysis on PV+ interneurons at 1d, 3d, 7d, 30d, 60d, and 120d post-injury in the 2mm-TBI cohort (**Fig. 11A**). We found similar patterns of neurodegeneration within this population of cells as seen in NeuN+ principal neurons. No significant reduction in absolute cell counts were found until 30d post-TBI (Sham = 13368.6 ± 420.9 hippocampal interneurons vs 30d = 9509.8 ± 621.8 hippocampal interneurons) which progressed throughout the observation period (**Fig. 11B**). Analysis by subregion revealed the DG suffered the largest loss of interneurons, with an average loss of interneurons of 33.1% at 30d which progressed to 66.2% loss by 120d (**Fig. 11C**). Overall, the hippocampus exhibited a 46.1% loss of interneurons by 120d post-TBI (**Fig. 11D**). Similar to the 2mm-TBI cohort, the 1mm-TBI cohort displayed a significant reduction in interneurons within the contralateral hippocampus at 4-months post-TBI (Sham = 13368.6 ± 420.9, 1mm = 8253.9 ± 677.9, 2mm = 7052.7 ± 549.3, $p < 0.0001$ vs Sham) (**Fig. 11E and F**). When normalized to sham, this equates to an overall loss of 38.3% hippocampal interneurons (**Fig. 11G**).

Since the ipsilateral hippocampus still largely remained in the 1mm-TBI cohort, we also used our stereology protocol to investigate interneuron loss around the impact site. Overall, we observed greater loss of interneurons in the ipsilateral compared to the

contralateral hippocampus (ipsi = 5345.6 ± 1085.3 interneurons, contra = 8253.9 ± 667.9 interneurons; ipsi = 60.1% loss, contra = 38.3% loss, p = 0.0465) (**Fig. 11H and I**). Though damage was more extreme around the site of impact, our results suggest the contralateral hippocampus also suffers large reductions in neurons and interneurons. These changes in cell density may alter the delicate neural circuits involved in balancing inhibition and excitation in the brain, ultimately resulting in increased potential for spontaneous seizures after TBI. A temporal relationship between epileptic seizure occurrence and neurodegeneration patterns in contralateral hemispheres can be found in **Fig. 12A and B**.

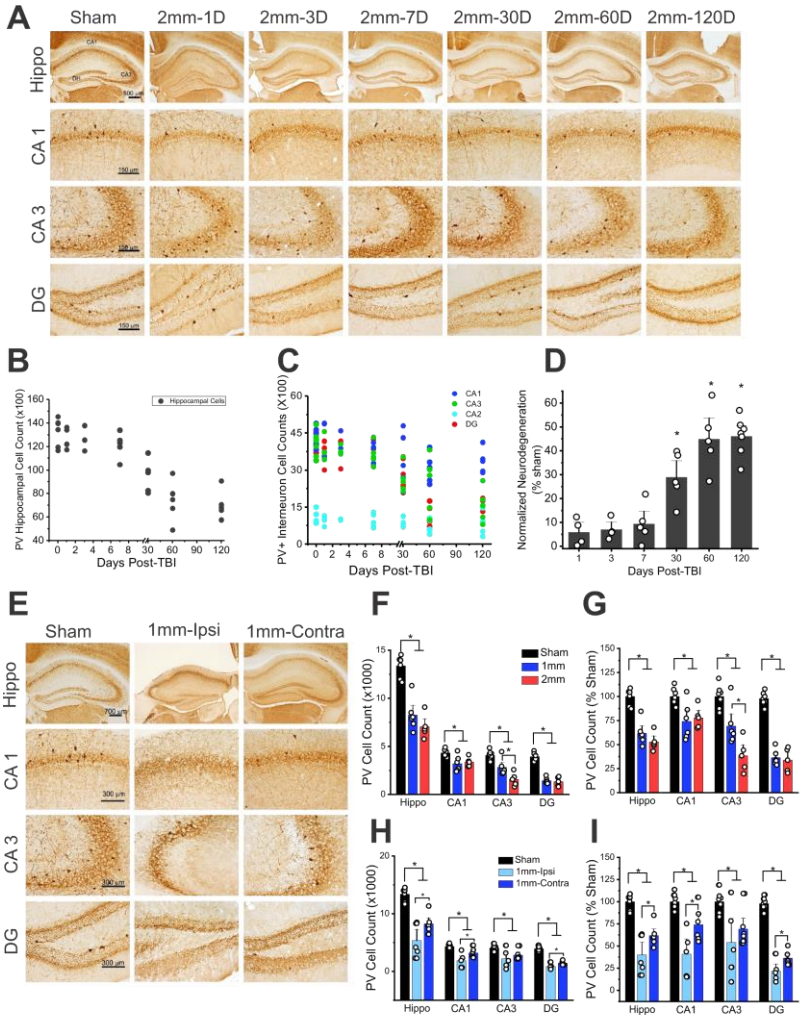

Figure 11: Loss of Inhibitory GABAergic Interneurons after TBI.
A, Time-course of contralateral hippocampal PV+ immunohistochemistry in Sham and TBI (2-mm) cohort at 1D, 3D, 7D, 30D, 60D, and 120D post-injury. Hippocampal images taken at 4x. CA1, CA3, and DG images taken at 20x. **B,** Total PV+ hippocampal cell count over time. **C,** PV+ cell counts divided into regions of interest CA1-CA3, DG & DH. **D,** Percent loss of PV+ cells over time, compared to Sham. **E,** Hippocampal and regional PV+ immunohistochemistry at 120D post-injury in Sham, 1mm-TBI ipsilateral hippocampus, and 1mm-TBI contralateral hippocampus. Hippocampal images taken at 4x. CA1, CA3, and DG images taken at 20x. **F,** Total PV+ cell count divided by hippocampus and region of interest at 120D post-injury in Sham, 1mm-TBI, and 2mm-TBI cohorts. **G,** PV+ cell count at 120D post-injury in Sham, 1mm-TBI, and 2mm-TBI cohorts normalized to Sham to show percent loss in regions of interest. **H,** Comparison of PV+ cell loss in ipsilateral versus contralateral hippocampus in 1mm-TBI cohort. **I,** Comparison of PV+ cell loss in ipsilateral versus contralateral hippocampus in 1mm-TBI cohort normalized to Sham to show percent loss in regions of interest.

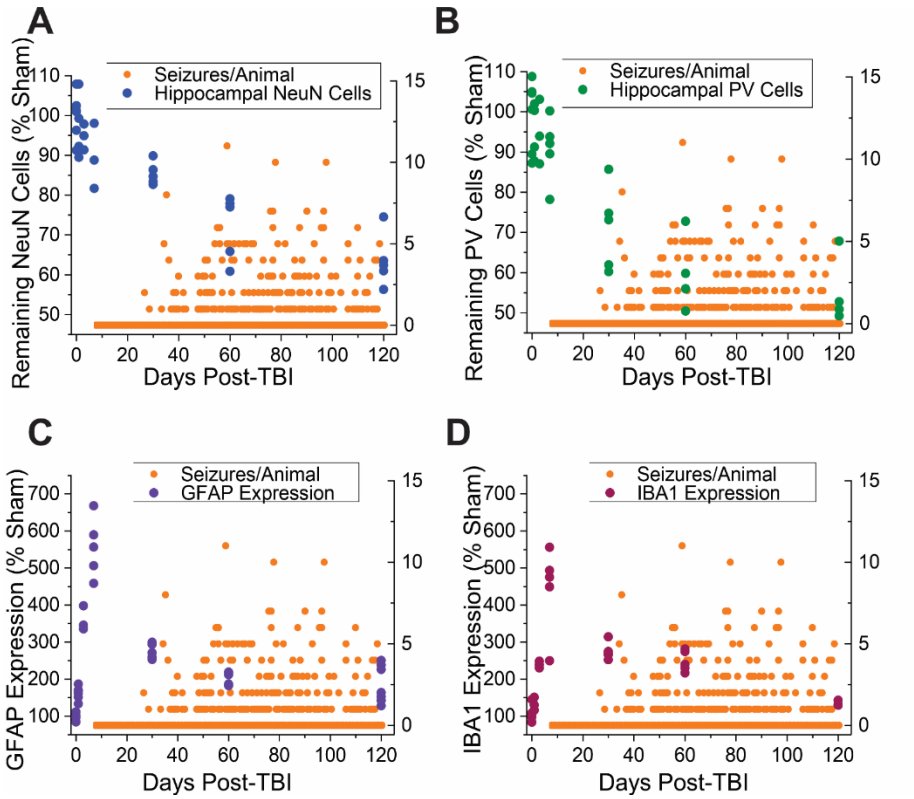

Figure 12: Histology Trend as a Function of Seizure Occurrence.

A, Scatter trend of remaining principal neurons over time, overlayed a scatterplot of seizure events over 120 days. Each blue dot represents the remaining cells for a specific animal. Likewise, each orange dot represents the number of seizures a single animal had on a corresponding day, such that each day has multiple data points ranging from 0-12. **B,** Scatter trend of remaining PV+ interneurons over time, overlayed a scatterplot of seizure events over 120 days. Each green dot represents the remaining cells for a specific animal. Likewise, each orange dot represents the number of seizures a single animal had on a corresponding day, such that each day has multiple data points ranging from 0-12. **C,** Scatter trend of %increase in astrogliosis over time, overlayed a scatterplot of seizure events over 120 days. Each purple dot represents the %astrogliosis for a specific animal. Likewise, each orange dot represents the number of seizures a single animal had on a corresponding day, such that each day has multiple data points ranging from 0-12. **D,** Scatter trend of %increase in microgliosis over time, overlayed a scatterplot of seizure events over 120 days. Each red dot represents the %microgliosis for a specific animal. Likewise, each orange dot represents the number of seizures a single animal had on a corresponding day, such that each day has multiple data points ranging from 0-12. Sample sizes for histology: Sham = 8; 2mm-TBI = 5 per time point. Sample sizes for seizure incidence 2mm-TBI= 15.

IV. 1.8 Widespread and Persistent Astrogliosis Occurs in PTE

To test whether neuroinflammation is directly involved in connecting the injury to PTE, we evaluated the temporo-spatial changes in cellular inflammation in the brain after TBI. Inflammation is a central component of the secondary injury catalyzed by TBI. Focal TBI injuries induce a sharp upregulation in glial fibrillary acidic protein (GFAP) as well as an increase of microglial infiltration and expression, which are often identified through changes in expression. These processes are classically defined as astrogliosis and microgliosis and are essential to protecting uninjured brain tissues from secondary damage (Anderson et al., 2016). However, prolonged gliosis can cause loss of homeostatic glial functions and contribute to poorer prognosis and comorbidities associated with TBI including epileptogenesis (Oleksii et al., 2019; Xu et al., 2019). Expression of GFAP+ and IBA1+ immunohistochemistry was used to determine the extent of astrogliosis and microgliosis after brain injury. Together, these stains are used as a measure of neuroinflammation or neuroprotection during different phases of injury or infection.

Significant increases in GFAP staining were observed in both the hippocampus and amygdala beginning at 3d post-injury and peaking at 7d (CA1= 400 ± 34.9%, CA3= 530.88 ± 22.55%, DG= 612.91 ± 47.84% increase over sham levels) (**Fig. 13A-C**). Higher GFAP expression persisted in the hippocampus throughout the study, and though levels began to drop at 30d post-injury, expression was still significantly higher than sham at 120d (CA1 $p = 0.0101$, CA3 $p = 0.0003$, DG $p < 0.0001$). At 30d post-injury, the contralateral amygdala still showed signs of inflammation but were not significant

following the initial week. Focal damage, such as TBI, can cause a global reaction of inflammation within the resident glial cells. Higher expression of useful markers, such as GFAP or IBA1, can be helpful in estimating reactivity in these cell types. However, higher expression can be as a result of either increased cell migration or by increased protein density on the resident cells (Khurgel and Ivy, 1996; Serrano-Pozo et al., 2013). Our data suggests this robust increase in GFAP is most likely a combination of cell migration within the region of interest as well as an accumulation of GFAP protein within those cells, suggesting highly reactive astrocytes in the first week after injury (**Fig. 13D**). Furthermore, we used a pathology scoring scale (0-5, 0 = no evidence of pathology, 5 = extreme evidence of pathology) to identify additional regions of the contralateral brain which may have shown increased pathology after injury. We found variability within these areas, with the most affected region being the piriform cortex (**Fig. 13E**). Images of these brain regions as well as a differential comparison between ipsilateral and contralateral hemispheres can be found in **Fig. 14**. As expected, lesser injury produced a reduced astrocytic response in the contralateral hemisphere. Within the 1mm cohort, GFAP expression in the hippocampus was similar to sham mice (**Fig. 13F**). However, due to the reduced tissue loss on the injured side, we were also able to capture chronic astrogliosis in the ipsilateral hippocampus. As **Fig. 13G** shows, these regions demonstrate prolonged activation of glial cells around the injury and surrounding areas.

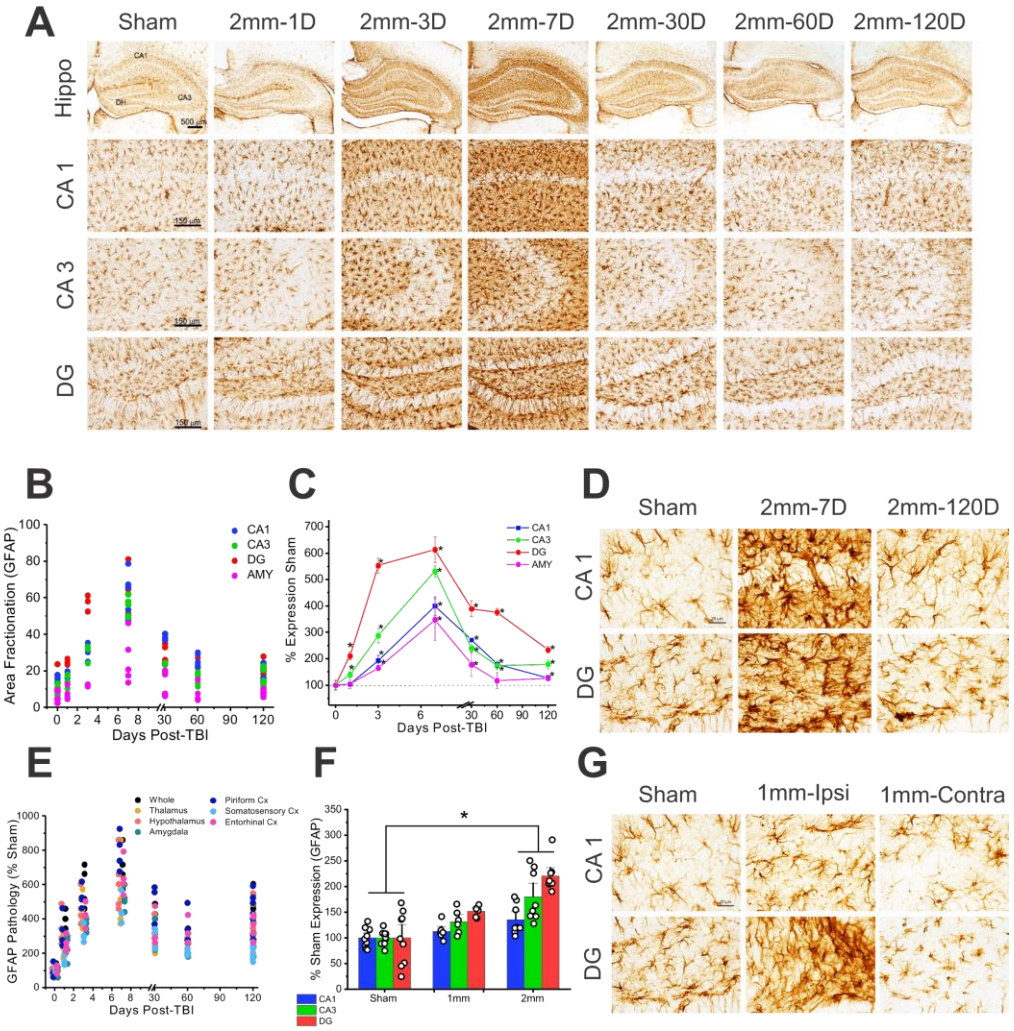

Figure 13: Immediate and Long-Lasting Astrogliosis following TBI.
A, Time-course of contralateral hippocampal GFAP+ immunohistochemistry in Sham and TBI (2-mm) cohort at 1D, 3D, 7D, 30D, 60D, and 120D post-injury to visualize astrogliosis. Hippocampal images taken at 4x. CA1, CA3, and DG images taken at 20x. **B,** Area fractionation for regions of interest CA1, CA3, DG, and Amygdala (AMY) in 2mm-TBI cohort over time. **C,** Densitometric analysis of GFAP+ expression in regions of interest in 2mm-TBI cohort over time expressed as percent Sham. **D,** Enlarged views of CA1 and DG in Sham cohort and 2mm-TBI cohort at 7D and 120D post-injury. Images taken at 40x. **E,** Qualitative scoring of GFAP+ expression in extrahippocampal regions of interest in 2mm-TBI cohort over time. Pathology scores were normalized to Sham and presented as percent increase to Sham average. **F,** Densitometric analysis of GFAP+ expression in regions of interest in Sham, 1mm-TBI, and 2mm-TBI cohorts at 120D post-injury. **G,** Regional GFAP+ immunohistochemistry at 120D post-injury in Sham, 1mm-TBI ipsilateral hippocampus and 1mm-TBI contralateral hippocampus. CA1 and DG images taken at 40x.

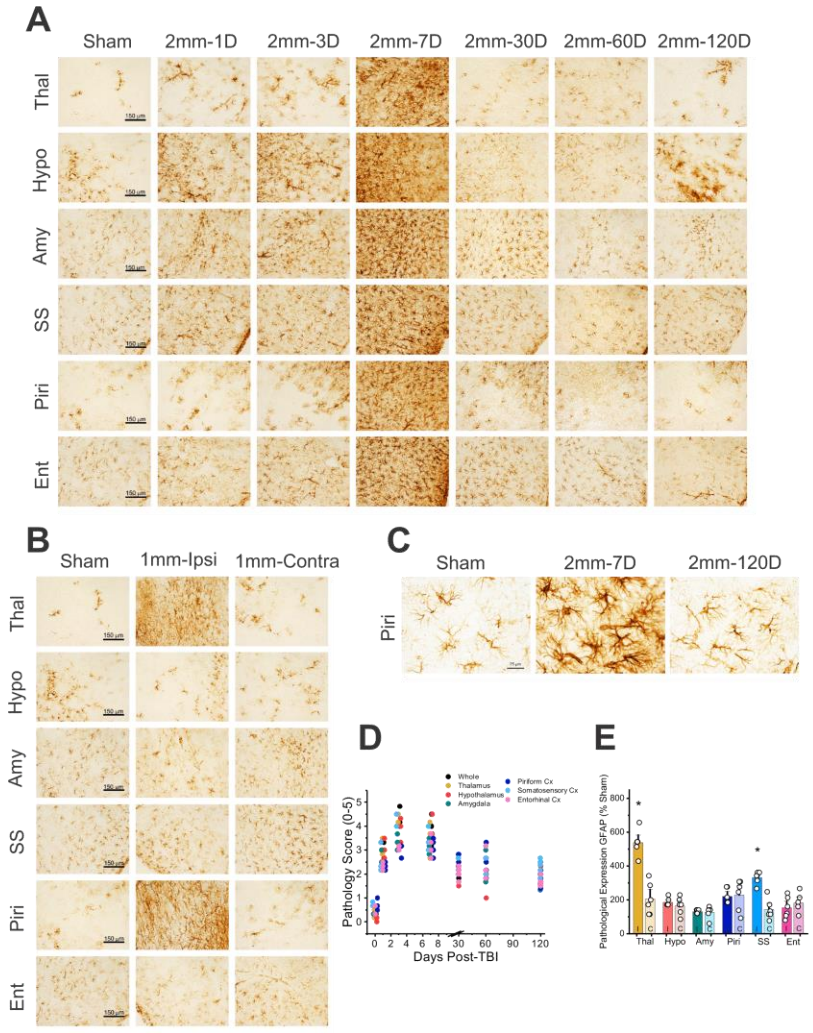

Figure 14: Time-Course Distribution of the Extent of TBI-Induced Astrogliosis in Extra-Hippocampal Brain Regions.

A, Time-course of extra-hippocampal regions of interest in contralateral hemisphere in Sham and 2mm-TBI cohort at 1D, 3D, 7D, 30D, 60D, and 120D post-injury to visualize astrogliosis. GFAP+ immunohistochemistry of Thalamus, Hypothalamus, Amygdala, Somatosensory Cortex, Piriform Cortex, and Entorhinal Cortex taken at 20X. **B,** Extrahippocampal regions of interest GFAP+ immunohistochemistry at 120D post-injury in Sham, 1mm-TBI ipsilateral hemisphere, and 1mm-TBI contralateral hemisphere. Images taken at 20X. **C,** Enlarged views of Piriform Cortex in Sham, 2mm-TBI 7D, and 2mm-TBI 120D. Images taken at 40X. **D,** Qualitative pathology scores on a scale of 0-5 (0 = no increase in expression from Sham; 5 = Significant increase in expression from Sham) over time in 2mm-TBI cohort. **E,** Comparison of GFAP+ pathology scores between ipsilateral (I) and contralateral (C) hemispheres in 1mm-TBI cohort.

IV. 1.9 Extensive and Long-lasting Microgliosis Arises in PTE

To illustrate the neuroimmune response following TBI, we conducted a densitometric time course study on IBA1-histochemistry for microglia. Microglia activation is critical for the clearance of pathogenic factors, promotion of tissue repair, and for general host defense. However, prolonged activation of microglia leads to microgliosis and overproduction of cytokines and cytotoxic factors such as reactive oxygen and nitrogen species (Kappock and Caradonna, 1996) (ROS and RNS). Animals underwent a 2mm CCI impact and were perfused at 1d, 3d, 7d, 30d, 60d, and 120d post-TBI. Expression of IBA1 dramatically increased within the first week, peaking at 7d within the hippocampus (**Fig. 15A-C**). The CA1 and CA3 regions saw the most robust upregulation, displaying 559.55 ± 18.41 % and 424.21 ± 27.97% increases compared to sham on 7d. At 120d post-injury, expression levels were still higher than naïve or sham mice, suggesting chronic agitation even past the onset of seizures (CA1 141.68 ± 5.6%, CA3 133.78 ± 5.9%, DG 137.5 ± 1.1%) (**Fig. 15D-F**). Diffuse increases in IBA1 expression can also been seen in extrahippocampal areas, with the piriform cortex and thalamus showing the greatest changes (**Fig. 15E**). In the ipsilateral hemisphere, we noted higher microglial expression around the lesion site, accumulating within the remaining cortical and thalamic regions. A time course of extrahippocampal images as well as differential expression between the ipsilateral and contralateral hemispheres can be found in **Fig. 16**. At 4 months post-injury, the 1 mm cohort showed little to no change in IBA1 expression in the contralateral hippocampus compared to sham (**Fig. 15F**). However, the ipsilateral hippocampus showed a strong increase of microglia, both

in number of microglia present and overall expression within the cells (**Fig. 15G**). Together, these results suggest secondary neuroinflammation not only affects the contralateral hemisphere but may also contribute to the initial loss of hippocampal cells seen in our model. A temporal relationship between epileptic seizure occurrence and neuroinflammation patterns in contralateral hemispheres can be found in **Fig. 16C-D**.

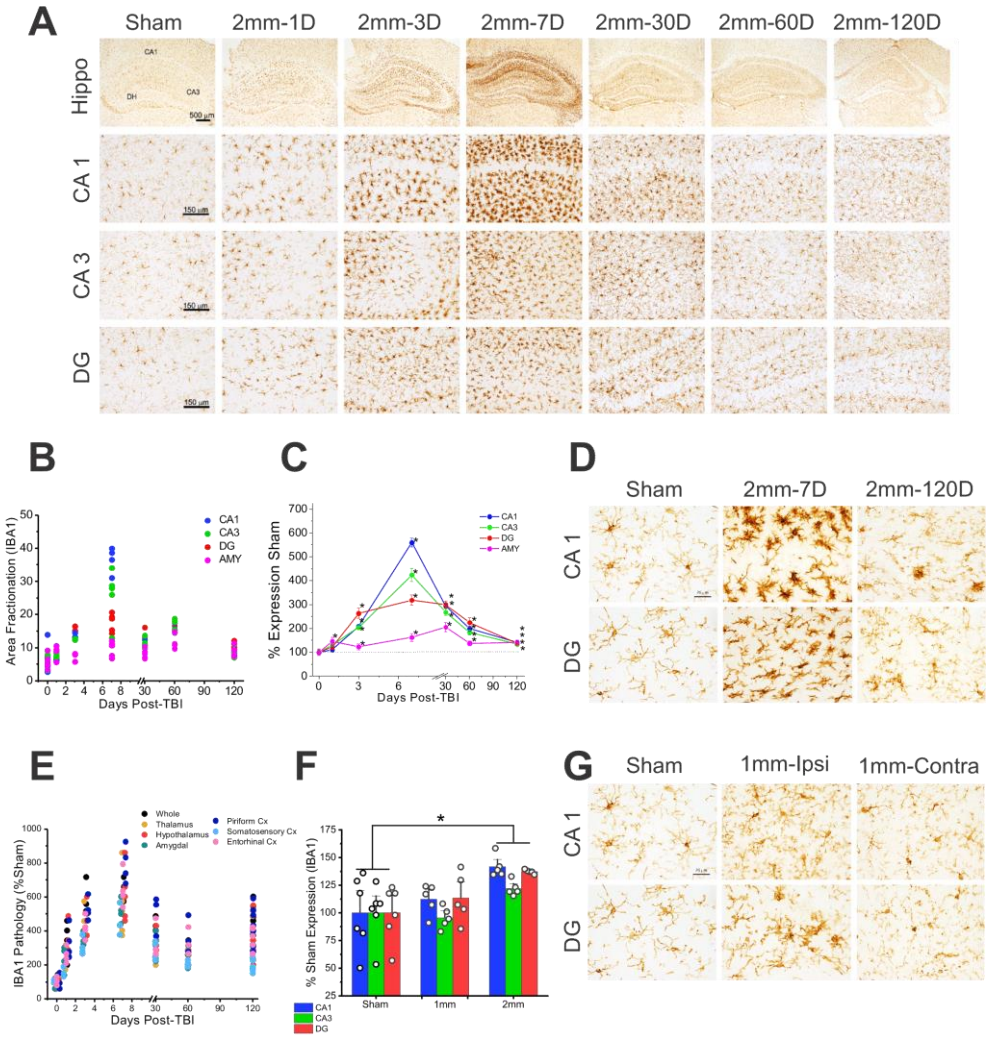

Figure 15: Extensive and Persistent Microgliosis following TBI.
A, Time-course of contralateral hippocampal IBA1+ immunohistochemistry in Sham and TBI (2-mm) cohort at 1D, 3D, 7D, 30D, 60D, and 120D post-injury to visualize microgliosis. Hippocampal images taken at 4x. CA1, CA3, and DG images taken at 20x. **B,** Area fractionation for regions of interest CA1, CA3, DG, and Amygdala (AMY) in 2mm-TBI cohort over time. **C,** Densitometric analysis of IBA1+ expression in regions of interest in 2mm-TBI cohort over time expressed as percent Sham. **D,** Enlarged views of CA1 and DG in Sham cohort and 2mm-TBI cohort at 7D and 120D post-injury. Images taken at 40x. **E,** Qualitative scoring of IBA1+ expression in extrahippocampal regions of interest in 2mm-TBI cohort over time. Pathology scores were normalized to Sham and presented as percent increase to Sham average. **F,** Densitometric analysis of IBA1+ expression in regions of interest in Sham, 1mm-TBI, and 2mm-TBI cohorts at 120D post-injury. **G,** Regional IBA1+ immunohistochemistry at 120D post-injury in Sham, 1mm-TBI ipsilateral hippocampus and 1mm-TBI contralateral hippocampus. CA1 and DG images taken at 40x.

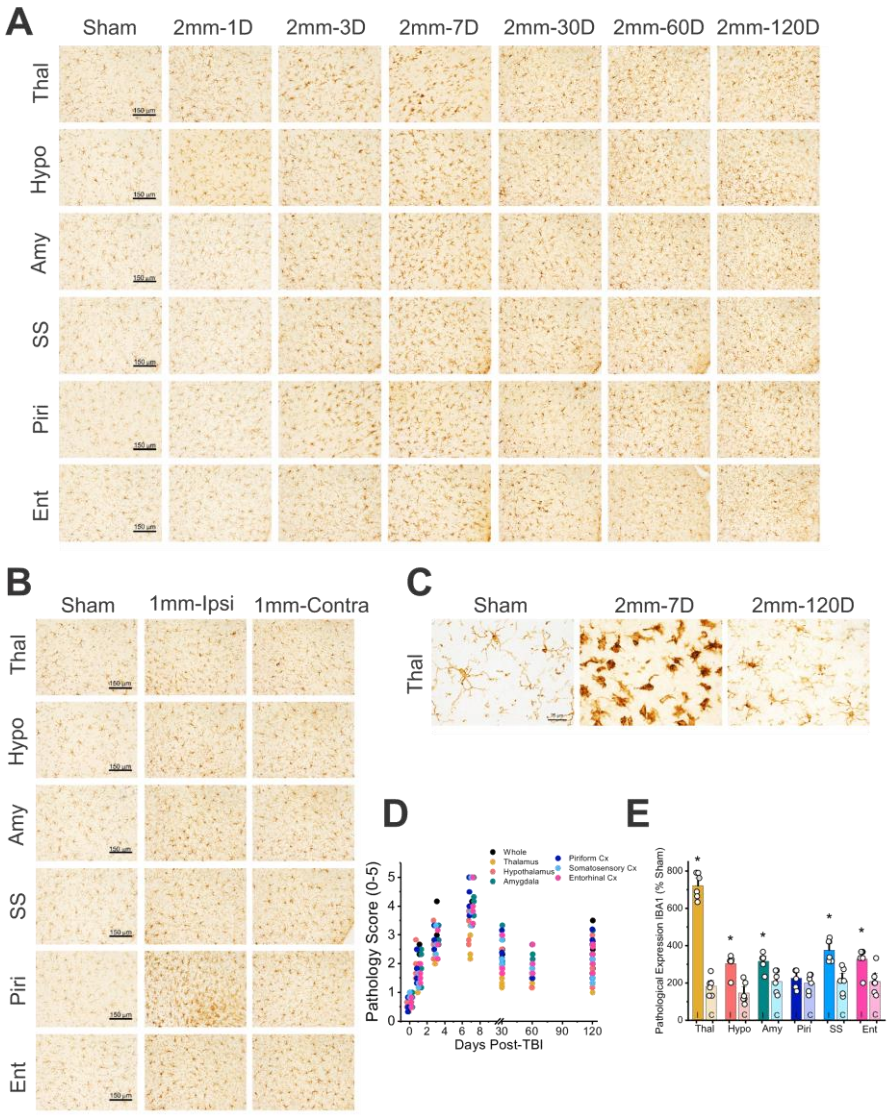

Figure 16: Time-Course Distribution of the Extent of TBI-Induced Microgliosis in Extra-Hippocampal Brain Regions.

A, Time-course of extrahippocampal regions of interest in contralateral hemisphere in Sham and 2mm-TBI cohort at 1D, 3D, 7D, 30D, 60D, and 120D post-injury to visualize microgliosis. IBA1+ immunohistochemistry of Thalamus, Hypothalamus, Amygdala, Somatosensory Cortex, Piriform Cortex, and Entorhinal Cortex taken at 20X. **B,** Extrahippocampal regions of interest IBA1+ immunohistochemistry at 120D post-injury in Sham, 1mm-TBI ipsilateral hemisphere, and 1mm-TBI contralateral hemisphere. Images taken at 20X. **C,** Enlarged views of Thalamus in Sham, 2mm-TBI 7D, and 2mm-TBI 120D. Images taken at 40X. **D,** Qualitative pathology scores on a scale of 0-5 (0 = no increase in expression from Sham; 5 = Significant increase in expression from Sham) over time in 2mm-TBI cohort. **E,** Comparison of IBA1+ pathology scores between ipsilateral (I) and contralateral (C) hemispheres in 1mm-TBI cohort.

IV. 1.10 Aberrant Neurogenesis in PTE

In order to better understand the fluctuation of neurogenesis after injury, we performed doublecortin (DCX) immunohistochemistry on brain slices taken from mice at 1d, 3d, 7d, 30d, 60d, and 120d post-injury, staining for late neuronal progenitor cells. The generation, maturation, and integration of newborn neurons is a tightly regulated process critical for normal hippocampal function, but this process can be disrupted by pathological insults such as TBI (Amrein et al., 2011; Ngwenya and Danzer, 2018). There is some controversy whether this disruption sparks an influx or efflux in neurogenesis. Some groups have found TBI increases cell proliferation (Gao et al., 2009; Dash et al., 2001; Urrea et al., 2007), while others report a decrease in new neurons after injury (Rola et al., 2006). However, these changes may be due in part to acute selective death of these newborn cells (Gao et al., 2008). To date, reports on neurogenesis after TBI have all been focused on the injured hippocampus, often using the contralateral hemisphere as a control. These methods do not consider widespread pathology which may affect the contralateral side as well.

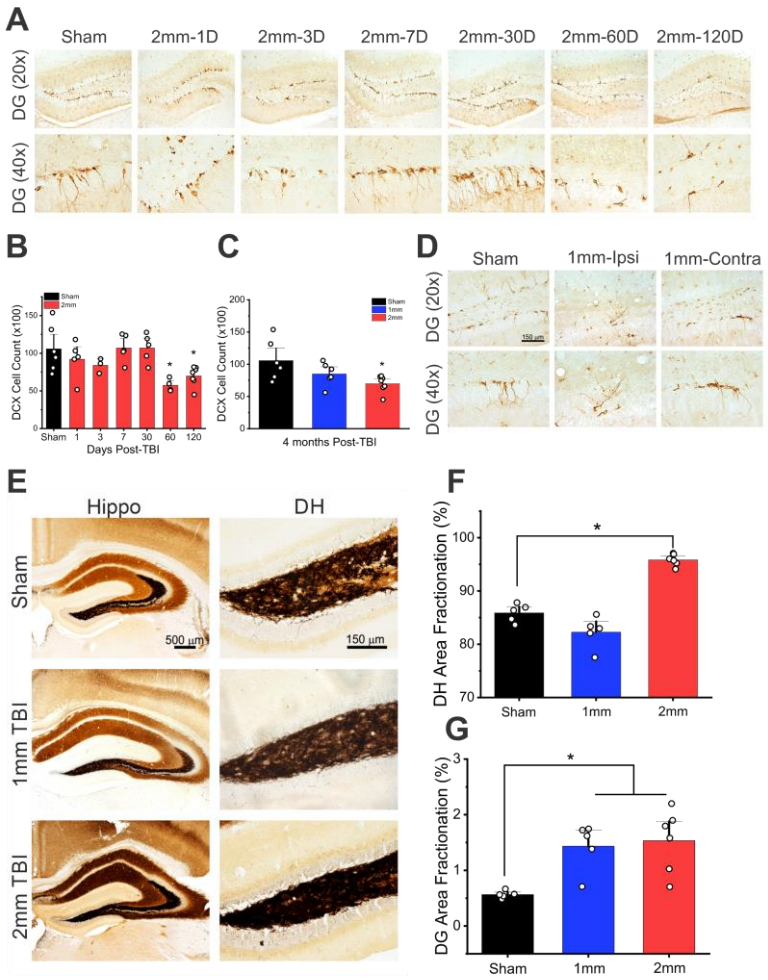

Figure 17: Fluctuations in Neurogenesis after TBI and Aberrant Mossy Fiber Sprouting in PTE.

A, Time-course of DCX+ immunohistochemistry in Sham and TBI (2-mm) cohorts at 1D, 3D, 7D, 30D, 60D, and 120D post-injury to visualize fluctuations in neurogenesis. Images taken in DG at 10X and 40X. **B,** Cell counts of DCX+ cells in DG over time. **C,** Cell count of DCX+ cells in Sham, 1mm-TBI, and 2mm-TBI contralateral hippocampus at 120D post-injury. **D,** DCX+ immunohistochemistry in Sham, 1mm-TBI ipsilateral hippocampus, and 1mm-TBI contralateral hippocampus at 120D post-injury. Images taken in DG at 10X and 40X. For all DCX+ calculations, n = 8 sham; n = 5 per 2mm-TBI time-point; n = 6 1mm-TBI. **E,** Images of TIMM stained hippocampus and dentate hilus (DH) in Sham, 1mm-TBI, and 2mm-TBI contralateral hippocampus at 120D post-injury to visualize aberrant mossy fiber sprouting. Images taken at 4X (hippocampus) and 20X (DH). **F,** Densitometric area fractionation of DH at 120D post-injury in Sham, 1mm-TBI, and 2mm-TBI. **G,** Densitometric area fractionation of DG granule and molecular layers at 120D post-injury in Sham, 1mm-TBI, and 2mm-TBI. For all TIMM calculations, sample sizes: Sham = 5, 2mm-TBI = 5, 1mm-TBI = 4.

Newborn neurons express DCX from their generation and maintain that expression for up to 3 weeks. The contralateral hippocampal dentate gyrus was counted using neurostereology methods described above and compared to sham counterparts. We found no significant changes in the number of newborn neurons in the first month post-TBI in the contralateral hippocampus (Sham = 10577.19 ± 1271.59 cells, 2mm-1d = 9200.17 ± 1429.23 cells, 2mm-3d = 8399.76 ± 572.17 cells, 2mm-7d = 10711.25 ± 818.51 cells; 2mm-30d = 10702.54 ± 838.19 cells). However, at 60d post-TBI, a steep drop in the number of DCX neurons was found, which persisted as a chronic reduction in neurogenesis compared to sham mice at 120d (2mm-60d = 5744.39 ± 417.39 cells, $p = 0.0158$; 2mm-120d = 7575.50 ± 719.84 cells, $p = 0.0177$) (**Fig. 17A and B**). These fluctuations in neurogenesis are contrasted by the 1mm cohort which saw no decrease in neurogenesis at 120d post-TBI in the contralateral hippocampus (1mm-120d = 8514.38 ± 719.07 cells) (**Fig. 17C and D**).

Regardless of a change in the rate of neurogenesis, cells born in the hilar and molecular layers of the dentate gyrus or at the CA3 border have been suggested to play a role in epileptogenesis (Scharfman et al., 2000; Danzer, 2019). Images of the hippocampus reveal evidence of ectopic newborn cells residing in the hilar and molecular regions of the dentate gyrus, rather than the granule layer. These neurons are most prevalent at 30d post-TBI (**Fig. 17A**). Our data suggests a chronic alteration in neurogenesis and the maturation of these cells in the hippocampus after injury which may relate to negative recovery seen after TBI.

IV. 1.11 Mossy Fiber Sprouting in the Hippocampus in PTE

Mossy fiber sprouting is a hallmark morphological index of temporal lobe epilepsy. Post-traumatic seizures are often facilitated through limbic circuits associated with aberrant sprouting of dentate gyrus granule mossy fibers in many rodent models of temporal lobe epilepsy (Bolkvadze and Pitkanen, 2012; Hunt et al., 2009; Kelly et al., 2015; Lemos and Cavalheiro, 1995). It has been known for some time that aberrant manifestation of mossy fibers from the hilar regions through the molecular layer of the dentate gyrus are not only found in murine models but are also indicative of clinical epilepsies (Scheibel et al., 1974). Timm's staining was used on serial sections of the hippocampus at 120d following injury to determine if our model showed signs of zinc-rich mossy fiber organization. Compared to the sham cohort, 1mm-TBI animals did not show a significant change in mossy fiber density within either the dentate gyrus (DG) or dentate hilus (DH) regions ($p=0.05876$). However, there was an intense increase in the density of mossy fibers in the contralateral hilar region of 2mm impact animals, verifying widespread axonal sprouting of excitatory granule cells ($p=.000636$). Sparse to evenly distributed granules in the supragranular region of the dentate gyrus can also be seen in some, but not all TBI mice (**Fig. 17E-G**). As seen with previous lab groups, the supragranular sprouting in the contralateral hippocampus did not reach significance and was more apparent within the dorsal versus ventral hippocampus (Bolkvadze and Pitkanen, 2012; Hunt et al., 2009, 2010). Of note, our TBI mice showed much darker Timm staining in the stratum oriens of the CA regions, compared to sham mice. This suggests the basal dendrites and axons may contain greater levels of zinc in these regions

and the pervasive axonal sprouting of granule cells leads to the rewiring of a reverberatory excitatory circuit ultimately resulting in reduced seizure threshold.

IV. 1.12 Progressive Sensorimotor and Behavior Dysfunction in PTE

To test whether PTE is associated with comorbid behavioral and neurological dysfunction, we evaluated the progressive changes in sensorimotor function of mice after TBI. TBI and PTE are associated with comorbidities, including poor functional outcomes, depression, and cognitive deficits (Moore et al., 2006; Catroppa et al., 2008; Dieter and Engel, 2019). Patients who have posttraumatic seizures have worse long-term functional outcomes compared to their non-epileptic counterparts (Tubi et al., 2019). **Fig. 18** shows the time-course alterations in motor and other behavior in mice after TBI. Acute changes in body weight are a sensitive indicator of overall health and disease progression. A detailed description of our health scale can be found in the materials and methods section of this article. Both cohorts of TBI mice experienced a persistent reduction in body weight (**Fig. 18A**), but only the 2mm cohort were found to have other notable health issues including swelling or discharge from the eyes, inability to support their own body weight while walking or sitting, as well as kyphosis (**Fig. 18B**). Though many of these health outcomes normalized back to sham-operated animals by 30d, TBI mice body weights were consistently lower than the sham cohort throughout the study.

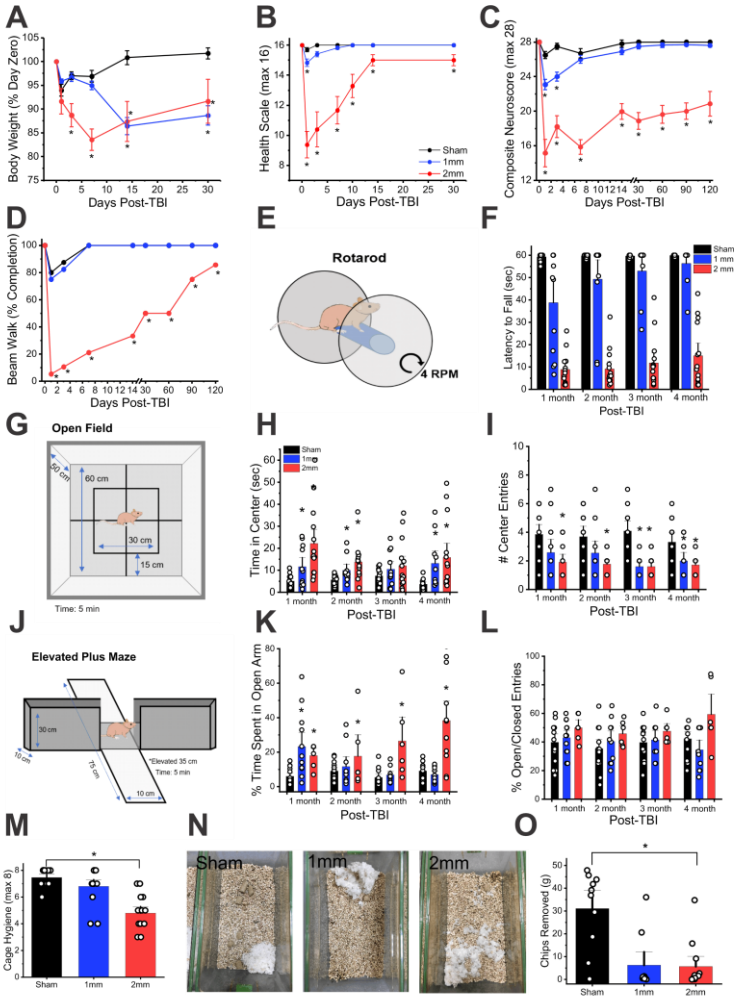

Figure 18: Sensorimotor and Behavior Functional Deficits after TBI and PTE in mice.

A, Changes in body weight over time, expressed as percent of day 0 body weight. **B,** Acute health recovery outcomes after TBI (max 16). **C,** Composite neuroscore over the 120-day observation period. It was set at max 28 score. **D,** Percent completion of ability to cross beam walk over time. **E,** Schematic of rotarod apparatus. Mice were placed on the rotarod cylinder for 60 s while it rotated at 4 rpm. **F,** Latency to fall from rotarod test. **G,** Schematic of open field apparatus. Mice were placed in center of arena and were free to explore for 5 min. **H,** Time spent in center square of open field arena. **I,** Number of entries into center square of open field arena. **J,** Schematic of elevated plus maze. Mice were placed into center of arena and were free to explore for 5 min. **K,** Percent time spent in open vs closed arms of elevated plus maze. **L,** Percent of entries into open arm vs closed arm. **M,** Cage hygiene index (max 8) at 120D post-TBI. **N,** Representative cages from Sham, 1mm-TBI, and 2mm-TBI cohort at 120D post-TBI. **O,** Amount of wood chips removed during burrowing test at 120-day post-injury.

Motor functional impairment

Acute and chronic functional impairment after TBI was investigated using three separate tests: Composite Neuroscore, Beam Walk, and Rotarod. Composite Neuroscore was graded on a scale of 0 (severely impaired) to 28 (normal) and focuses on responses to left/right propulsion by push, hind and forelimb flexion, as well as grip strength. 1mm TBI mice displayed some functional impairment assessed by Neuroscore in the first week after injury but improved to sham levels by 7d. Compared to both the sham and 1mm cohorts, 2mm-TBI mice showed severe impairments during the first week post-injury and gained little improvement after 14d (**Fig. 18C**). Since many 2mm-TBI mice were unable to complete the beam walk, we converted this behavioral assessment to a completion index. Only 5% of TBI mice were able to complete the beam walk on 1d. By 14d, this percent completion increased to 33% of TBI mice, and to 86% by 120d (**Fig. 18D**). Contrastingly, the 1mm cohort differed little from the sham group, with 75% of mice completing the beam walk test on 1d and improving to a 100% completion rate on 7d.

The rotarod test was completed at monthly increments after injury. The rotarod was held steady at a speed of 4 RPM for a duration of 60 s. All sham mice completed the task without difficulty, whereas TBI cohorts showed some impairment at all observation points (**Fig. 18E-F**). The 1mm cohort remained on the rotarod apparatus for an average of 38.78 ± 6.5 s at 1 month, compared to only 8.87 ± 1 s by the 2mm cohort. By 4 months post-TBI, the 1mm cohort had significantly improved their time, staying on for an average of 56.32 ± 2.44 s ($p > 0.05$ vs sham), whereas the 2mm cohort exhibited

much less improvement (2mm = 15.05 ± 3.81 s; $p < 0.001$ vs sham). Overall, these functional tests show trends of greatest improvement during the first two weeks following injury, with little improvement during the remainder of the study.

Anxiety behavior assessment

Anxiety-like behaviors were assessed at regular intervals throughout the study with the open field (OF) and elevated plus maze (EPM) tests. Instead of relying on learned responses or noxious stimuli which produce a conditioned response (i.e., treats, food/water deprivation, loud noises, electric shock), these tests exploit the animal's natural conflict between exploring a novel environment and seeking a secure shelter/protection. The degree of thigmotaxis has been previously validated as a measure of anxiogenic behavior—increased thigmotaxis suggests higher levels of anxiety (Seinbenhener and Wooten, 2015). We calculated the time spent within the center and perimeter regions as a function of total testing time (5 min) (**Fig. 18G**). Similar to previous reports (Popovitz et al., 2019), we found that TBI mice spent significantly longer amounts of time in the center zone of the open field arena compared to sham animals at 1 month post-TBI (1mm vs sham $p = 0.0183$; 2mm vs sham $p=0.0006$) (**Fig. 18H**), though number of entries into the center decreased in the TBI cohorts (4 month center entries Sham= 3.31 ± 0.43, 1mm = 2 ± 0.39, 2mm = 1.71 ± 0.19; $p = 0.018$ sham vs 1mm, $p = 0.0019$ sham vs 2mm) (**Fig. 18I**). These trends and differences held steady for all tested time points. Furthermore, TBI mice showed less activity than sham mice, indicating the opposite impact of brain injury on anxious behavior.

To further support our results, elevated plus maze was also performed on these cohorts on a different testing day. Animals were placed in the center of a 'plus' shaped maze consisting of two open arms and two closed arms (**Fig. 18J**). Animals were observed for 5 min, taking into consideration ambulatory activity, open and closed arm entries, and general exploratory behavior. Increased time spent and entries on/into the open arms suggests anxiolytic behavior (Walf and Frye, 2007). In general, we found TBI mice spent significantly longer amounts of time on the open vs closed arms (**Fig. 18K**). However, 1mm mice showed similar behavior to the sham cohort after the first testing period of 1-month post-TBI. Percent of open vs closed entries was similar between cohorts, suggesting severely injured mice spent more time in the open arms per entry than the other cohorts (**Fig. 18L**). Together, with the open field data, our results point towards anxiolytic behaviors in TBI mice. However, due to the reduction of overall ambulatory behavior within these tests, we conclude that TBI induces a diminished environmental awareness compared to sham controls resulting in altered exploratory behavior in these mice.

Depressive-like mood deficits

The assessment of distress, suffering, and depression are also potential comorbidities following brain injuries. Cage hygiene and burrowing performance observed in the animal's home cage can be valuable in assessing long-term brain malfunction and anhedonia (Jirkof, 2014). Construction of nests and the cleanliness of a cage if common in rodent species. Cage hygiene was assessed at 4 months post-TBI on a

scale of 0-8 (0 = very disorderly vs 8 = clean, healthy cage). We observed the nest complexity and amount of used nest material, location(s) of fecal and urinary waste, and the gathering of food by nest area. Sham mice typically built very fluffy, complex nests residing in a corner of the cage. Food pellets were often seen in or around the nest area, and fecal droppings/urination typically took place in 1-2 areas which were in corners or areas of the cage far from their nest. 1mm-TBI mice had similar nesting and cage hygiene behaviors to sham mice, but sometimes built fewer complex nests—using less of the provided nesting materials. Contrastingly, 2mm-TBI showed much more disorderly cages. Nesting material was often not used or spread throughout the cage with no discernable nest area. Fecal matter was more frequently spread out throughout the cage as well. The cage hygiene and nesting performance was significantly lower in 2mm-TBI mice compared to sham or 1mm-TBI animals (**Fig. 18M**). Example cage images can be seen in **Fig. 18N**. Furthermore, the burrowing test can be used to assess changes in typical burrowing behavior. Briefly, a tube with one closed end and one open end is filled with 50 g of novel woodchips and placed in the home cage. After 2 hours, we measured the weight of woodchips displaced from the tube. Sham mice removed a significantly higher amount of woodchips with an average of 31.1 ± 5.3 g, compared to an average of 6.2 ± 3.9 g or 5.7 ± 3.0 g woodchips in the 1mm and 2mm TBI groups, respectively ($p = 0.0014$ sham vs 1mm; $p = 0.0003$ sham vs 2mm) (**Fig. 18O**).

IV. 1.13 PTE is associated with Disrupted Discrimination and Spatial Memory

To test whether PTE mice show cognitive deficits, we evaluated the object recognition and spatial memory function in mice. Perhaps the most debilitating consequences of TBI are those of reduced cognitive functioning. Especially when TBI occurs at a critical developmental stage, patients experience chronic alteration in behavior, attention, memory, education, and ability to learn (Catroppa et al., 2008). Cognitive deficits caused by TBI can interfere with a patient's ability to work, perform activities of daily living, effect relationships or leisure time for years after the initial event (Rabinowitz and Levin, 2014). To investigate the long-term changes in cognitive function after TBI between moderate and severe injury, we used the Novel Object Recognition Test (NORT) and the Morris Water Maze (MWM). NORT has been used for decades to assess memory based off the innate exploratory behavior of the mouse and its preference for novelty (Ennaceur et al., 1988).

Object recognition memory

At approximately 1-month increments after TBI, mice were habituated to an open field arena for 5 min. Following habituation phase, the learning phase consisted of two 5 min trials in which an identical object was placed in two opposite corners of the arena. Mice were given free access to explore these objects at leisure. Twenty-four hours following the learning phase, one of the familiar objects was replaced with a novel object (**Fig. 19A**). At all observed time-points, 2mm-TBI mice showed reduced time spent investigated the novel object compared to the familiar object (**Fig. 19B and C**). A

decrease in percent time spent investigating the novel object was also seen in 1mm-TBI mice, though this data was not significantly lower than sham mice. These results suggest that TBI-induced cognitive deficits on memory occur early on and persist long after the recovery period.

Spatial learning and memory

Our results are further supported by MWM. Following all other testing procedures, mice were trained in a hidden platform water maze assessment. The learning phase lasted 4 days with each day having six 60 s trials (starting locations N, W, E, NW, NE, SW; platform located in SE quadrant). After reaching the platform or maxing out the time in each trial, the mouse was guided to the platform and remained for 15 s before being placed in a cage to dry off. Two testing days were used to assess memory—the first occurred 24 hours after the final learning day, and the second occurred 5 days following the final learning day (**Fig. 19D**). To evaluate the active process of learning, we investigated the latency and distance to the platform during the four learning days. Swimming speed was determined to be different between the sham and TBI mice, which affects latency to the platform. However, distance is not affected by speed and may be a better indicator of test performance under these conditions. Trial data for each learning day were averaged for each mouse before obtaining the cohort averages. Representative traces from learning day 2 of sham, 1mm, 2mm mice can be seen in **Fig. 19E**. Sham mice learned to reach the platform quickly, taking only 7.94 ± 1.63 s to travel a 131.9 ± 20.5 cm path by learning day 4. The 1mm cohort also learned to reach the platform

faster with each consecutive day, though their scores for time and distance were significantly impaired compared to sham mice (Day 1 1mm= 35.9 ± 2.13 s and 605.9 ± 42.8 cm; Day 4 1mm= 15.52 ± 1.45s and 244.8 ± 38.8 cm). Similarly, the 2mm-TBI mice showed severe deficits in cognitive function assessed by MWM. Though some learning did take place, there was little improvement in their latency and distance to platform throughout the learning trial period (Day 1 2mm= 41.23 ± 7.1 s and 660.9 ± 92.5 cm; Day 4 2mm= 35.61 ± 5.98 s and 418.8 ± 46.6 cm) (**Fig. 19F and G**).

We conducted two memory probes on days 1 and 5 following the final learning trials to assess short-term and long-term memory. The hidden platform was removed from the water tank, and mice were given 60 s to search for the previously stationed platform. Time spent in the target quadrant was calculated to determine memory function, since mice had previously learned where the platform was supposed to be located. Cohorts of 1mm and 2mm TBI mice showed significant memory deficits at both time-points, as they spent less time in the target quadrant compared to sham mice (**Fig. 19H**). Thus, these results show striking deficits in MWM test in which TBI mice took significantly more time and distance to learn the location of the hidden platform compared to sham mice. They also spent less time in the target quadrant searching for the platform on memory probe days, suggesting that not only is the learning process affected by brain injury but that retrieval of learned responses is also impaired.

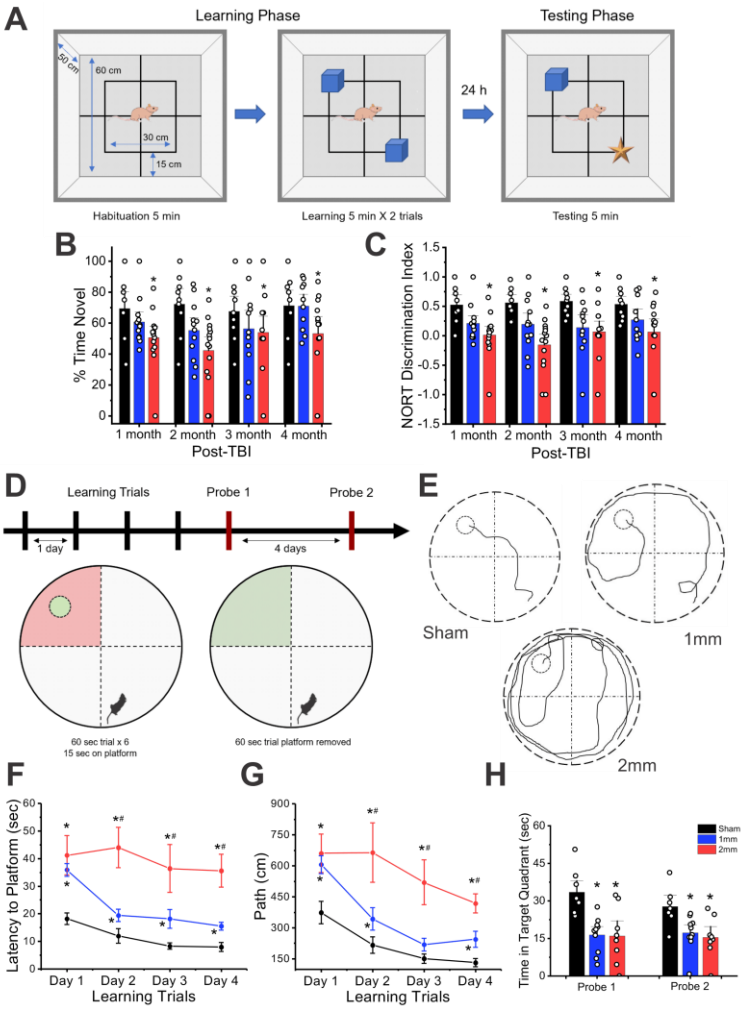

Figure 19: Long-term Memory Dysfunction in PTE mice.

A, Schematic of novel object recognition test (NORT). For full methodology, see methods section. **B,** Percent time spent investigating the novel object vs familiar object. **C,** Discrimination index (DI) calculates the discrimination between the novel and familiar objects by subtracting the time spent exploring the familiar object from the time spent exploring novel object and dividing the result by the total time of exploration. **D,** Schematic of Morris water maze protocol used at 4 months post-TBI. Mice had four days of learning trials each with 6- 60s trials. After each trial, mice were placed on platform for 15 s before being removed from arena. 24 hr and 5 days following last learning trial, the platform was removed, and mice were given 60 s to explore arena. Time spent in target quadrant was calculated on probe days. **E,** Representative path traces from learning trial day 3 in Sham, 1mm-TBI, and 2mm-TBI cohorts. **F,** Average latency to platform (sec) during learning trials. **G,** Average distance (cm) traveled to reach platform. **H,** Time spent in target quadrant on probe days during Morris water maze.

IV. 2 Targeting Epigenetic Pathways Reduces Inflammation and Provides Neuroprotection in a Mouse Model of Post-Traumatic Epilepsy

Nearly 70 million traumatic brain injuries (TBI) occur worldwide every year, representing an ever-growing public health crisis (Dewan et al., 2018). Initial and secondary damage from TBI can lead to catastrophic life-long disabilities, including the onset of the acquired seizure disorder, post-traumatic epilepsy (PTE). Due to the heterogenous underlying pathophysiology of PTE at different phases of the disease, determining an appropriate drug regimen for improving the prognosis of affected patients is challenging. Currently, there are no therapeutics in clinical use which can halt or prevent epileptogenesis following TBI.

Recently, our lab found an intimate role between epigenetic regulation and the control of epileptogenesis in a kindling model of temporal lobe epilepsy (Reddy et al., 2018). Epigenetics refers to modifications, such as acetylation or methylation to the DNA or accompanying histone proteins causing alterations in gene expression without directly altering the genetic code. Histone acetylation is controlled by two opposing proteins, histone acetyltransferases (HATs) and histone deacetylases (HDACs). These enzymes play a critical role in chromatic remodeling and the regulation of gene expression. TBI is known cause persistent hyperactivation of HDACs within the hours following initial injury, contributing to upstream excitotoxic and inflammatory cascades (Gao et al., 2006; Zhang et al., 2008). TBI-induced inflammatory responses are driven primarily by resident microglial cells acting together with additional immune effectors. Ramified microglia transform to an activated phenotype with shorter processes and

migrate to the site of injury. Prolonged neuroinflammation can exacerbate neurodegeneration and lead to poorer prognosis (Rock and Kono, 2008). Recently, Patnala et al. demonstrated the HDAC inhibitor, sodium butyrate, epigenetically augments the microglial inflammatory response by concurrently downregulating pro-inflammatory mediators such as NOS2 and TNF-α and upregulating the anti-inflammatory cytokine IL-10 (2017). Furthermore, studies on HDAC inhibition therapy have revealed *in vitro* and *in vivo* neuroprotective effects in CNS disorders such as ischemic stroke (Kim et al., 2007), spinal cord injury (Zhang et al., 2018), Huntington's disease (Ferrante et al., 2003), and acquired learning disabilities (Dash et al., 2009).

Sodium butyrate is a broad Class I and II histone deacetylase inhibitor with blood brain barrier permeability (Stilling et al., 2016). Sodium butyrate is a natural product of the intestinal microbial fermentation during digestion and like other HDACi in its class, it has been shown to stop the proliferation of cancer cells, induce differentiation, alter gene expression, and stimulate apoptosis (Kruh, 1981). Given its wide range of neuroprotective effects and role in epigenetic modification of inflammatory disorders (Furusawa et al., 2013), we sought to investigate sodium butyrate as a potential therapeutic agent for PTE and its associated comorbidities. Our results demonstrate how post-injury administration of sodium butyrate (SB) modifies seizure progression and neuropathology following TBI, resulting in improved quality of life.

IV. 2.1 Systemic Sodium Butyrate Administration Normalizes TBI-induced Increase in HDAC Activity

To induce a diffuse cortical-hippocampal TBI, we chose a CCI model calibrated to severe injury in adult male mice aged 12-16 weeks. Previous studies of PTE, including work in our own lab, have shown a moderate 1mm injury produces 0-40% incidence of spontaneous recurrent seizures (SRS) (Kochanek et al., 2006; Hunt et al., 2009; Golub and Reddy, 2021). Therefore, to produce a reliable incidence of epilepsy, we utilized a severe 2mm impact depth (4.0 m/s, 3 mm diameter, 80 ms dwell). Sham animals underwent the same protocol, with exclusion of the impact. Following TBI-injury, mice were assigned to untreated, or sodium butyrate treated cohorts. Sodium butyrate was administered 600mg/kg i.p. twice daily for 21 days, with first injection starting 1 hr post-TBI. Untreated mice were administered vehicle injections. The rationale for this dosing scheme was multifactional. We aimed to assess a treatment regimen that would reasonably approximate the timing of first dose given by emergency medical technicians with continued long-term therapy throughout the critical latency period before SRS onset. Mortality at 120d post-injury was 28% in the TBI cohort, 10% in the SB cohort, and 0% in the Sham cohort.

To determine the extent of inhibition on HDAC activity following TBI, we used a fluorometric Boc-Lys(Ac)-AMC assay at 4 hr, 24 hr, and 72 hr post-TBI in cortex and ipsilateral hippocampus tissues (Reddy et al., 2018). For further validation of prolonged hyperactivation of HDAC activity, we also performed the Boc-Lys(Ac)-AMC assay at 1-month post-injury in the cortex, representing a timepoint that is one week following the

last administration of sodium butyrate. Sodium butyrate has been previously shown to be an inhibitor of histone deacetylase (HDAC) enzymes, and preserves acetylation at H2A, H3, and H4 histones (Vidali et al., 1978). TBI is known to induce a sharp increase in HDAC activity within the first hours following injury, leading to decreased acetyl-H3 and acetyl-H4 proteins (Gao et al., 2006).

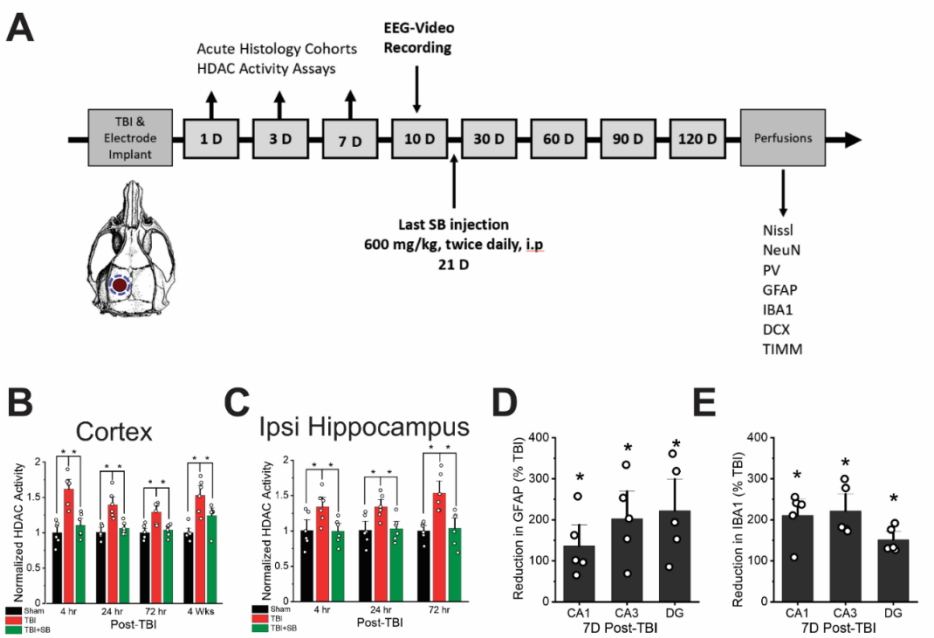

Figure 20: Systemic Sodium Butyrate Administration Normalizes TBI-Induced Hyperactivation of HDAC.

A, Experimental design. TBI surgeries occurred over the left hippocampus, with the diameter of craniectomy being 1mm wider than the impact site. Acute histology was taken on days 1, 3, and 7 post-TBI. EEG recording began on 10d post-TBI allowing for full recovery from surgery. Sodium butyrate injections were given twice daily for up to 21d post-TBI. Behavioral testing occurred at all time-points listed. Perfusions for chronic immunohistochemistry took place following the last behavior testing timepoint. **B,** HDAC activity assay in the cortex of Sham, TBI, and SB cohorts displayed in relative units normalized to Sham. Sample size: triplicates from n=6 mice/group. **C,** HDAC activity assay in the ipsilateral hippocampus of Sham, TBI, and SB cohorts displayed in relative units normalized to Sham. Sample size: triplicates from n=6 mice/group. **D,** Percent reduction in GFAP markers by systemic sodium butyrate administration, expressed as %TBI. Sample size: n=5/group. **E,** Percent reduction in IBA1 markers by systemic sodium butyrate administration, expressed as %TBI. Sample size: n=5/group.

TBI induced a sharp 34-54% increase in HDAC activity over sham in the ipsilateral hippocampus that remained steady over the first 72 hr post-injury (**Fig. 20B**). This robust change was also seen up to 1-month post-TBI in the cortex (sham=1.001 ± 0.041-0.066 relative units vs 4hr-TBI=1.619±0.091; 24hr-TBI=1.396±0.077; 72hr-TBI=1.301±0.060; 4wk-TBI=1.528±0.0962) (**Fig. 20C**). Sodium butyrate administration significantly ameliorated the spike in HDAC activity in both the ipsilateral hippocampus and cortex at all time-points ($p>0.05$; cortex: 4hr-SB=1.105±0.001; 24hr-SB=1.063±0.035; 72hr-SB=1.037±0.035; 4wk-SB=1.241±0.039) (**Fig. 20B-C**). The specialized response of neuroinflammation by microglia is regulated by epigenetic mechanisms including the modulation of H3K9 acetylation (Patnala et al., 2016). The normalization of TBI-induced hyperacetylation by sodium butyrate was associated with a significant reduction in expression of neuroinflammatory markers GFAP and Iba-1. At 7d post-injury, sodium butyrate reduced expression of GFAP by 186.9±43.5% and Iba-1 by 194.4±22.5% in the contralateral hippocampus compared to the untreated cohort ($p>0.001$). **Fig. 20D-E** show reduction of GFAP and Iba-1 by region of interest (CA1, CA3, DG) compared to TBI. These results suggest that normalization of HDAC activity by sodium butyrate may act at promotors which affect the immune response, thereby acting as an anti-inflammatory agent.

IV. 2.2 Sodium Butyrate Treatment Suppresses Acute Inflammation after TBI

To further define the neuroprotective role of SB treatment against inflammation, we performed an acute time-course of immunohistochemistry on GFAP+ and Iba-1+ at

1d, 3d, and 7d post-TBI. TBI causes an upregulation of the intermediary filament, glial fibrillary acidic protein (GFAP), in astrocytes as well as an increase of microglial infiltration and activated morphology (Iba-1) (Golub and Reddy, 2021). Though these processes can be essential for protecting against secondary damages, prolonged astrogliosis and microgliosis is a critical contributor to poorer prognosis and comorbidities associated with TBI (Oleskii et al., 2019). Excessive release of pro-inflammatory mediators can exacerbate cell loss. Previous studies have shown sodium butyrate significantly reduces *Stat1* gene expression in activated microglia, an essential transcription factor for driving the immune response (Patnala et al., 2016).

Densitometric analysis of hippocampal regions CA1, CA3, and DG indicated that GFAP expression increased at similar rates at 1d and 3d post-injury compared to sham. However, by 7d post injury, sodium butyrate treatment significantly reduced GFAP expression in all three regions of interest (CA1: TBI=521.73±32.22% vs SB=385.48±34.08, p=0.0197, CA3: TBI=599.92±23.93% vs SB=397.62±44.78%, p=0.0004; DG: TBI=573.78±44.79% vs SB=351.68±51.58%, p=0.0117) (**Fig. 21A-E**).

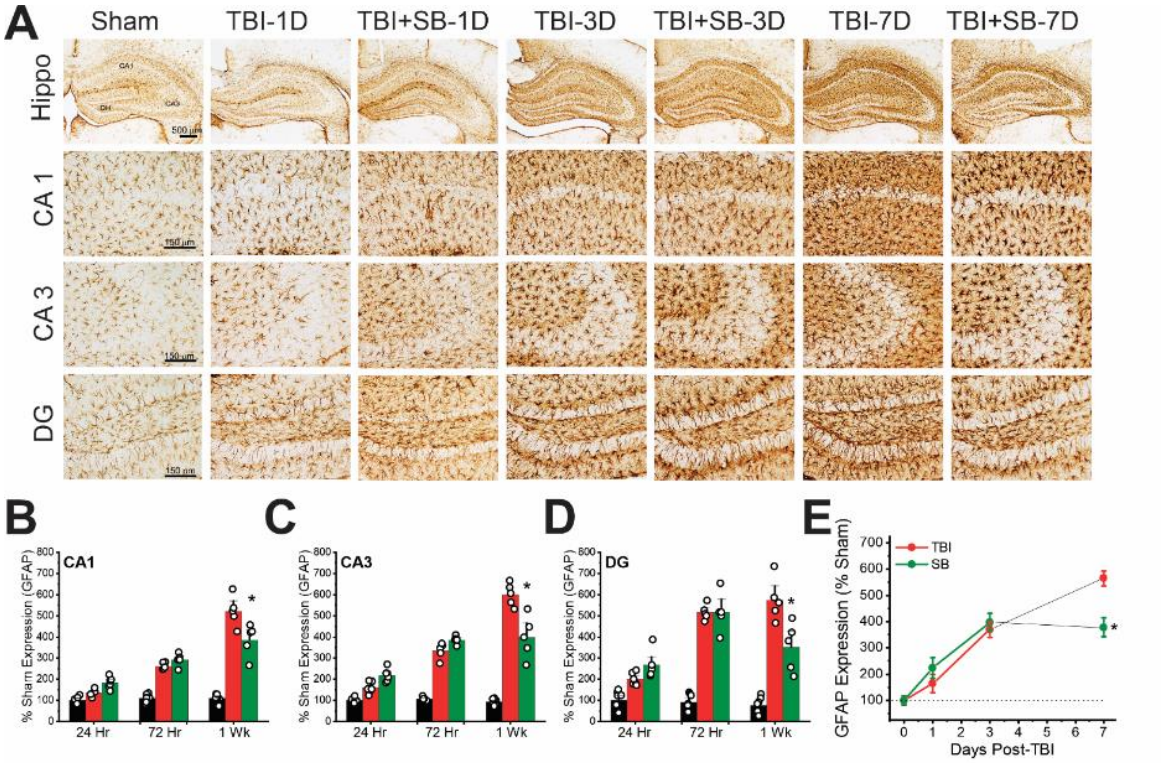

Figure 21: Sodium Butyrate Treatment Suppresses Acute Astrogliosis after TBI.

A, Acute time-course of contralateral hippocampal GFAP+ immunohistochemistry in Sham, TBI, and SB cohorts at 1d, 3d, and 7d post-injury to visualize astrogliosis. Hippocampal images taken at 4x. CA1, CA3, and DG images taken at 20x. **B,** Densitometric analysis of GFAP+ expression in CA1 in Sham, TBI, and SB cohorts expressed as percent Sham. **C,** Densitometric analysis of GFAP+ expression in CA3 in Sham, TBI, and SB cohorts expressed as percent Sham. **D,** Densitometric analysis of GFAP+ expression in DG in Sham, TBI, and SB cohorts expressed as percent Sham. **E,** Total hippocampal change in GFAP+ expression between TBI and SB cohorts over time, expressed as percent Sham.

A similar pattern was observed with Iba-1. Overtime, the contralateral hippocampus shows a dramatic increase in both number of microglia present and general expression within the cells in the TBI cohorts compared to sham; however, by 7d post-injury, sodium butyrate administration significantly lowered Iba-1 expression in the CA1, CA3, and DG (CA1: TBI=681.31±28.33 vs SB=471.01±26.47, $p>0.0001$; CA3: TBI=463.43±25.57 vs SB=241.87±27.45, $p>0.0001$; DG: TBI=318.79±21.67 vs SB=167.41±13.50, $p>0.0001$) (**Fig. 22A-E**). Our results suggest that sodium butyrate acts to significantly modify the immune response, reducing both microglial and astrocytic activation and recruitment to the contralateral hippocampus.

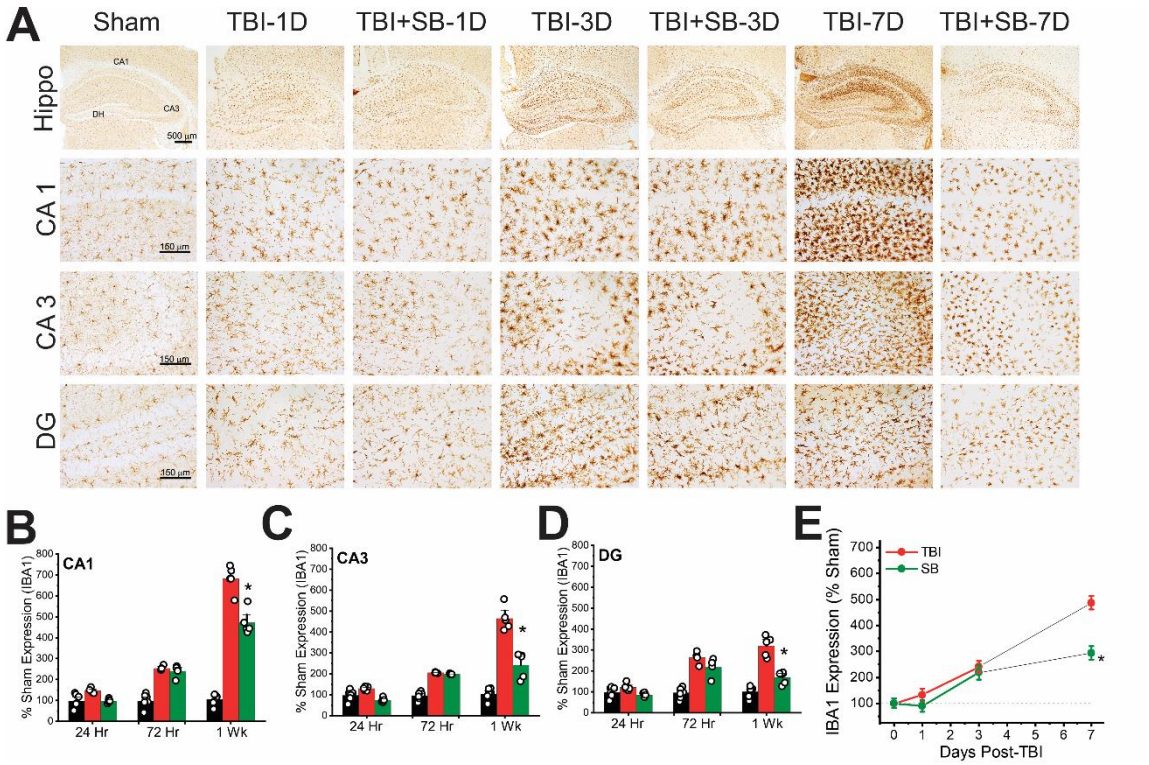

Figure 22: Sodium Butyrate Treatment Suppresses Acute Microgliosis after TBI.

A, Acute time-course of contralateral hippocampal IBA1+ immunohistochemistry in Sham, TBI, and SB cohorts at 1d, 3d, and 7d post-injury to visualize microgliosis. Hippocampal images taken at 4x. CA1, CA3, and DG images taken at 20x. **B,** Densitometric analysis of IBA1+ expression in CA1 in Sham, TBI, and SB cohorts expressed as percent Sham. **C,** Densitometric analysis of IBA1+ expression in CA3 in Sham, TBI, and SB cohorts expressed as percent Sham. **D,** Densitometric analysis of IBA1+ expression in DG in Sham, TBI, and SB cohorts expressed as percent Sham. **E,** Total hippocampal change in IBA1+ expression between TBI and SB cohorts over time, expressed as percent Sham.

IV. 2.3 Sodium Butyrate Reduces Progressive Tissue Loss and Lesion Volume

To examine the effect of sodium butyrate treatment on lesion volume after TBI, we used stereological volume counting techniques to measure progressive tissue loss around the impact site at 1d and 120d after injury. Coronal slices throughout the entirety of impact diameter were photographed and evaluated. Representative slices showing dorsal and ventral hippocampi can be seen in **Fig. 23A**. We observed substantial losses of tissue, encompassing both the upper cortical and hippocampal areas at 1d post-injury (Total lesion volume, Sham = 0.4123±0.111 mm^3 ; TBI = 6.041±0.943 mm^3 ; TBI+SB = 6.439±1.172; Hippocampal lesion volume, Sham = 0.1813±0.050 mm^3; TBI = 3.322±0.682 mm^3; TBI+SB = 2.719±0.599) (**Fig. 23B-C**). Tissue loss in the TBI cohorts extended into the thalamus at 120d post-injury, though total lesion volume was significantly reduced by sodium butyrate treatment (Total lesion volume, TBI = 22.49±1.21 mm^3 ; TBI+SB = 18.06±1.49 mm^3, p=0.0414) (**Fig. 23D-E**). Our results suggest beginning sodium butyrate treatment 1-hr post-injury is not adequate for preventing initial damage from TBI; however, long-term treatment did provide neuroprotection against progressive necrosis and tissue loss.

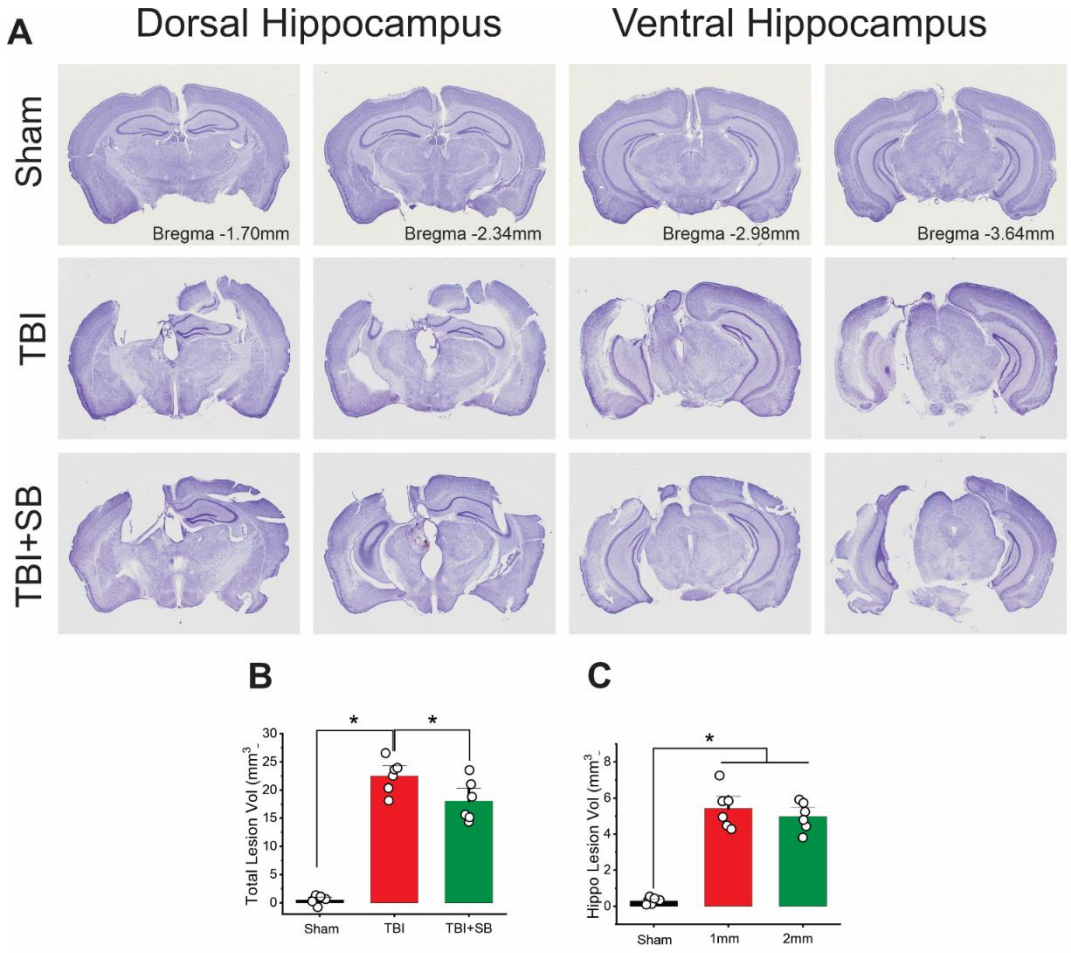

Figure 23: Sodium Butyrate Reduces Progressive Tissue Loss and Lesion Volume.

A, Coronal slices of whole brain showing dorsal and ventral hippocampus in Sham, TBI, and SB cohorts. **B,** Total lesion volume in Sham, TBI, and SB cohorts at 1d post-injury. Sample size n=5/group. **C,** Hippocampal lesion volume in Sham, TBI, and SB cohorts at 1d post-injury. Sample size n=5/group. **D,** Total lesion volume at 120d post-injury in Sham, TBI, and SB cohorts. Sample size n=6/group **E,** Hippocampal lesion volume at 120d post-injury in Sham, TBI, and SB cohorts. Sample size n=6/group. *p<0.05 vs. Sham or TBI group, when appropriate (n = 5-6 per group); one-way ANOVA with Bonferroni or Tukey HSD post hoc test.

IV. 2.4 HDACi Therapy Reduces Burden of Post-Traumatic Seizures

Electrophysiological events play a key role in the progression of brain injury, including excitotoxicity, spontaneous recurrent seizures (SRS), epileptiform discharges, and changes in sleep cycle. EEG seizure activity can occur in the absence of overt behavioral manifestations common to status-induced or temporal lobe seizures. Therefore, it is critical that continuous EEG monitoring for the duration of the experiment be used to confirm any epileptic event. Following TBI, mice were implanted with an EEG electrode for 24/7 video-EEG recording in the contralateral hippocampus. Recording began immediately following a 10-day recovery period.

Eighty-five percent of TBI mice and 75% of SB mice developed seizures over time. TBI mice displayed a robust evolution of seizure activity, beginning at 21d post-injury in some animals. Sodium butyrate treatment did not prevent the development of electrographic SRS and the latency to first seizure was similar between cohorts. However, sodium butyrate treatment significantly modified seizure burden by reducing both daily seizure frequency and average seizure duration (**Fig. 24A-E**). Average daily seizures per animal ranged from 0 – 4.8±1.09 in the TBI cohort, with highest frequency towards the end of the observation period. This frequency was reduced to 0 – 1±0.632 seizures with HDACi therapy (**Fig. 24A**). Cumulative seizures per cohort fell from 626 in untreated to 103 in treated mice, and average number of seizures per animal dropped from 62.6±14.3 to 17.2±3.5 (p=0.0382) (**Fig. 24F-G**). Similarly, we observed a significant reduction in average seizure duration and total time seizing between cohorts

(Avg duration, TBI=42.5±5.62s vs SB=31.58±1.72s, p=0.0214; Total time seizing, TBI=444.53 min vs SB=64.21 min, p<0.001) (**Fig. 24H-I**).

To determine whether HDACi therapy effected seizure threshold after TBI, we used the 6 Hz corneal stimulation test. As with our previous studies, we pretested additional cohorts of non-implanted mice for a seizure threshold of 35 mA, the average 6 Hz threshold for our strain of mice. Seizure thresholds began to fall dramatically as early as 7d post-injury in both groups. By 120d post-injury, the untreated mice displayed a threshold of 52.4±5.73% of their day zero measurement. However, we observed a plateaued reduction in the SB cohort which leveled off by 30d post-injury with a final reading of 70.5±7.92% (**Fig. 24J-K**). Together, these results suggest HDACi therapy modifies the progression and burden of chronic seizures following TBI by ameliorating the reduction in seizure threshold.

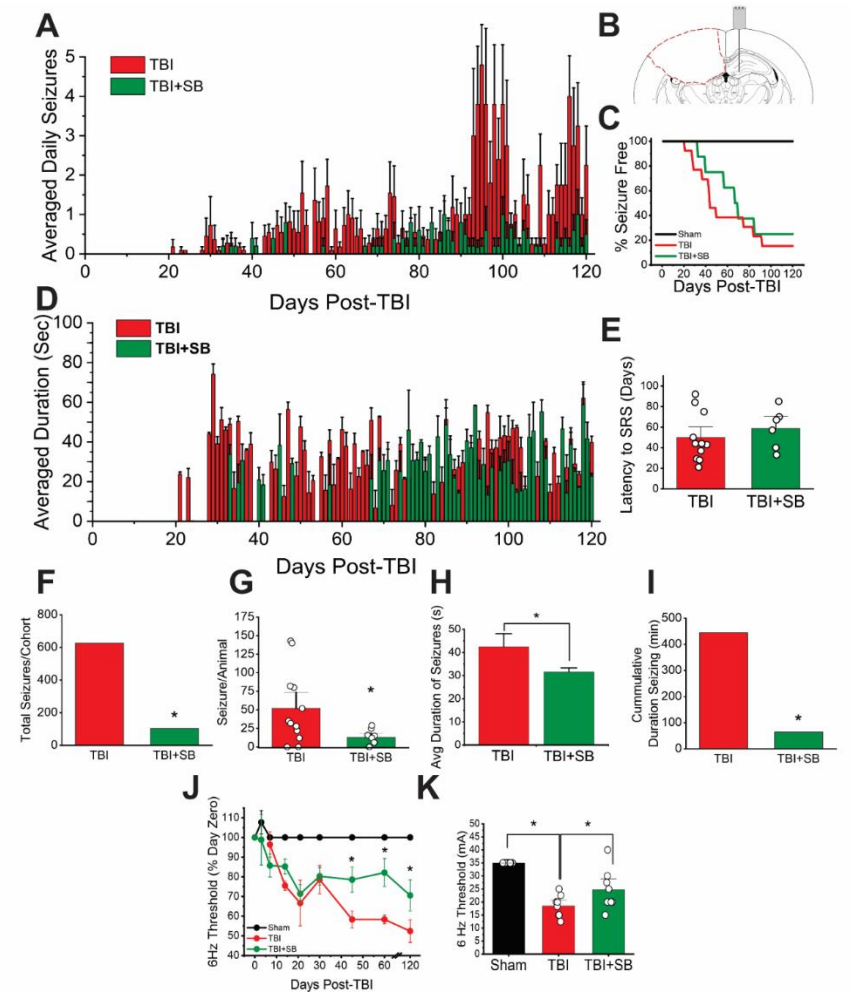

Figure 24: Sodium Butyrate Therapy Reduces Burden of Post-Traumatic Seizures. **A,** Average seizures per day per animal over 120-day observation period for both TBI and TBI+SB cohorts. Following two-week recovery period from CCI, mice were hooked to 24/7 video-EEG recording. Seizures were identified through a custom MatLab algorithm. Only responding animals were used for calculations. **B,** Representative atlas of TBI impact area and corresponding electrode placement in contralateral hippocampus. **C,** Incidence curve of epileptic animals over time, showing latency to first spontaneous recurrent seizure (SRS). **D,** Average duration of seizures per day over 120 days. All seizure events on each day from responding mice were used in calculations. **E,** Average latency to first SRS. **F,** Total number of seizures over 120-day observation period within TBI and SB cohorts. **G,** Average number of seizures per animal within TBI and SB cohorts. **H,** Average duration of seizures. All seizure events from responding mice were used in calculations. **I,** Cumulative duration of time seizing in min between TBI and SB cohorts. **J,** Seizure threshold in TBI and SB cohorts over time. Additional non-implanted cohorts were generated to determine seizure thresholds using the 6Hz model. **K,** 6Hz seizure threshold of Sham, TBI, and SB cohorts at 120 days post-injury.

IV. 2.5 HDACi Therapy Reduces Frequency of Epileptiform Discharges

Next, we analyzed the EEG output using a customized MatLab code for non-motor epileptiform discharges which have been known to be associated with the human condition of TBI and hippocampal atrophy (Vespa et al., 2010). Previous work in our lab has shown that these short bursts of non-convulsive seizure activity often precede generalized ictal events (Golub and Reddy, 2021). Electrographic discharges lasting between 3-9s were identified in 92% of the TBI and 75% of the SB cohorts, though frequency of discharges was significantly lower with sodium butyrate treatment. Average frequency ranged from 0 – 4.72 ± 2.74 per day per animal in the TBI cohort, compared to 0 - 1.6 ± 1.12 in the SB cohort (**Fig. 25A-B**, $p<0.0001$). Onset of epileptiform activity did not differ between cohorts. Average duration of discharges was similar between groups, but cumulative time spent experiencing epileptiform discharges was significantly lowered with HDAC inhibition therapy. The TBI cohort spent a total of 106.2 min having non-convulsive discharges over the 120-day observation period versus only 7.8 min in the SB cohort ($p<0.0001$). Likewise, the number of total discharges per cohort and per animal were significantly reduced in the treated group (Total cohort discharges, TBI=1125 vs SB=89, $p<0.0001$; avg discharge per animal, TBI=92.5±23.5 vs SB=14.8±4.2, $p=0.0354$) (**Fig. 25C-H**). Onset of epileptiform activity did not differ between cohorts (**Fig. 25I**). Together, our data shows sodium butyrate administration significantly reduces the frequency of EEG abnormalities following TBI, suggesting long-term improvement in brain circuitry and functionality.

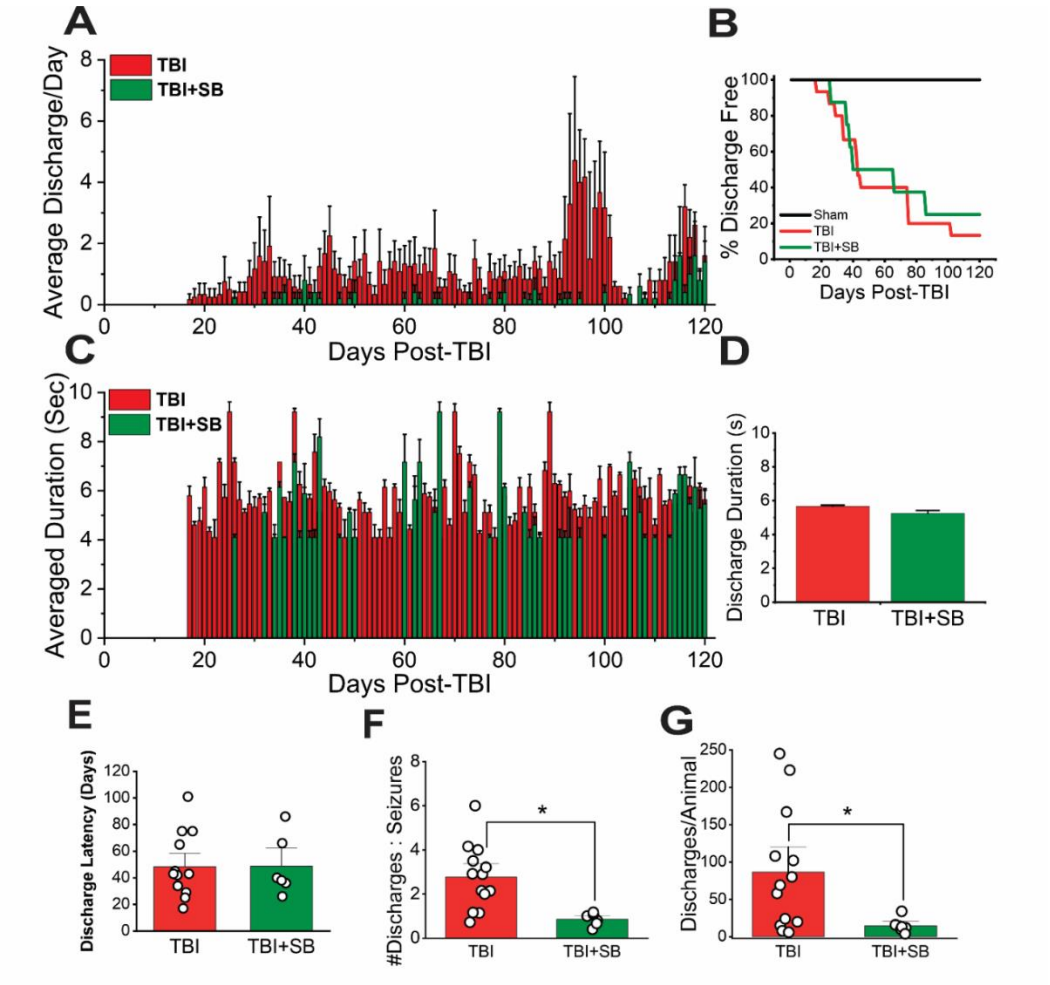

Figure 25: Butyrate Therapy Reduces Frequency of Epileptiform Discharges. **A,** Average epileptiform discharges per day per animal over 120-day observation period for both TBI and SB cohorts. Following a mandatory recovery period from CCI, mice were hooked to 24/7 video-EEG recording. Epileptiform discharges (3 – 9s) were identified through a custom Matlab script. Only responding animals were used for calculations. **B,** Incidence curve showing latency to first epileptiform discharge over time. Sham animals did not experience any epileptiform discharge activity. **C,** Average duration of discharges per day over 120 day observation period. All epileptiform discharge events on each day from responding mice were used in calculations. **D,** Average duration of discharges between TBI and SB cohorts. **E,** Cumulative minutes spent experiencing discharges for TBI and SB cohorts during observation period. **F,** Total number of discharges within TBI and SB cohorts. **G,** Average number of discharges per animal within TBI and SB cohorts. **H,** Ratio of number of discharges to number of seizures for each responding animal. Only animals which experiences both seizures and discharges were used for calculation. **I,** Average latency to first epileptiform discharge.

IV. 2.6 Sodium Butyrate Ameliorates Neurodegeneration

To determine if HDAC inhibition therapy could reduce long-term neurodegeneration, we performed stereological analysis on NeuN+ principal neurons and PV+ interneurons in the contralateral hippocampus at 7d and 120d post-TBI. Progressive necrosis and neuron loss are critical contributing factors to the development of seizures as well as the cognitive impairment and psychological changes which are often associated with TBI (Tai et al., 2016; Dieter and Engel, 2019). Consistent with our previous findings, no NeuN+ and PV+ cell loss was observed in the contralateral hippocampus in either cohort at 7d post-injury (**Fig. 26A and D**). However, at 120d post-injury, TBI mice showed significant loss of both cell types. TBI mice showed significant loss of NeuN+ cells in all hippocampal regions of interest compared to sham, with the greatest loss (>43%) within the CA3 (Total Hippocampus: Sham=625523.3±14484.92 vs TBI=397559.8±18790.04, $p<0.0001$). Sodium butyrate treated animals maintained 86.8% of NeuN+ hippocampal cells relative to sham mice, representing a significant rescue of 23.3% of TBI-induced neurodegeneration (Total Hippocampus: TBI=397559.8±18790.04 cells vs SB=543217.99±14525.45 cells, $p>0.0001$) (**Fig. 26B-C**).

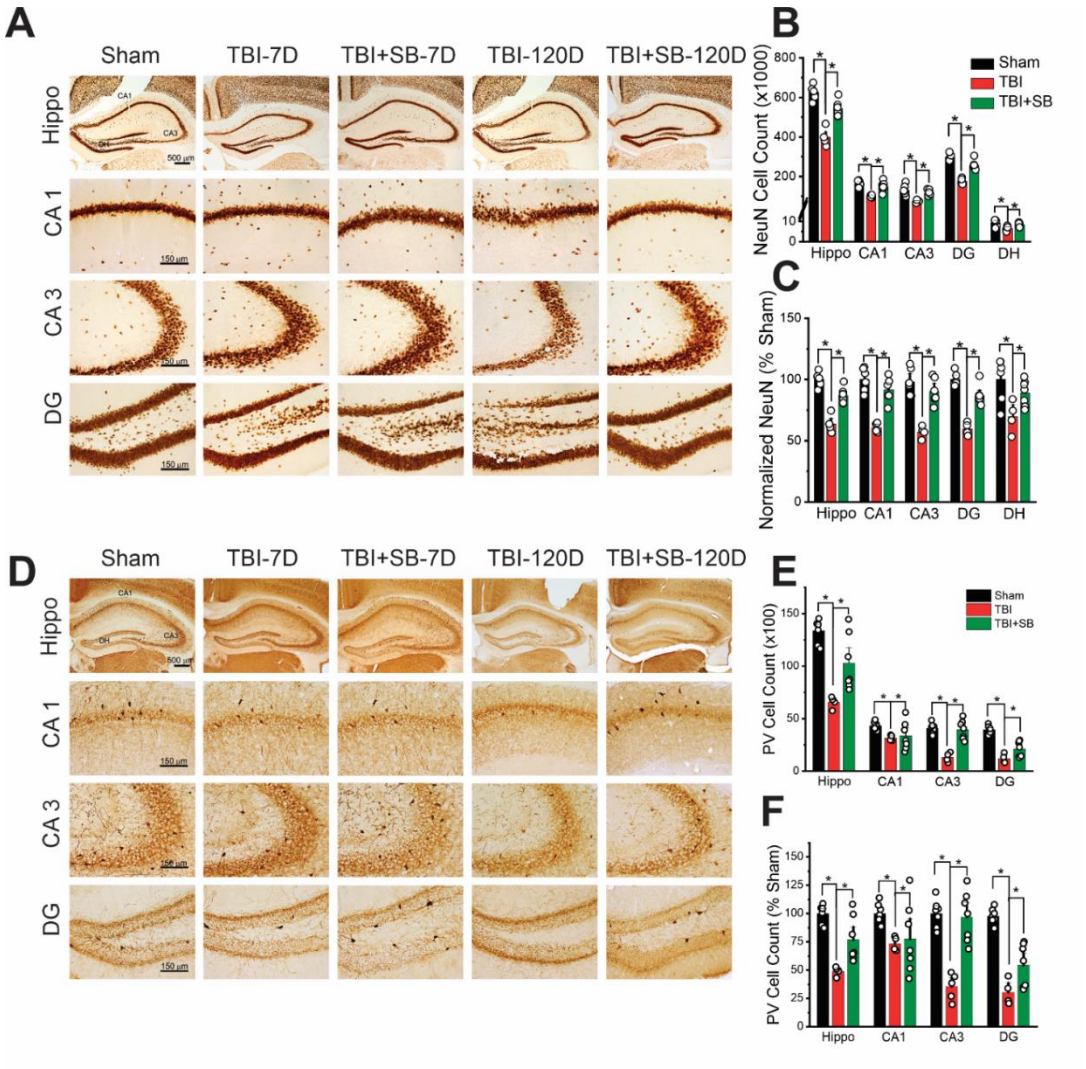

Figure 26: Sodium Butyrate Ameliorates Neurodegeneration.
A, NeuN+ immunohistochemistry of the contralateral hippocampus in Sham, TBI, and SB cohorts at 7d and 120d post-injury to visualize healthy principal neurons. Hippocampal images taken at 4x. CA1, CA3, and DG images taken at 20x. **B,** Total NeuN cell count divided by hippocampus and regions of interest at 120d post-injury in Sham, TBI, and SB cohorts. **C,** NeuN+ cell count at 120d post-injury in Sham, TBI, and SB cohorts normalized to Sham to show percent loss in regions of interest. **D,** PV+ immunohistochemistry of the contralateral hippocampus in Sham, TBI, and SB cohorts at 7d and 120d post-injury to visualize healthy GABAergic interneurons. Hippocampal images taken at 4x. CA1, CA3, and DG images taken at 20x. **E,** Total PV cell count divided by hippocampus and regions of interest at 120d post-injury in Sham, TBI, and SB cohorts. **F,** PV+ cell count at 120d post-injury in Sham, TBI, and SB cohorts normalized to Sham to show percent loss in regions of interest.

Likewise, we observed a striking decrease in the absolute cell count of GABAergic interneurons in the contralateral hippocampus at 120d post-TBI in the untreated mice. This population of interneurons plays a central role in information processing by regulating neuronal activity, balancing inhibitory/excitatory circuitry, and synchronizing network oscillations (Mann and Paulsen, 2007). Only 51% of PV+ cells remained in the contralateral hippocampus of TBI mice at 120d post-injury (Total Hippocampus, Sham=13368.64±446.94 cells vs TBI=6811.6±280.53 cells, $p<0.0001$). The DG displayed the greatest loss of PV+ interneurons in TBI mice with losses upwards of 69%. However, sodium butyrate treatment impeded this loss, showing a rescue of 24.1% of TBI-induced PV+ cell loss (Total hippocampus, TBI=6811.6±280.53 cells vs SB=10270.62±1006.98 cells; $p=0.0319$). Total remaining hippocampal PV+ interneurons in the sodium butyrate cohort was 78.83% relative to sham counts (**Fig. 26E-F)**. Regional cell counts and percent neurodegeneration between cohorts can be found in **Fig. 26B-C and E-F**). Together, our results suggest HDAC inhibition can provide robust long-term neuroprotection from TBI-induced neurodegeneration.

IV. 2.7 Sodium Butyrate Rescues Rate of Neurogenesis and Reduces Aberrant Mossy Fiber Sprouting

To investigate the immediate and long-term effect of HDAC inhibition on neurogenesis, we performed an acute time-course of DCX+ immunohistochemistry for 1d, 3d, and 7d post-TBI. We also stained tissues at 120d, a time-point after most animals displayed SRS. Within the hippocampus, neurogenesis is found arising from

proliferating cells at the border between the dentate hilus and granule cell layer. DCX is expressed in newborn neurons for up to 3 weeks after their generation during adult neurogenesis (Brown et al., 2003). The pattern of newly generated DCX+ cells was examine using unbiased stereological quantification within the contralateral dentate gyrus containing the hilar region (**Fig. 27A**).

During the first week post-injury, we observed minimal fluctuation in the number of newborn neurons between sham, TBI, and SB cohorts (7d DCX: Sham=10577.19±1271.59 cells, TBI=10711.25±818.5 cells, SB=9793.3±1641.47 cells, $p>0.05$) (**Fig. 27B**). However, at 120d post-injury we observed a significant 34% reduction in doublecortin expressing neurons in the TBI cohort (Sham=10469±1187.41 cells vs TBI=6995.22±491.86 cells, $p=0.0177$). Sodium butyrate treated mice maintained a similar rate of neurogenesis to sham mice throughout the 120-day observation period, suggesting HDAC inhibition therapy rescues long-term neurogenesis after TBI (SB=9343.87±830.92 cells) (**Fig. 27C-D**).

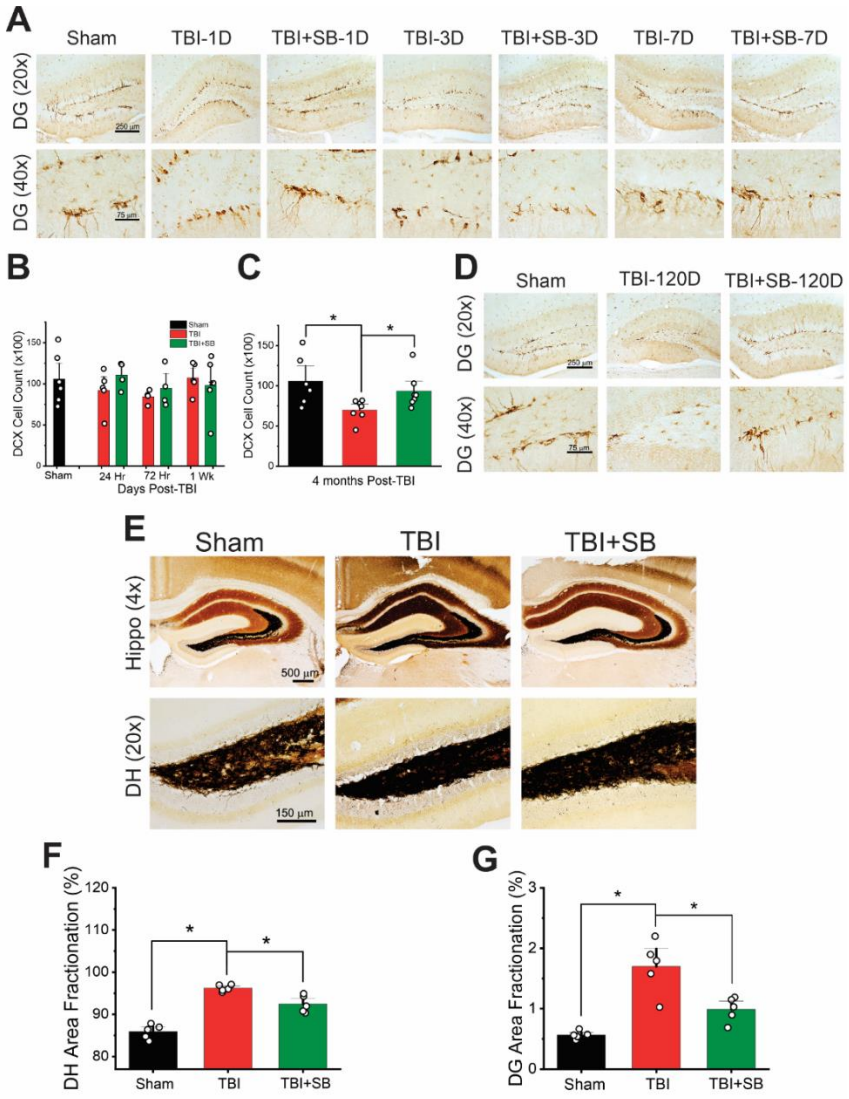

Figure 27: Sodium Butyrate Rescues Rate of Neurogenesis and Reduces Aberrant Mossy Fiber Sprouting.

A, Acute time-course of DCX+ immunohistochemistry in Sham, TBI, and SB cohorts at 1d, 3d, and 7d post-injury to visualize fluctuations in neurogenesis. Images taken in DG at 10x and 40x. **B,** Cell counts of DCX+ cells in DG over time. **C,** Cell count of DCX+ cells in Sham, TBI, and SB cohorts in the contralateral hippocampus at 120d post-injury. **D,** DCX+ immunohistochemistry in Sham, TBI, SB in the contralateral hippocampus at 120d post-injury. Images taken in DG at 10x and 40x. For all DCX+ calculations, n=8 sham, n=5 per TBI and SB cohort. **E,** Images of TIMM stained hippocampus and dentate hilus (DH) in Sham, TBI, and SB contralateral hippocampus at 120d post-injury to visualize aberrant mossy fiber sprouting. Images taken at 4x (hippocampus) and 20x (DH). **F,** Densitometric area fractionation of DH at 120d post-injury in Sham, TBI, and SB cohorts. **G,** Densitometric area fractionation of DG granule and molecular layers at 120d post-injury in Sham, TBI, and SB cohorts.

A classic hallmark of epileptogenesis is the aberrant sprouting of mossy fibers within the hilar and granule layers of the dentate gyrus (Lemos and Cavalheiro, 1995; Scheibel et al., 1974). We performed Timm's staining on coronal brain slices at 120d after injury to compare organization of mossy fibers within the hippocampal sections contralateral to the lesion site. Sham mice did not show evidence of abnormal mossy fiber sprouting. Both TBI and SB cohorts displayed darkened regions within the dentate hilus which could be seen beginning to extend into the granule layer at higher magnification (**Fig. 27E**). Area fractionation analysis found a significant increase in Timm staining within both the DH and DG regions in the TBI cohort compared to sham (DH: Sham=85.89±0.75% fractionation vs TBI=96.19±0.36% fractionation, p=0.0001; DG: Sham=0.56±0.03% fractionation vs TBI=1.70±0.2% fractionation, p=0.0004). Sodium butyrate treatment reduced density of mossy fibers in both regions of interest compared to untreated mice (DH: SB=92.42±0.92% fractionation, p=0.0051; DG: SB=0.99±0.09% fractionation, p=0.0111) (**Fig. 27F-G**).

IV. 2.8 Sodium Butyrate Reduces Chronic Inflammation

Based on the data obtained from the effects of HDACi on acute neuroinflammation, we sought to determine if sodium butyrate influences long-term astro- and micro-gliosis. We performed GFAP and Iba-1 immunohistochemistry at 120d post-TBI. Quantitative evaluation was performed using densitometric analysis via NIH Image J software to capture subtle increases in astrocytes and microglia expression relative to sham-injured mice.

Extensive staining of astrocytes and activated microglia was persistent both around the remaining tissues surrounding the injury site as well as within the contralateral hippocampus in TBI mice 120d post-injury (**Fig. 28A and D**). GFAP is upregulated in astrocytes during scar formation and immune responses, therefore GFAP+ immunohistochemistry was used to visualize chronic astrogliosis. At 120 days post-TBI, we observed an increase in GFAP expression ranging from 152.5 – 201.15% relative to sham mice within the subregions of the contralateral hippocampus. Sodium butyrate treated mice also showed signs of long-term neuroinflammation, however, expression was significantly reduced across all subregions when compared to TBI mice (CA1: TBI =152.5±7.91% vs SB=124.1±6.65%, p=0.0205; CA3: TBI=201.15±13.4% vs SB=132.66±7.24%, p=0.0008; DG: TBI=197.83±12.61% vs SB=137.36±9.63%, p=0.0024) (**Fig. 28B-C**).

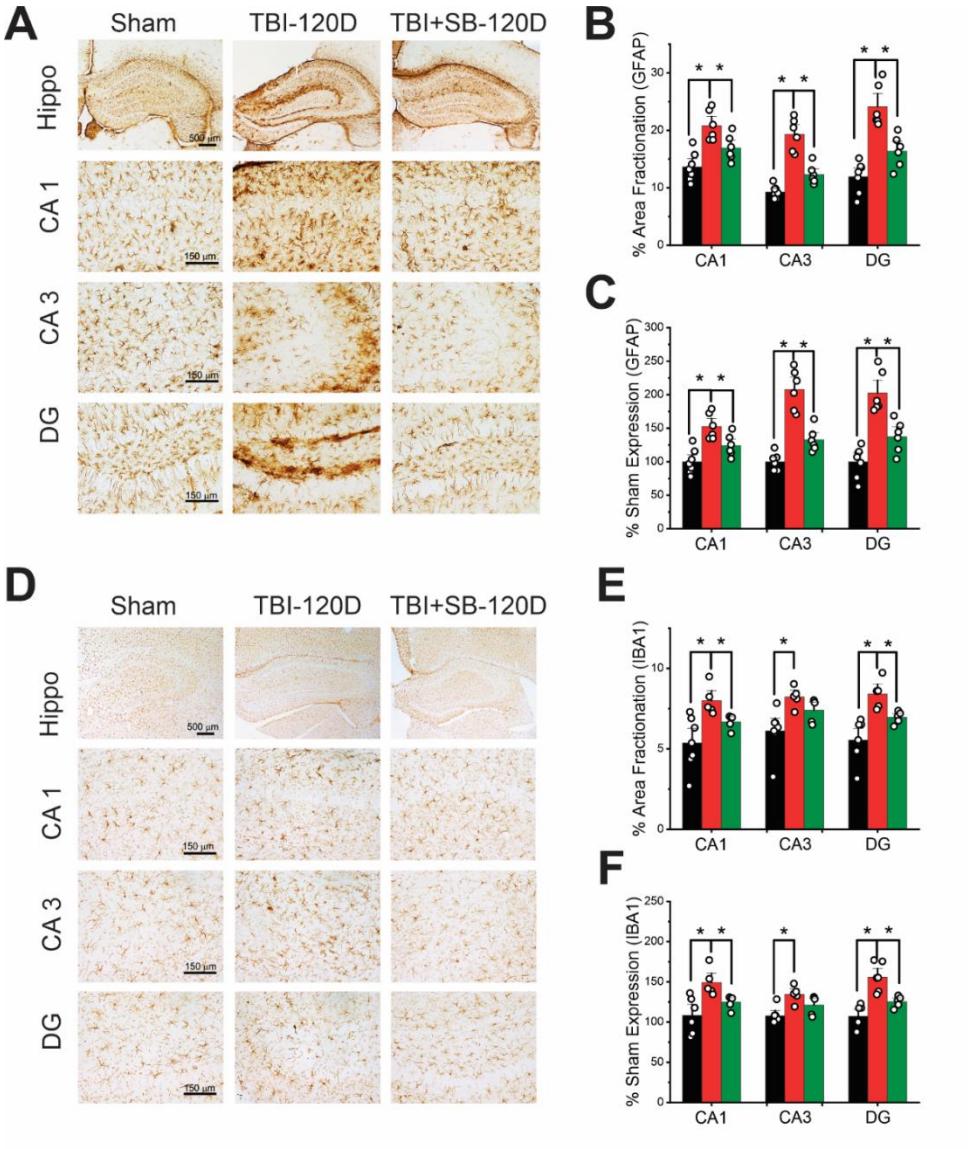

Figure 28: Sodium Butyrate Reduces Chronic Inflammation.
A, Hippocampal and regional (CA1, CA3, & DG) GFAP+ immunohistochemistry at 120d post-injury in Sham, TBI, and SB cohorts to visualize chronic astrogliosis. Images taken at 4x (hippocampus) and 20x (CA1, CA3, DG). **B,** Area fractionation of GFAP+ staining for regions of interest CA1, CA3, & DG in Sham, TBI, and SB cohorts at 120d post-injury. **C,** Densitometric analysis of GFAP+ expression in regions of interest at 120d post-injury, expressed as percent Sham. **D,** Hippocampal and regional (CA1, CA3, & DG) IBA1+ immunohistochemistry at 120d post-injury in Sham, TBI, and SB cohorts to visualize chronic microgliosis. Images taken at 4x (hippocampus) and 20x (CA1, CA3, DG). **E,** Area fractionation of IBA1+ staining for regions of interest CA1, CA3, & DG in Sham, TBI, and SB cohorts at 120d post-injury. **F,** Densitometric analysis of IBA1+ expression in regions of interest at 120d post-injury, expressed as percent Sham.

An antibody against Iba-1 was used to visualize microglia and blood-derived macrophages. Aberrant expression of Iba-1 was not as robust as with the GFAP staining, though significant upregulation was still seen in all subregions at 120d post-injury in untreated mice (**Fig. 28D**). Iba-1 expression in untreated TBI mice ranged between 134.54 – 155.76% relative to the sham cohort, suggesting neuroinflammation had not subsided even 4 months after injury. However, sodium butyrate treatment attenuated the TBI-induced increase of Iba-1 expression by 24.45% in the CA1 and by 30.4% in the DG (CA1: TBI=149.09±6.48% vs SB=124.65±3.39%, p=0.0208; DG: TBI=155.56±6.79% vs SB=125.36±2.84%, p=0.0063). Additionally, at 120d post-injury, sodium butyrate treated mice showed no difference in Iba-1 expression within the CA3 compared to sham mice (p=0.0856) (**Fig. 28E-F**). Together, these results suggest that HDACi therapy not only reduced acute inflammatory processes, but that these anti-inflammatory properties provide long-term neuroprotective benefits.

IV. 2.9 Sodium Butyrate Treatment Improved Motor Function and Reduced Cognitive Impairment Induced by TBI

To assess major health outcomes after TBI, we took body weight measurements and evaluated health scores over the initial 30d post-injury. Mice were evaluated for their coat fur condition, eye health, and active/inactive behavior. TBI mice experienced a 17% loss of their respective day zero body weight over the first week post-injury and did not fully recover by 30d. Sodium butyrate treated mice also experienced an initial weight loss; however, they recovered to normal body weight by 7d post-injury (p=0.0062 vs

untreated mice) (**Fig. 29A**). Likewise, we observed a significantly faster improvement in overall health outcomes when assessed with the health scale as well as composite neuroscore (**Fig. 29B-C**).

Motor function and balance was examined via a beam walk test and 60 sec rotarod test. Due to the severe impairment of balance seen in TBI mice, we modified the beam walk test to a completion test with a non-tapered rod. Even though the width of the rod was larger than the width of the mouse, both TBI and SB cohorts showed severe motor and balance deficits while attempting to cross the beam. By 120d post-injury, both cohorts improved so that 86% of TBI and 100% of SB mice successfully completed the beam walk; however, the SB cohort improved at a rate significantly faster than the untreated mice ($p=0.0143$) (**Fig. 29D**). We also observed gradual, but significant, improvement during the monthly rotarod assessment. The rotation speed was fixed at slow 4 rpm such that it was easy for both sham and injured mice to complete with little learning effect. Mice were given three consecutive trials lasting 60s and their times were averaged before calculating group means. TBI and SB mice showed similar latency to fall at 30d and 60d post-injury (30d: Sham=59.26±0.38 sec vs TBI=8.87±1.9 sec vs SB=16.6±2.61 sec, $p>0.05$; 60d: Sham=59.73±0.15 sec vs TBI=9.12±2.29 sec vs SB=14.96±2.39 sec, $p>0.05$), though sodium butyrate trended a longer duration on the rotarod. At 90d and 120d post-TBI, sodium butyrate treated mice could remain on the rotating rod for a longer duration than TBI mice (90d: Sham=59.67±0.16 sec vs TBI=11.78±2.88 sec vs SB=27.46±5.34 sec, $p=0.0161$; 120d: Sham=59.87±0.09 sec vs TBI=15.05±3.7 sec vs SB=29.89±4.9 sec, $p=0.0262$) (**Fig. 29E**). Furthermore, anxiety is

a common comorbidity seen in the human condition of TBI, therefore, we performed the open field test in monthly increments to identify anxiety-like behaviors between cohorts (Hiott and Labbate, 2002). Untreated mice spent a significantly longer amount of time in the center of the arena compared to both the sham and SB treated mice ($p<0.05$ vs sham and SB at all time-points). Furthermore, TBI mice were less active in the open field arena compared to Sham and SB cohorts. Together these results suggest chronic changes in instinctual behaviors (**Fig. 29F**).

Lastly, we sought to investigate the cognitive dysfunction associated with severe TBI and whether HDAC inhibition therapy could alleviate these changes. Morris water maze has been the gold standard for identifying sensitive changes in cognitive function/dysfunction in rodent models (Wagner et al., 2013). The learning phase consisted of four days of six 60 s trials, each with a different cardinal starting position (**Fig. 29G**). After reaching the platform or maxing out the time in each trial, the mouse was guided to the platform and remained for 15 s before being placed in a cage to dry off. Swimming speed was determined to be different between sham and injured mice, but not between TBI and SB cohorts. Though swim speed affects latency to platform, distance to platform is independent of time and perhaps is a better indicator of test performance under these conditions. Nonetheless, our results show significant differences in both latency (Sham=8.09±1.12 s vs TBI=36.27±4.82 s, $p=0.0003$) and path distance (Sham=128.4±23.1 cm vs TBI=444.6±41.3 s, $p=0.0048$) to platform in untreated TBI mice compared to sham on the final learning day. Both measurements

improved in sodium butyrate treated mice (latency: SB=23.61±1.94 s, p=0.0246 vs TBI; distance: 351.2±35.1 cm, p=0.0416 vs TBI) (**Fig. 29I-J**).

Two testing days in which the platform was removed from the water arena were used to assess memory. The first occurred 24 hr following the last learning trial and the second occurred five days following the final learning day. Sham mice spent over 55.8% and 46.3% of the 60 s memory trials searching in the target quadrant for the platform, suggesting memory retention of platform location. Contrarily, TBI and SB cohorts spent significantly less time in the target quadrant on both memory probe trials (probe 1: TBI=26.7%, SB=35%; probe 2: TBI=25.5%, SB=33.8%). Post-hoc comparisons of TBI and SB cohorts showed that SB mice did not perform better than TBI mice on either probe day, suggesting a deficit in long-term retention for both injured cohorts compared to sham.

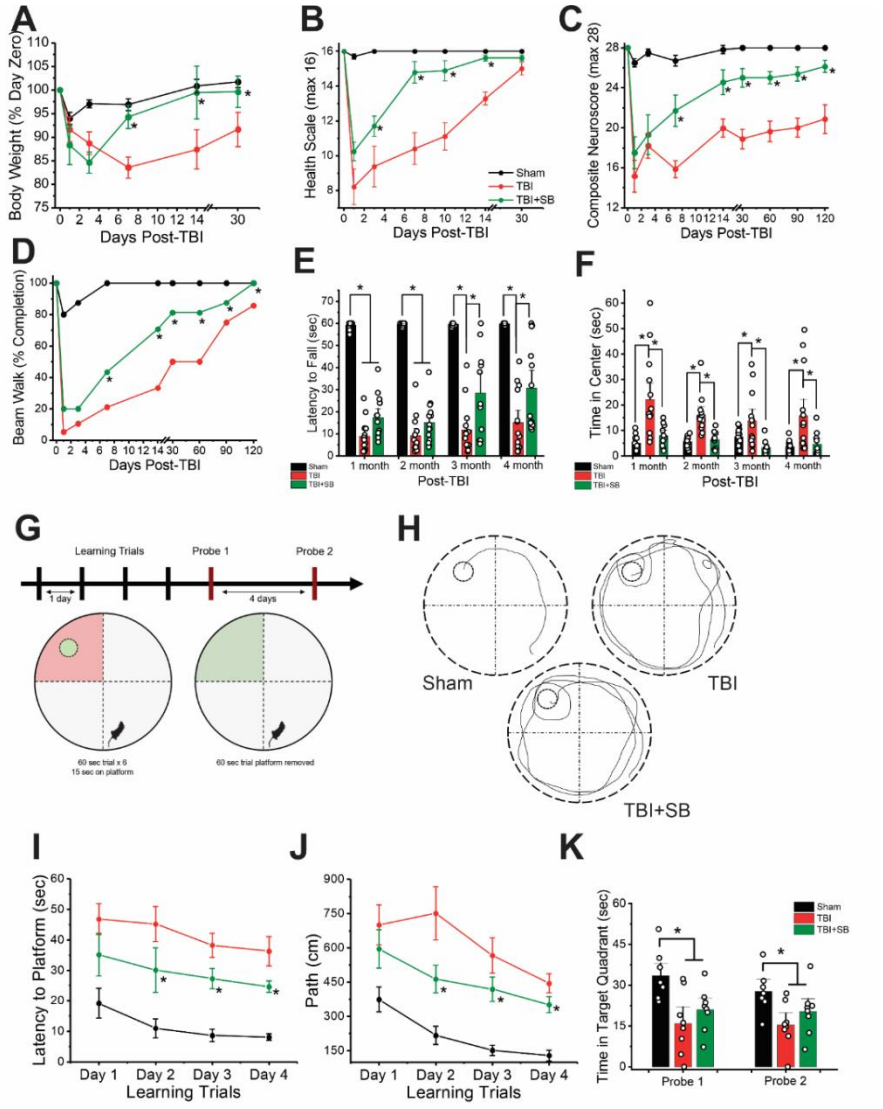

Figure 29: Sodium Butyrate Treatment Improved Motor Function and Reduced Cognitive Impairment Induced by TBI.

A, Changes in body weight over time, expressed as percent of day 0 body weight. **B,** Acute health recovery outcomes after TBI (max=16). **C,** Composite neuroscore over the 120-day observation period (max=28). **D,** Percent completion of ability to cross beam walk apparatus over time. **E,** Latency to fall from rotarod test. **F,** Time spent in center square of open field apparatus. Mice were placed in center of arena and were free to explore for 5 min. Time in center and number of center entries were recorded during test. **G,** Schematic of Morris water maze protocol used at 4 months post-TBI. Full description in methods. **H,** Representative path traces from learning trial day 3. **I,** Average latency to platform (sec) during learning trials. **J,** Average distance (cm) traveled to reach platform during learning trials. **K,** Time spent in target quadrant on probe days during Morris water maze.

IV. 3 Broad and Narrow Spectrum HDAC Inhibitors as Potential Antiepileptogenics in a Mouse Model of Post-Traumatic Epileptogenesis

Traumatic brain injury (TBI) is a worldwide health problem that causes death and disability in both young and aged individuals. TBI is the leading cause of an acquired epilepsy disorder, post-traumatic epilepsy (PTE), characterized by secondary injury cascades such as immediate inflammation, changes in neuroexcitation, and ultimately leading to spontaneous recurrent seizures (SRS). In contrast to primary injury which requires preventative strategies such as helmets and other protective equipment, secondary damage pathologies can be alleviated with therapeutic interventions. Although several efforts have been made to manage injury-induced damage and seizures, clinical significance has yet to be observed. This is, in part, due to the fact that much of the research investigating antiepileptogenesis treatments has thus far been studied using post-status epilepticus models, even though acquired human epilepsies are more likely to arise from injury, stroke, or infection (Klein et al., 2018). Moreover, variation between rodent strains, injury induction, and interpretation between research groups further complicates the understanding of an appropriate therapeutic timeline. A critical priority of epilepsy research is to develop new therapeutic strategies which halt or prevent epileptogenesis after brain injury, thereby reducing seizure burden and improving quality of life for at-risk patients.

Epigenetic modifications have been implicated in a diverse set of neuronal processes, both salubrious and pathological, including synaptic responses to learning and memory, normal aging, immune responses, and central nervous system disorders.

Simply defined, epigenetics refers to the plastic changes in gene expression that occur without direct alteration of the DNA sequence itself. Modifications include histone or DNA acetylation, methylation, phosphorylation, ubiquitination, etc. Post-translational histone modifications have been the most widely studied epigenetic change, both in the CNS and periphery.

The role of epigenetic mechanisms such as histone acetylation in recovery outcomes have been increasingly studied in neurological conditions including intracerebral hemorrhage, chronic pain, and epilepsy (Reddy et al., 2017; Borgonetti and Galeotti, 2021; Bonsack and Sukumari-Ramesh, 2021). Previous studies have demonstrated hypoacetylation of histones in the acute phase of TBI (Zhang et al., 2008). Restoring homeostatic levels of lysine acetylation at these histones reduces maladaptive immune responses via the downregulation of pro-inflammatory mediators such as TNF-α and NOS2 (Patnala et al., 2017). Moreover, administration of HDAC inhibitors, such as sodium butyrate, valproate, and trichostatin A, have decreased lesion volume and improved blood-brain barrier integrity after CNS injury (Dash et al., 2010; Sukumari-Ramesh et al., 2016).

SAHA (Vorinostat) is a broad spectrum HDAC inhibitor, with reported effects on both Class I and Class II HDACs. SAHA is currently approved by the United States FDA and other drug regulatory authorities worldwide for the management of cutaneous T-cell lymphoma and is currently undergoing investigation for other indications including glioma, breast cancer, HIV infection, lung cancer, and leukemia (ClinicalTrials.gov). Entinostat (previously MS-275), on the other hand, is a potent

narrow-spectrum HDAC inhibitor with micromolar affinity for class I HDAC1 and HDAC3 (Simonini et al., 2006). Clinical evaluation of entinostat is currently underway for cancers and other indications but has also shown promising preclinical results in central nervous system disorders. Entinostat administration in aged, dementia mice restored their capacity to respond to the anti-psychotic, haloperidol (Montalvo-Ortiz et al., 2014). Furthermore, entinostat rescues innate anxiety by enhancing acetylation of H3 proteins in the cingulate cortex (Sah et al., 2019). We have recently found that the use of the broad spectrum HDAC inhibitor, sodium butyrate, produced beneficial disease modifying effects in both an electrical kindling model of temporal lobe epilepsy (Reddy et al., 2017) as well as a PTE model in mice (Golub and Reddy, 2021b/Aim 2). This signifies that future research is warranted to investigate the properties of HDAC inhibitors and their role in altering the epileptogenic process. Using our previously validated models of post-traumatic seizures (Golub and Reddy, 2021a/Aim 1), we sought to investigate the therapeutic effects of broad vs narrow spectrum HDAC inhibition on the prevention and modification of PTE and its associated comorbidities.

IV. 3.1 Effects of SAHA Treatment on Seizure Incidence, Frequency, and Duration Post-TBI

To test the therapeutic effects of the broad-spectrum HDAC inhibitor, SAHA, on post-traumatic seizures, we utilized both a moderate (1mm) and severe (2mm) injury model. Mice were randomly placed into either Sham, 1mm, or 2mm TBI cohorts. Administration of SAHA (25 mg/kg, twice daily, i.p.) or vehicle began 1-hr post injury

to ensure the subjects had fully awoken from the surgical procedure and continued for up 21 days. Mice were recorded by continuous video-EEG for 120 days post-injury to evaluate the electrographic and behavioral components of epileptiform activity. Seizures were analyzed via a customized MATLAB script before visual validation of true positives by unbiased technician and power spectral analysis.

Incidence of PTE within the moderate injury groups was not significantly changed with HDAC inhibition, as 67% of untreated mice and 56% of treated mice displayed seizure activity during the observation period. The physiological characteristics of seizures were similar between responders in both groups, as the average duration and behavioral responses were unchanged with SAHA administration (1mm TBI= 39±6 s, 1mm TBI+SAHA= 37.5±3 s). The latency period between injury and first seizure trended longer in SAHA-treated mice, though this parameter did not reach significance. However, frequency of seizures was significantly reduced with SAHA treatment (1mm TBI= 0.67±0.12 seizures/day, 1mm TBI+SAHA= 0.12±0.06 seizures/day; $p<0.0001$). This translated to a significant reduction in seizure burden over the 4-month observation period with reduced total number of seizures per animal as well as shorter accumulated seizure duration (**Fig. 30A-E**). A timeline of seizure occurrence, both daily and weekly, as well as average seizure duration throughout the observation period can be found in **Fig. 30.**

Seizure threshold to electrical or chemical stimulation can also be a sensitive indicator of hyperactivity in the brain. Therefore, at 4-months post-TBI, we utilized the 6Hz method of seizure threshold testing to identify the minimum current intensity

needed to evoke seizure occurrence. Injured mice displayed a significantly lower seizure threshold compared non-injured sham mice. As expected from the incidence results, SAHA treatment did not significantly increase or decrease seizure threshold to 6Hz stimulation after moderate brain injury.

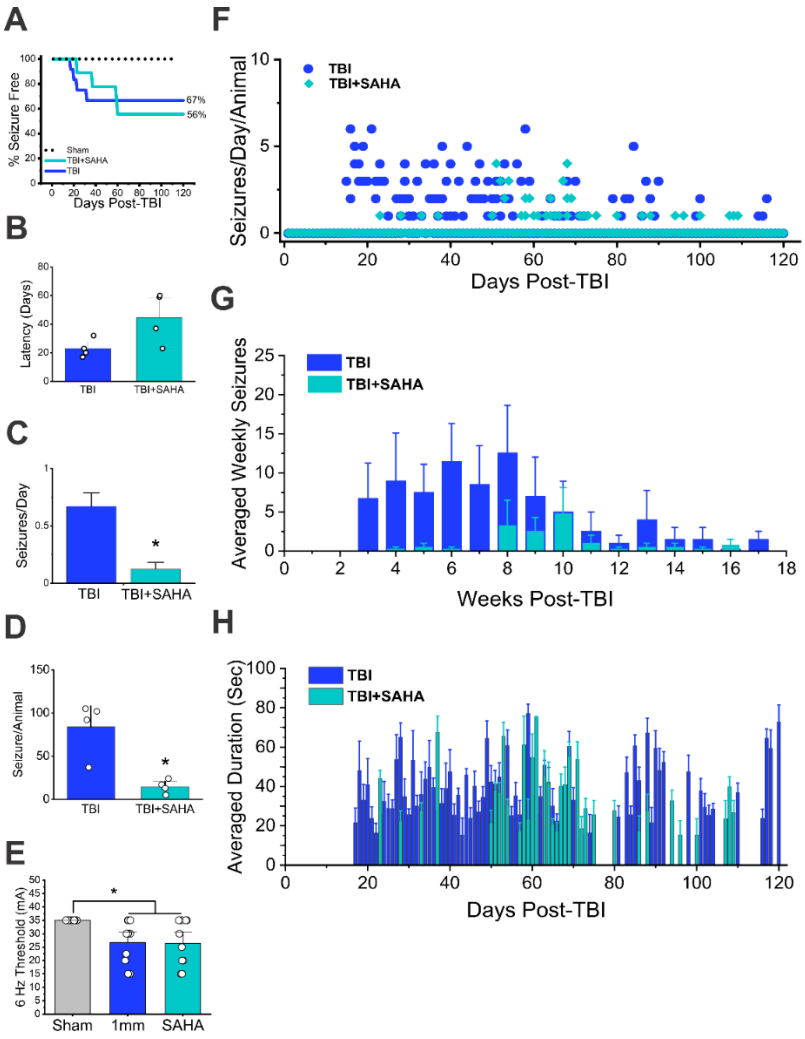

Figure 30: Effect of SAHA Treatment on Moderate TBI-induced Seizures.
A, Incidence curve of epileptic animals over time, showing latency to first spontaneous recurrent seizure (SRS). **B,** Average latency to first SRS in treated and untreated 1mm-TBI cohorts. **C,** Average frequency of seizures per day **D, N**umber of seizures per animal within 1mm-TBI and 1mm-TBI+SAHA cohorts. **E,** Seizure threshold of Sham, 1mm-TBI, and 1mm-TBI+SAHA cohorts at 120 days post-injury using the 6 Hz model of threshold. **F,** Scatter plot of seizures per day per animal over 120-day observation period for both 1mm-TBI and 1mm-TBI+SAHA cohorts. Following two-week recovery period from TBI, mice were hooked to 24/7 video-EEG recording. Only responding animals were used for calculations (TBI n=4, SAHA n=4). **G,** Average number of weekly seizures per animal in responding animals. **H,** Average duration of seizures per day over 120 days. All seizure events on each day from responding mice were used in calculations. *p<0.05 vs. Sham group or TBI, when appropriate (n= 15 animals/group, unless as indicated above for responders only).

Similarly, we performed the same study in severe 2mm-injured cohorts. Again, mice were continuously recorded via video-EEG for 120 days post-injury. SAHA treatment in the severe-TBI cohort significantly reduced incidence of epileptic seizures (2mm-TBI= 81.3% vs 2mm-TBI+SAHA = 42.9%; p=0.0295) (**Fig. 31A**). The latency period was not altered within this cohort, with most animals exhibiting seizures approximately 50 days post-injury (**Fig. 31B**). We observed a significant reduction in seizure frequency with HDAC inhibition treatment (2mm TBI= 0.88±0.034 seizures/day, 2mmTBI+SAHA= 0.23±0.027 seizures/day; p<0.0001) (**Fig. 31C**). The total number of seizures per animal trended lower in SAHA-treated mice but did not quite reach significance (**Fig. 31D**). As with the 1mm cohorts, timelines of daily and weekly seizure occurrence as well as average seizure duration throughout the observation period can be found in **Fig. 31.**

Lastly, we performed the 6 Hz seizure threshold model at 4 months post-injury. Injured mice showed a significantly lowered threshold to 6Hz stimulation compared to sham-injured mice. Though SAHA was only administered for the first 21 days post-TBI, treatment resulted in a significantly ameliorated chronic reduction of seizure threshold associated with TBI. Together, the results of these moderate and severe TBI studies suggest that HDAC inhibition therapy reduces seizure burden and has the potential of preventing both seizure occurrence and frequency long after the conclusion of drug therapy.

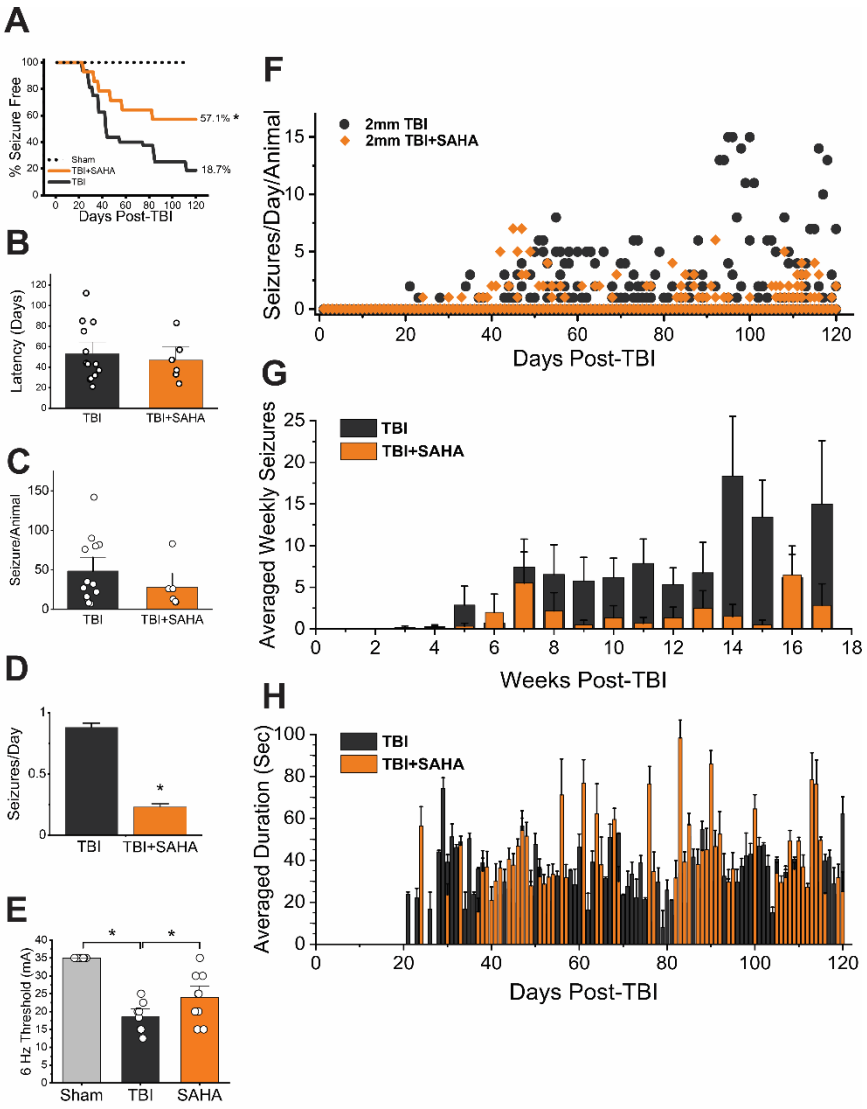

Figure 31: Effect of SAHA Treatment on Severe TBI-induced Seizures.
A, Incidence curve of epileptic animals over time, showing latency to first spontaneous recurrent seizure (SRS). **B,** Average latency to first SRS in treated and untreated 2mm-TBI cohorts. **C,** Average frequency of seizures per day between untreated and treated 2mm-TBI cohorts. **D, N**umber of seizures per animal within 2mm-TBI and 1mm-TBI+SAHA cohorts. **E,** Seizure threshold of experimental cohorts at 120 days post-injury using the 6 Hz model of threshold. **F,** Scatter plot of seizures per day per animal over 120-day observation period for both 2mm-TBI and 2mm-TBI+SAHA cohorts. Following two-week recovery period from TBI, mice were hooked to 24/7 video-EEG recording. Only responding animals were used for calculations (TBI n=13, SAHA n=6). **G,** Average number of weekly seizures per animal in responding animals. **H,** Average duration of seizures per day over 120 days. All seizure events on each day from responding mice were used in calculations.

IV. 3.2 Effects of Entinostat Treatment on Seizure Incidence, Frequency, and Duration Post-TBI

To evaluate the effects of the narrow-spectrum HDAC inhibitor, Entinostat, we performed a concurrent cohort of 2mm TBI+Entinostat animals. Beginning 1-hr post-injury, Entinostat (10 mg/kg, once daily, i.p.) was injected for 21 days. As with the previous cohorts, these mice were single-housed and recorded with continuous video-EEG for 120 days post-TBI. At 4-months post-injury, we performed a 6Hz seizure threshold test to identify changes in hyperexcitability.

Entinostat significantly reduced incidence of PTE, with only 33.3% of treated mice vs 81.3% untreated mice exhibiting spontaneous seizures ($p<0.0111$) (**Fig. 32A**). Latency to first seizure ranged between 35-100 days, suggesting the therapeutic window was unchanged with Entinostat treatment. Moreover, seizure duration was similar to both untreated and SAHA-treated 2mm-TBI cohorts, averaging 41 ± 3 s (**Fig. 32B**). We also found Entinostat treatment significantly reduced seizure frequency over the 120-day observation period (2mm-TBI= 0.88±0.03 seizures/day, 2mm-TBI+Ent= 0.52±0.02 seizures/day; $p=0.0004$) (**Fig. 32C**). However, the cumulative number of seizures per animal was unchanged between responders in both the treated and untreated cohorts (**Fig. 32D**), suggesting the manifestation of epilepsy symptoms in responding mice were similar once they appeared. Lastly, 6Hz threshold testing demonstrated Entinostat has neuroprotective properties which lead to a significant rescue in the current intensity needed to evoke a seizure (**Fig. 32E**).

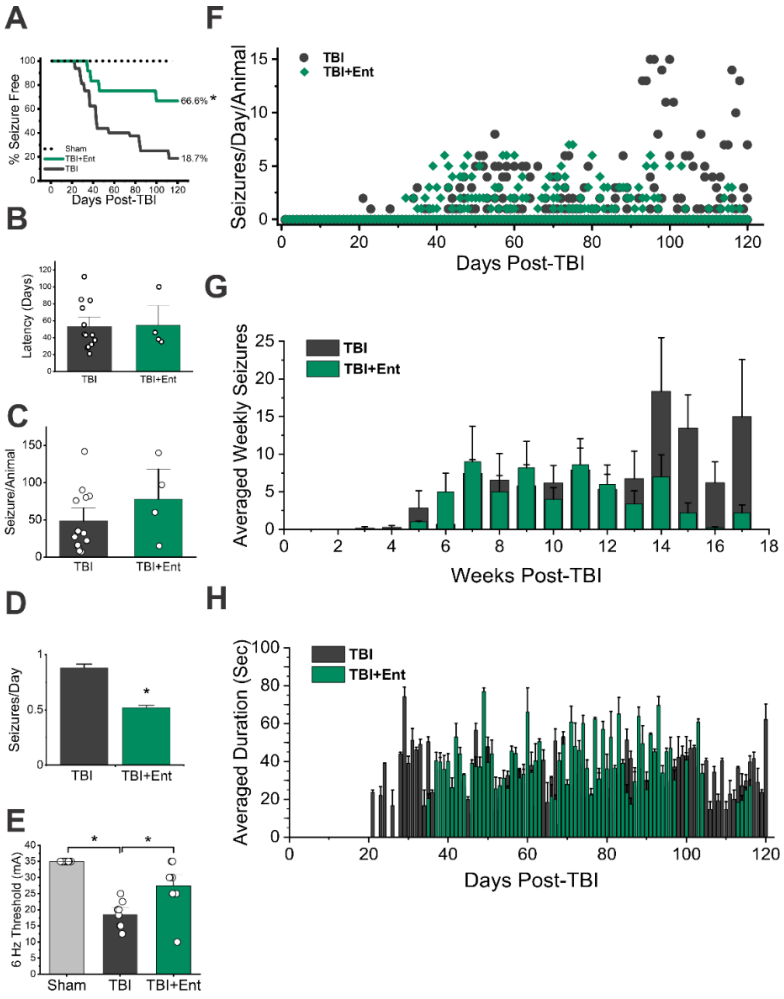

Figure 32: Effect of Entinostat Treatment on Severe TBI-induced Seizures. **A,** Incidence curve of epileptic animals over time, showing latency to first spontaneous recurrent seizure (SRS). **B,** Average latency to first SRS in treated and untreated 2mm-TBI cohorts. **C,** Average frequency of seizures per day between untreated and treated 2mm-TBI cohorts. **D, N**umber of seizures per animal within 2mm-TBI and 1mm-TBI+Ent cohorts. **E,** Seizure threshold of Sham, 2mm-TBI, and 2mm-TBI+Ent cohorts at 120 days post-injury using the 6 Hz model of threshold. **F,** Scatter plot of seizures per day per animal over 120-day observation period for both 2mm-TBI and 2mm-TBI+Ent cohorts. Following two-week recovery period from TBI, mice were hooked to 24/7 video-EEG recording. Seizures were identified through a custom MatLAB algorithm and then validated by an unbiased researcher via power spectra analysis. Only responding animals were used for calculations (TBI n=13, Ent n=4). **G,** Average number of weekly seizures per animal in responding animals. **H,** Average duration of seizures per day over 120 days. All seizure events on each day from responding mice were used in calculations.

IV. 3.3 Effect of SAHA Treatment on Epileptiform Discharges

To identify any therapeutic effect of the broad-spectrum HDAC inhibitor, SAHA, on epileptiform activity, we analyzed continuous video-EEG output through a customized MATLAB script for the 120-day observation period post-injury. Epileptiform discharges were defined as short bursts of hyperactive non-convulsive seizure activity lasting between 3-9s. Moderate brain injury resulted in 42% incidence of discharge activity in untreated mice and 44% incidence in the SAHA-treated group (**Fig. 33A**). As with the seizure comparisons between these cohorts, the latency to discharge output was trending longer but did not reach significance (**Fig. 33D**). Epileptiform discharge frequency was significantly reduced with SAHA treatment (1mm-TBI= 1.64±0.11 discharges/day, 1mm-TBI+SAHA= 0.27±0.052 discharges/day; $p<0.0001$) and animals exhibited significantly fewer total discharges over the observation period (1mm-TBI= 202±68 discharges/animal, 1mm-TBI+SAHA= 87±22 discharges/animal; $p=0.0489$) (**Fig. 33A-G**). However, the ratio of discharges to seizures between treated and untreated mice was unchanged, suggesting symptom pathology manifested similarly in responding animals after moderate brain injury.

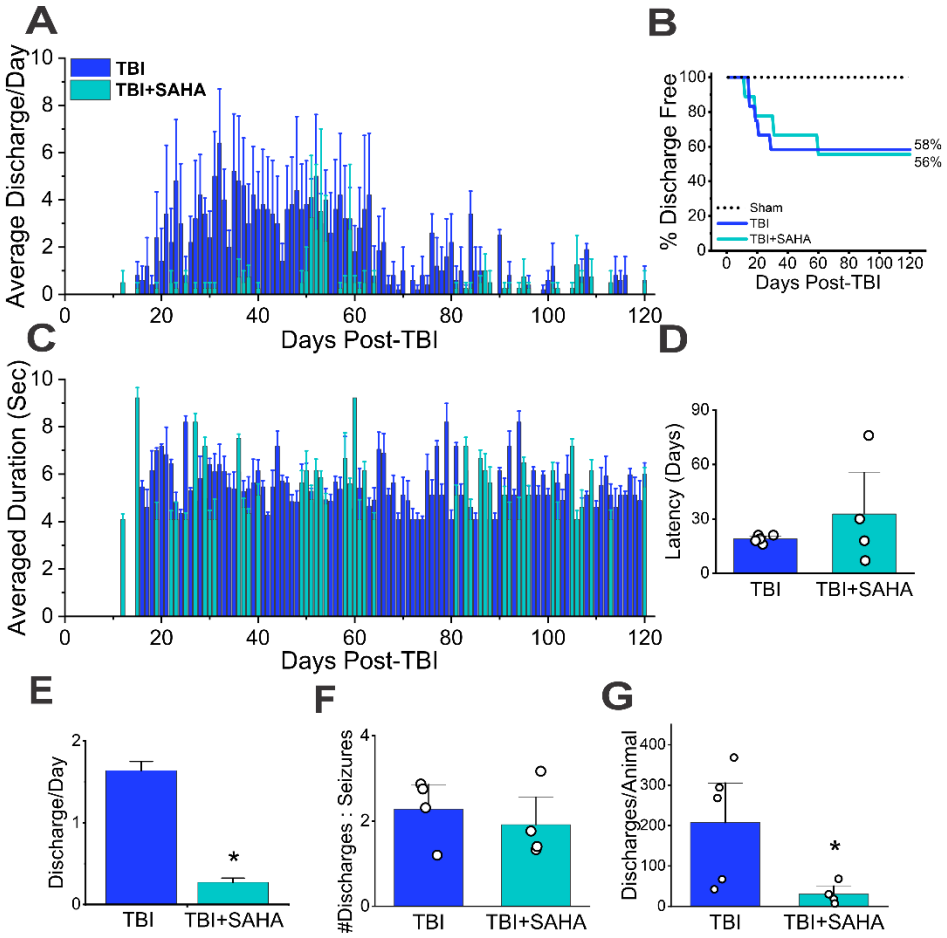

Figure 33: Effect of SAHA Treatment on Moderate TBI-induced Epileptiform Discharges.

A, Average epileptiform discharges per day per animal over 120-day observation period for both 1mm-TBI and 1mm-SAHA cohorts. Following a mandatory recovery period from TBI, mice were hooked to 24/7 video-EEG recording. Epileptiform discharges (3 – 9s) were identified through a custom MatLAB script. Only responding animals were used for calculations (TBI: n=5, SAHA: n=4). **B,** Incidence curve showing latency to first epileptiform discharge over time. Sham animals did not experience any epileptiform discharge activity. **C,** Average duration of discharges per day over 120-day observation period. All epileptiform discharge events on each day from responding mice were used in calculations. **D,** Latency to first epileptiform discharge. **E,** Frequency of discharges/day between treated and untreated cohorts. **F,** Ratio of number of discharges to number of seizures for each responding animal. Only animals which experienced both seizures and discharges were used for calculation (TBI: n=4, SAHA: n=4). **G,** Number of discharges per animal over 120-day observation period within TBI and SAHA cohorts.

A similar pattern was found within the severe TBI cohorts. Epileptiform discharges were observed in 57% of SAHA-treated mice and 87% untreated 2mm-TBI mice but did not reach significance ($p=0.0755$). Interestingly, discharges in this group were observed after a shorter latency period compared to untreated mice (2mm-TBI= 48±7 days, 2mm-TBI+SAHA= 28±3 days; $p=0.0298$). However, SAHA treatment significantly reduced discharge frequency (2mm-TBI= 1.11±0.043 discharges/day, 2mm-TBI+SAHA= 0.43±0.049 discharges/day; $p<0.0001$). Moreover, SAHA-treated mice exhibited a lower ratio of discharges to seizures ($p=0.038$), though overall, the total number of discharges from responding animals was unchanged with SAHA treatment (**Fig. 34A-G**).

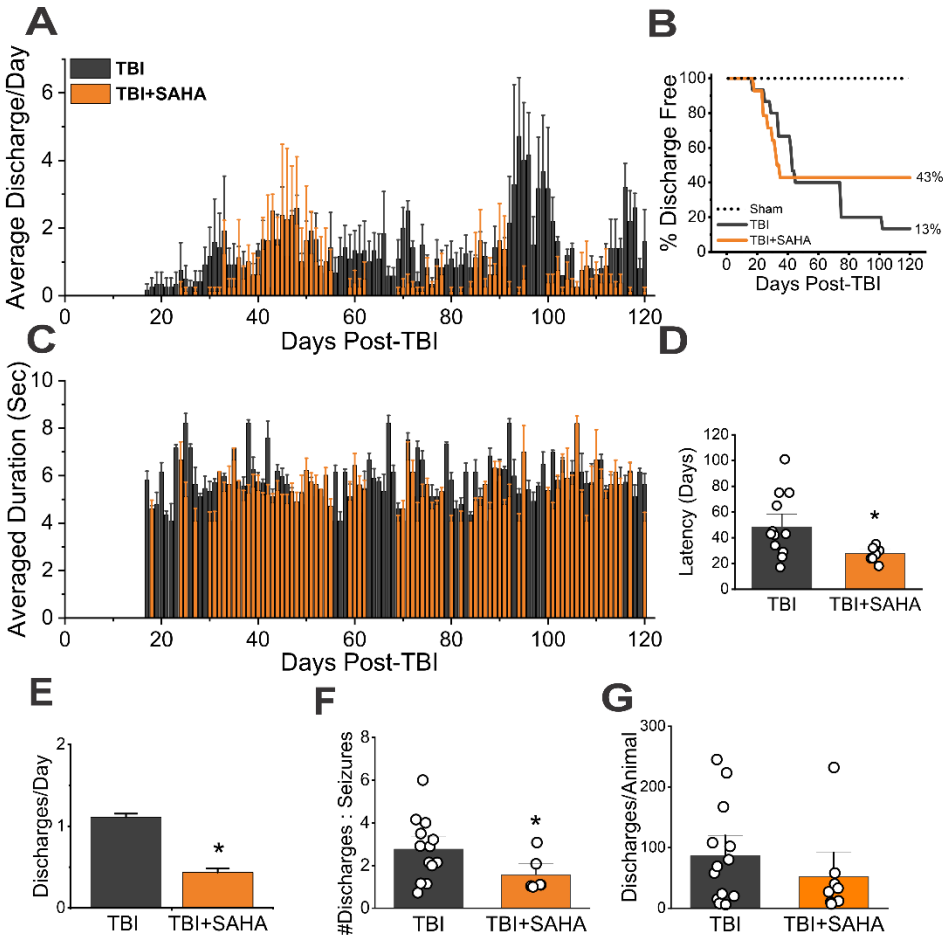

Figure 34: Effect of SAHA Treatment on Severe TBI-induced Epileptiform Discharges.

A, Average epileptiform discharges per day per animal over 120-day observation period for both 2mm-TBI and 2mm-SAHA cohorts. Following a mandatory recovery period from TBI, mice were hooked to 24/7 video-EEG recording. Epileptiform discharges (3 – 9s) were identified through a custom MatLAB script. Only responding animals were used for calculations (TBI: n=13, SAHA: n=7). **B**, Incidence curve showing latency to first epileptiform discharge over time. Sham animals did not experience any epileptiform discharge activity. **C**, Average duration of discharges per day over 120-day observation period. All epileptiform discharge events on each day from responding mice were used in calculations. **D**, Latency to first epileptiform discharge. **E**, Frequency of discharges/day between treated and untreated cohorts. **F**, Ratio of number of discharges to number of seizures for each responding animal. Only animals which experienced both seizures and discharges were used for calculation (TBI: n=13, SAHA: n=6). **G**, Number of discharges per animal over 120-day observation period within TBI and SAHA cohorts.

IV. 3.4 Effect of Entinostat Treatment on Epileptiform Discharges

Treatment with the narrow-spectrum HDAC inhibitor, Entinostat, resulted in significantly less incidence of epileptiform discharges during the 120-day observation period. We observed short bursts of non-convulsive hyperactivity in 87% of 2mm-TBI untreated mice, whereas only 50% of treated mice exhibited discharges ($p=0.0349$). This result expanded on the seizure data for this cohort, suggesting Entinostat may have disease modification properties which help prevent secondary epileptogenesis after TBI.

Occurrence of discharges began approximately 28 days following injury within responding mice of the Entinostat-treated cohort, similar to untreated mice. As with our previous groups, discharge onset was generally before the presence of spontaneous seizures (**Fig. 35A**). The ratio of discharges to seizures as well as the total number of discharges per animal were found to be unaffected by Entinostat administration. However, surprisingly, the frequency of discharges was higher in the treated group compared to non-treated mice (2mm-TBI= 1.11±0.043 discharges/day, 2mm-TBI+Ent= 1.61±0.084 discharges/day; $p=0.003$) (**Fig. 35A-G**), suggesting that, in general, total duration of epileptic activity was reduced with Entinostat treatment as there were significantly fewer seizures.

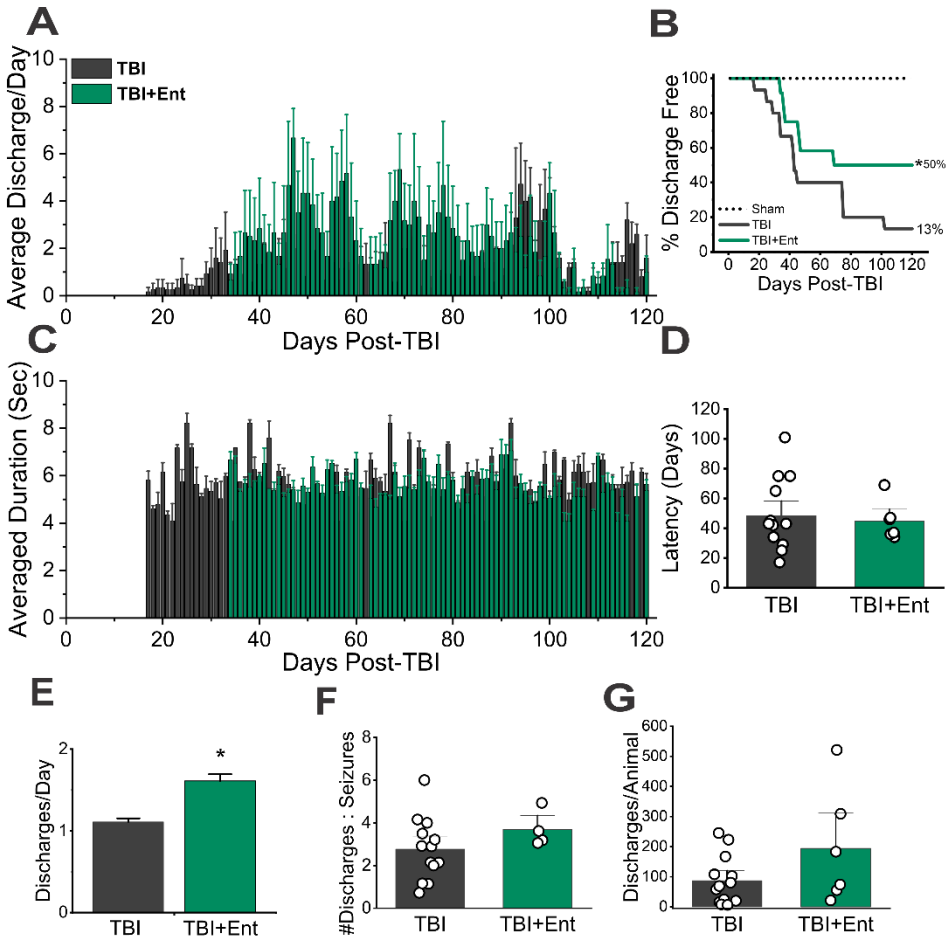

Figure 35: Effect of Entinostat Treatment on Severe TBI-induced Epileptiform Discharges.

A, Average epileptiform discharges per day per animal over 120-day observation period for both 2mm-TBI and 2mm-Ent cohorts. Following a mandatory recovery period from TBI, mice were hooked to 24/7 video-EEG recording. Epileptiform discharges (3 – 9s) were identified through a custom MatLAB script. Only responding animals were used for calculations (TBI: n=13, Ent: n=7). **B,** Incidence curve showing latency to first epileptiform discharge over time. Sham animals did not experience any epileptiform discharge activity. **C,** Average duration of discharges per day over 120-day observation period. All epileptiform discharge events on each day from responding mice were used in calculations. **D,** Latency to first epileptiform discharge. **E,** Frequency of discharges/day between treated and untreated cohorts. **F,** Ratio of number of discharges to number of seizures for each responding animal. Only animals which experienced both seizures and discharges were used for calculation (TBI: n=13, Ent: n=6). **G,** Number of discharges per animal over 120-day observation period within TBI and Ent cohorts.

IV. 3.5 Pharmacokinetic Study of SAHA Administration in Blood and Brain

Previous research using rodent models to systemically administer entinostat has found beneficial results within the central nervous system, suggesting entinostat permeates the blood-brain barrier (BBB) at therapeutically relevant levels (Simonini et al., 2006; Montalvo-Ortiz et al., 2014; Murphy et al., 2014; Ma et al., 2018). Therefore, we performed a pharmacokinetic study using SAHA to determine the extent to which this compound could cross the BBB. Following a similar surgery and treatment protocol, Sham and 2mm-TBI mice were administered either 25 mg/kg or 100 mg/kg SAHA per day (i.p.) for 7 days, beginning 1 hr post-surgery. For this experiment, sham mice did not undergo a craniotomy, so that we could be certain the integrity of the BBB stayed fully intact. Whole brain tissue and plasma were collected 30 min following the final dose. **Fig. 36** shows the results of the pharmacokinetic study in the brain, plasma, and as a ratio of each other. Higher doses of SAHA resulted in greater levels of the drug present in both the brain and plasma, though injured mice show significantly increased levels of SAHA in the brain. Furthermore, the ratio of brain to plasma levels of SAHA remained similar between sham and TBI mice in the low dose but were significantly elevated with the high dose. These results suggest that SAHA can permeate the BBB, but not easily as it tends to stay peripherally. Moreover, TBI impact shatters the integrity of the BBB thereby allowing for greater influx of SAHA to the brain and central nervous system.

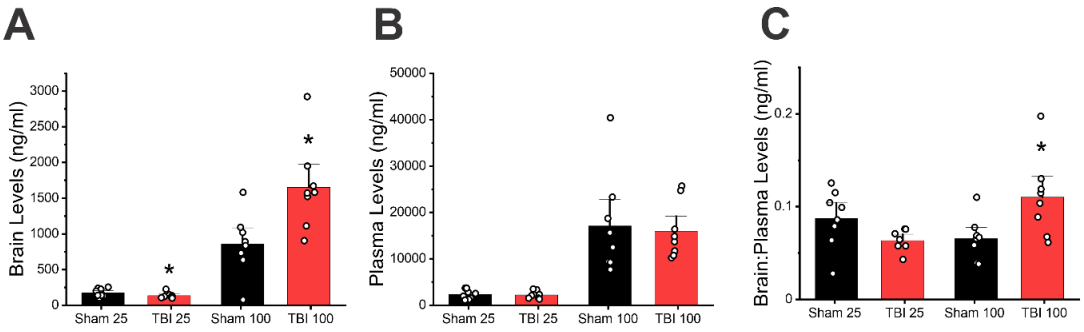

Figure 36: Pharmacokinetic Study of SAHA Administration for BBB Permeability Pharmacokinetic study of SAHA administration after Sham or 2mm-TBI surgery. Animals were administered SAHA treatment (either 25 mg/kg or 100 mg/kg) for 7 days, beginning 1 hr post-surgery. Whole brain tissue and plasma were extracted 30 min after the last dose. **A,** Brain levels of SAHA (ng/ml) between Sham or 2mm-TBI injury groups and 25 mg/kg or 100 mg/kg doses. **B,** Plasma levels of SAHA (ng/ml) between Sham or 2mm-TBI injury groups and 25 mg/kg or 100 mg/kg doses. **C,** Ratio of brain to plasma levels of SAHA between Sham and 2mm-TBI cohorts and 25 mg/kg or 100 mg/kg doses, expressed as ng/ml. *p<0.05 vs Sham. ANOVA with Bonferroni or Tukey HSD post hoc test, Kruskal-Wallis test followed by Mann-Whitney U-test.

IV. 3.6 SAHA Treatment Reduces TBI-Induce Chronic Neuroinflammation

To evaluate the effect of SAHA treatment on chronic pathologies, we used immunohistochemistry techniques to illustrate changes in astrocytic and microglia expression at 4-months post-injury. Within the moderate (1mm) injury cohorts, GFAP+ immunohistochemistry revealed a 27% increase over sham mice in astrogliosis in the CA3 and 36% in the DG regions of the contralateral hippocampus (CA3, p=0.0174; DG, p=0.0034). SAHA treatment successfully normalized GFAP+ expression (CA3, p=0.0435; DG, p=0.0002) (**Fig. 37A-C**). No changes were observed in microglial expression between non-injured and moderate injury animals (**Fig. 37D-F**).

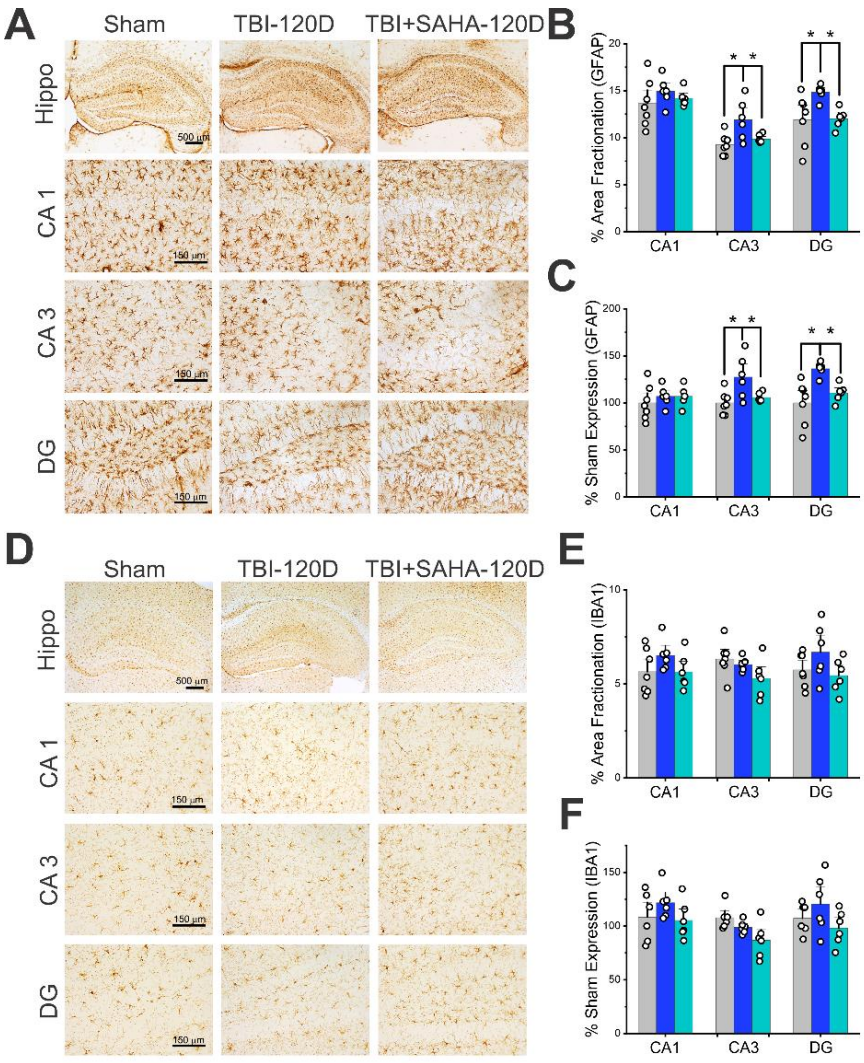

Figure 37: SAHA Treatment Reduces Chronic Inflammation after Moderate TBI. **A,** Hippocampal and regional (CA1, CA3, & DG) GFAP+ immunohistochemistry at 120d post-injury in Sham, 1mm-TBI, and 1mm-TBI+SAHA cohorts to visualize chronic astrogliosis. Images taken at 4x (hippocampus) and 20x (CA1, CA3, DG). **B,** Area fractionation of GFAP+ staining for regions of interest CA1, CA3, & DG in Sham, 1mm-TBI, and SAHA cohorts at 120d post-injury. **C,** Densitometric analysis of GFAP+ expression in regions of interest at 120d post-injury, expressed as percent Sham. **D,** Hippocampal and regional (CA1, CA3, & DG) IBA1+ immunohistochemistry at 120d post-injury in Sham, 1mm-TBI, and SAHA cohorts to visualize chronic microgliosis. Images taken at 4x (hippocampus) and 20x (CA1, CA3, DG). **E,** Area fractionation of IBA1+ staining for regions of interest CA1, CA3, & DG in Sham, 1mm-TBI, and SAHA cohorts at 120d post-injury. **F,** Densitometric analysis of IBA1+ expression in regions of interest at 120d post-injury, expressed as percent Sham.

After severe TBI injury, overexpression of the astrocytic (GFAP) and microglial (Iba1) markers was much more evident. At 4-months post-injury, 2mm-TBI mice revealed a robust increase in GFAP expression in all contralateral hippocampal subregions (CA1=52.5±7.9%, p=0.0004; CA3=107.9±12.4%, p=0.0002; DG= 102.6±12.6%, p<0.0001). As with the 1mm cohorts, we observed a significant reduction of astrogliosis with SAHA treatment in all subregions (CA1, p=0.001; CA3, p=0.0002; DG, p=0.0059) (**Fig. 38A-C**).

Though microgliosis was not noteworthy after moderate injury, severe TBI resulted in a striking increase of Iba1+ at 4-months post-injury. The DG showed the greatest microgliosis, demonstrating approximately 56% greater expression over non-injured controls (p=0.0003). The CA1 and CA3 were also found to have considerably higher expression over sham mice (CA1=49.1±7%, p=0.0091; CA3= 34.5±4.2%, p=0.0025). Once again, we found SAHA treatment ameliorated this increase in Iba1 expression in the CA1 (p=0.0036) and CA3 (p=0.0099). Though the DG was not significant, a trend of reduction was also found in this subregion (DG, p=0.0984) (**Fig. 38D-F**). Since astrocytes and microglia are both involved in neuroinflammation, our data suggests SAHA may act to reduce pro-inflammatory cascades after injury.

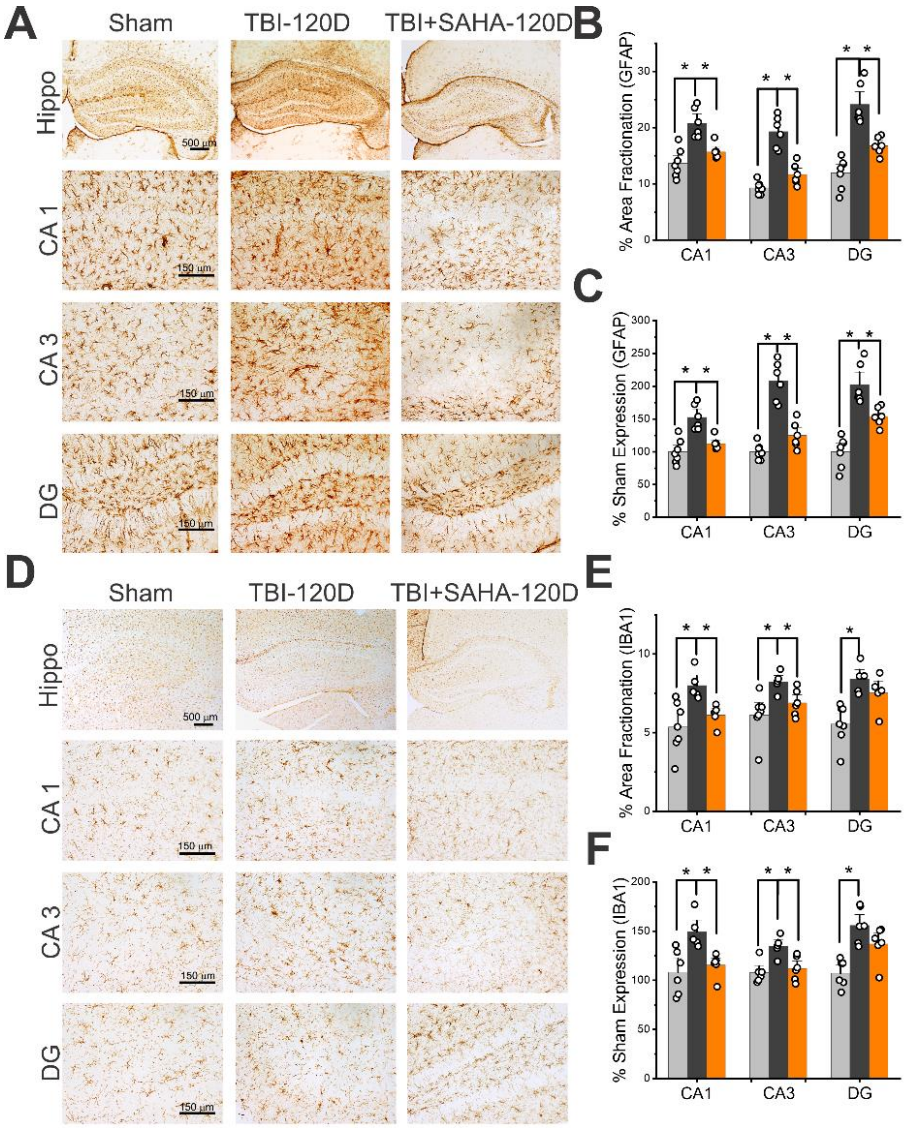

Figure 38: SAHA Treatment Reduces Chronic Inflammation after Severe TBI. **A,** Hippocampal and regional (CA1, CA3, & DG) GFAP+ immunohistochemistry at 120d post-injury in Sham, 2mm-TBI, and 2mm-TBI+SAHA cohorts to visualize chronic astrogliosis. Images taken at 4x (hippocampus) and 20x (CA1, CA3, DG). **B,** Area fractionation of GFAP+ staining for regions of interest CA1, CA3, & DG in Sham, 2mm-TBI, and SAHA cohorts at 120d post-injury. **C,** Densitometric analysis of GFAP+ expression in regions of interest at 120d post-injury, expressed as percent Sham. **D,** Hippocampal and regional (CA1, CA3, & DG) IBA1+ immunohistochemistry at 120d post-injury in Sham, 2mm-TBI, and SAHA cohorts to visualize chronic microgliosis. Images taken at 4x (hippocampus) and 20x (CA1, CA3, DG). **E,** Area fractionation of IBA1+ staining for regions of interest CA1, CA3, & DG in Sham, 2mm-TBI, and SAHA cohorts at 120d post-injury. **F,** Densitometric analysis of IBA1+ expression in regions of interest at 120d post-injury, expressed as percent Sham.

IV. 3.7 Entinostat Treatment Reduces TBI-Induce Chronic Neuroinflammation

Entinostat treatment also resulted in a positive anti-inflammatory effect. GFAP expression was found to be significantly reduced in all hippocampal subregions at 4-months post-injury (CA1, p=0.0079; CA3, p=0.0028; DG, p=0.0044) (**Fig. 39A-C**). Likewise, Entinostat treated mice displayed significantly reduced microglial expression, suggesting an ameliorated inflammatory response compared to untreated mice (CA1, p=0.0011; CA3, p=0.0001; DG, p=0.0003) (**Fig. 39D-F**). Together these results suggest that both HDAC inhibitors, SAHA and Entinostat, can alleviate neuroinflammatory cascades as well as glial scarring, often associated with brain injury. Moreover, reduction of acute inflammation has been shown to reduce other pathologies, such as neurodegeneration and behavioral recovery outcomes.

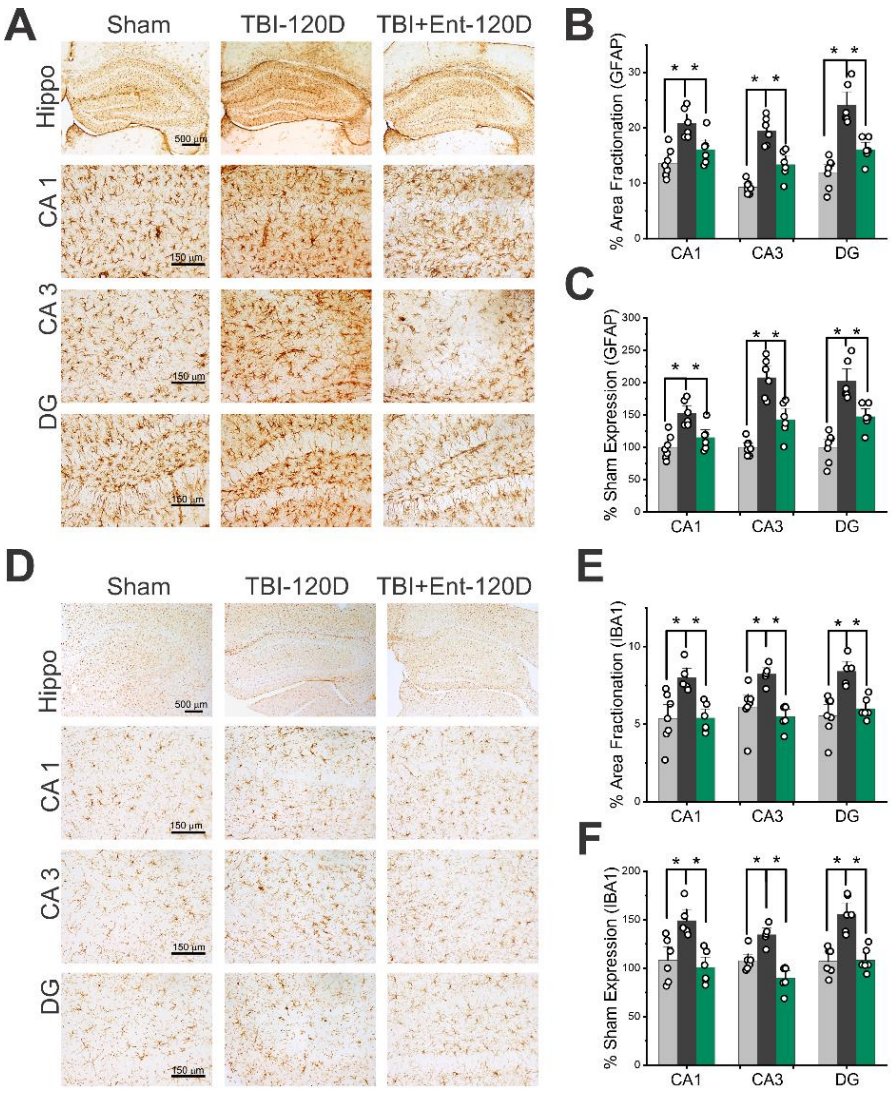

Figure 39: Entinostat Treatment Reduces Chronic Inflammation after Severe TBI. **A,** Hippocampal and regional (CA1, CA3, & DG) GFAP+ immunohistochemistry at 120d post-injury in Sham, 2mm-TBI, and 2mm-TBI+Ent cohorts to visualize chronic astrogliosis. Images taken at 4x (hippocampus) and 20x (CA1, CA3, DG). **B,** Area fractionation of GFAP+ staining for regions of interest CA1, CA3, & DG in Sham, 2mm-TBI, and Ent cohorts at 120d post-injury. **C,** Densitometric analysis of GFAP+ expression in regions of interest at 120d post-injury, expressed as percent Sham. **D,** Hippocampal and regional (CA1, CA3, & DG) IBA1+ immunohistochemistry at 120d post-injury in Sham, 2mm-TBI, and Ent cohorts to visualize chronic microgliosis. Images taken at 4x (hippocampus) and 20x (CA1, CA3, DG). **E,** Area fractionation of IBA1+ staining for regions of interest CA1, CA3, & DG in Sham, 2mm-TBI, and Ent cohorts at 120d post-injury. **F,** Densitometric analysis of IBA1+ expression in regions of interest at 120d post-injury, expressed as percent Sham.

IV. 3.8 SAHA Treatment on Long-term Sensorimotor and Behavioral Dysfunction

To assess health and recovery outcomes after moderate and severe brain injury, we took body weight measurements and evaluated health status over the initial 30d period post-TBI. We utilized the same composite health scoring protocol described in a previous paper (Golub and Reddy, 2021a; 2021b/Aim 1; 2). Briefly, mice were evaluated for their coat fur condition, eye health, and active/inactive behaviors. Additional behavior testing, including composite neuroscore functioning, beam walk, cage hygiene index, rotarod, burrowing, novel object recognition, and Morris water maze were also performed at regular intervals to assess sensorimotor or cognitive functioning. Following Sham or TBI surgery, TBI mice from all cohorts demonstrated weight loss in the first 30 days after injury. No significant interaction was found between injury depth or drug administration in body weight progression during the first month after injury (**Fig. 40-42A**).

TBI results in a wide range of sensorimotor and cognitive deficits, though location and severity of injury influence recovery outcomes and quality of life. With a lesser severity, it is expected that there is a lesser deficit in behavioral functioning. Within the 1mm cohorts, both treated and untreated mice performed similarly across all functional tests (**Fig. 40A-D, G**). However, on the psychiatric-focused tasks, such as cage hygiene index and the burrowing tasks, SAHA-treated animals performed significantly better than their untreated cohort. Cage hygiene was evaluated before cage changes in all groups. Sham cages typically appeared tidy, with large, fluffy nests created from the provided enrichment materials. Urine and fecal matter were constrained

to one or two corners of the cage, generally opposite their nest. On the contrary, TBI mice kept much more disorganized cages, with bedding often spread around the cage or left unused. Moreover, urine and fecal matter would also be spread throughout the cage instead of having a fixed location. On the other hand, SAHA-treated mice showed similar nesting and organized behaviors to sham-operated mice, suggesting HDAC inhibition treatment contributed to improvement in behavioral functioning ($p=0.0098$) (**Fig. 40E-F**). Disorderly cages in mice have often been attributed to dysfunction and depression-like behaviors (Deacon, 2006). Moreover, SAHA-treated mice removed more woodchips from the burrowing tube compared to untreated mice (Sham= 31.1±5.6 g; 1mm-TBI= 8.4±3.7g; 1mm-TBI+SAHA= 42.6±4.6g, $p<0.0001$) (**Fig. 40H**). Cage hygiene and burrowing tasks both focus on depression-like activities or behavioral dysfunction such that animals who score lower on the hygiene scale or remove less woodchips during the burrowing tasks are considered to be exhibiting depression-like symptoms. Therefore, from this data, we can conclude that SAHA treatment reduced long-term depression-like symptoms after TBI. This trend also kept true with the severe 2mm-TBI+SAHA cohort and narrow spectrum Entinostat-treated groups (next sections), though in these cohorts we also observed significant improvement in functionality.

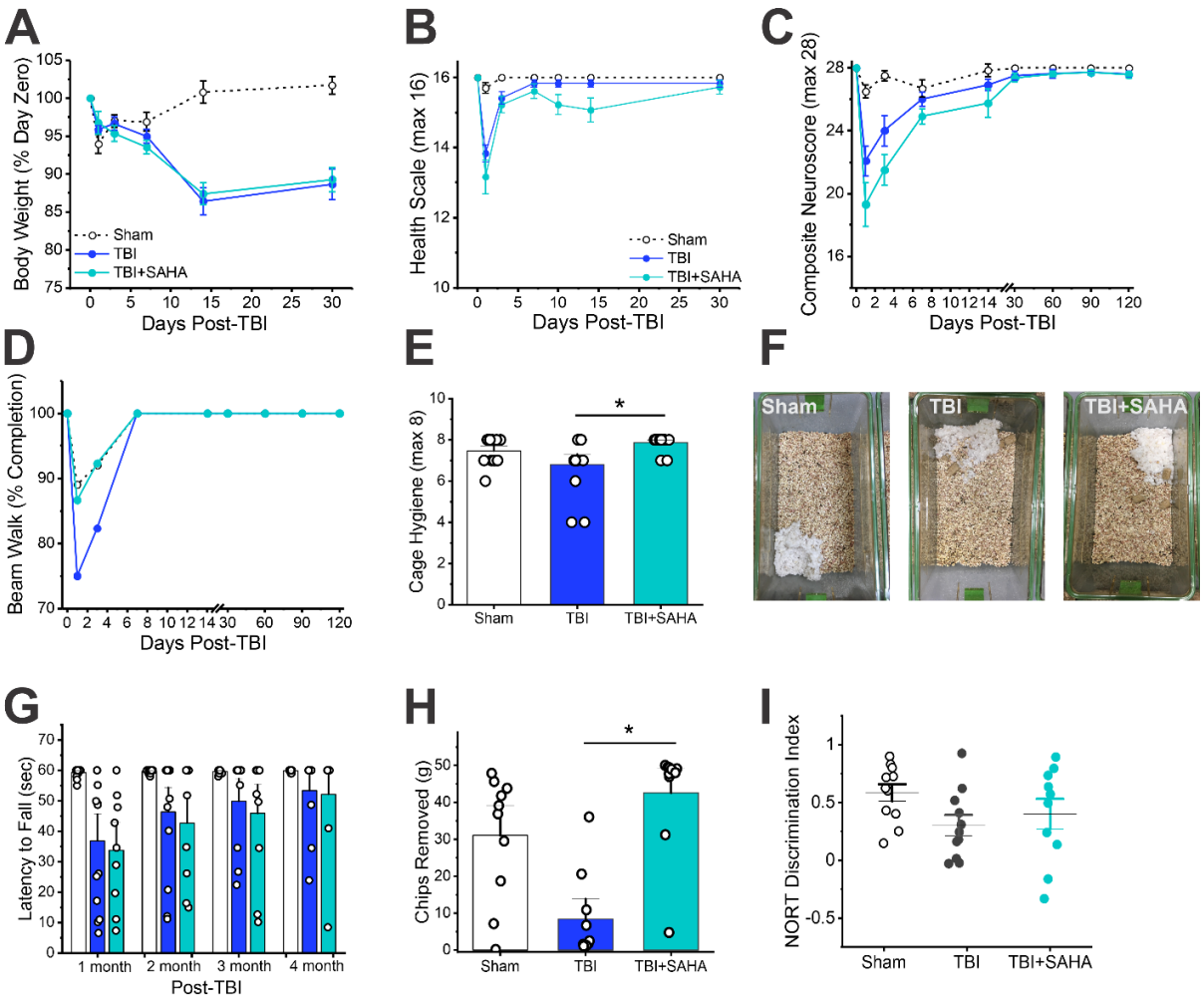

Figure 40: Effect of SAHA Treatment on Functional Recovery after Moderate TBI. **A,** Changes in body weight over time, expressed as percent of day 0 body weight. **B,** Acute health recovery outcomes after moderate TBI (health scale max=16 points). Full description of test in methods. **C,** Composite neuroscore over the 120-day observation period (max score=28 points). **D,** Percent completion of ability to cross beam walk apparatus over time. **E,** Cage hygiene index (max 8). **F,** Representative pictures of home cages from Sham, 1mm-TBI, or 1mm-TBI+SAHA mice. **G,** Latency to fall from rotarod test in 1-month increments post-injury. **H,** Amount of wood chips removed during burrowing test at 4-months post-injury. **I,** NORT discrimination index, as determined from the amount of time spent investigating the novel object versus old object, as a function of total investigation time. NORT was performed 4 months post-injury.

Within the 2mm-TBI cohorts, SAHA treatment resulted in faster recovery of overall health, as reported by the health scale (Day 3, $p<0.0001$; Day 7, $p=0.0237$) (**Fig. 41B**). As early as 1-day post-injury, we observed significantly improved sensorimotor function with twice-daily SAHA administration. SAHA-treated mice completed the beam walk task at a higher percentage than untreated mice ($p=0.0144$), and composite neuroscores revealed enhanced recovery, especially with respect to the grip strength component ($p<0.0001$) (**Fig. 41C-D**). These changes were observed as early as 1-day post-TBI and continued to improve over the 120-day observation period. The rotarod test was used to track improvement in balance and motor coordination over 4 months. In this task, mice must walk forward on a rotating beam to remain upright and not fall off. We kept the rotation of the rod set to 4 rpm, a speed at which sham and naive mice have maintained balance for a full minute without issue. Though no improvements were seen between SAHA-treated and untreated mice at 1-month, SAHA-treated mice successfully stayed on the rotating rod for a longer duration at months 2, 3, and 4 post-TBI compared to untreated mice ($p= <0.0001 - 0.0438$) (**Fig. 41G**).

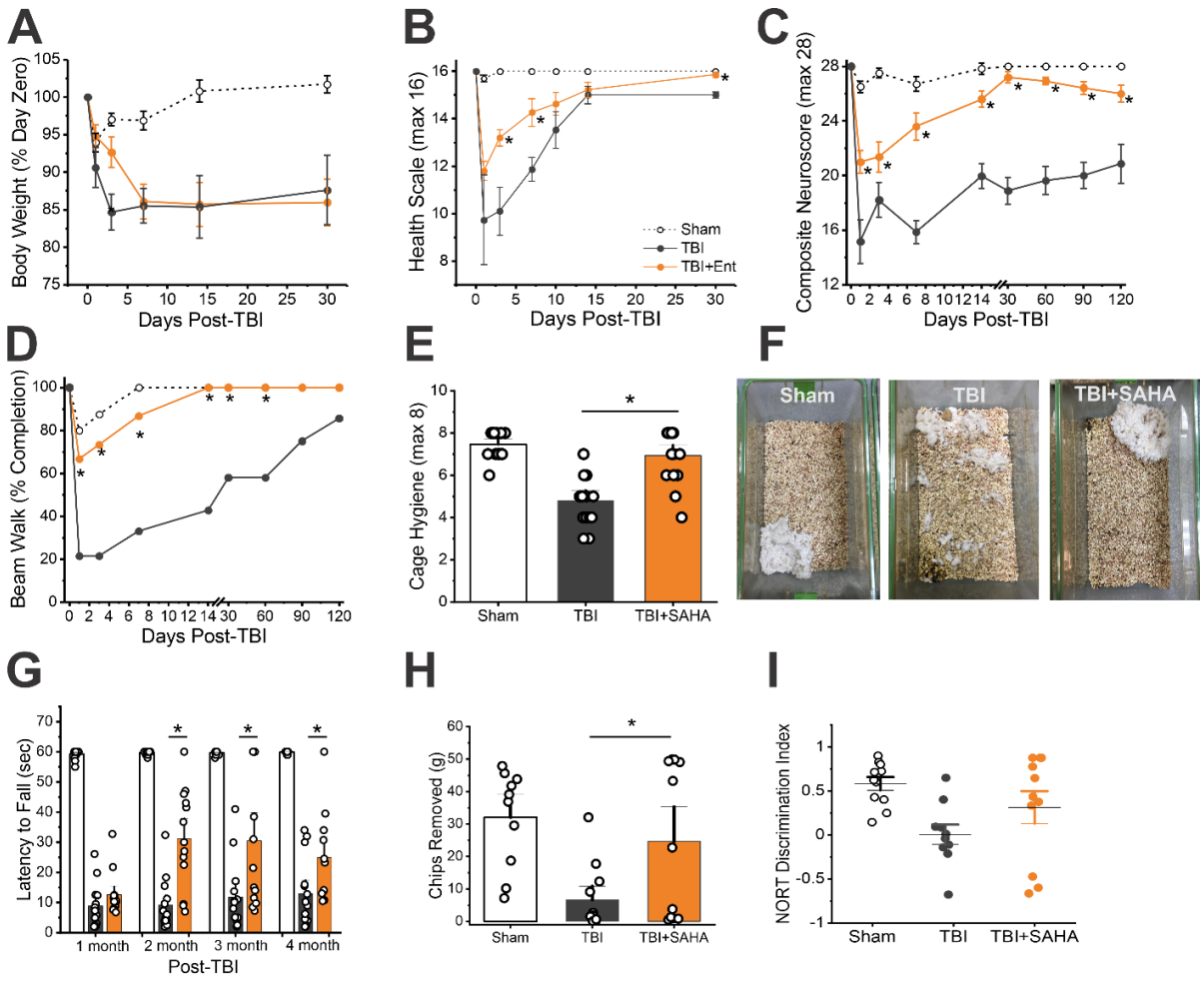

Figure 41: SAHA Treatment Improves Functional Recovery after Severe TBI. **A,** Changes in body weight over time, expressed as percent of day 0 body weight. **B,** Acute health recovery outcomes after severe TBI (health scale max=16 points). Full description of test in methods. **C,** Composite neuroscore over the 120-day observation period (max score=28 points). **D,** Percent completion of ability to cross beam walk apparatus over time. **E,** Cage hygiene index (max 8). **F,** Representative pictures of home cages from Sham, 2mm-TBI, or 2mm-TBI+SAHA mice. **G,** Latency to fall from rotarod test in 1-month increments post-injury. **H,** Amount of wood chips removed during burrowing test at 4-months post-injury. **I,** NORT discrimination index, as determined from the amount of time spent investigating the novel object versus old object, as a function of total investigation time. NORT was performed 4 months post-injury.

IV. 3.9 Entinostat Treatment on Long-term Sensorimotor and Behavioral Dysfunction

Similarly, we identified recovery and behavioral improvements with administration of the narrow-spectrum HDAC inhibitor, Entinostat. We observed faster recovery and overall health outcomes as early as 1-day post-injury ($p=0.0003$) (**Fig. 42B**). Entinostat-treated mice also had higher success in completing the beam walk task throughout the 120-day observation period compared to untreated mice (Day 1, $p=0.0367$). The neuroscore test reached significance at 7-days post-injury, in which Entinostat-treated mice showed improved function over their untreated counterparts ($p=0.0007$) (**Fig. 42C-D**). Improvement in acute behavioral functioning translated to rehabilitated rotarod ability over time. Once again, we observed little improvement in stability and motor function, as tested by the rotarod task, at 1-month post-injury. However, Entinostat treatment resulted in significantly improved rotarod performance at months 2, 3, and 4 ($p= 0.0104 – 0.0323$) (**Fig. 42G**). Together, our results suggest HDAC inhibition treatment, whether broad or narrow spectrum, helps to ameliorate motor deficits and improve recovery outcomes after severe TBI.

We also used behavioral tests to look at psychiatric behavioral dysfunction after severe TBI. Cages of 2mm-TBI mice were extremely unkept, with nesting materials strewn across most of the cage bottom. In some cages, the enrichment materials were left untouched or used as a latrine area. SAHA-treated mice constructed cleaner cages, with large, fluffy nests comparable to sham mice ($p<0.0001$) (**Fig. 42E-F**). We also found SAHA-treated mice performed better during the burrowing task compared to untreated mice, removing a greater amount of woodchips from the filled tube (2mm-TBI=

6.6±2.8g removed; 2mm-TBI+SAHA= 24.7±7.1 g removed, p=0.034) (**Fig. 42H**). Similarly, Entinostat treatment resulted in higher cage hygiene scores compared to untreated TBI mice ($p<0.0001$) as well as better performance during the burrowing task (2mm-TBI+Ent= 34.5±5.8g removed, $p<0.0001$) (**Fig. 42E-F, H**). Together, these results suggest HDAC inhibition treatment ameliorates negative psychiatric deficits, such as depression-like activity, often associated with TBI.

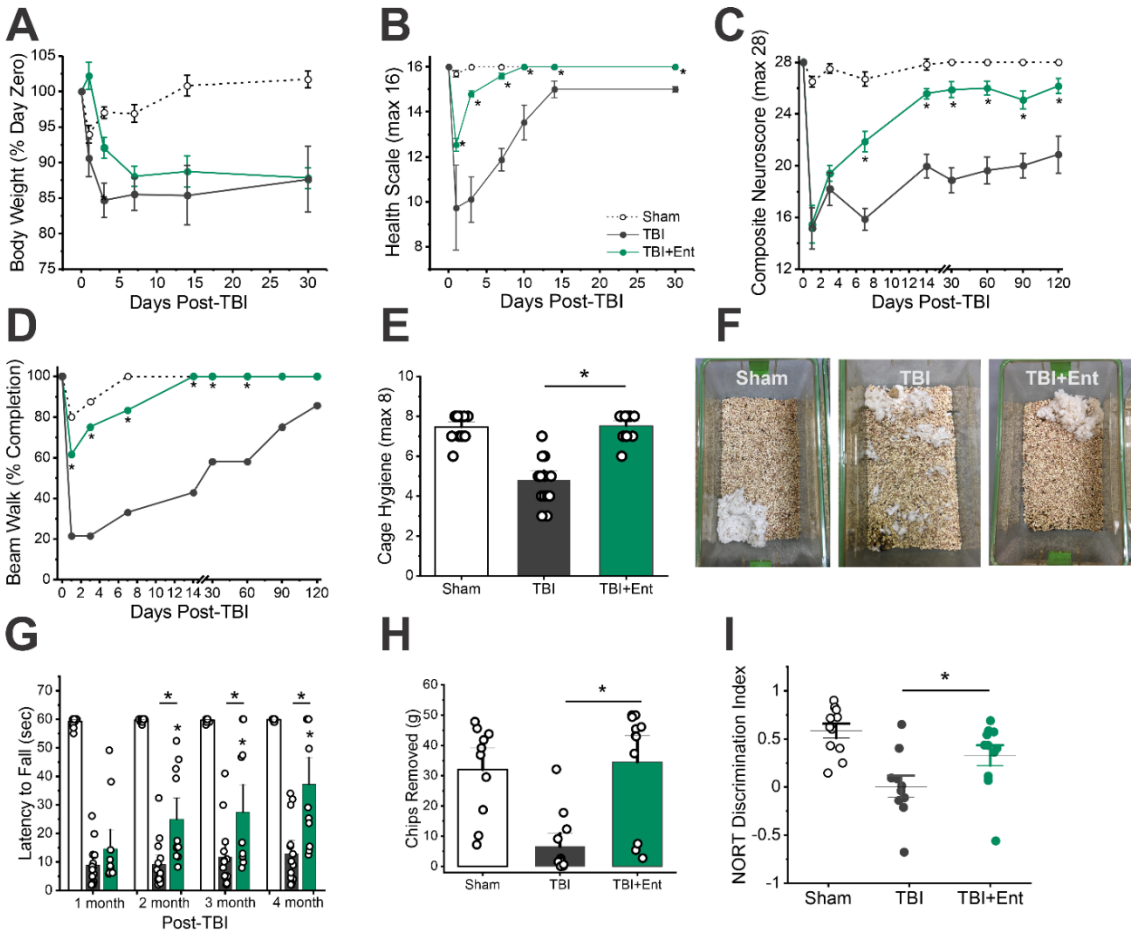

Figure 42: Entinostat Treatment Improves Functional Recovery after Severe TBI. **A,** Changes in body weight over time, expressed as percent of day 0 body weight. **B,** Acute health recovery outcomes after severe TBI (health scale max=16 points). Full description of test in methods. **C,** Composite neuroscore over the 120-day observation period (max score=28 points). **D,** Percent completion of ability to cross beam walk apparatus over time. **E,** Cage hygiene index (max 8). **F,** Representative pictures of home cages from Sham, 2mm-TBI, or 2mm-TBI+Ent mice. **G,** Latency to fall from rotarod test in 1-month increments post-injury. **H,** Amount of wood chips removed during burrowing test at 4-months post-injury. **I,** NORT discrimination index, as determined from the amount of time spent investigating the novel object versus old object, as a function of total investigation time. NORT was performed 4 months post-injury.

IV. 3.10 SAHA Treatment on Cognitive Outcomes following TBI

Cognitive functioning is a major concern after brain injury. The hippocampus plays a major role in learning and memory tasks. Therefore, we sought to investigate whether HDAC inhibition treatment would ameliorate cognitive deficits often seen after TBI. At 4 months after injury, we performed the Novel Object Recognition Task (NORT) and the Morris Water Maze (MWM) tests. The NORT test was used to examine non-spatial learning and memory, since this task requires functionality of multiple brain regions including the hippocampus, whereas the MWM task focuses on hippocampal-dependent spatial memory.

As a result of a moderate traumatic injury, we observed cognitive deficits in both 1mm-TBI cohorts, which were not ameliorated with SAHA treatment. TBI mice from both cohorts suffered a significant memory deficit, as evidenced by a reduced preference to investigate the novel object during exploration compared to sham-operated mice (**Fig. 40I**). During the MWM test, we found sham, 1mm-TBI, and 1mm-TBI+SAHA mice completed the task progressively faster during the four days of learning trials, suggesting all cohorts learned the location of the hidden platform. However, both TBI cohorts exhibited memory deficits during the testing days which occurred 1- and 5-days post-learning (**Fig. 43A-D**). Though SAHA treatment did not appear to alleviate cognitive deficits after moderate injury, we did observe improvements after severe TBI.

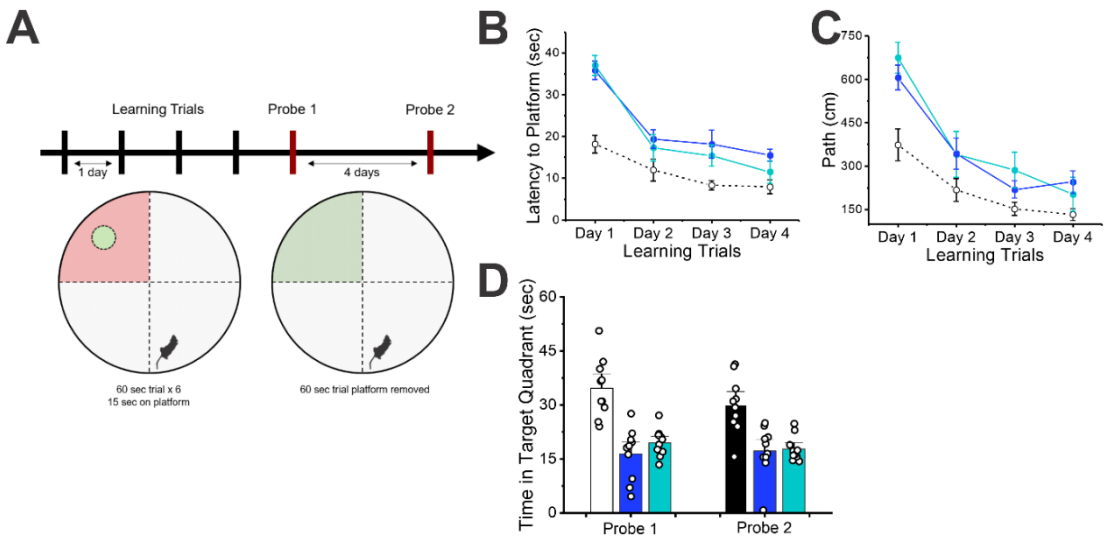

Figure 43: Effect of SAHA Treatment on Cognitive Function after Moderate TBI. **A,** Schematic of Morris water maze protocol used at 4 months post-TBI (1mm). Mice had four days of consecutive learning trials, each with 6-60s trials. After each trial, mice were placed on platform for 15 s before being removed from arena. At 24 hr and 5 days following last learning trial, the platform was removed, and mice were given 60 s to explore arena. Time spent in target quadrant was calculated on probe days. **B,** Average latency to platform (sec) during learning trials in Sham, 1mm-TBI, and 1mm-TBI+SAHA cohorts. (Sample sizes: Sham, n=10; TBI, n=12; SAHA, n=12). **C,** Average distance (cm) traveled to reach platform during learning trials in Sham, TBI, and SAHA cohorts. **D,** Time spent in target quadrant on probe days during Morris water maze.

Within the 2mm-TBI cohorts, SAHA treated mice demonstrated a progressively shorter latency to reach the hidden platform in the MWM task compared to untreated TBI mice. This was coupled with a decreased pathway. Latency to reach the hidden platform and path distance were significant on days 2-4 of the learning phase compared to untreated mice ($p=0.0126 – 0.0404$). Swim speeds between severe TBI cohorts was not significantly different, suggesting that this faster task completion and shorter distance was a drug effect. Furthermore, on both the short-term (1 day) and long-term (5 day) memory tasks, SAHA treated mice spent longer in the target quadrant searching for the removed platform, suggesting greater memory retention than untreated mice (Short-term, $p=0.0304$; Long-term, $p=0.0089$) (**Fig. 44A-D**). Similarly, SAHA-treated mice performed better on the NORT task compared to untreated mice, though this data did not reach significance ($p=0.1690$) (**Fig. 41I**).

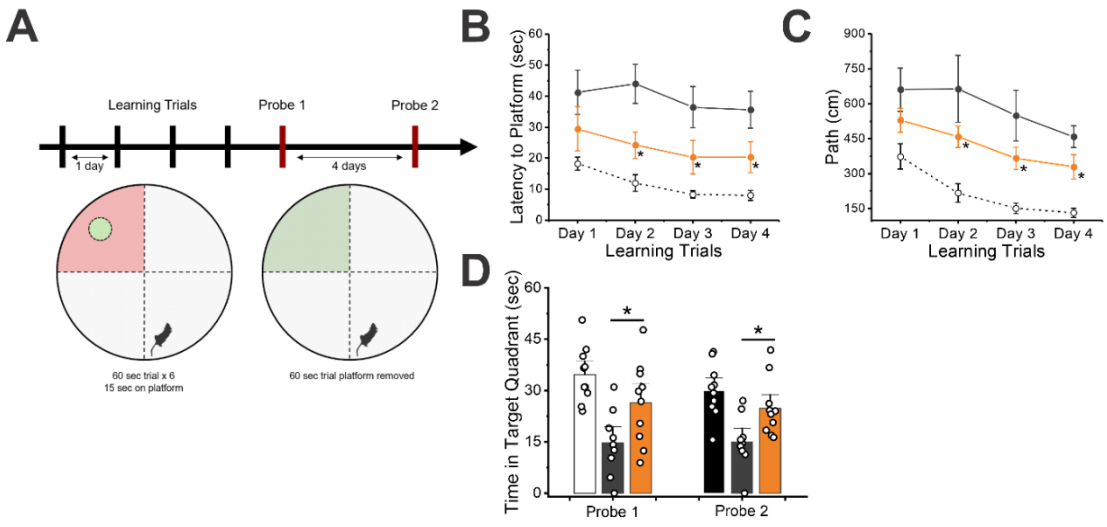

Figure 44: Effect of SAHA Treatment on Cognitive Function after Severe TBI. **A,** Schematic of Morris water maze protocol used at 4 months post-TBI (2mm). Mice had four days of consecutive learning trials, each with 6-60s trials. After each trial, mice were placed on platform for 15 s before being removed from arena. At 24 hr and 5 days following last learning trial, the platform was removed, and mice were given 60 s to explore arena. Time spent in target quadrant was calculated on probe days. **B,** Average latency to platform (sec) during learning trials in Sham, 2mm-TBI, and 2mm-TBI+SAHA cohorts. (Sample sizes: Sham, n=10; TBI, n=9; SAHA, n=10). **C,** Average distance (cm) traveled to reach platform during learning trials in Sham, TBI, and SAHA cohorts. **D,** Time spent in target quadrant on probe days during Morris water maze.

IV. 3.11 Entinostat Treatment on Cognitive Outcomes following TBI

Entinostat-treated mice also completed the MWM task with shorter latency and distance to reach the hidden platform on days 2-4 compared to untreated 2mm-TBI mice ($p<0.05$). Of note, on day 3 of learning trials, Entinostat-treated mice only latency to platform and not path distance reached significance. Short-term (1 day) and long-term (5 day) memory probes demonstrated Entinostat-treated mice spent a longer duration in the target quadrant compared to untreated mice, suggesting treatment rescued TBI-induced cognitive deficits in memory at both time points (**Fig. 45A-D**). Moreover, NORT revealed a similar rescue of cognition, as Entinostat-treated animals exhibited a higher discrimination index towards the novel object compared to untreated mice ($p= 0.0493$) (**Fig. 42I**). Together, our results suggest that HDAC inhibition treatment plays a role in adaptive recovery outcomes resulting in improved sensorimotor coordination, psychiatric function, and even better performance on learning/memory tasks. Furthermore, Entinostat-treated animals tended to perform better than SAHA-treated animals, especially on health and cognitive tasks, suggesting it may be a more optimal treatment for severe TBI.

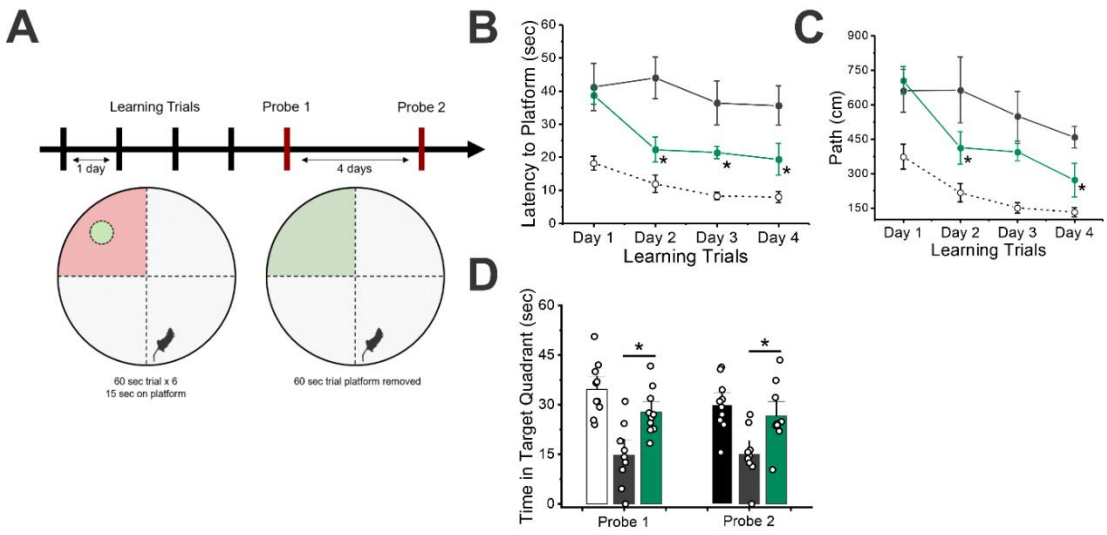

Figure 45: Effect of Entinostat Treatment on Cognitive Function after Severe TBI. **A,** Schematic of Morris water maze protocol used at 4 months post-TBI (2mm). Mice had four days of consecutive learning trials, each with 6-60s trials. After each trial, mice were placed on platform for 15 s before being removed from arena. At 24 hr and 5 days following last learning trial, the platform was removed, and mice were given 60 s to explore arena. Time spent in target quadrant was calculated on probe days. **B,** Average latency to platform (sec) during learning trials in Sham, 2mm-TBI, and 2mm-TBI+Ent cohorts. (Sample sizes: Sham, n=10; TBI, n=9; Ent, n=10). **C,** Average distance (cm) traveled to reach platform during learning trials in Sham, TBI, and Ent cohorts. **D,** Time spent in target quadrant on probe days during Morris water maze.

CHAPTER V

DISCUSSION

V. 1 Contusion Brain Damage in Mice for Modelling of Post-Traumatic Epilepsy with Contralateral Hippocampal Sclerosis

To our knowledge, this study is the first attempt to comprehensively advance a contusion brain injury in mice for post-traumatic epilepsy, which is characterized by spontaneous seizures, neuropathology, and behavioral dysfunction. Apart from the primary tissue damage from initial injury, a pathological secondary damage can result from focal and diffuse inflammatory responses. Signals of microgliosis and astrogliosis in the contralateral hippocampus peaked within the first week following injury and lasted for nearly four months. The hallmark response of neurodegeneration of principal and inhibitory cells was evident starting at 30 days post-TBI. To further illustrate the impact of these histological changes on post-traumatic epileptogenesis, we overlaid seizure output over 120 days with neuropathological outcomes over the same period. Both astrogliosis and microgliosis peaked in the early stages of epileptogenesis; however, progressive loss of PV+ interneurons and NeuN+ cells corresponded with the onset and progression of SRS (**Fig. 46**). This temporal remodeling of brain circuitry through maladaptive immune responses in conjunction with robust cell loss provides a strong credence as a potential mechanism of post-traumatic epileptogenesis. These PTE models hold great promise for deeper understanding of the pathogenesis and identifying therapeutic interventions for PTE.

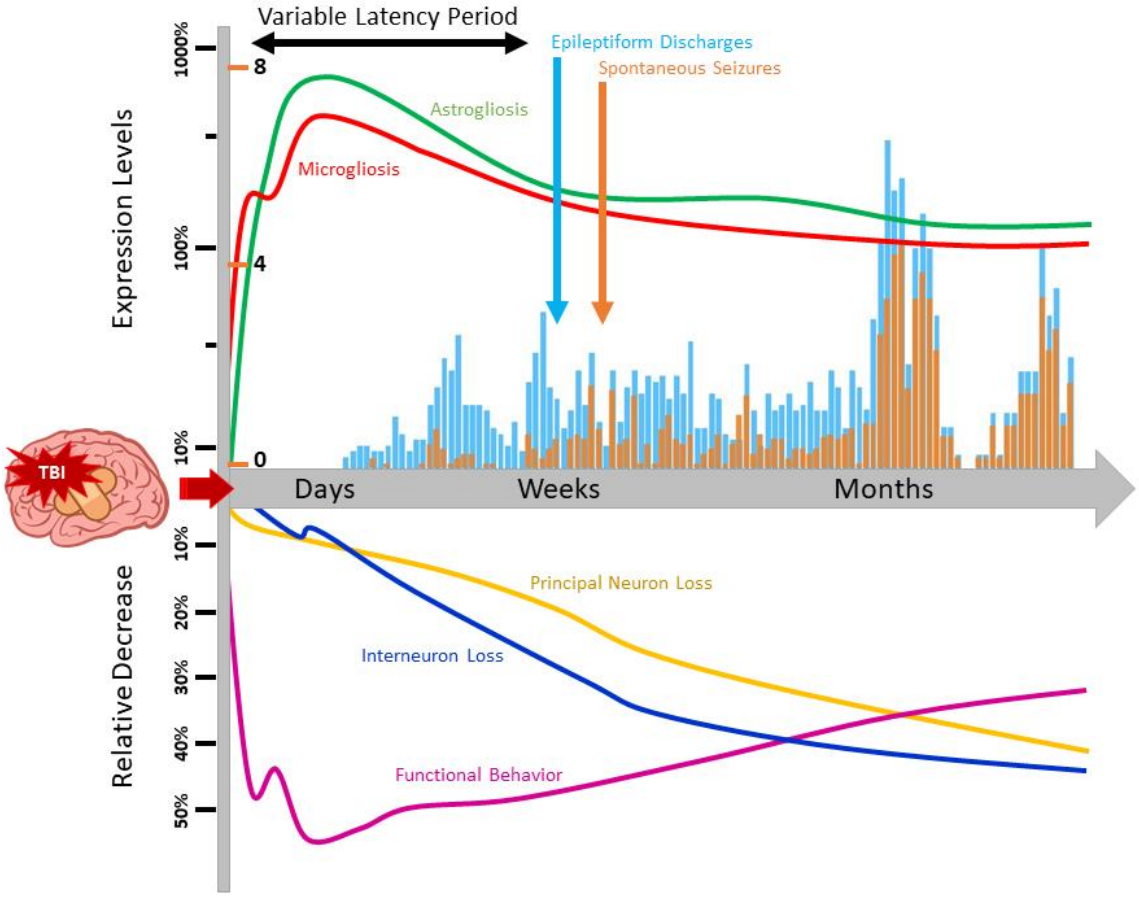

Figure 46: Summary of TBI-induced Pathologies of Epileptogenesis.
TBI induces a number of overlapping pathologies which effect epileptogenesis and recovery. Early stages of injury, both maladaptive and repair, include inflammatory cascades via astrocytes and microglia. This neuroinflammation peaks approximately 1 week after injury. Neurodegeneration near the impact site is initiated by direct damage; however, contralateral cell loss was observed in this model as early as 1 month after injury. Seizures and epileptiform discharges emerged from responding animals within 4-8 weeks post-TBI in most cases. Lastly, functional recovery was an ongoing process that improved over time.

PTE occurs as temporal lobe epilepsy in 35-62% of cases, affecting the limbic circuits within the hippocampus and amygdala (Zhu et al., 2019; Diaz-Arrastia et al., 2000). Given the location and depths of injury used in this mouse model, we expected the focus of PTE to be the hippocampus. We identified hyperexcitability and seizures in both groups of mice. The severe TBI cohort had significantly higher incidence of chronic epilepsy and displayed a robust inflammatory response leading to progressive neurodegeneration and behavioral deficits. Intriguingly, functional recovery still occurred concurrently with progressive neurodegeneration. Therefore, it is likely that recovery from injury is a separate mechanism to the development of epileptogenesis and seizure induction. The moderate TBI cohort also displayed chronic seizures and behavioral deficits, and as expected, these functional changes were less severe. More intriguingly, seizures developed more quickly in the moderate-cohort compared to the severe-cohort (20 vs 53 days), and responders had a higher average cumulative seizures (84 vs 47 seizures/animal). This suggests that SRS frequency may be worse after moderate than severe injury, even though risk of chronic seizures is much lower.

The risk of PTE increases with severity of brain injury (Englander et al., 2003), though differences in seizure frequency under varying impact depths has not been fully investigated. Our data shows significant differences in brain architecture between the two TBI cohorts. The severe (2mm)-impact created a vast, expanding lesion which encompassed much of the surrounding cortical tissue and the ipsilateral hippocampus. TBI creates a brain state geared towards active recovery and compensation for lost tissue, often leading to maladaptive inflammation and neuron loss (Hunt et al., 2013).

Overtime, we found the impact was not isolated solely to the injured hemisphere. Increased expression of GFAP and IBA1 was found globally, peaking within the first week and continuing throughout the 4-month observation period, suggesting long-lasting neuroinflammation. Furthermore, significant loss of inhibitory interneurons and principal neurons was observed beginning at 30d post-injury and progressing up to 120d period and beyond. The contralateral hippocampus is forced to overcompensate for the lost tissue, inducing a transient increase in newborn neurons. Ectopic granule cells and overall loss of inhibitory circuitry through degeneration of PV+ interneurons create a state of hyperexcitability and reduced seizure threshold (Hester and Danzer, 2013). The vulnerable non-impacted hippocampus serves as the focal point of seizures in the 2mm-TBI cohort, but only after the secondary consequences of TBI exceed the brain's repair capabilities. Our graphical abstract summarizes the major changes seen within our model of PTE. We project that selective tissue loss, under these TBI conditions, essentially removed the likely focal point of seizure generation (i.e. ipsilateral cortex and hippocampus), similar to a resective epilepsy surgery (Wyler et al., 1995; West et al., 2016).

In contrast, the moderate (1mm)-impact inevitably generated a smaller lesion, encompassing only the surrounding cortical tissue, leaving both hippocampi susceptible to maladaptive repair processes. We found extensive loss of inhibitory interneurons at 4-months post-TBI. Contralateral interneuron loss was comparable to the 2mm cohort, but loss within the ipsilateral hippocampus was significantly higher (60% PV+ cell loss ipsilateral vs 38% PV+ cell loss contralateral). Similarly, we found the ipsilateral

hemisphere to have much higher microglial inflammation compared to the contralateral hemisphere. Though both hippocampi suffered from secondary damages from TBI, they were both largely intact and extremely susceptible to reorganization in function, resulting in an accelerated epileptic state in susceptible responders with SRS.

Mechanisms by which TBI produces PTE are likely complex; herein, we have identified one potential pathway within the contralateral hippocampus following initial injury. Generally, TBI models focus on the injured side only, and in some cases use the contralateral hemisphere to normalize changes that are occurring ipsilaterally (Shandra and Robel, 2020; Hunt et al., 2009, 2010). However, our data suggests that the surviving tissue from the contralateral side is contributing to a greater extent to the epileptogenic changes happening in the brain and may be providing a primary or alternate focus for seizure generation in the case of severe injury. Tong et al. hinted at the potential on contralateral damage after CCI in mice, with findings of progressive white matter damage extending to the contralateral subcortices at 3 days after injury (2002). Though excellently portrayed, this study only tracked neuropathology within the first 21 days post-TBI. Few studies following this have intentionally characterized the damages which extend to the uninjured hemisphere overtime, thereby highlighting the importance of the present study. Interestingly, we found severe neurodegeneration within both sides of the hippocampus within the 1mm-TBI cohort, though damage was more extensive in the ipsilateral side. If true, possible future treatment options may include targeting such distant regions, since damage is not restricted to the impact site and its surrounding tissues.

While TBI promotes plasticity and reorganization in the limbic structures, there are likely other sites or cortical regions that regulate mood and behavior. We probed this notion with several behavioral analyses throughout the epileptogenic period. We found that the moderate (1mm)-TBI cohort had only a transient change in motor ataxia, which recovered within a few weeks after injury. The severe (2mm)-injury resulted a striking dysfunction, which was prolonged through the observation period. More than 60% of TBI patients experience psychiatric disorders up to 5 years post-injury, including impaired memory and depression (Whelan-Goodinson et al., 2009). We noted depressive-like symptoms in both TBI cohorts during the burrowing test, and a more graded depressive response within the cage hygiene index. TBI mice showed significant changes in anxiety (amygdala-mediated) behavior during the open field and elevated plus maze tests. Consistent with hippocampal sclerosis, mice with PTE exhibited marked memory deficits in the NORT and water-maze tests. These results are highly consistent with the vast literature on TBI-induced permanent memory dysfunction and interventions that correct neurodegeneration in the hippocampus to improve memory after TBI (Zhu et al., 2019).

There are some caveats to our practical protocol for vEEG. Longitudinal vEEG studies are the most useful for investigating changes in neuronal circuitry by reducing the amount of missed data of seizure occurrence. In this study, animals were given a mandatory 10-day recovery period following TBI impact. We found that this recovery time allowed the mice to better recover and reduced risk of premature death in the cohorts but limited our early recording abilities. Nevertheless, we noticed post-traumatic

seizures in most cases and variable incidence in both cohorts. Accordingly, the epileptiform data is presented using only responding mice from each cohort. We did not explore the mechanisms underlying the differences in the pathological response between responders vs non-responders in each TBI cohort. Besides an emphasis on disparities between epileptic and non-epileptic cohorts following TBI, our ongoing studies are investigating the potential age- and sex-differences in PTE outcomes.

TBI-related PTE in humans is highly variable and dependent on susceptible factors. Deciphering such factors may offer an integrated approach to PTE research. Rodent models have inherent limitation because rodent brain is lissencephalic and has relatively little white matter and gyri than human brain. Moreover, due to this complexity, it is not feasible to create identical symptoms associated with the human condition; however, a consistently reproducible model of PTE with SRS is crucial to elucidating the pathogenesis of PTE. Here, we reveal comparable features in the most comprehensive study of PTE to date, providing two PTE model options. The moderate PTE model may be best to investigate the process of epileptogenesis since subgroups of animals with and without spontaneous seizures should arise, thus giving researchers the opportunity to investigate intracohort pathologies. Furthermore, the severe PTE model produces high incidence of spontaneous seizures, thereby creating a much-needed platform for exploration of therapeutic modalities for prevention and treatment of PTE.

An overarching goal of this study was to validate a mouse PTE model. Experimental models of PTE which reflect the human condition are urgently needed to unravel the mystery of epileptogenesis and test new therapeutic options. Here we show a

multifaceted approach to PTE research in which we investigate the progressive epileptiform activity, histopathological changes, and functional deficits at two different injury levels. Our findings validate that SRS develops progressively following brain damage in mice. The neuropathology is highly consistent with neuronal lesion, atrophy, or network rewiring within the hippocampus. An injury-severity dependent tissue lesion and contralateral hippocampus sclerosis with neuronal loss and inflammation were strongly evident with the onset and severity of PTE, as well as concomitant behavior and cognitive deficits. Thus, this mouse model could be of value in evaluating pathophysiology and novel treatment for PTE.

V. 2 Targeting Epigenetic Pathways Reduces Inflammation and Provides Neuroprotection in a Mouse Model of Post-Traumatic Epilepsy

Understanding and treating PTE presents with a unique challenge due to its position at the meeting point of epileptology and neurotrauma. Pathologic risk factors for PTE vary greatly by the brain region affected, including contusion, subdural hematoma, BBB disruption, prolonged inflammation, and neurodegeneration (Bolkvadze and Pitkanen, 2012). Severity of injury is also strongly correlated with the development of spontaneous recurrent seizures (Annegers et al., 1998). Unfortunately, there are no currently available treatments for effectively slowing or preventing epileptogenesis after TBI. HDAC inhibitors, such as sodium butyrate, have been shown to alleviate the inflammatory response in lung injury (Liang et al., 2013), spinal cord injury (Zhang et al., 2018), and stroke (Park and Sohrabji, 2016), as well as possess other protective

effects which may be beneficial in subduing secondary injury cascades after TBI (Shein et al., 2009; Nikolian et al., 2019). Therefore, the current study aimed to investigate the therapeutic potential of sodium butyrate on posttraumatic seizures and its associated comorbidities.

The neuroprotective effects of HDAC inhibitors have been associated with their ability to restore histone acetylation levels disrupted in CNS disorders and during injury (Ferrante et al., 2003; Rouaux et al., 2004). Consistent with these reports, we observed a robust increase in HDAC activity after TBI in the cortex and hippocampus, suggesting regional reduction in acetylated H3 protein (Gao et al., 2006). Systemic administration of sodium butyrate normalized HDAC hyperactivation throughout the first month post-injury, confirming both availability and activity of this agent within the injured brain. HDAC inhibitors have also been shown to convey anti-inflammatory effects in rodent models through their ability to reduce COX-2 levels, and decrease IL-6, IL-12, and IFN-γ (Hull et al., 2016). Our observations expand on previous findings, as we show sodium butyrate reduces microglial accumulation and lessens GFAP and iba-1 expression within the contralateral hippocampus.

Mature astrocytes in the healthy brain are largely postmitotic; however, following TBI a subset of scar-forming astrocytes reenter the cell cycle to increase astrocyte numbers at the site of injury (Buffo et al., 2008). Additionally, resident microglia accumulate to the site of injury and alter their morphology into an active state after CNS injury. We identified a significant reduction in GFAP and iba-1 immunohistochemistry in the contralateral hippocampus after 7 days of sodium butyrate

treatment. This acute response to treatment likely contributed to the significant reduction in chronic inflammation and neurodegeneration seen at 120 days post-TBI. Maladaptive immune responses in the brain can disrupt the balance of neuronal excitability, impair cell survival, and further weaken the integrity of the blood brain barrier such that the brain becomes susceptible to blood-borne molecules and circulating pathogens (Vezzani and Granata, 2005). Therefore, a timely reduction of neuroinflammation enhances the potential of interrupting epileptogenesis and improving quality of life.

A serious neurologic complication of TBI is the increased risk of seizures, either by direct result of trauma or long-term alteration of neuronal networks resulting in chronic epilepsy. Currently, there is no clinically viable treatment for the prevention or prophylaxis of post-traumatic seizures. To determine if global network hyperexcitability could be modified by HDAC inhibition therapy, we continuously monitored brain function using video-EEG. Monitoring brain function through continuous EEG overcomes several confounds present in data from studies with intermittent recordings. Primarily, the advantages come from the ability to determine false negative events and preventing overestimation of ictal frequency. We observed significant augmentation of seizure burden in sodium butyrate treated mice. Though latency to first seizure and incidence did not differ between cohorts, sodium butyrate treated mice experienced far fewer seizures, and these seizures were shorter in duration. The data shown in this report mimic the results found with sub-chronic administration of sodium butyrate in a kindling model of temporal lobe epilepsy (Reddy et al., 2015). HDAC inhibition therapy retarded the development of limbic epileptogenesis, reduced behavioral responses to seizures, and

showed erasure of the epileptic state in mice without affecting after-discharge signal. Likewise, we observed a substantial rescue of TBI-induced reduction of seizure threshold with sodium butyrate treatment in the current study. Though only a few studies have reviewed the potential role of HDAC signaling in epileptogenesis, data has shown promising results for disease modification (Zhang et al., 2008; Dash et al., 2009; Shein et al., 2009; Younus and Reddy, 2017; Nikolian et al., 2019; Chang et al., 2019).

HDAC inhibitors alter neuronal plasticity and memory, often demonstrating multifactorial roles in preserving tissues and promoting functional recovery (Ganai et al., 2016). We observed strong evidence of functional improvement and recovery outcomes with sodium butyrate administration. Treated mice regained body weight, improved neurofunctional scores, and performed motor/balance tasks more effectively than non-treated mice after TBI. Furthermore, our results suggested HDAC inhibition therapy contributed to significant improvement in psychological and cognitive outcomes during the open field anxiety and Morris water maze studies. Learning trials of the water maze test suggested learning occurred in all cohorts as latency and path to platform improved with each consecutive day. Previous studies have shown HDAC inhibition not only rescues learning and memory deficits after stroke and fear conditioning, but also enhanced these processes in naïve rodents (Stefanko et al., 2009; Fass et al., 2013). This mechanism likely involves increased acetylation in neuronal histones H3 and H4, especially within the CA1 and CA3 of the hippocampus (Miller et al., 2008). Interestingly, we found neither the TBI nor SB cohorts showed memory retention of

platform location during probe trials, suggesting learning did not manifest as long-term retention and memory.

Cognitive impairment in epileptic patients has been well documented and, in some cases, long-term use of antiepileptic drugs to control seizures can contribute to memory dysfunction (Ronen et al., 2003; Brooks-Kayal et al., 2014; Mula and Trimble, 2009). The hippocampus plays a critical role in both learning and memory, especially during spatial learning tasks such as Morris water maze. Additionally, the hippocampus is one of the most excitable structures in the brain. One highly studied form of memory in the hippocampus is long-term potentiation (LTP). There are many similarities between the processes of LTP and seizures (Meador, 2007). LTP is most easily induced at bandwidths which are active during high-frequency ictal activity, and both seizures and LTP require activation of NMDA receptors. These shared characteristics suggest overlapping processes may be disrupted in pathologies such as TBI. Ongoing seizure progression, as seen in PTE models, can saturate the hippocampal synapses with long-term facilitation, thereby decreasing their capacity for plasticity and disrupting similar processes such as LTP and memory. Supporting this, repeated electroconvulsive seizures have been linked to reduced LTP (Reid and Stewart, 1997). In our study, we observed large hippocampal lesions and SRS in both TBI and SB cohorts. It is perhaps unlikely a single drug could completely rescue cognitive function in these severe cases; however, significant improvement in the learning process shows therapeutic potential of HDAC inhibition to improve quality of life.

Our previous work which extensively characterized post-traumatic epileptogenesis (PTE) determined that certain aspects of the disorder are progressive overtime, such as neurodegeneration and lesion volume (Golub and Reddy, 2021). This implies a therapeutic window exists to halt or modify disease course. Our experiments were designed to determine whether administration of the HDAC inhibitor, sodium butyrate, after TBI was disease modifying (i.e., prevents the development or reduces the severity of chronic epilepsy). HDAC inhibition therapy can provide a sustainable benefit, with neuroprotective effects seen well after administration has ended (Shein et al., 2009). As opposed to immediate or pre-injury treatments, our data is relevant to the treatment of TBI and PTE patients who may not receive medical attention for hours or days after injury. Investigations into the epigenetic processes has revealed significant changes to the epigenome in both a TBI and epileptic brain (Sweatt, 2013). These alterations can cause dramatic shifts in gene expression, potentially conferring maladaptive or beneficial effects on the disease state. In this study, we demonstrated that HDAC inhibition slowed the progressive nature of lesion formation and neurodegeneration, ultimately resulting in a decreased seizure burden and improved motor-neurological function.

In conclusion, our data provides significant evidence that targeting HDAC pathways can improve quality of life and reduce seizure burden of PTE, including reducing acute and chronic inflammation, ameliorating cell death, decreasing aberrant mossy fiber sprouting, and improving motor and cognitive functions. Several HDAC inhibitors are already approved for other clinical indications and have a favorable safety

profile in humans. Therefore, these agents represent a promising and timely means of expanding the range of therapeutic agents available for treating TBI and PTE affected patients.

V. 3 Broad and Narrow Spectrum HDAC Inhibitors as Potential Antiepileptogenics in a Mouse Model of Post-Traumatic Epilepsy

Our results show that HDAC inhibition treatment after TBI exerts a significant therapeutic effect on post-traumatic seizures and comorbidities associated with PTE. We observed a remarkable reduction in the incidence of epilepsy in treated mice—whether they were treated with the broad-spectrum inhibitor, SAHA, or the narrow-spectrum inhibitor, entinostat. We found that this reduction in seizure burden was not limited to a reduction of responding animals, but also to seizure frequency. Moreover, expression of GFAP and Iba1 has been linked to neuroinflammation, which contributes to the epileptogenic process. Restoring homeostatic lysine acetylation at histone proteins reduces maladaptive immune responses via the downregulation of pro-inflammatory mediators (Patnala et al., 2017). Indeed, SAHA and entinostat treatment reduced chronic inflammation at 4-months post-TBI, implying treatment lessened the inflammatory response at an early stage after injury and improved pathology. Behavioral testing revealed mice treated with HDAC inhibitors exhibited better health outcomes overall, including improvements in motor function, reduction of psychiatric ailments, and rescued cognition. Together, we found this therapy to be largely successful in abrogating the epileptogenic process after TBI.

HDAC activity has been implicated in numerous cellular processes and pathways, and some studies suggest these roles have a dual effect on the regulation of neuronal viability (Bardai et al., 2012). However, accumulating evidence supports the notion that hypoacetylation of histones and transcriptional dysfunction play a critical role in the development of chronic neurological conditions, particularly neurodegenerative disorders such as dementia and Huntington's (Chuang et al., 2009). Though not considered a classical neurodegenerative disorder, epilepsy disorders are known to exhibit neuronal cell loss and progressive cognitive decline, resembling a neurodegenerative disease (Ono and Galanopoulou, 2019). HDAC inhibition therapy has neuroprotective effects both in vivo and in vitro; however, the benefits of broad vs narrow spectrum HDAC inhibitors, or vice versa, have yet to be fully explored, especially within the context of epileptogenesis. Rather than using broad-based therapies, focusing on targeted pharmacological treatments may be more therapeutically beneficial and result in fewer off-target consequences or negative side effects. Within that line of thought, we used a narrow spectrum HDAC inhibitor, entinostat, with specificity towards Class I HDAC1 and HDAC3, and compared the results to the broad-spectrum Class I and II HDAC inhibitor, SAHA, which is currently FDA approved for T-cell lymphoma and undergoing clinical trials for other indications. We chose entinostat as our narrow-spectrum compound due to the prevalence of HDACs 1 and 3 in the brain, as well as their interaction with each other. The HDAC1-HDAC3 interaction is greatly elevated under conditions of neurodegeneration and injury. Knocking down HDAC3 suppresses HDAC1-induced neurotoxicity, and vice versa (Bardai et al., 2012).

Furthermore, the neurotoxic effect of overexpression of either of these HDAC proteins is inhibited by treatment of IGF-1, expression of Akt, or inhibition of GSK3β (Bardai and D'Mello, 2011).

In a previous study, we observed significant disease modifying effects of sodium butyrate administration, both within an electrical kindling model of temporal lobe epilepsy (Reddy et al., 2017) and post-traumatic epilepsy (Golub and Reddy, 2021b/Aim 2). These studies provide a scientific basis of HDAC inhibitors as therapeutic interventions in acquired epilepsies. Furthermore, a previous experiment by Brandt et al. reported extended treatment with valproate, an anti-seizure medication with HDAC inhibition properties, prevented hippocampal damage and behavioral dysfunction occurring after status epilepticus, though it did not prevent spontaneous post-status epilepticus seizures (2006). Although these studies did not reduce incidence of seizures after TBI, the data indicate strong disease modifying effects of treatment that may extend to the whole class of compounds.

The first major finding in the present study was that both SAHA- and entinostat-treated cohorts showed a significant reduction in the incidence of post-traumatic seizures and discharges over the 120-day observation period. Within the severe TBI cohorts, we observed spontaneous recurrent seizures in 81% of untreated, 43% of SAHA-treated, and only 33% entinostat-treated mice. This data revealed a consistent relief in seizure burden not only with the significant reduction of responding animals, but also in the frequency of seizures within the treatment groups. To highlight the potential therapeutic value of our results, we performed 6 Hz seizure threshold testing at 4-months post-TBI.

Unsurprisingly, severe TBI mice exhibited a significant drop in the amperes needed to stimulate a seizure, whereas treated mice, either with SAHA or entinostat, displayed a significantly rescued threshold to electrically stimulated seizures. Combined with the reduced incidence of epilepsy within these cohorts, our results suggest a robust effect of HDAC inhibition for interrupting the epileptogenic process.

Positive results from the continuous video-EEG recording were backed up by a reduction of chronic inflammation in the contralateral hippocampus. At 4 months post-injury, overexpression of GFAP and Iba1 immunohistochemistry was still present after severe TBI in untreated mice. HDAC inhibition treatments, such as sodium butyrate, are known to possess anti-inflammatory mechanisms in CNS injuries by downregulating pro-inflammatory signaling of NF-κB, thereby reducing upregulation of inflammasome transcription and their interaction with caspase-associated cell death (Guo et al., 2015; Park and Sohrabji, 2016; Jiang et al., 2020). In a similar response to our previous studies using sodium butyrate (Golub and Reddy, 2021b/Aim 2), we observed an amelioration of chronic inflammation with both SAHA and entinostat treatment regimens. We expect that early treatment with HDAC inhibitors reduced acute inflammation, resulting in a snowball effect of positive recovery outcomes such as improved motor functional behavior, rescued cognition, lessened neuronal cell loss, and reduced seizure burden. Targeting inflammation in epileptogenesis has long been a therapeutic strategy in preclinical epilepsy models, with a wide variation in results (for review see: Dey et al., 2016). Translating these results to the clinical setting have been challenging due to the complexity of the inflammatory networks and specificity of the small molecules used.

Multi-target compounds, such as HDAC inhibitors, or combinational drug studies using currently available anti-seizure medications may maximize efficacy and overcome treatment resistance in refractory conditions such as status epilepticus or PTE.

HDAC inhibition has been implicated in alleviating cell loss and improving neurological recovery after stroke and brain injury (Zhao et al., 2019). TBI rodents characteristically display cognitive impairment and psychiatric comorbidities such as depressive-like and anxiety-like behaviors (Kosari-Nasab et al., 2019; Piao et al., 2019). Both preclinical and clinical findings have demonstrated that anxiety- and trauma-related disorders, such as post-traumatic stress disorder, are accompanied by dynamic changes to the epigenome, suggesting that epigenetic modification may affect chronic stress and behavioral responses associated with brain injury (Matosin et al., 2017; Daskalakis et al., 2018). Furthermore, previous studies involving cytotoxic lesions of the hippocampus have found reduced nesting and burrowing behaviors, suggesting changes in emotionality (Deacon et al., 2002). In the present studies, we observed positive reductions in psychiatric comorbidities within the HDACi-treated cohorts. Both SAHA- and entinostat-treated mice produced clean, complex nests within their home cages. Furthermore, they indicated healthy food storage and burrowing habits compared to the untreated counterparts. Though we only recorded these behaviors towards the end of the observation period, changes in hygiene behavior were seen as early as the first week post-injury in grooming behaviors and collated health scale scores. Our data echo that of previous studies in which anti-depressive like behaviors were observed as a result of pharmacological administration of HDAC inhibitors, owing to their modulation of a

wide number of depression-related genes such as BDNF and CREB (Tsankova et al., 2006; Covington et al., 2009; Sun et al., 2016).

HDAC inhibitors may be a promising therapy against cognitive decline or impairment (Penney and Tsai, 2014). In our study, we demonstrated that treatment with HDAC inhibitors for the first 21 days post-TBI was associated with improved cognition, as tested by the NORT and MWM tasks, at the 4-month follow-up. NORT is a commonly used behavioral test which exploits the inherent preference of mice for novelty, thereby revealing memory recognition for previously encountered objects. NORT involves multiple brain regions, including the cortices, hippocampus, and thalamus, to evaluate non-spatial learning. This contrasts the Morris Water Maze task, which is a hippocampal-dependent spatial learning task. Owing to the location and severity of injury within the severe TBI mice (cortex and hippocampus), we expected to find significant alteration in cognitive abilities. TBI mice performed poorly on both tasks, spending a lesser percentage of time investigating the novel object during the NORT task as well as taking longer to find the hidden platform during MWM. SAHA treatment resulted in a trend for improved NORT results, though the data did not reach significance. Additionally, SAHA-treated mice performed significantly better in MWM compared to untreated mice. Entinostat-treated mice, however, performed better in all cognitive tasks compared to untreated mice. The discrepancy within these results may stem from the variance in tested regions of interest (i.e., hippocampal-dependent vs multiple regions), or in the innate density of expression in targeted HDAC proteins. The different HDAC isoforms have a specific pattern of distribution both among the cell

types (i.e., astrocytes, neurons, etc.), but also regionally (Baltan et al., 2011). Compared to other Class I HDAC isoforms, HDACs 1 and 3 are more heavily expressed within the cortices and hippocampus—two regions required for learning and memory. Perhaps, this regional disbursement partially explains the differences we observed in these cognition tasks between the broad-spectrum compound, SAHA, and narrow-spectrum inhibitor, entinostat.

Initial impact induces a state of precipitous pro-inflammatory cascades, leading to accumulation of reactive species, hyperexcitability, and cell death. Delayed onset of pathologies suggests a prolonged influence of these processes on the epileptic state, suggesting both early and extended therapy may be needed to confer an antiepileptogenic effect. One critical issue that has yet to be settled within the field of epilepsy is the duration of treatment within the window of opportunity needed to interrupt the underlying processes of epileptogenesis, thereby halting or preventing the development of spontaneous seizures following brain injury. This debate stems from several reasons, but perhaps the most pressing are the variation of latency periods between rodent models and the lack of subsequent translation to clinical trials in epilepsy or TBI patients (Temkin, 2009; Klein and Tyrlikova, 2020; for review on tested compounds in PTE models see Golub and Reddy, 2021/introduction). Much of the antiepileptogenesis treatments have thus far been studied in post-status epilepticus models, even though acquired human epilepsies are more likely to arise from injury, stroke, or infections (Klein et al., 2018). Recent studies have demonstrated stroke-induced, and therefore CNS injury-induced, seizures may have a more rapid onset than

previously thought (Lösher, 2020). Here, we chose to administer therapy from 1 hr post-TBI, and then twice daily for 21 days. This regimen allowed for mice to recover from anesthesia, but also accounted for the average time an ambulance can arrive on scene in an emergency. Furthermore, based on our earlier studies, we noted the earliest onset of spontaneous epileptic seizures after TBI was 3 weeks post-injury. Therefore, we aimed to administer therapy for the full duration of the potential therapeutic window. Moreover, SAHA-treatment was split between two 25 mg/kg doses per day, as a single dose containing 50 mg/kg resulted in minor side effects such as lethargy and gastrointestinal issues (i.e., reduced interest in food). With entinostat, on the other hand, we observed no negative side effects with administration.

In conclusion, we investigated the therapeutic potential of a broad- and narrow-spectrum HDAC inhibitor for controlling seizures and comorbidities associated with PTE. We observed neuroprotective effects from both agents within the severe 2mm-TBI model, such as reduced inflammation, neurodegeneration, and significant reduction of seizure burden. These results corresponded to reduced aberrant mossy fiber sprouting and a rescued threshold to 6 Hz stimulation, indicating a disruption of the epileptogenic process in those cohorts. Though both treatment regimens produced several beneficial effects, entinostat treatment resulted in an extremely low incidence of seizures. Overall health and recovery progressed better with entinostat, rather than SAHA, as we did not observe any negative side effects with administration. Our results warrant future studies continue to explore additional HDAC inhibitor compounds or combinational studies for the prevention and modification of acquired epilepsy disorders.

CHAPTER V

CONCLUSIONS

Post-traumatic epilepsy is a chronic neurological disorder characterized by devastating spontaneous recurrent seizures triggered by an initial brain injury event. This occurs via epileptogenesis, the process by which a normal brain becomes epileptic due to underlying progressions of inflammation, hyperexcitability, and epigenetic modifications. Epigenetics, which refers to a set of functional changes in gene expression without altering the DNA itself, is emerging as an important driver in many brain diseases. However, the potential of treatments based on epigenetic pathways has not been widely tested in epilepsy disorders, whether acquired or otherwise. In this set of three aims, we optimized a model of TBI to be better suited for the study of PTE and tested the efficacy of both broad and narrow spectrum HDAC inhibitors on injury-induced seizures.

Within the aim 1 studies, we developed an innovate model of PTE by optimizing the existing controlled-cortical impact model of TBI. We performed a full characterization of acute and chronic behavioral testing, which allowed for a greater understanding of recovery outcomes and translational properties of therapeutic interventions. We also provide a histological time-course of TBI- and epilepsy-associated pathologies including neuroinflammation, neurodegeneration, neurogenesis, and aberrant mossy fiber sprouting. These results allow researchers to interpret an optimum therapeutic window as well as determine targeted pathways for intervention. Furthermore, we recorded long-term 24/7 video-EEG for up to 120 days post-injury

using a hippocampal depth electrode. Continuous EEG is critical for verifying the diagnosis of epilepsy and evaluating the progression of epileptiform activity during the latency period. To our knowledge, this dissertation and chapter represent the first time such an extensive characterization of PTE has been completed and verified in mice, thus giving the field a useful mechanism for studying critically needed novel therapeutics to prevent or halt the epileptogenic process after TBI.

Within the aim 2 studies, we investigated the therapeutic potential of epigenetic HDAC inhibitors as interventions for epileptogenesis after TBI. Using sodium butyrate as our drug of choice, we demonstrate the potent anti-inflammatory properties of sodium butyrate, which ultimately led to positive disease modifying effects such as reduced neurodegeneration and ameliorated behavioral deficits. We found that even though sodium butyrate treatment did not reduce incidence of epilepsy after TBI, it did reduce the overall seizure burden of responding mice via the significant reduction of seizure frequency and duration compared to untreated mice. These results provide a scientific basis for further investigating the clinical and translational potential of HDAC inhibition for PTE and other epilepsy disorders.

In aim 3, we sought to find an optimum compound for HDAC inhibition therapy for PTE. Using SAHA (suberanilohydroxamic acid) as a broad spectrum HDAC inhibitor and Entinostat (MS-275) as a narrow spectrum HDAC inhibitor, we tested these compounds in both moderate and severe TBI mice. We found that SAHA administration within the moderate TBI cohort produced modest disease modifying effects. However, SAHA was found to be very effective in preventing PTE development

in severe TBI model. Similarly, the narrow-spectrum Entinostat produced significant reduction on PTE development in severe TBI model. They both ameliorated the TBI-related comorbidities. Overall, these results indicate the potential utility of broad and narrow spectrum HDAC inhibitors preventing PTE and its associated comorbidities in at risk individuals after severe TBI.

REFERENCES

Abbasi B and Goldenholz DM. (2019) Machine learning applications in epilepsy. *Epilepsia* 60(10): 2037-2047.

Adeyemo BO, Biederman J, Zafonte R, Kagan E, Spencer TJ, Uchida M, Kenworthy T, Spencer AE, and Faraone SV. (2014) Mild traumatic brain injury and ADHD: a systematic review of the literature and meta-analysis. *J Atten Disord* 18(7): 576-584.

Agoston DV, Shutes-David A, and Peskind ER. (2017) Biofluid biomarkers of traumatic brain injury. *Brain Inj* 31(9): 1195-1203.

Agoston DV, Vink R, Helmy A, Risling M, Nelson D, and Prins M. (2019) How to translate time: the temporal aspects of rodent and human pathobiological processes in traumatic brain injury. *J Neurotrauma* 36: 1724-1737.

Agrawal A, Timothy J, Pandit L, and Manju M. (2006) Post-traumatic epilepsy: An overview. *Clin Neurol Neurosurg* 108(5): 433-439.

Ahmed F, Plantman S, Cernak I, and Agoston DV. (2015) The temporal pattern of changes in serum biomarker levels reveals complex and dynamically changing pathologies after exposure to a single low-intensity blast in mice. *Front Neurol* 6: 114.

Alyu F and Dikmen M. (2017) Inflammatory aspects of epileptogenesis: contribution of molecular inflammatory mechanisms. *Acta Neuropsychiatr* 29(1): 1-16.

Amrein I, Isler K, and Lipp HP. (2011) Comparing adult hippocampal neurogenesis in mammalian species and orders: influence of chronological age and life history stage. *Eur J Neurosci* 34(6): 978-987.

Anderson MA, Burda JE, Ren Y, Ao Y, O'Shea TM, Kawaguchi R et al. (2016) Astrocyte scar formation aids central nervous system axon regeneration. *Nature* 532: 195-200.

Andrade P, Nissinen J, and Pitkanen A. (2017) Generalized seizures after experimental traumatic brain injury occur at the transition from slow wave to rapid eye movement sleep. *J Neurotrauma* 34: 1482-1487.

Andrade-Valenca LP, Dubeau F, Mari F, Zelmann R, and Gotman J. (2011) Interictal scalp fast oscillations as a marker of the seizure onset zone. *Neurology* 77(6): 524-531.

Andrioli A, Alonso-Nanclares L, Arellano JI, and DeFelipe J. (2007) Quantitative analysis of parvalbumin-immunoreactive cells in the human epileptic hippocampus. *Neurosci* 149: 131-143.

Annegers JF, Hauser WA, Coan SP, and Rocca WA. (1998) A population-based study of seizures after traumatic brain injuries. *N Eng J Med* 338(1): 20-24.

Asnaghi L, Bruno P, Priulla M, and Nicolin A. (2004) Mtor: a protein kinase switching between life and death. *Pharmacol Res* 50: 545-549.

Atkins CM, Truettner JS, Lotocki G, Sanchez-Molano J, Kang Y, Alonso OF, Sick TJ, Dietrich WD, and Bramlett HM. (2010) Post-traumatic epilepsy seizure susceptibility is attenuated by hypothermia therapy. *Eur J Neurosci* 32(11): 1912-1920.

Avsar E and Empson RM. (2004) Adenosine acting via A1 receptors, controls the transition to status epilepticus-like behavior in an in vitro model of epilepsy. *Neuropsychopharmacol* 47: 427-437.

Babbage DR, Yim J, Zupan B, Neumann D, Tomita MR, and Willer B. (2011) Meta-analysis of facial affect recognition difficulties after traumatic brain injury. *Neuropsychology* 25(3): 277-285.

Baik EJ, Kim EJ, Lee SH, and Moon C. (1999) Cyclooxygenase-2 selective inhibitors aggravate kainic acid induced seizure and neuronal cell death in the hippocampus. *Brain Res* 843(1-2): 118-129.

Bailes JE, Dashnaw ML, Petraglia AL, and Turner RC. (2014) Cumulative effects of repetitive mild traumatic brain injury. *Prog Neurol Surg* 28: 50-62.

Baltan S, Bachleda A, Morrison RS, and Murphy SP. (2011) Expression of histone deacetylases in cellular compartments of the mouse brain and the effects of ischemia. *Transl Stoke Res* 2(3): 411-423.

Bardai FH and D'Mello SR. (2011) Selective toxicity by HDAC3 in neurons: regulation by Akt and GSK3beta. *J Neurosci* 31(5): 1746-1751.

Bardai FH, Price V, Zaayman M, Wang L, and D'Mello SR. (2012) Histone Deacetylase-1 (HDAC1) is a molecular switch between neuronal survival and death. *J Biol Chem* 287(42): 35444-35453.

Bar-Klein G, Lublinksy S, Kamintsky L, Noyman I, Veksler R, Dalipaj H, et al. (2017) Imaging blood-brain barrier dysfunction as a biomarker for epileptogenesis. *Brain* 140: 1692-1705.

Barnes CA. (1979) Memory deficits associated with senescence: a neurophysiological and behavioral study in the rat. *J Comp Physiol Psychol* 93: 74-104.

Barnes DE, Kaup A, Kirby KA, Byers AL, Diaz-Arrastia R, and Yaffe K. (2014) Traumatic brain injury and risk of dementia in older veterans. *Neurology* 83(4): 312-319.

Barlow DH. (2004) Anxiety and its disorders: The nature and treatment of anxiety and panic. 2nd edition. Guilford Press, New York. DH Barlow. 1-36.

Barton ME, Klein BD, Wolf HH, and White S. (2001) Pharmacological characterization of the 6-Hz psychomotor seizure model of partial epilepsy. *Epilepsy Res* 47(3): 217-227.

Bao Y, Bramlett HM, Atkins CM, Truettner JS, Lotocki G, Alonso OF, and Dietrich WD. (2011) Post-traumatic seizures exacerbate histopathological damage after fluid-percussion brain injury. *J Neurotrauma* 28(1): 35-42.

Baumann CR, Stocker R, Imhof HG, Trentz O, Hersberger M, Mignot E, and Bassetti CL. (2005) Hypocretin-1 (orexin A) deficiency in acute traumatic brain injury. *Neurology* 65: 147-149.

Baumann CR, Werth E, Stocker R, Ludwig S, and Bassetti CL. (2007) Sleep-wake disturbances 6 months after traumatic brain injury: a prospective study. *Brain* 130: 1873-1883.

Behr C, Levesque M, Ragsdale D, and Avoli M (2015) Lacosamide modulates interictal spiking and high-frequency oscillations in a model of mesial temporal lobe epilepsy. *Epilepsy Res* 115: 8-16.

Benabid AL, Benazzous A, and Pollak P. (2002) Mechanisms of deep brain stimulation. *Mov Disord* 17: S73-S74.

Benar, G.G., Chauviere, L., Bartolomei, F., and Wendling, F. (2010) Pitfalls of high-pass filtering for detecting epileptic oscillations: A technical note on "false" ripples. Clinical *Neurophysiology*, 121: 301-310.

Bergsneider M, Hovda DA, Shalmon E, Kelly DF, Vespa PM, Martin NA, et al. (1997) Cerebral hyperglycolysis following severe traumatic brain injury in humans: a positron emissions tomography study. *J Neurosurg* 86: 241-251.

Bevins RA and Besheer J. (2006) Object recognition in rats and mice: a one-trial non-matching-to-sample learning task to study 'recognition memory'. *Nat Protoc* 1: 1306-1311.

Bhatt D, Hazari A, Yamakawa GR, Salberg S, and Sgro M, et al. (2020) Investigating the cumulative effects of Δ9-tetrahydrocannabinol and repetitive mild traumatic brain injury on adolescent rats. *Brain Commun* 2(1): fcaa042.

Biber K, Pinto-Duarte A, Wittendorp MC, Dolga AM, Fenandes CC, Von Frijtag Drabbe Kunzel J, et al. (2008) Interleukin-6 upregulates neuronal adenosine A1 receptors: implications for neuromodulation and neuroprotection. *Neuropharmacology* 33: 2237-2250.

Biederman J, Feinberg L, Chan J, Adeyemo BO, Woodworth KY, Panis W, McGrath N, Bhatnagar S, Spencer TJ, Uchida M, Kenworthy T, Grossman R, Zafonte R, and Faraone SV. (2015) Mild traumatic brain injury and attention-deficit hyperactivity disorder in young student athletes. *J Nerv Ment Dis* 203(11): 813-819.

Binder DK and Steinhauser C. (2006) Functional changes in astroglial cells in epilepsy. *Glia* 54(5): 358-368.

Bissler JJ, McCormack FX, Young LR, Elwing JM, Chuck G, Leonard JM, Schmithorst VJ, Laor T, Brody AS, Bean J, Salisbury S, and Franz DN. (2008) Sirolimus for angiomyolipoma in tuberous sclerosis complex or lymphangioleiomyomatosis. *N Engl J Med* 358: 140-151.

Bockaert J and Marin P. (2015) Mtor in brain physiology and pathologies. *Physiol Rev* 95: 1157-1187.

Bolkvadze T and Pikanen A. (2012) Development of post-traumatic epilepsy after controlled cortical impact and lateral fluid-percussion-induced brain injury in the mouse. *J Neurotrauma* 29(5): 789-812.

Bolkvadze T, Rantala J, Puhakka N, Andrade P, and Pitkanen A. (2015) Epileptogenesis after traumatic brain injury in Plau-deficient mice. *Epilepsy Behav* 51: 19-27.

Bolkvadze T, Puhakka N, and Pitkanen A. (2016) Epileptogenesis after traumatic brain injury in Plaur-deficient mice. *Epilepsy Behav* 60.

Bombardier CH, Fann JR, Temkin NR, Esselman PC, Barber J, and Dikmen SS. (2010) Rates of major depressive disorder and clinical outcomes following traumatic brain injury. *JAMA* 303(19): 1938-1945.

Bonfield CM, Lam S, Lin Y, and Greene S. (2013) The impact of attention deficit hyperactivity disorder on recovery from mild traumatic brain injury. *J Neurosurg Pediatr* 12: 97-102.

Bonsak F and Sukumari-Ramesh S. (2021) Entinostat improves acute neurological outcomes and attenuates hematoma volume after intracerebral hemorrhage. *Brain Res* 1752: 147222.

Borgonetti V and Galeotti N. (2021) Combined inhibition of histone deacetylases and BET family proteins as epigenetic therapy for nerve injury-induced neuropathic pain. *Pharmacol Res* 156: 105431.

Borovecki F, Lovrecic L, Zhou J, Jeong H, Then F, Rosas HD, Hersch SM, Hogarth P, Bouzou B, Jensen RV, and Krainc D. (2005) Genome-wide expression profiling of

human blood reveals biomarkers for Hungtinton's disease. *Proc Natl Acad Sci USA* 102(31): 11023-11028.

Bragin A, Wilson CL, and Engle J Jr. (2000) Chronic epileptogenesis requires development of a network of pathologically interconnected neuron clusters: a hypothesis. *Epilepsia* 41(6): S144-152.

Bragin A, Wilson CL, Almajano J, Mody I, and Engel J Jr. (2004) High-frequency oscillation after status epilepticus: epileptogenesis and seizure genesis. *Epilepsia* 45(9): 1017-1023.

Brandt C, Gastens AM, Sun MZ, Hausknecht M, and Lösher W. (2006) Treatment with valproate after status epilepticus: effect on neuronal damage, epileptogenesis, and behavioral alterations in rats. *Neuropharmacology* 51(4): 789-804.

Brooks-Kayal AR, Bath KG, Berg AT, Galanopoulou AS, Holmes GL, Jensen FE, Kanner AM, O'Brien TJ, Whittemore VH, Winawer MR, Patel M, and Scharfman HE, (2013) Issues related to symptomatic and disease-modifying treatments affecting cognitive and neuropsychiatric comorbidities of epilepsy. *Epilespia* 54: 44-60.

Brown JP, Couillard-Despres S, Cooper-Kuhn CM, Winkler J, Aigner L, and Kuhn HG, (2003) Transient expression of doublecortin during adult neurogenesis. *J. Compar. Neurol*. 467(1), 1-10

Buckmaster PS, Ingram EA, and Wen X. (2009) Inhibition of the mammalian target of rapamycin signaling pathway suppresses dentate granule cell axon sprouting in a rodent model of temporal lobe epilepsy. *J Neurosci* 29: 8259-8269.

Buffo A, Rite I, Tripathi P, Lepier A, Colak D, Horn AP, Mori T, and Gotz B. (2008) Origin and progeny of reactive gliosis: A source of multipotent cells in the injured brain. *Proc. Natl. Acad. Sci. USA* 105(9), 3581-3586.

Bugay V, Bozdemir E, Vigil FA, Chun SH, Zamora DO, Rule G, Shapiro MS, Lechleiter JD, and Brenner R. (2019) A mouse model of repetitive blast traumatic brain injury reveals post-trauma seizures and increased neuronal excitability. *Neurotrauma* 37: 2.

Butler CR, Boychuk JA, Smith BN. (2015) Effects of rapamycin treatment on neurogenesis and synaptic reorganization in the dentate gyrus after controlled cortical impact injury in mice. *Front Syst* Neurosci 9:163.

Butler CR, Boychuk JA, Smith BN. (2016) Differential effects of rapamycin treatment on tonic and phasic GABAergic inhibition in dentate granule cells after focal brain injury in mice. *Exp Neurol* 280:30–40.

Calzolari E, Chepisheva M, Smith RM, Mahmud M, Hellyer PJ, Thatis V, Arshad Q, Jolly A, Wilson M, Rust H, Sharp DJ, and Seemungal BM. (2021) Vestibular agnosia in traumatic brain injury and its link to imbalance. *Brain* 144(1): 128-143.

Campbell JN, Gandhi A, Singh B, and Churn SB. (2014) Traumatic brain injury causes a tacrolimus-sensitive increase in non-convulsive seizures in a rat model of post-traumatic epilepsy. *Int J Neurol Brain Disord* 1(1): 1-11.

Carlson SW, Madathil SK, Sama DM, Gao X, Chen J, and Saatman KE. (2014) Conditional overexpression of insulin-like growth factor-1 enhances hippocampal neurogenesis and restores immature neuron dendritic processes after traumatic brain injury. *J Neuropathol* 73(8): 734-746.

Carron S, Dezsi G, Ozturk E, Nithianantharajah J, and Jones NC. (2019) Cognitive deficits in a rat model of temporal lobe epilepsy using touchscreen-based translational tools. *Epilepsia* 60(8): 1650-1660.

Carron SF, Sun M, Shultz SR, and Rajan R. (2019) Inhibitory neuronal changes following a mixed diffuse-focal model of traumatic brain injury. *J Comp Neurol* 528(2): 175-198.

Castellani RJ and Perry G. (2019) Tau biology, tauopathy, traumatic brain injury, and diagnostic challenges. *J Alzheimers Dis* 67(2): 447-467.

Catroppa C, Anderson VA, Morse SA, Haritou L, and Rosenfeld JV. (2008) Outcome and predictors of functional recovery 5 years following pediatric traumatic brain injury. *J Pediatr Psychol* 33: 707-718.

Cavazos JE, Golarai G, and Sutula TP. (1991) Mossy fiber synaptic reorganization induced by kindling: time course of development, progression, and permanence. *J Neuro* 11: 2795-2803.

Cazalis F, Feydy A, Valabregue R, Pelegrini-Issac M, Pierot L, and Azouvi P. (2006) fMRI study of problem-solving after severe traumatic brain injury. *Brain Injury* 20(10): 1019-1028.

Ceylan MF and Akca OF. (2013) Secondary attention deficit/hyperactivity disorder due to right basal ganglia injury: A case report. *J Exp Clin Med* 30: 189-191.

Chang, P., Williams, A.M., Bhatti, U.F., Biesterveld, B.E., Liu, B., Nikolian, V.C., Dennahy, I., Lee, J., Li, Y., and Alam, H.B., 2019. Valproic acid attenuates neural apoptosis, inflammation, and degeneration 30 days after traumatic brain injury, hermorrhagic shock, and polytrauma in a swine model. *J Am Coll Surg* 228(3): 265-275.

Chauvette S, Soltani S, Seigneur J, and Timofeev I. (2017) In vivo models or cortical acquired epilepsy. *J Neurosci Meth* 260: 185-201.

Chen JW, Ruff RL, Eavey R, Wasterlain CG. (2009) Posttraumatic epilepsy and treatment. *J Rehabil Res Dev* 46(6): 685-696.

Chen K, Neu A, Howard AL, Foldy C, Echegoyen J, Hilgenberg L, Smith M, Mackie K, and Soltesz I. (2007) Prevention of plasticity of endocannabinoid signaling inhibits persistent limbic hyperexcitability caused by developmental seizures. *J Neurosci* 27: 46-58.

Chuang D-M, Leng Y, Marinova Z, Kim H-J, and Chiu C-T. (2009) Multiple roles of HDAC inhibition in neurodegenerative conditions. *Trends Neuro* 32(11): 591-601.

Christensen J, Pedersen MG, Pedersen CB, Sidenius P, Olsen J, and Vestergaard M. (2009) Long-term risk of epilepsy after traumatic brain injury in children and young adults: a population-based cohort study. *Lancet*. 373: 1105-1110.

Chrzaszcz M, Venkatesan C, Dragisic T, Watterson DM, and Wainwright MS. (2010) Minozac treatment prevents increased seizure susceptibility in a mouse "two-hit" model of closed skull traumatic brain injury and electroconvulsive shock-induced seizures. *J Neurotrauma* 27(7): 1283-1295.

Citraro R, Leo A, De Caro C, Neci V, and Cantafio MEG, et al. (2020) Effects of histone deacetylase inhibitors on the development of epilepsy and psychiatric comorbidity in WAG/Rij rats. *Mol Neurobiol* 57(1): 408-421.

Clossen BL and Reddy DS. (2017) Novel therapeutic approaches for disease-modification of epileptogenesis for curing epilepsy. *Biochim. Biophys. Acta*. 1863(6): 1519-1538.

Coan AC, Appenzeller S, Bonilha L, Li LM, and Cendes F. (2009) Seizure frequency and lateralization affect progression of atrophy in temporal lobe epilepsy. *Neurology* 73(11): 834-842.

Cornford EM and Oldendorf WH. (1986) Epilepsy and the blood-brain barrier. *Adv Neurol* 44: 787-812.

Covington HE, Maze I, LaPlant QC et al. (2009) Antidepressant action of histone deacetylase inhibitors. *J Neurosci* 29: 11451-11460.

Cullen KD, Harris J, Browne K, Wolf J, Duda J, Meaney D, Margulies S, and Smith D. (2016) A porcine model of traumatic brain injury via head rotational acceleration. *Meth Mol Bio* 1462: 289-324.

Curia G, Levitt M, Fender JS, Miller JW, Ojemann J, and D'Ambrosio R. (2011) Impact of injury location and severity on posttraumatic epilepsy in the rat: Role of frontal neocortex. *Cereb Cortex* 21(7): 1574-1592.

Croll SD, Goodman JH, and Scharfman HE. (2004) Vascular endothelial growth factor (VEGF) in seizures: a double-edged sword. *Adv Exp Med Biol* 548: 57-68.

Crosio C, Heitz E, Allis CD, and Borrelli E. (2003) Chromatin remodeling and neuronal response: multiple signaling pathways induce specific histone H3 modifications and early gene expression in hippocampal neurons. *J Cell Sci* 116: 4905-4914.

Cross JH and Lagae L. (2020). The concept of disease modification. *Eur J Pediatric Neurol* 24: 43-46.

D'Alessandro R, Ferrara R, Benassi G, Lenzi PL, and Sabattini L. (1988) Computed tomographic scans in posttraumatic epilepsy. *Arch Neurol* 45: 42-43.

D'Ambrosio R, Eastman CL, Darvas F, Fender JS, Verley DR, Farin FM et al. (2013) Mild passive focal cooling prevents epileptic seizures after head injury in rats. *Ann Neurol* 73: 199-209.

D'Ambrosio R, Fairbanks JP, Fender JS, Born DE, Doyle DL, and Miller JW. (2004) Post-traumatic epilepsy following fluid percussion injury in the rat. *Brain* 127: 304-314.

D'Ambrosio R, Fender JS, Simon EA, Born DE, Doyle DL, and Miller JW. (2005) Progression from frontal-parietal to mesial-temporal epilepsy after fluid percussion in the rat. *Brain* 128: 174-188.

Dadas A and Janigro D. (2019) Breakdown of blood brain barrier as a mechanism of post-traumatic epilepsy. *Neurobiol Dis* 123: 20-26.

Dantzer R, O'Connor JC, Freund GG, Johnson RW, and Kelley KW. (2008) From inflammation to sickness and depression: when the immune system subjugates the brain. *Nat Rev Neurosci* 9: 46.

Danzer SC. (2019) Adult neurogenesis in the development of epilepsy. *Epilepsy Curr* 19(5): 316-320.

Darrah SD, Miller MA, Ren D, Hoh NZ, Scanlon JM, Conley YP, et al. (2013) Genetic variability in glutamic acid decarboxylase genes: associations with post-traumatic seizures after severe TBI. *Epilepsy Res* 103: 180-194.

Dash PK, Mach SA and Moore AN. (2001) Enhanced neurogenesis in the rodent hippocampus following traumatic brain injury. *J Neurosci Res* 63(4): 313-319.

Dash PK, Redell JB, Hergenroeder G, Zhao J, Clifton GL, and Moore A. (2010) Serum ceruloplasmin and copper are early biomarkers for traumatic brain injury-associated elevated intracranial pressure. *J Neurosci Res* 88(8): 1719-1726.

Dash PK, Orsi SA, and Moore AN. (2009) Histone deacetylase inhibition combined with behavioral therapy enhances learning and memory following traumatic brain injury. *FASEB J* 23: 4266-4275.

Dash PK, Orsi SA, Zhang M, Grill RJ, Pati S, Zhao J, Moore AN. (2010). Valproate administered after traumatic brain injury provides neuroprotection and improves cognitive function in rats. *PLoS One* 5: e11383.

Daskalakis NP, Rijal CM, King C, Huckins LM, and Ressler KJ. (2018) Recent genetics and epigenetics approaches to PTSD. *Curr Psychiatry Rep* 20(5): 30.

Davis KA, Sturges BK, Vite CH, Ruedebusch V, and Worrell G, et al. (2011) A novel implanted device to wirelessly record and analyze continuous intracranial canine EEG. *Epilepsy Res* 96: 116-122.

De La Garza RI and Asnis GM. (2003) The non-steroidal anti-inflammatory drug diclofenac sodium attenuates IFN-alpha induced alterations to monoamine turnover in prefrontal cortex and hippocampus. *Brain Res* 997: 70-79.

De Oliveira CO, Reimer AG, Da Rocha AB, Grivicich I, Schneider RF, Roisenberg I, Regner A, Simon D. (2007) Plasma von Willebrand factor levels correlate with clinical outcome of severe traumatic brain injury. *J Neurotrauma* 24(8): 1331-1338.

De Grauw X, Thurman D, Xu L, Kancherla V, and DeGrauw T. (2018) Epidemiology of traumatic brain injury-associated epilepsy and early use of anti-epileptic drugs: An analysis of insurance claims data, 2004-2014. *Epilepsy Res* 146: 41-49.

Deacon RMJ, Croucher A, and Rawlins JNP. (2002) Hippocampal cytotoxic lesion effects of species-typical behaviors in mice. *Behav Brain Res* 132(2): 203-213.

Deacon RMJ. (2006) Burrowing in rodents: a sensitive method for detecting behavioral dysfunction. *Nature Proto* 1, 118-121.

Deuschl G, Schade-Brittinger C, Krack P, Volkmann J, Schafer H et al. (2006) A randomized trial of deep-brain stimulation for Parkinson's disease. *N Engl J Med* 355: 896-908.

Dewan MC, Rattani A, Gupta S, Baticulon RE, Hung Y, Punchak M, Agrawal A, Adeleye A, Shrime MG, Rubiano AM, Rosenfeld JV, and Park KB. (2018) Estimating the global incidence of traumatic brain injury. *J. Neurosurg*. 1, 1-18.

Dey A, Kang X, Qiu J, Du Y, and Jiang J. (2016) Anti-inflammatory small molecules to treat seizures and epilepsy: from bench to bedside. *Trends Pharmacol Sci* 37(6): 463-484.

Diamond ML, Ritter AC, Failla MD, Boles JA, Conley YP, Kochanek PM, et al. (2015) IL-1β associations with posttraumatic epilepsy development: a genetics and biomarker cohort study. *Epilepsia* 56: 991-1001.

Diamond ML, Ritter AC, Jackson EK, Conley YP, Kochanek PM, Boison D, et al. (2015) Genetic variation in the adenosine regulatory cycle is associate with posttraumatic epilepsy development. *Epilepsia* 56: 1198-1206.

Diaz-Arrastia R, Agostini MA, Frol AB, Mickey B, Fleckenstein J, Bigio E, et al. (2000) Neurophysiologic and neuroradiologic features of intractable epilepsy after traumatic brain injury in adults. *Arch. Neurol*. 57: 1611–1616. doi: 10.1001/archneur.57.11.1611

Dieter JN and Engel SD. (2019) Traumatic brain injury and posttraumatic stress disorder: Comorbid consequences of war. *Neurosci. Insights*. 31(14): 1179069519892933.

Dickstein SG, Bannon K, Castellanos FX, and Milham MP. (2006) The neural correlates of attention deficit hyperactivity disorder: An ALE meta-analysis. *J Child Psychol Psychiatry* 47: 1051-1062.

Diekhof EK, Geier K, Falkai P, and Gruber O. (2011) Fear is only as deep as the mind allows: a coordinate-based meta-analysis of neuroimaging studies on the regulation of negative affect. *Neuroimage* 58(1): 275-285.

Ding K, Gupta PK, and Diaz-Arrastia. (2016) Epilepsy after traumatic brain injury. In: Translational research in traumatic brain injury. Eds: Laskowitz D and Grant G. CRC Press/Taylor and Francis Group. Taylor & Francis, LLC, Boca Raton, FL.

Dinocourt C, Gallagher SE, and Thompson SM. (2006) Injury-induced axonal sprouting in the hippocampus is initiated by activation of trkB receptors. *Eur J Neurosci* 24: 1857-1866.

Dixon KJ. (2017) Pathophysiology of traumatic brain injury. *Phys Med Rehab Clinics North America* 28(2): 215-225.

Duclos C, Dumont M, Wiseman-Hakes C, Arbour C, Mongrain V, Gaudreault PO, Khoury S, Lavigne G, Desautels A, and Gosselin N. (2014) Sleep and wake disturbances following traumatic brain injury. *Pathol Biol* 62: 252-261.

Dudek FE and Spitz M. (1997) Hypothetical mechanisms for the cellular and neurophysiologic basis of secondary epileptogenesis: proposed role of synaptic reorganization. *J Clin Neurophysiol* 14: 90-101.

Dudek FE and Staley KJ. (2012) The time course and circuit mechanisms of acquired epileptogenesis. *In Japsper's basic mechanisms of the epilepsies* (ed. Noebels JL, et al.) National Center for Biotechnology Information, Bethesda, MD.

DVBIC. DoD TBI Statistics 2000-2019 Q3. Falls Church, VA: Defense and Veterans Brain Injury Center. (2019) p. 1-5.

Eakin K, Rowe RK, and Lifshitz J. (2015) Modeling fluid percussion injury, in *Brain Neurotrauma: Molecular, neuropsychological, and rehabilitation aspects*. Chapter 19. Ed. FH Kobeissy. FL: CRC Press.

Eastman CL, Verley DR, Fender JS, Stewart TH, Nov E, Curia G, and D'Ambrosio R. (2011) Antiepileptic and Antiepileptogenic Performance of Carisbamate after head injury in the rat: blind and randomized studies. *J Pharmacol Exp Thera* 336: 779-790.

Eastman CL, Verley DR, Fender JS, Temkin NR, and D'Ambrosio R. (2010) ECoG studies of valproate, carbamazepine and halothane in frontal lobe epilepsy induced by head injury in the rat. *Exp Neurol* 224(2): 369-388.

Echegoyen J, Armstrong C, Morgan RJ, and Soltesz I. (2009) Single application of a CB1 receptor antagonist rapidly following head injury prevents long-term hyperexcitability in a rat model. *Epilepsy Res* 85: 123-137.

Edwards III G, Zhao J, Dask PK, Soto C, and Moreno-Gonzalez I. (2020) Traumatic brain injury induces tau aggregation and spreading. *J Neurotrauma* 37(1): 80-92.

Efendioglu M, Basaran R, Akca M, Ceman D, Demirtas C, and Yildirim M. (2020) Combination therapy of gabapentin and *N*-acetylcysteine against posttraumatic epilepsy in rats. *Neurochem Res* 45: 1802-1812.

Engel J, Pitkanen A, Loeb JA, Dudek FE, Bertram EH, Cole AJ, et al. (2013) Epilepsy biomarkers. *Epilepsia* 54(4): 61-69.

Englander J, Bushnik T, Duong TT, Cifu DX, Zafonte R, Wright J, et al. (2003) Analyzing risk factors for late posttraumatic seizures: a prospective, multicenter investigation. *Arch Phys Med Rehabil* 84: 365-373.

Englander J, Cifu DX, and Diaz-Arrastia R. (2015) Seizures after traumatic brain injury. *Arch Phys Med Rehabil* 95: 1223-1224.

Ennaceur A and Delacour J. (1988) A new one-trial test for neurobiological studies of memory in rats. 1: Behavioral data. *Behav Brain Res* 31: 47-59.

Enomoto T, Osugi T, Satoh H, McIntosh TK, and Nabeshima T. (2005) Pre-injury magnesium treatment prevents traumatic brain injury—Induced hippocampal ERK activation, neuronal loss, and cognitive dysfunction in the radial-arm maze test. *J Neurotrauma* 22(7): 783-792.

Eslami M, Ghanbari E, Sayyah M, Etemadi F, Choopani S, and Soleimani M et al. (2016) Traumatic brain injury accelerates kindling epileptogenesis in rats. *Neurological Res* 42: 91-98.

Ewell LA, Fischer KB, Leibold C, Leutgeb S, and Leutgeb JK. (2019) The impact of pathological high-frequency oscillations on hippocampal network activity in rats with chronic epilepsy. eLife. 8: e42148.

Fabene P, Bramanti P, and Constantin G. (2010) The emerging role for chemokines in epilepsy. *J Neuroimmunol* 224(2): 22-27.

Fann JR, Ribe AR, Pedersen HS, Fenger-Gron M, Christensen J, Benros ME, Vestergaard M. (2018) Long-term risk of dementia among people with traumatic brain injury in Denmark: a population-based observational cohort study. *Lancet Psychiatry* 5(5): 424-431.

Farrant M and Nusser Z. (2005) Variations on an inhibititory theme: phasic and tonic activation of GABAA receptors. *Nat Rev Neurosci* 6: 215-229.

Fass DM, Reis SA, Ghosh B, Hennig KM, Joseph NF, Zhao WN, Nieland TJ, Guan JS, Kuhnle CE, Tang W, Barker DD, Mazitschek R, Schreiber SL, Tsai LH, and Haggarty SJ (2013) Crebinostat: a novel cognitive enhancer that inhibits histone deacetylase activity and modulates chromatin-mediated neuroplasticity. *Neuropharmacol*. 64, 81-96.

Faul M. et al. (2010) Traumatic Brain Injury in the United States: Emergency Department Visits, Hospitalizations and Deaths, 2002–2006, Centers for Disease Control and Prevention.

Fenwick T and Anderson V. (1999) Impairments of attention following childhood traumatic brain injury. *Child Neuropsychol* 5: 213-223.

Ferrante RJ, Kubilus JK, Lee J et al. (2003) Histone deacetylase inhibition by sodium butyrate chemotherapy ameliorates the neurodegenerative phenotype in Huntington's disease mice. *J. Neurosci*. 23: 9418-9427.

Frankowski JC, Kim YJ, and Hunt RF. (2019) Selective vulnerability of hippocampal interneurons to graded traumatic brain injury. *Neurobiol Dis* 129: 208-216.

Friedman A. (2011) Blood-brain barrier dysfunction, status epilepticus, seizures, and epilepsy: a puzzle of a chicken and egg? *Epilepsia* 52(8): 19-20.

Friedman SD, Brooks WM, Jung RE, Chiulli SJ, Sloan JH, Montoya BT, et al. (1999) Quantitative proton MRS predicts outcome after traumatic brain injury. *Neurology* 52: 1384-1391.

Friess SH, Ichord RN, Owens K, Ralston J, and Rizol R, et al. (2007) Neurobehavioral functional deficits following closed head injury in the neonatal pig. *Exp Neurol* 204(1): 234-243.

Filibian M, Frasca A, Maggioni D, Micotti E, Vezzani A, and Ravizza T. (2012) In vivo imaging of glia activation using 1H-magnetic resonance spectroscopy to detect putative biomarkers of tissue epieleptogenicity. *Epilepsia* 53: 1907-1916.

Finkelstein, E.A. et al., 2006. Incidence and Economic Burden of Injuries in the United States, Oxford University Press.

Foffani G, Uzcategui YG, Gal B, and Menedez de la Prida L. (2007) Reduced spike-timing reliability correlates with the emergence of fast ripples in the rat epileptic hippocampus. *Neuron* 55: 930-941.

Franklin, K.B.J., and Paxinos, G., 1997. The mouse brain in stereotaxic coordinates, 1st ed. Academic Press: New York.

Galic MA, Riazi K, Heida JG, Mouihate A, Fournier NM, Spencer SJ, Kalynchuk LE, Teskey GC, and Pittman QJ. (2008) Postnatal inflammation increases seizure susceptibility in adult rats. *J Neurosci* 28(27): 6904-6913.

Galic MA, Riazi K, Henderson AK, Tsutsui S, and Pittman QJ. (2009) Viral-like brain inflammation during development causes increased seizure susceptibility in adult rats. *Neurobiol Dis* 36(2): 343-351.

Ganai, S.A., Ramadoss, M., and Mahadevan, V., 2016. Histone deacetylase (HDAC) inhibitors – Emerging roles in neuronal memory, learning, synaptic plasticity and neural regeneration. Curr. Neuropharmacol. 14(1), 55-71.

Gao WM, Chadha MS, Kline AE, Clark RS, Kochanek PM, Dixon CE, and Jenkins LW. (2006) Immunohistochemical analysis of histone H3 acetylation and methylation – evidence for altered epigenetic signaling following traumatic brain injury in immature rats. *Brain Res* 1070: 31-34.

Gao X, Deng-Bryant Y, Cho W, Carrico KM, Hall ED, and Chen J. (2008) Selective death of newborn neurons in the hippocampal dentate gyrus following moderate experimental traumatic brain injury. *J Neurosci Res* 86(10): 2258-2270.

Gao X, Enikolopov G, and Chen J. (2009) Moderate traumatic brain injury promotes proliferation of quiescent neural progenitors in the adult hippocampus. *Exp Neurol* 219(2): 516-523.

Gardner RC, Burke JF, Nettiksimmons J, Goldamn S, Tanner CM and Yaffe K. (2015) Traumatic brain injury in later life increases risk for Parkinson disease. *Ann Neurol* 77(6): 987-995.

Garner R, La Rocca M, Vespa P, Jones N, Monti MM, Toga AW, and Duncan D. (2019) Imaging biomarkers of posttraumatic epileptogenesis. *Epilepsia* 00: 1-12.

Gerbatin RR, Silva LF, Hoffmann MS, Della-Pace LD, do Nascimento PS, Kegler A, de Zorzi VN, Cunha JM, Botelho P, Neto JBT, Furian AF, Oliveira MS, Fighera MR, and Royes LFF. (2019) Delayed creatine supplementation counteracts reduction of GABAergic function and protects against seizures susceptibility after traumatic brain injury in rats. Prog *Neuropsychopharmacol Biol Psychiatry* 92: 328-338.

Gerring JP, Brady KD, Chen A, Vasa R, Grados M, Bandeen-Roche KJ, Bryan RN, and Denckla MB. (1998) Premorbid prevalence of ADHD and development of secondary ADHD after closed head injury. *J Can Acad Chil Adolesc Psychiatry* 37: 647-654.

Ghadiri T, Vakilzadeh G, Hajali V, and Khodagholi F. (2019) Progesterone modulates post-traumatic epileptogenesis through regulation of BDNF-TrkB signaling and cell survival-related pathways in the rat hippocampus. *Neurosci Lett* 709: 134384.

Gilbert KS, Kark SM, Gehrman P, and Bogdanova Y. (2015) Sleep disturbances, TBI PTSD: Implications for treatment and recovery. *Clin Psychol Rev* 40: 195-212.

Gill R, Chang PK, Prenosil GA, Deane EC, and McKinney RA. (2013) Blocking brain-derived neurotrophic factor inhibits injury-induced hyperexcitability of hippocampal CA3 neurons. *Eur J Neurosci* 38(11): 3554-3566.

Golarai G, Greenwood AC, Feeney DM, Connor JA. (2001) Physiological and structural evidence for hippocampal involvement in persistent seizure susceptibility after traumatic brain injury. *J Neurosci* 21(21): 8523-8537.

Gold EM, Su D, Lopez-Velazquez L, Haus DL, Perez H, Lacuesta GA, Anderson AJ, and Cummings BJ. (2013) Functional assessment of long-term deficits in rodent models of traumatic brain injury. *Regen Med* 8(4): 13.41.

Golub VM, Brewer J, Wu X, Kuruba R, Short J, Manchi M, Swonke M, Younus I, and Reddy DS, (2015) Neurostereology protocol for unbiased quantification of neuronal injury and neurodegeneration. *Front. Aging Neurosci*. 7: 196.

Goodrich GS, Kabakov AY, Hameed MQ, Dhamne SC, Rosenberg PA, Rotenberg A. (2013) Ceftriaxone treatment after traumatic brain injury restores expression of the glutamate transporter, GLT-1, reduces regional gliosis, and reduces post-traumatic seizures in the rat. *J Neurotrauma* 30: 1434-1441.

Goshen I and Yirmiya R. (2007) The role of pro-inflammatory cytokines in memory processes and neural plasticity. In Ader R et al. Psychoneuroimmunology, 4th edition. Elsevier, Inc.

Gottlicher M, Minucci S, Zhu P et al. (2001) Valproic acid defines a novel class of HDAC inhibitors inducing differentiation of transformed cells. *EMBO J* 20: 6969-6978.

Gu F, Parada I, Yang T, Longo FM, and Prince DA. (2018) Partial TrkB receptor activation suppresses cortical epileptogenesis through actions on parvalbumin interneurons. *Neurobiol Dis* 113: 45-58

Guo D, Zeng L, Brody DL, Wong M. (2013) Rapamycin attenuates the development of posttraumatic epilepsy in a mouse model of traumatic brain injury. *PLOS one*, 8(5): e64078.

Guo H, Callaway JB, and Ting JP. (2015) Inflammasomes: mechanism of action, role in disease and therapeutics. *Nat Med* 21(7): 677-687.

Gupta A, Elgammal FS, Proddutur A, Shah S, and Santhakumar V. (2012) Decrease in tonic inhibition contributes to increase in dentate semilunar granule cell excitability after brain injury. *J Neurosci* 32: 2523-2537.

Guyás AI, and Freund TT. (2015) Generation of physiological and pathological high frequency oscillations: the role of perisomatic inhibition in sharp-wave ripple and interictal spike generation. *Curr. Opin. Neurobiol*. 31: 26-32.

Graber KD and Prince DA. (1999) Tedrodotoxin prevents posttraumatic epileptogenesis in rats. *Ann Neurol* 46: 234-242.

Graber KD and Prince DA. (2006) Chronic partial cortical isolation, in *Animal Models of Epilepsy*. Eds. A Pitkanen, PA Schwarzkroin, and S Moshe. Elsevier: New York, pps. 477-494.

Grovola MR, Paleologos N, Wofford KL, Harris JP, Browne KD, et al. (2020) Mossy cell hypertrophy and synaptic changes in the hilus following mild diffuse traumatic brain injury in pigs. *J Neuroinflammation* 17(44). Doi:10.1186/s12974-020-1720-0

Gurkoff GG, Giza CC, Shin D, Auvin S, Sankar R, and Hovda DA. (2009) Acute neuroprotection to pilocarpine-induced seizures is not sustained after traumatic brain injury in the developing rat. *Neuroscience* 164(2): 862-876.

Haghighi F, Ge Y, Chen S, Xin Y, Umli MU, De Gasperi R, Gma Sosa MA, Ahlers ST, and Elder GA. (2015) Neuronal DNA methylation profiling of blast-related traumatic brain injury. *J Neurotrauma* 32: 1200-1209.

Hall ED, Bryant YD, Cho W, and Sullivan PG. (2008) Evolution of post-traumatic neurodegeneration after controlled cortical impact traumatic brain injury in mice and rats as assessed by the de Olmos silver and fluorojade staining methods. *J Neurotrauma* 25(3): 235-247.

Hall ED, Bryant YD, Cho W, and Sullivan PG (2008) Evolution of post-traumatic neurodegeneration after controlled cortical impact traumatic brain injury in mice and rats as assessed by the de Olmos silver and fluorojade staining methods. *J Neurotrauma*. 25(3): 235-247.

Haltiner AM, Temkin NR, and Dikmen SS. (1997) Risk of seizure recurrence after the first late posttraumatic seizure. *Arch Phys Med Rehabil* 78: 835-840.

Hameed MQ, Hsieh T, Morales-Quezada L, Lee HH, Damar U, MacMullin PC, Hensch TK, and Rotenberg A. (2018) Ceftriaxone Treatment Preserves Cortical Inhibitory Interneuron Function via Transient Salvage of GLT-1 in a Rat Traumatic Brain Injury Model. *Cerebral Cortex* 29(11): 4506-4518.

Hamm RJ, Pike BR, Temple MD, O'Dell DM, and Lyeth BG. (1995) The effect of postinjury kindled seizures on cognitive performance of traumatically brain-injured rats. *Exp Neurol* 136(2): 143-148.

Hammond FM, Corrigan JD, Ketchum JM, Malec JF, Dams-O'Connor K, Hart T, Novack TA, Bogner J, Dahdah MN, and Whiteneck GG. (2019) Prevalence of medical and psychiatric comorbidities following traumatic brain injury. *J Head Trauma Rehabil* 34(4): E1-E10.

Hammond FM, Hart T, Bushnik T, Corrigan JD, and Sasser H. (2004) Change and predictors of change in communication, cognition, and social function between 1 and 5 years after traumatic brain injury. *J Head Trauma Rehab* 19: 314-328.

Han K, Chapman SB, and Krawczyk DC. (2015) Altered amygdala connectivity in individuals with chronic traumatic brain injury and comorbid depressive symptoms. *Front Neurol* 6: 231.

Hånell A, Clausen F, Bjork M, Jansson K, Philipson O, Nilsson LNG, Hillered L, Weinreb PH, Lee D, McIntosh TK, Gimbel DA, Strittmatter SM, and Marklund N. (2010) Genetic deletion and pharmacological inhibition of Nogo-66 receptor impairs cognitive outcome after traumatic brain injury in mice. *Neurotrauma* 27(7): 1297-1309.

Haselkorn ML, Shellington DK, Jackson EK, Vagni VA, Janesko-Feldman K, Dubey RK, Gillespie DG, Cheng D, Bell MJ, Jenkins LW, Homanics GE, Schermann J, and Kochanek PM. (2010) Adenosine A1 receptor activation as a brake on the microglial response after experimental traumatic brain injury in mice. *J Neurotrauma* 27(5): 901-910.

Hazama A, Ziechmann R, Arul M, Krishnamurthy S, Galgano M, and Chin LS. (2018) The Effect of Keppra Prophylaxis on the Incidence of Early Onset, Post-traumatic Brain Injury Seizures. *Cureus* 10(5): e2674.

Heggeness MH, Strong N, Wooley PH, and Yang SY. (2017) Quiescent pluripotent stem cells reside within murine peripheral nerves that can be stimulated to proliferate by recombinant human bone morphogenic protein 2 or by nerve trauma. *Spine J* 17(2): 252-259.

Hesam S, Khoshkholgh-Sima B, Pourbadie HG, Babpour V, Zendedel M, Sayyah M. (2018) Monophosphoryl Lipid A and Pam3Cys Prevent the Increase in Seizure Susceptibility and Epileptogenesis in Rats Undergoing Traumatic Brain Injury. *Neurochem Res* 43(10): 1978-1985.

Hester MS and Danzer SC. (2013) Accumulation of abnormal adult-generated hippocampal granule cells predicts seizure frequency and severity. *J. Neurosci*. 33(21): 8926-8936.

Hillary FG, Slocomb J, Hills EC, Fitzpatrick NM, Medaglia JD, Wang J, Good DC, Wylie GR. (2011) Changes in resting connectivity during recovery from severe traumatic brain injury. *Int J Psychophysiol* 82: 115-123.

Hiott, W.D. and Labbate, L., (2002). Evaluation and management of neurobehavioral syndromes of traumatic brain injury. *Neuro. Rehab*. 17(4), 345-355.

Hogg MC, Raoof R, El Naggar H, Monsefi N, Delanty N, O'Brien DF, et al. (2019) Elevation of plasma tRNA fragments precedes seizures in human epilepsy. *J Clin Invest* 129: 2946-2951.

Holtman L, van Vliet EA, Edelbroek PM, Aronica E, and Gorter JA. (2010) COX-2 inhibition can lead to adverse effects in a rat model for temporal lobe epilepsy. *Epilepsy Res* 91(1): 49-56.

Huang Y, Doherty JJ, and Dingledine R. (2002) Altered histone acetylation at glutamate receptor 2 and brain-derived neurotrophic factor genes is an early event triggered by status epilepticus. *J Neurosci* 22: 8422-8428.

Huang Y, Zhao F, Wang L, Yin H, Zhou C, and Wang X. (2012) Increased expression of histone deacetylases 2 in temporal lobe epilepsy: a study of epileptic patients and rat models. *Synapse* 66: 151-159.

Hudak AM, Trivedi K, Harper CR, Booker K, Caesar RR, Agostini M, et al. (2004) Evaluation of seizure-like episodes in survivors of moderate and severe traumatic brain injury. *J. Head Trauma Rehabil*. 19: 290–295.

Hull, E.E., Montgomery, M.R., and Leyva, K.J. (2016) HDAC inhibitors as epigenetic regulators of the immune system: impacts on cancer therapy and inflammatory diseases. *BioMed. Res. Internatl*. 2016, 8797206.

Hunt RF, Haselhorst LA, Schoch KM, Bach EC, Rios-Pilier J, Scheff SW, Saatman KE, and Smith BN. (2012) Posttraumatic mossy fiber sprouting is related to degree of cortical damage in three mouse strains. *Epilepsy Res* 99(1-2): 167-170.

Hunt RF, Scheff SW and Smith BN. (2009) Posttraumatic epielsy after controlled cortical impact injury in mic. *Exp Neurol* 215: 243-252.

Hunt RF, Scheff SW, and Smith BN. (2010) Regionally localized recurrent excitation in the dentate gyrus of a cortical contusion model of posttraumatic epilepsy. *J Neurophysiol* 103: 1490-1500.

Hunt RF, Scheff SW, and Smith BN. (2011) Synpatic reorganization of inhibitory hilar interneuron circuitry after traumatic brain injury in mice. *J Neurosci* 31: 6880-6890.

Hwang JY, Aromolaran KA, and Zukin RS. (2017) The emerging field of epigenetics in neurodegeneration and neuroprotection. *Nat Rev Neurosci* 18(6): 347-361.

Ibhazehiebo K, Gavrilovici C, de la Hoz CL, Ma SC, Rehak R, Kaushik G, Meza Santoscoy PL, Scott L, Nath N, and Kim DY. (2018) A novel metabolism-based phenotypic drug discovery platform in zebrafish uncovers HDACs 1 and 3 as a potential combined anti-seizure drug target. *Brain* 141: 744–761.

Ibrahim S, Hu W, Wang X, Gao X, He C, and Chen J. (2016) Traumatic brain injury causes aberrant migration of adult-born neurons in the hippocampus. *Sci Rep* 6: 21793.

Immonen R, Harris NG, Wright D, Johnston L, Manninen E, Smith G, Paydar A, Branch C, and Grohn O. (2019) Imaging biomarkers of epileptogenicity after traumatic brain injury – preclinical frontiers. *Neurobiol Dis* 123: 75-85.

Immonen R, Kharatishvili I, Grohn O, and Pitkanen A. (2013) MRI biomarkers for post-traumatic epileptogenesis. *J Neurotrauma* 30(14): 1305-1309.

Ivens S, Kaufer D, Flores LP, Bechmann I, Zumsteg D, Tomkins O, Seiffert E, Heinemann U, and Friedman A. (2007) TGF-beta receptor-mediated albumin uptake into astrocytes is involved in neocortical epileptogenesis. *Brain* 130(2): 535-547.

Jackson ML, Srivastava AK, and Cox Jr. CS. (2017) Preclinical progenitor cell therapy in traumatic brain injury: a meta-analysis. *J Surg Res* 214: 38-48.

Jacobs J and Zijlmans M. (2020) HFO to measure seizure propensity and improve prognostication in patients with epilepsy. *Epilespy Curr* 20(6): 338-347.

Jefferys JG, Menendez de la Prida L, Wendling F, Bragin A, Avoli M, Timofeev I, and Lopes da Silva FH. (2012) Mechanisms of physiological and epileptic HFO generation. Prog. Neurobiol. 98, 250-264.

Jiang L, Wang J, Liu Z, Jiang A, Li S, Wu D, Zhang Y, Zhu X, Zhou E, Wei Z, and Yang Z. (2020) Sodium butyrate alleviates lipopolysaccharide-induced inflammatory responses by down-regulation of NF-κB, BLRP3, signaling pathway, and activating histone acetylation in bovine macrophages. *Front Vet Sci* 7: 579674.

Jiao H, Wang Z, Liu Y, Wang P, Xue Y. (2011) Specific role of tight junction proteins claudin-5, occluding, and ZO-1 of the blood-brain barrier in a focal cerebral ischemic insult. *J Mol Neurosci* 44(2): 130-139.

Jirkof P. (2014) Burrowing and nest building behavior as indicators of well-being in mice. *J. Neurosci. Methods*. 234: 139-146.

Jirsch JD, Urrestarazu E, LeVan P, Olivier A, Dubeau F, Gotman J. (2006) High-frequency oscillations during human focal seizures. *Brain* 129: 1593-1608.

Johnson VE, Stweart W, Weber MT, Cullen DK, Siman R, and Smith DH. (2016) SNTF immunostaining reveals previously undetected axonal pathology in traumatic brain injury. *Acta Neuropathol* 131: 115-125.

Jones NC, Nguyen T, Corcoran NM, Velakoulis D, Chen T, Grundy R, O'Brien TJ, and Hovens CM. (2012) Targeting hyperphosphorylated tau with sodium selenate suppresses seizures in rodent models. *Neurbiol Dis* 45(3): 897-901.

Jorge RE, Robinson RG, Moser D, Tateno A, Crespo-Facorro B, and Arndt S. (2004) Major depression following traumatic brain injury. *Arch Gen Psychiatry* 61(1): 42-50.

Jupp B, Williams J, Binns D, Hicks RJ, Cardamone L, Jones N, et al. (2012) Hypometabolism precedes limbic atrophy and spontaneous recurrent seizures in a rat model of TLE. *Epilepsia* 53: 1233-1244.

Kaitaro T, Koskinen S, and Kaipio ML. (1995) Neuropsychological problems in everyday life: A 5-year follow-up study of young severely closed-head-injured patients. *Brain Inj* 9: 713-727.

Kanbayashi T, Kodama T, Kondo H, et al. (2009) CSF histamine contents in narcolepsy, idiopathic hypersomnia and obstructive sleep apnea syndrome. *Sleep* 32(2): 181-187.

Kappock JT and Caradonna JP. (1996) Pterin-dependent amino acid hydroxylases. Chem. Rev. 96(7), 2659-2756.

Kasahara M, Menon DK, Salmond CH, Outtrim JF, Taylor Tavares JC, Carpenter TA, Pickard JD, Sahakian BJ, and Stamatakis EA. (2010) Altered functional connectivity in the motor network after traumatic brain injury. *Neurology* 75: 168-176.

Katayama T, Tanaka H, Yoshida T, Uehara T, and Minami M. (2009) Neuronal injury induces cytokine-induced neutrophil chemoattractant-1 (CINC-1) production in astrocytes. *J Pharmacol Sci* 109(1): 88-93.

Kelley KA, Ho L, Winger D, Freire-Moar J, Borelli CB, Aisen PS, and Pasinetti GM. (1999) Potentiation of excitotoxicity in transgenic mice overexpressing neuronal cyclooxygenase-2. *Am J Pathol* 155: 995-1004.

Kelly KM, Miller ER, Lepsveridze E, Kharlamov EA, and Mcedlishvili Z. (2015) Posttraumatic seizure and epilepsy in adult rats after controlled cortical impact. *Epilepsy Res* 117: 104-116.

Kendirli MT, Rose DT, and Bertram EH. (2014) A model of posttraumatic epilepsy after penetrating brain injuries: Effect of lesion size and metal fragments. *Epilepsia* 55(12): 1969-1977.

Kernie SG, Erwin TM, and Parada LF. (2001) Brain remodeling due to neuronal and astrocytic proliferation after controlled cortical injury in mice. *J Neurosci Res* 66(3): 317-326.

Kharatishvili I, Nissinen JP, McIntosh TK, Pitkanen A. (2006) A model of posttraumatic epilepsy induced by lateral fluid-percussion brain injury in rats. *Neurosci* 140: 685-697.

Kharatishvili I, Immonen R, Grohn O, and Pitkanen A. (2007) Quantitative diffusion MRI of hippocampus as a surrogate marker for post-traumatic epileptogenesis. *Brain* 130(12): 3155-3168.

Khurgel M and Ivy GO. (1996) Astrocytes in kindling: relevance to epileptogenesis. Epilepsy Res. 26, 163-175.

Kim, H.J., Rowe, M., Ren, M., Hong, J.S., Chen, P.S., and Chuang, D.M. (2007) Histone deacetylase inhibitors exhibit anti-inflammatory and neuroprotective effects in a rat permanent ischemic model of stroke: multiple mechanisms of action. *J. Pharmacol. Exp. Ther.* 321, 892-901.

Klein P, Dingledine R, Aronica E, Bernard C, Blumcke I, Boison D, et al. (2018) Commonalities in epileptogenic processes from different acute brain insults: Do they translate? *Epilepsia* 59, 37-66.

Klein P and Tyrlikova I. (2020) No prevention or cure of epilepsy as yet. *Neuropharmacology* 168, 107762.

Knutsen LJS and Murray TF. (1997) Adeosine and ATP in epilepsy. In: Purinergic approaches in experimental therapeutics. Editors: Jacobson KA and Jarvis MF. Chapter 22. NY: Wiley-Liss Inc, 423-447.

Kobau R, Zahran H, Thurman DJ, Zack MM, Henry TR, and Schachter SC et al. Centers for Disease Control and Prevention (CDC) (2008) Epilepsy surveillance among adults-19 states, Behavioral Risk Factor Surveillance System, 2005. *MMWR Surveill Summ* 57: 1-20.

Kochanek PM, Hendrich KS, Dixon CE, Schinding JK, Williams DS, and Ho C. (2002) Cerebral blood flow at one year after controlled cortical impact in rats: assessment by magnetic resonance imaging. *J Neurotrauma* 19(9): 1029-1037.

Kochanek PM, Vagni VA, Janesko KL, Washington CB, Crumrine PK, Garman RH, et al. (2006) Adenosine A1 receptor knockout mice develop lethal status epilepticus after experimental traumatic brain injury. *J Cereb Blood Flow Metab* 26: 565-575.

Koenig JB, Cantu D, Low C, Sommer M, Noubary F, Croker D, Whalen M, Kong D, and Dulla CG. (2019) Glycolytic inhibitor 2-deoxyglucose prevents cortical hyperexcitability after traumatic brain injury. *JCI Insight* 5(11): e126506.

Kosari-Nasab M, Shokouhi G, Azarfarin M, Bannazadeh Amirkhiz M, Mesgari Abbasi M, and Salari AA. (2019) Serotonin 5-HT1A receptors modulate depression-related symptoms following mild traumatic brain injury in male adult mice. *Metab Brain Dis* 34(2): 575-582.

Kovacs SK, Leonessa F, Grimes J, and Ling GSF. (2014) A neuropathology approach to understanding of explosive blast TBI seizure risk. *J Neurol Disord Stroke* 2(3): 1071.

Kraemer DL and Awad IA. (1994) Vascular malformations and epilepsy: clinical considerations and basic mechanisms. *Epilepsia* 35(6): S30-43.

Krueger DA, Wilfong AA, Holland-Bouley K, Anderson AE, Argicola K, Tudor C, Mays M, Lopez CM, Kim MO, and Franz DN. (2013) Everolimus treatment of refractory epilepsy in tuberous sclerosis complex. *Ann Neurol* 74: 679-687.

Kruh, J., 1981. Effects of sodium butyrate, a new pharmacological agent, on cells in culture. *Mol. Cell. Biochem*. 42(2), 65-82.

Kulkarni S and Dhir A. (2009) Cyclooxygenase in epilepsy: from perception to application. *Drugs Today* 45: 135-154.

Kumar RG, Breslin KD, Ritter AC, Conley YP, and Wagner AK. (2019) Variability with astroglial glutamate transport genetics is associated with increased risk for post-traumatic seizures. *J Neurotrauma* 36: 230-238.

Kuruba R, Hattiangady B, Parihar V, Shuai B, and Shetty AK. (2011) Differential susceptibility of interneurons expressing neuropeptide Y or parvalbumin in the aged hippocampus to acute seizure activity. *PLoS One*. 6: e24493. 10.1371/journal.pone.0024493

Kyyriäinen J, Bolkvadze T, Koivisto H, Lipponen A, Perez LO, Ndode-Ekane XE, Tanila H, and Pitkanen A. (2019) Deficiency of urokinase-type plasminogen activator and its receptor affects social behavior and increases seizure susceptibility. *Epilepsy Res* 151: 67-74.

Lauro C, Di Angelantonio S, Cipriani R, Sobrero F, Antonilli L, Brusadin V, et al. (2008) Activity of adenosine receptors type 1 is required for CX 3 CL1-mediated neuroprotection and neuromodulation in hippocampal neurons. *J Immunol* 180: 7590-7596.

Lehre KP and Danbolt NC. (1998) The number of glutamate transporter subtype molecules at glutamatergic synapses: chemical and stereological quantification in young adult rat brain. *J Neurosci* 18: 8751-8757.

Lemos T, and Cavalheiro EA. (1995) Suppression of pilocarpine-induced status epilepticus and the late development of epilepsy in rats. *Experimental Brain Research*. 102: 423-428.

Levenson JM, Roth TL, Lubin FD, Miller CA, Huang IC, Desai P, Sweatt JD et al. (2006) Evidence that DNA (cytosine-5) methyltransferase regulates synaptic plasticity in the hippocampus. *J Biol Chem* 281: 15763-15773.

Li H, Graber KD, Jin S, McDonald W, Barres BA, and Prince DA. (2012) Gabapentin decreases epileptiform discharges in a chronic model of neocortical trauma. *Neurobiol Dis* 48(3): 429-438.

Liang, X., Wang, R.S., Wang, F., Liu, S., Guo, F., Sun, L., Wang, Y.J., Sun, Y.X., and Chen, X.L., 2013. Sodium butyrate protects against severe burn-induced remote acute lung injury in rats. *PLoS One* 8(7), e68786.

Lighthall JW. (1988). Controlled cortical impact: a new experimental brain injury model. *J Neurotrauma* 5: 1-15.

Lin W, Harnod T, Lin C, and Kao C. (2019) Mortality risk and risk factors in patients with posttraumatic epilepsy: A population-based cohort study. *Int J Environ Res Pub Health* 16(4): 589.

Lister RG. (1987) The use of a plus-maze to measure anxiety in the mouse. *Psychopharmacology*. 92(2): 180-185.

Littlejohn EL, Scott D, and Saatman KE. (2020) Insulin-like growth factor-1 overexpression increases long-term survival of posttrauma-born hippocampal neurons while inhibiting ectopic migration following traumatic brain injury. *Acta Neuropathologica Comm* 8: 46.

Liu J, Reeves C, Michalak Z, Coppola A, Diehl B, Sisodiya SM, and Thom M. (2014) Evidence for mtor pathway activation in a spectrum of epilepsy-associated pathologies. *Acta Neuropathol Commun* 2: 71.

Liu S, Zheng P, Wright DK, Dezsi G, Braine E, Nguyen T, Corcoran NM, Johnston LA, Hovens CM, Mayo JN, Hudson M, Shultz SR, Jones NC, and O'Brien TJ. (2016) Sodium selenate retards epileptogenesis in acquired epilepsy models reversing changes in protein phosphatase 2A and hyperphosphorylated tau. *Brain* 139: 1919-1938.

Löscher W, Schwartz-Porche D, Frey H-H, and Schmidt D. (1985) Evaluation of epileptic dogs as an animal model of human epilepsy *Arzneimittelforschung (Drug Res)* 35: 82-87.

Lösher W. (2020) The holy grail of epilepsy prevention: Preclinical approaches to antiepileptogenic treatments. *Neuropharmacology* 167, 107605/

Lotrich FE, Albusaysi S, and Ferrel RE. (2013) Brain-derived neurotrophic factor serum levels and genotype: association with depression during interferon-alpha treatment. *Neuropsychopharmacology* 38(6): 985-995.

Lowenstein DH, Thomas MJ, Smith DH, and McIntosh TK. (1992) Selective vulnerability of dentate hilar neurons following traumatic brain injury: a potential mechanistic link between head trauma and disorders of the hippocampus. *J Neurosci* 12: 4846-4853.

Lu XM, Hartings JA, Si Y, Balbir A, Cao Y, and Tortella FC. (2011) Electrocortical pathology in a rat model of penetrating ballistic-like brain injury. *J Neurotrauma* 28(1): 71-83.

Lu XM, Shear DA, Graham PB, Bridson GW, Uttamsingh V, Chen Z, Leung LY, and Tortella FC. (2015) Dual therapeutic effects of C-10068, a dextromethorphan derivative, against post-traumatic nonconvulsive seizures and neuroinflammation in a rat model of penetrating ballistic-like brain injury. *J Neurotrauma* 32(20): 1621-1632.

Lucke-Wold BP, Nguyen L, Turner RC, Logson AF, Chen, Y, Smith KE, Huber JD, Matsumoto R, Rosen CL, Tucker ES, Richter E. (2015) Traumatic brain injury and epilepsy: Underlying mechanisms leading to seizure. *Seizure* 33: 13-23.

Ma K, Qin L, Matas E, Duffney FJ, Liu A, and Yan Z. (2018) Histone deacetylase inhibitor MS-275 restores social and synaptic function in a Shank3-deficient mouse model of autism. *Neuropsychopharmacology* 43(8): 1779-1788.

Madathil SK, Carlson SW, Brelsfoard JM, Ye P, D'Ercole AJ, and Saatman KE. (2013) Astrocyte-specific overexpression of insulin-like growth factor-1 protects hippocampal neurons and reduces behavioral deficits following traumatic brain injury in mice. *PLOS One* 8(6): e67204.

Magnuson J, Leonessa F, and Ling GS. (2012) Neuropathology of explosive blast traumatic brain injury. *Curr Neurol Neurosci Rep* 12(5): 570-579.

Mahler B, Carlsson S, Andersson T, Adelow C, Ahlborn A, Tomson T. (2015) Unprovoked seizures after traumatic brain injury: a population-based case-control study. *Epilepsia*. 56: 1438-1444.

Makovac E, Meeten F, Watson DR, Herman A, Garfinkel SN, Critchley H, and Ottaviani C. (2016) Alterations in amygdala-prefrontal functional connectivity account for excessive worry and autonomic dysregulation in generalized anxiety disorder. *Biol Psychiatry* 80(10): 786-795.

Malec JF, Ketchum JM, Hammond FM, Corrigan JD, Dams-O'Connor K, Hart T, Novack T, Dahdah M, Whiteneck GG, and Bogner J. (2019) Longitudinal effects of medical comorbidities on functional outcome and life satisfaction after traumatic brain injury: An individual growth curve analysis of NIDILRR traumatic brain injury model system data. *J Head Trauma Rehabil* 34(5): E24-E35.

Malec JF, Van Houtven CH, Tanielian T, Atizado A, and Dorn MC. (2017) Impact of TBI on caregivers of veterans with TBI: Burden and interventions. *Brain Injury* 31(9): 1235-1245.

Mann, E.O. and Paulsen, O., 2007. Role of GABAergic inhibition in hippocampal network oscillations. *Trends Neurosci*. 30, 343-349.

Marchi N, Angelov L, Masaryk T, Fazio V, Granata T, Hernandez N, Hallene K, Diglaw T, Franic L, Najm I, and Janigro D. (2007) Seizure-promoting effect of blood-brain barrier disruption. *Epilepsia* 48(4): 732-742.

Marchi N, Granata T, Ghosh C, and Janigro D. (2012) Blood-brain barrier dysfunction and epilepsy: Pathophysiologic role and therapeutic approaches. *Epilepsia* 53(11): 1877-1886.

Marion DW. (1999) Management of traumatic brain injury: past, present, and future. *Clin Neurosurg* 45: 184. 191.

Marmarou A, Foda MA, van den Brink W, Campbell J, Kita H, and Demetriadou K. (1994). A new model of diffuse brain injury in rats. Part I: Pathophysiology and biomechanics. *J Neurosurg* 80(2): 291-300.

Marty S, Berzaghi Mda P, and Berninger B. (1997) Neurotrophins and activity-dependent plasticity of cortical interneurons. *Trends Neurosci* 20(5): 198-202.

Matosin N, Cruceanu C, and Binder EB. (2017) Preclinical and clinical evidence of DNA methylation changes in response to trauma and chronic stress. *Chronic Stress* 1: 2470547017710764.

McCormick DA and Contreras D. (2001) On the cellular and network bases of epileptic seizures. *Annu Rev Physiol* 63: 815-846.

McIntosh TK, Vink R, Noble L, et al. (1989) Traumatic brain injury in the rat: characterization of a lateral fluid percussion model. *Neurosci* 28: 233-244.

McKee AC, Cantu RC, Nowinski CJ, Hedley-Whyte ET, and Gavett BE, et al. (2009) Chronic traumatic encephalopathy in athletes: progressive tauopathy after repetitive head injury. *J Neuropathol Exp Neurol* 68:709-735.

Meador, K.J., 2007. The basic science of memory as it applies to epilepsy. *Epilepsia* 48(9), 23-35.

McManus CM, Brosnan CF, and Berman JW. (1998) Cytokine induction of MIP-1 alpha and MIP-1 beta in human fetal microglia. *J Immunol* 160(3): 1449-1455.

Meany DF, Smith DH, Shreiber DI, Bain AC, Miller RT, and Ross DT, et al. (1995) Biomechanical analysis of experimental diffuse axonal injury. *J Neurotrauma* 12: 689-694.

Mez J, Daneshvar DH, and Kiernan et al. (2017) Clinicopathological evaluation of chronic traumatic encephalopathy in players of American football. *JAMA* 318(4): 360-370.

Miller AH, Maletic V, and Raison CL. (2009) Inflammation and its discontents: the role of cytokines in the pathophysiology of major depression. *Biol Psychiatry* 65: 732-741.

Miller, C.A., Campbell, S.L., and Sweatt, J.D. (2008) DNA methylation and histone acetylation work in concert to regulate memory formation and synaptic plasticity. *Neurobiol. Learn Mem*. 89(4), 599-603.

Mula, M. and Trimble, M.R., 2009. Antiepileptic drug-induced cognitive adverse effects: potential mechanisms and contributing factors. CNS Drugs 23, 121-137

Miller MA, Conley Y, Scanlon JM, Ren D, Ilyas Kamboh M, Niyonkuru C, et al. (2010) APOE genetic associations with seizure development after severe traumatic brain injury. *Brain Inj* 24: 1468-1477.

Miszczuk D, Debski KJ, Tanila H, Lukasiuk K, and Pitkanen A. (2016) Traumatic brain injury increases the expression of Nos1, Aβ clearance, and epileptogenesis in APP/PS1 mouse model of Alzheimer's disease. *Mol Neurobiol* 53: 7010-7027.

Montalvo-Ortiz JL, Keegan J, Gallardo C, Gerst N, and Tetsuka K, et al. (2014) HDAC inhibitors restore the capacity of aged mice to respond to haloperidol through modulation of histone acetylation. *Neuropsychopharmacology* 39(6): 1469-1478.

Moore EL, Terryberry-Spohr L, and Hope DA. (2006) Mild traumatic brain injury and anxiety sequelae: a review of the literature. *Brain Inj*. 20: 117-132.

Morganti-Kossmann MC, Yan E, and Bye N. (2010) Animal models of traumatic brain injury: is there an optimal model to reproduce human brain injury in the laboratory? *Injury* 41(S1): S10-S13.

Morris R. (1984) Developments of a water-maze procedure for studying spatial-learning in the rat. *J Neurosci Meth* 11: 47-60.

Morse AM and Garner DR. (2018) Traumatic brain injury, sleep disorders, and psychiatric disorders: An underrecognized relationship. *Med Sci* 6(15): 6010015.

Mountney A, Shear DA, Potter B, and Marcsisin SR. (2013) Ethosuximide and phenytoin dose-dependently attenuate acute nonconvulsive seizures after traumatic brain injury in rats. *J Neurotrauma* 30(23): 1973-1982.

Mtchedlishvili Z, Lepveridze E, Xu H, Kharlamov E, Lu B, and Kelly KM. (2010) Increase of GABAA receptor-mediated tonic inhibition in dentate gyrus granule cells after traumatic brain injury. *Neurobiol Dis* 38: 464-475.

Mukherjee S, Zeitouni S, Cavarsan CF, and Shaprio LA. (2013) Increased seizure susceptibility in mice 30 days after fluid percussion injury. *Front Neurol* 4: 28.

Murphy SP, Lee RJ, McClean ME, Pemberton HE, Uo T, Morrison RS, Bastian C, and Baltan S. (2014) MS-275, a class I histone deacetylase inhibitor, protects the p53-deficent mouse against ischemic injury. *J Neurochem* 129(3): 509-515.

Muyon C, Eakin KC, Sweet JA, and Miller JP. (2014) Decreased bursting and novel object-specific cell firing in the hippomcapus after mild traumatic brain injury. *Brain Res* 1582: 220-226.

Nagalakshmi B, Sagarkar S, Sakharkar AJ. (2018) Epigenetic mechanisms of traumatic brain injuries. *Prog Mol Biol Transl Sci* 157: 263-298.

Nakagawa A, Manley GT, Gean AD, Ohtani K, Armonda R, Tsukamoto A, Yamamoto H, Takayama K, and Tominaga T. (2011) Mechansims of primary blast-induced traumatic brain injury: insights from shock-wave research. *J Neurotrauma* 28(6): 1101-1119.

Neal EG, Chaffe H, Schwartz RH, Lawson MS, Edwards N, Fitzsimmons G, Whitney A, and Cross JH. (2008) The ketogenic diet for the treatment of childhood epilepsy: a randomized controlled trial. *Lancet Neurol* 7(6): 500-506.

Nelson ED, Kavalali ET, and Moteggia LM. (2008) Activity-dependent suppression of miniature neurotransmission through the regulation of DNA methylation. *J Neurosci* 28: 395-406.

Nemes A, Najm IM, Gale JT, Ying Z, Johnson M, and Gonzalez-Martinez J. (2016) Underlying cortical dysplasia as risk factor for traumatic epilepsy: An animal study. *J Neurotrauma* 33(20): 1883-1891.

Ngwenya LB, Mazumder S, Porter ZR, Minnema A, Oswald DJ, and Farhadi HF. (2018) Implantation of neuronal stem cells enhances object recognition without increasing neurogenesis after lateral fluid percussion injury in mice. *Stem Cells Int* 2018: 4209821.

Nikolian VC, Dennahy IS, Weykamp M, Williams AM, Bhatti UF, Eidy H, Ghandour MH, Chtrakilin K, Li Y, and Alam HB. (2019) Isoform 6-selective histone deacetylase inhibition reduces lesion size and brain swelling following traumatic brain injury and hemorrhagic shock. *J. Trauma Acute Care Surg*. 86(2): 232-239

Nilsson P, Ronne-Engstrom E, Flink R, Ungerstedt U, Carlson H and Hillered L. (1994) Epileptic seizure activity in the acute phase following cortical impact trauma in rat. *Brain Res*. 637: 227-232.

Nishino S, Ripley B, Overeem S, Lammers GJ, and Mignot E. (2000) Hypocretin (orexin) deficiency in human narcolepsy. *Lancet* 355: 39-40.

Nissinen J, Andrade P, Natunen T, Hiltunen M, Malm T, Kanninen K, Soares JI, Shatillo O, Sallinen J, Ndode-Ekane XE, and Pitkanen A. (2017) Disease-modifying effect of atipamezole in a model of post-traumatic epilepsy. *Epilepsy Res* 136: 18-34.

Nita DA, Cisse Y, Timofeev I, and Steriade M. (2006) Increased propensity to seizures after chronic cortical deafferentation in vivo. *J Neurophysiol* 95(2): 902-913.

Oaklander AL. (2011) Neuropathic itch. *Semin Cuta Med Surg* 30(2): 87-92.

Oleksii S, Winemiller AR, Heithoff BP, Munoz-Ballester C, George KK, Benko MJ, Zuidoek IA, Bessner MN, Curley DE, Edwards III GF, Mey A, Harrington AN, Kitchen JP, and Robel S. (2019) Repetitive diffuse mild traumatic brain injury causes an atypical astrocyte response and spontaneous recurrent seizures. *J Neurosci* 39(1): 1944-1963.

Ono T and Galanopoulou AS. (2019) Epilepsy and epilepsy syndrome. *Adv Exp Med Biol* 724: 99-113.

Ouyang W, Yan Q, Zhang Y, and Fan Z. (2017) Moderate injury in motor-sensory cortex causes behavioral deficits accompanied by electrophysiological changes in mice adulthood. *PLOS One* 12(2): e0171976.

Osier ND and Dixon CE. (2016) The controlled cortical impact model: Applications, considerations for researchers, and future directions. *Front Neurol* 7: 134.

Ostergard T, Sweet J, Kusyk D, Herring E, Miller J. (2016) Animal models of post-traumatic epilepsy. *J Neuro Meth* 272: 50-55.

Palacios EM, Sala-Llonch R, Junque C, Roig T, Tormos JM, Bargallo N, et al. (2013) Resting-state functional magnetic resonance imaging activity and connectivity and cognitive outcome in traumatic brain injury. *JAMA Neurol* 70: 845-851.

Park MJ and Sohrabji F. (2016) The histone deacetylase inhibitor, sodium butyrate, exhibits neuroprotective effects for ischemic stroke in middle-aged female rats. *J Neuroinflammtion* 13(1): 300.

Paterno R, Folweiler KA, and Cohen AS. (2017) Pathophysiology and treatment of memory dysfunction after traumatic brain injury. *Curr Neurol Neurosci* 17: 52.

Patnala R, Arumugam TV, Gupta N, and Dheen ST. (2016) HDAC inhibitor sodium butyrate-mediated epigenetic regulation enhances neuroprotective function of microglia during ischemia stroke. *Mol. Neurobiol*. 54: 6391-6411.

Paudel YN, Shaikh MF, Shah S, Kumari Y, Othman I. (2018) Role of inflammation in epilepsy and neurobehavioral comorbidities: Implication for therapy. *Eur J Pharmcol* 15: 145-155.

Penney J and Tsai L-H. (2014) Histone deacetylases in memory and cognition. *Sci Signal* 7:12.

Perek-Polnik M, Jozwiak S, Jurkiewicz E, Perek D, and Kotulska K. (2012) Effective everolimus treatment of inoperable, life-treatening subependymal giant cell astrovytoma and intractable epilepsy in a patient with tuberous sclerosis complex. *Eur J Paediatr Neurol* 16: 83-85.

Perucca P, Smith G, Santana-Gomez C, Bragin A, and Staba R. (2019) Electrophysiological biomarkers of epileptogenicity after traumatic brain injury. *Neurobiol Dis* 123: 69-74.

Piacentino M, Beggio G, Zordan L, and Bonanni P. (2018) Hippocampal deep brain stimulation: persistent seizure control after bilateral extra-cranial electrode fracture. *Neurol Sci* 39(8): 1431-1435.

Piao CS, Holloway AL, Hong-Routson S, and Wainwright MS. (2019) Depression following traumatic brain injury in mice is associated with down-regulation of hippocampal astrocyte glutamate transporters by thrombin. *J Cereb Blood Flow Metab* 39(1): 58-73.

Piccenna L, Shears G, and O'Brien TJ. (2017) Management of post-traumatic epilepsy: An evidence review over the last 5 years and future directions. *Epilepsia Open* 2: 123-144.

Pijet B, Stefaniuk M, Kostrzewska-Ksiezyk A, Tsilibary PE, Tzinia A, and Kaczmarek L. (2018) Elevation of MMP-9 levels promotes epileptogenesis after traumatic brain injury. *Molecular Neurobiol* 55: 9294-9306.

Ping X and Jin X. (2016a) Chronic posttraumatic epilepsy following neocortical undercut lesion in mice. *PLOS One* 11(6): e0158231.

Ping X and Jin X. (2016b) Transition from initial hypoactivity to hyperactivity in cortical layer V pyramidal neurons after traumatic brain injury in vivo. *J Neurotrauma* 33(4): 354-361.

Pingue V, Mele C, and Nardone A. (2021) Post-traumatic seizures and anti-epileptic therapy as predictors of the functional outcome in patients with traumatic brain injury. *Sci Rep* 11: 4708.

Pischiutta F, Micotti E, Zanier ER. (2018) Single severe traumatic brain injury produces progressive pathology with ongoing contralateral white matter damage one year after injury. *Exp Neurol* 300:167-178.

Pitkanen A. and Bolkvadze T. Head Trauma and Epilepsy. In: Noebels, J.L., Avoli, M., Rogawski, M.A., 2012. Jasper's Basic Mechanisms of the Epilepsies. 4th Edition. Bethesda (MD); 2012.

Pitkanen A, Lukasiuk K, Dudek FE, and Staley KJ. (2015) Epileptogenesis. *Cold Spring Harb Perspect Med* 5(10): a022822.

Pitkanen A, Nissinen J, Nairismagi J, Lukasiuk K, Grohn OHJ, Mitettinen R, and Kauppinen R (2002) Progression of neuronal damage after status epilepticus and during spontaneous seizures in a rat model of temporal lobe epilepsy. *Prog Brain Res* 135: 67-83.

Polascheck N, Bankstahl M, and Loscher W. (2010) The COX-2 inhibitor parecoxib is neuroprotective but not antiepileptogenic in the pilocarpine model of temporal lobe epilepsy. *Exp Neurol* 224(1): 219-233.

Ponsford J. (2017) Anxiety and depression following TBI. In RM McMillian, RW (Ed.), Neurobehavioral Disability and Social Handicap Following Traumatic Brain Injury, pp. 167.

Ponsford J and Kinsella G. (1992) Attentional deficits following closed-head injury. *J Clin Exp Neuropsychol* 14: 822-838.

Price JL and Drevets WC. (2012) Neural circuits underlying the pathophysiology of mood disorders. *Trends Cogn Sci* 16(1): 61-71.

Purcell SM, Manoach DS, Demanuele C, Cade BE, Mariani S, Cox R, Panagiotaropoulou G, Saxena R, Pan JQ, Smoller JW, Redline S, and Stickgold R. *Nat Commun* 8: 15930.

Raabe A, Schmitz AK, Pernhorst K, Grote A, von der Brelie C, Urbach H, Friedman A, Becker AJ, Elger CE, and Niehusmann P. (2012) Cliniconeuropathologic correlations show astroglial albumin storage as a common factor in epileptogenic vascular lesions. *Epilepsia* 53: 539-548.

Rabinowitz AR and Levin HS. (2014) Cognitive sequelae of traumatic brain injury. *Psychia. Clin. N. Am*. 37: 1-11.

Raible DJ, Frey LC, Cruz Del Angel Y, Russek SJ, and Brooks-Kayal AR. (2012) GABA(A) receptor regulation after experimental traumatic brain injury. *J Neurotrauma* 29: 2548-2554.

Rapport II RL and Penry JK. (1973) A survey of attitudes toward the pharmacological prophylaxis of posttraumatic epilepsy. *J Neurosurg* 38: 159-166.

Rao MS, Hattiangady B, Reddy DS, and Shetty AK. (2006) Hippocampal neurodegeneration, spontaneous seizures, and mossy fiber sprouting in the F344 rat model of temporal lobe epilepsy. *J. Neuroscience Res*. 83: 1088-1105.

Rao V and Lyketsos C. (2002) Psychiatric aspects of traumatic brain injury. *Pyschiatr Clin N America* 25: 43-69.

Raoof R, Bauer S, El Naggar H, Connolly NMC, Brennan GP, Brindley E, et al. (2018) Dual-center, dual-platform microRNA profiling identifies potential plasma biomarkers of adult temporal lobe epilepsy. *EBrioMedicine* 38: 127-141.

Raoof R, Jimenez-Mateos EM, Bauer S, Tackenberg B, Rosenow F, Lang J, et al. (2017) Cerebrospinal fluid microRNAs are potential biomarkers of temporal lobe epilepsy and status epilepticus. *Sci Rep* 7: 3328.

Ravizza T and Vezzani A. (2006) Status epilepticus induces time-dependent neuronal and astrocytic expression of interleukin-1 receptor type I in the rat limbic system. *Neuroscience* 137(1): 301-308.

Raymont V, Salazar AM, Lipski R, Goldman D, Tasick G, and Grafman J. (2010) Correlates of posttraumatic epilepsy 35 years following combat brain injury. *Neurology*. 75(3): 224-229.

Reddy DS and Estes WA. (2016) Clinical potential of neurosteroids for CNS disorders. *Trends Pharmacol Sci* 37(7): 543-561.

Reddy DS, Wu X, Golub V, Dashwood WM and Dashwood RH. (2018) Measuring histone deacetylase inhibition in the brain. Cur. Proto. Pharmacol. 81(1):e41.

Reddy SD, Clossen BL, and Reddy DS. (2017) Epigenetic histone deacetylation inhibition prevents the development and persistence of temporal lobe epilepsy. *J Pharmacol Exper Thera* 367(1): 244939.

Reeves TM, Lyeth BG, Phillips LL, Hamm RJ, and Povlishcok JT. (1997) The effects of traumatic brain injury on inhibition in the hippocampus and dentate gyrus. *Brain Res* 757(1): 119-132.

Reid AY, Bragin A, Giza CC, Staba RJ, and Engel J Jr. (2016) The progression of electrophysiologic abnormalities during epileptogenesis after experimental traumatic brain injury. *Epilepsia* 57(10): 1558-1567.

Reid IC and Stewart CA. (1997) Seizure, memory and synaptic plasticity. *Seizure* 6(5): 351-359

Rezai AR, Sederberg PB, Bogner J, Nielson DM, Zhang J, Mysiw WJ, et al. (2016) Improved function after deep brain stimulation for chronic, severe traumatic brain injury. *Neurosurgery* 79: 204-210.

Ripley DL and Politzer T. (2010) Vision disturbance after TBI. *NeuroRehab* 27: 215-216.

Ritter AC, Kammerer CM, Brooks MM, Conley YP, and Wagner AK. Genetic variation in neuronal glutamate transport genes and associations with posttraumatic seizure. *Epilepsia* 57: 984-993.

Rivera C, Li H, Thomas-Crusells J, Lahtinen H, Viitanen T, Nanobashvili A, Kokaia Z, Airaksinen MS, Voipio J, Kaila K, and Saarma M. (2002) BDNF-induced TrkB activation down-regulated the K^+ - Cl^- cotransporter KCC2 and impairs neuronal Cl^- extrusion. *J Cell Biol* 159: 747-752.

Robel S and Sontheimer H. (2016) Glia as drivers of abnormal neuronal activity. *Nat* Neurosci 19(1): 28-33.

Rock KL and Kono H. (2008) The inflammatory response to cell death. *Annu. Rev. Pathol.* 3: 99-126.

Rodgers KM, Dudek FE, and Barth DS. (2015) Progressive, seizure-like, spike-wave discharges are common in both injured and uninjured Sprague-dawley rats: implications for the fluid percussion injury model of post-traumatic epilepsy. *J Neurosci* 35(24): 9194-9204.

Rola R, Mizumatsu S, Otsuka S, Morhardt DR, Noble-Haeusslein LJ, Fishman K, Potts MB, and Fike JR. (2006) Alterations in hippocampal neurogenesis following traumatic brain injury in mice. *Exp Neurol* 202(1): 189-199.

Ronen GM, Streiner DL, and Rosenbaum P. (2003) Health-related quality of life in childhood epilepsy: moving beyond 'seizure control with minimal adverse effects'. *Health Qual. Life Outcomes* 1: 36.

Rosenfeld JC, McFarlane AC, Bragge P, Armonda RA, Grimes JB, and Ling GS. (2013) Blast-related traumatic brain injury. *Lancet Neurol* 12: 882-893.

Rouaux, C., Loeffler, J.P., and Boutillier, A.L., 2004. Targeting CREB-binding protein (CBP) loss of function as a therapeutic strategy in neurological disorders. *Biochem. Pharmacol.* 68(6), 1157-1164.

Sagarkar S, Bhamburker T, Shelkar G, Choudhar A, Kokare DM, Sakharkar AJ. (2017) Minimal traumatic brain injury causes persistent changes in DNA methylation at BDNF gene promoters in rate amygdala: a possible role in anxiety-like behaviors. *Neurobiol Dis* 106: 101-109.

Sah A, Sotnikov S, Kharitonova M, Schmuckermair C, and Diepold RP, et al. (2019) Epigenetic mechanisms within the cingulate cortex regulate innate anxiety-like behavior. *In J Neuropsychopharmacol* 22(4): 317-328.

Salazar AM and Grafman J. (2015) Post-traumatic epilepsy: clinical clues to pathogenesis and paths to prevention. *Handb Clin Neurol* 128: 525-538.

Salazar AM, Jabbari B, Vance SC, Grafman J, Amin D, and Dillon JD. (1985) Epilepsy after penetrating head injury. I. Clinical correlates: a report of the Vietnam Head Injury Study. *Neurology*. 35(10):1406-1414

Sanchez-Elexpuru G, Serratosa JM, and Sanchez MP. (2017) Sodium selenate treatment improves symptoms and seizure susceptibility in a mailin-deficient mouse model of Lafora disease. *Epilepsia* 58(3): 467-475.

Saraiva AL, Ferreira AP, Silva LF, Hoffmann MS, Dutra FB, Furian AF, Oliveira MS, Fighera MR, and Royes LFF. (2012) Creatine reduces oxidative stress markers but does not protect against seizure susceptibility after severe traumatic brain injury. *Brain Res Bull* 97(2-3): 180-186.

Schaefer SY, Mutha PK, Haaland KY, and Sainburg RL. (2012) Hemispheric specialization for movement control produces dissociable difference in online corrections after stroke. *Cereb. Cortex*. 22: 1407-1419.

Scharfman HE, Goodman JH, and Sollas AL. (2000) Granule-like neurons at the hilar/CA3 border after status epilepticus and their synchrony with area CA3 pyramidal cells: functional implications of seizure-induced neurogenesis. *J. Neurosci*. 20(16): 6144-6158.

Scheff SW, Baldwin SA, Brown RW, and Kraemer PJ. (2009) Morris water maze deficits in rats following traumatic brain injury: Lateral controlled cortical impact. *J Neurotrauma* 14(9): 615-627.

Scheibel ME, Crandall PH, and Scheibel AB. (1974) The hippocampal-dentate complex in temporal lobe epilepsy. *Epilepsia*. 55-80.

Scher AI, Wu H, Tsao JW, Blom HJ, Feit P, Nevin RL, et al. (2011) MTHFR C677T genotype as a risk factor for epilepsy including post-traumatic epilepsy in a representative military cohort. *J Neurotrauma*28: 1739-1745.

Schierhout G, and Roberts I. (2001) Anti-epileptic drugs for preventing seizures following acute traumatic brain injury. *Cochrane Database Syst. Rev*. CD000173.

Schiff ND, Giacino JT, Kalmar K, Victor JD, Baker K, Gerber M, et al. (2013) Medial septal nucleus theta frequency deep brain stimulation improves spatial working memory after traumatic brain injury. *J Neurotrauma* 30: 119-30.

Schonberger J, Birk N, Lachner-Piza D, Dumpelmann M, Schulze-Bonhage A, and Jacobs J. (2019) . *Ann. Clin. Transl. Neurol*. 6(12): 2479-2488.

Schultz SR, Cardamone L, Liu YR, Hogan RE, Maccotta L, Wright DK, Zheng P, Koe A, Gregoire M, Williams JP et al. (2013) Can structural or functional changes following traumatic brain injury in the rat predict epileptic outcome? *Epilepsia* 54(7): 1240-1250.

Schwartz JRL and Roth T. (2008) Neurophysiology of sleep and wakefulness: Basic science and clinical implications. *Curr Neuropharmacol* 6(4): 367-378.

Schwartzkroin PA, Wenzel HJ, Lyeth BG, Poon CC, Delance A, Van KC, Campos L, and Nguyen DV. (2010) Does ketogenic diet alter seizure sensitivity and cell loss following fluid percussion injury? *Epilepsy Res* 92(1): 74-84.

Seiffert E, Dreier JP, Ivens S, Bechmann I, Tomkins O, Heinemann U, and Friedman A. (2004) Lasting blood-brain barrier disruption induces epileptic focus in the rat somatosensory cortex. *J Neurosci* 24(36): 7829-7836.

Seinbenhener ML, and Wooten MC. (2015) Use of the open field maze to measure locomotor and anxiety-like behavior in mice. *J. Vis. Exp*. 96: 52434.

Semple BD, O'Brien TJ, Gimlin K, Wright DK, Kim SE, Casillas-Espinosa PM, Webster KM, Petrou S, and Noble-Haeusslein LJ. (2017) Interleukin-1 Receptor in Seizure Susceptibility after Traumatic Injury to the Pediatric Brain. *J Neurosci* 37(33): 7864-7877.

Serrano-Pozo, A, Gomez-Isla T, Growdon JH, Frosch MP, and Hyman BT. (2013) A phenotypic change but not proliferation underlies glial responses in Alzheimer disease. *Am. J. Pathol*. 182: 2332-2344.

Shandra O and Robel S. (2020) Inducing post-traumatic epilepsy in a mouse model of repetitive diffuse traumatic brain injury. *J Vis Exp* 156: e60360.

Sharma R and Laskowitz DT. (2012) Biomarkers in traumatic brain injury. *Curr Neurol Neurosci Rep* 12(5): 560-569.

Shay N, Yeates KO, Walz NC, Stancin T, Taylor HG, Beebe DW, Caldwell CT, Krivitzky L, Cassedy A, and Wade SL. (2014) Sleep problems and their relationship to cognitive and behavioral outcomes in young children with traumatic brain injury. *J Neurotrauma* 31: 1305-1312.

Shekleton JA, Parcell DL, Redman JR, Phipps-Nelson J, Ponsford JL, and Rajaratnam SM. (2010) Sleep disturbance and melatonin levels following traumatic brain injury. *Neurology* 74: 1732-1738.

Shein NA, Grigoriadis N, Alexandrovich AG, Simeonidou C, Lourbopoulos A, Polyzoidou E, Trembovler V, Mascagni P, Dinarello CA, and Shohami E. (2009) Histone deacetylase inhibitor ITF2357 is neuroprotective, improves functional recovery, and induces glial apoptosis following experimental traumatic brain injury. *FAEB J.* 23(12): 4266-4275.

Shimon B, Shavit-Stein E, Altman K, Pick CG, and Maggio N. (2020) Thrombin as key mediator of seizure development following traumatic brain injury. *Front Pharmacol* 10: 1532.

Shin SS, Dixon CE, Okonkwo DO, and Richardson RM. (2014) Neurostimulation for traumatic brain injury. *J Neurosurg* 121: 1219-1231.

Shultz SR, Cardamone L, Liu YR, Hogan RE, Maccotta L, Wright DK, et al. (2014) Can structural or functional changes following traumatic brain injury in the rat predict epileptic outcome? *Epilepsia* 54: 1240-1250.

Sick T, Wasserman J, Bregy A, Sick J, Dietrich WD, and Bramlett HM. (2017) Increased expression of epileptiform spike/wave discharges one year after mild, moderdte, or severe fluid percussion brain injury in rats. *J Neurotrauma* 34(16): 2467-2474.

Silva LF, Hoffmann MS, Gerbatin R, Fiorin F, Dobrachinski F, Mota BC, Wouters ATB, Pavarini SP, Soares FAA, Fighera MR, and Royes LFF. (2013) Treadmill exercise protects against pentylenetetrazol-induced seizures and oxidative stress after traumatic brain injury. *J Neurotrauma* 30(14): 1278-1287.

Simonini MV, Camargo LM, Dong E, Maloku E, Veldic M, Costa E, and Guidotti A. (2006) The benzamide MS-275 is a potent, long-lasting brain region-selective inhibitor of histone deacetylases. *PNAS* 103(5), 1587-1592.

Sloviter RS. (1987) Decreased hippocampal inhibition and a selective loss of interneurons in experimental epilepsy. *Science*. 235: 73-76.

Smith DH, Chen X-H, Nonaka M, Trojanowski JQ, and Lee VM-Y, et al. (1999) Accumulation of amyloid beta and tau and the formation of neurofilament inclusions following diffuse brain injury in the pig. *J Neuropathol and Exp Neurol* 58(9): 982-992.

Smith D, Rau T, Poulsen A, MacWilliams Z, Patterson D, Kelly W, and Poulsen D. (2018) Convulsive seizures and EEG spikes after lateral fluid-percussion injury in the rat. *Epilepsy Res* 147: 87-94.

Smyth K, Sandhu SS, Crawford S, Dewey D, Parboosingh J, and Barlow KM. (2014) The role of serotonin receptor alleles and environmental stressors in the development of post-concussive symptoms after pediatric mild traumatic brain injury. *Dev Med Child Neruol* 56: 73-77.

Sng J, Hideo Taniura CG, and Yoneda Y. (2006) Histone modifications in kainic-induced status epilepticus. *Euro J Neurosci* 23(5): 1269-1282.

Staba RJ. (2012) Normal and pathologic high-frequency oscillations In: Jasper's Basic Mechanisms of the Epilepsies, (Bethesda, MD).

Statler KD, Scheerlinck P, Pouliot W, Hamilton M, White HS, and Dudek FE. (2009) A potential model of pediatric posttraumatic epilepsy. *Epilepsy Res* 86(2-3): 221-223.

Statler KD, Swank S, Abildskov T, Bigler ED, and White HS. (2008) Traumatic brain injury during development reduces minimal clonic seizure threshold at maturity. *Epilepsy Res* 80(2): 163-170.

Stefanko, D.P., Barrett, R.M., Ly, A.R., Reolon, G.K., and Wood, M.A., 2009. Modulation of long-term memory for object recognition via HDAC inhibition. *Proc. Natl. Acad. Sci. USA* 106(23), 9447-9452.

Steinmetz S, Tipold A, and Löscher W. (2013) Epilepsy after head injury in dogs: A natural model of posttraumatic epilepsy. *Epilepsia* 54: 580–58.

Stevens MC, Lovejoy D, Kim J, Oakes H, Kureshi I, Witt ST. (2012) Multiple resting state network functional connectivity abnormalities in mild traumatic brain injury. *Brain Imaging Behav* 6: 293-318.

Stilling, R.M., van de Wouw, M., Clarke, G., Stanton, C., Dinan, T.G., Cryan, J.F., (2016) The neuropharmacology of butyrate: the bread and butter of the microbiota-gut-brain axis? *Neurochem. Int.* 99: 110-132.

Sukumari-Ramesh S, Alleyne CH, and Dhandapani KM. (2016) The histone deacetylase inhibitor syberoylanilide hydroxamic acid (SAHA) confers acute neuroprotection after intracerebral hemorrhage in mice. *Transl Stroke Res* 7(2): 141-148.

Sun J, Wang F, Hong G, Pang M, Xu H, Li H, Tian F, and Fang R et al. (2016) Antidepressant-like effects of sodium butyrate and its possible mechanisms of action in mice exposed to chronic unpredictable mild stress. *Neurosci Lett* 618: 159-166.

Sun Z, Liu S, Kharlamov EA, Miller ER, and Kelly KM. (2018) Hippocampal neuropeptide Y protein expression following controlled cortical impact and posttraumatic epilepsy. *Epilepsy & Behav* 87: 188-194.

Sutula T, Cascino G, Cavazos J, Parada I, and Ramirez L. (1989) Mossy fiber synaptic reorganization in the epileptic human temporal lobe. *Ann Neurol* 26: 321-330.

Sutula TP and Dudek FE. (2007) Unmasking recurrent excitation generated by mossy fiber sprouting in the epileptic dentate gyrus: an emergent property of a complex system. *Prog Brain Res* 163: 541-563.

Sweatt JD. (2013) The emerging field of neuroepigenetics. *Neuron* 80(3): 624-632.

Szemere E and Jokeit H. (2015) Quality of life is social – Towards an improvement of social abilities in patients with epilepsy? *Seizure* 26.

Szu JI, Chaturvedi S, Patel DD, and Binder DK. (2020) Aquaporin-4 dysreguilation in a controlled cortical impact injury model of posttraumatic epilepsy. *Neurosci* 428: 140-153.

Tagge CA, Fisher AM, Minaeva OV, Gaudreau-Balderrama A, and Moncaster JA, et al. (2018) Concussion, microvascular injury, and early tauopathy in young athletes after impact head injury and an impact concussion mouse model. *Brain* 141(2): 422-458.

Tai, X.Y., Duncan, J., Fox, N., Baxendale, S., Liu, J., Michalak, Z., et al. (2016) Hyperphosphorylated tau in refractory epilepsy patients correlates with cognitive decline: a study of temporal lobe resections. *Brain*. 2441-2455.

Tang L, Ge Y, Sodickson DK, Miles L, Zhou Y, Reaume J, et al. (2011) Thalamic resting-state functional networks: disruption in patients with mild traumatic brain injury. *Radiology* 260: 831-840.

Taylor CA, Bell JM, Breiding MJ, and Xu L. (2017) Traumatic brain injury-related emergency department visits, hospitalizations, and deaths – United States, 2007 and 2013. *MMWR Surveill Summ* 66(9): 1-16.

Temkin NR. (2009) Preventing and treating posttraumatic seizures: the human experience. *Epilepsia* 50: 10-13.

Temkin NR, Jarell AD, and Anderson DG. (2001) Antiepileptogenic agents: How close are we? *Drugs* 61: 1045-1055.

Thomas MJ, Watabe AM, Moody TD, Makhinson M, and O'Dell TJ. (1998) Postsynaptic complex spike bursting enables the induction of LTP by theta frequency synaptic stimulation. *J Neurosci* 18(18): 7118-7126.

Thrane AS, Rappold PM, Fujita T, Torres A, Bekar L et al. (2011) Critical role of aquaporin-4 (AQP4) in astrocytic Ca2+ signaling events elicited by cerebral edema. *Proc Natl Acad Sci USA* 108(2): 846-851.

Timofeev I, Sejnowski TJ, Bazhenov M, Chauvette S, and Grand LB. (2013) Age dependency of trauma-induced neocortical epileptogenesis. *Front Cell Neurosci* 7: 154.

Tobin RP, Mukherjee S, Kain JM, Rogers SK, Henderson SK, Motal HL, Newell Rogers MK, and Shapiro LA. (2014) Traumatic brain injury causes selective, CD74-dependent peripheral lymphocyte activation that exacerbates neurodegeneration. *Acta Neuropathol Commun* 2: 143.

Tomkins O, Feintuch A, Benifla M, Cohen A, Friedman A, and Shelef I. (2011) Blood-brain barrier breakdown following traumatic brain injury: a possible role in posttraumatic epilepsy. *Cardiovasc Psychiatry Neurol* 2011: 765923.

Tomkins O, Shelef I, Kaizerman I, Eliushin A, Afawi Z, Misk A, Gidon M, Cohen A, Zumsteg D, and Friedman A. (2008) Blood-brain barrier disruption in post-traumatic epilepsy. *J Neurol Neurosurg Psychiatry* 79(7): 774-777.

Tong, W., Igarashi, T., Ferriero, D.M., and Noble, L.K., 2002. Traumatic brain injury in the immature mouse brain: Characterization of regional vulnerability. *Exp. Neurol*. 176(1): 106-116.

Topolnik L, Steriade M, and Timofeev I. (2003a) Hyperexcitability of intact neurons underlies acute development of trauma-related electrographic seizures in cats in vivo. *Eur J Neurosci* 18: 486-496.

Topolnik L, Steriade M, and Timofeev I. (2003b) Partial cortical deafferentation promotes development of paroxysmal activity. *Cereb Cortex* 13(8): 883-893.

Tropeano MP, Spaggiari R, Ileyassoff H, Park KB, Kolias AG, Hutchinson PJ, and Servadei F. (2019) A comparison of publication to TBI burden ratio of low- and middle-income countries versus high-income countries: how can we improve worldwide care of TBI? *Neurosurg Focus* 47(5): E5.

Tsankova NM, Berton O, Renthal W, Kumar A, Neve RL, and Nestler EJ. (2006) Sustained hippocampal chromatin regulation in a mouse model of depression and antidepressant action. *Nat Neurosci* 9: 519-525.

Tubi MA, Lutkenhoff E, Blanco MB, McArthur D, Villablanca P, Ellingson B, et al. (2019) Early seizures and temporal lobe trauma predict post-traumatic epilepsy: a longitudinal study. *Neurobiol Dis* 123: 115-121.

Ulyanova AV, Koch PF, Cottone C, Grovola MR, Adam CD, Browne KD, and Weber MT et al. (2018) Electrophysiological signature reveals laminar structure of the porcine hippocampus. *eNeuro* 5(5): 0102-18.

Urrea, C., Castellanos, D.A., Sagen, J., Tsoulfas, P., Bramlett, H.M., and Dietrich, W.D., 2007. Widespread cellular proliferation and focal neurogenesis after traumatic brain injury in rats. *Restor. Neurol. Neurosci*. 25(1), 65-76.

Vallat-Azouvi C, Weber T, Legrand L, and Azouvi P. (2007) Working memory after severe traumatic brain injury. *J Int Neuropsychol Soc* 13: 770-780.

van der Naalt J. (2001) Prediction of outcome in mild to moderate head injury: A review. *J Clin Exp Neuropsychol* 23(6): 837-851.

van Vliet EA, da Costa Araujo S, Redeker S, van Schaik R, Aronica E, and Gorter JA. (2007) Blood-brain barrier leakage may lead to progression of temporal lobe epilepsy. *Brain* 130(2): 521-534.

Vespa, P.M., McArthur, D.L., Xu, Y., Eliseo, M., Etchepare, M., Dinov, I., Alger, J., Glenn, T.P., and Hovda, D., 2010. Nonconvulsive seizures after traumatic brain injury are associated with hippocampal atrophy. *Neurology*. 75(9), 792-798.

Vezzani A, Friedman A, and Dingledine RJ. (2013) The role of inflammation in epileptogenesis. *Neuropharmacology* 69: 16-24.

Vezzani A and Granata T. (2005) Brain inflammation in epilepsy: experimental and clinical evidence. Epilepsia 46(11), 1724-1743.

Vezzani A, Maroso M, Balosso S, Sanchez MA, and Bartfai T. (2011) IL-1 receptor/Toll-like receptor signaling in infection, inflammation, stress and neurodegeneration couples hyperexcitability and seizures. *Brain Behav Immun* 25(7): 1281-1289.

Vidali, G., Boffa, L.C., Bradbury, E.M., and Allfrey, V.G., (1978) Suppression of histone deacetylation by butyrate leads to accumulation of multi-acetylated forms of histones H3 and H4 and increased DNase I-sensitivity of the associated DNA sequences. *Proc. Natl. Acad. Sci. U.S.A.* 75, 2239-2243.

Vigil FA, Bozdemir E, Bugay V, Chun SH, Hobbs M, Sanchez I, Hastings SD, Veraza RJ, Holstein DM, Sprague SM, Carver CM, Cavazos JE, Brenner R, Lechleiter JD, and Shapiro MS. (2020) Prevention of brain damage after traumatic brain injury by

pharmacological enhancement of KCNQ (Kv7, "M-type") K+ currents in neurons. *J Cereb Blood Flow Metab* 40(6): 1256-1273.

Villasana LE, Kim KN, Westbrook GL, and Schnell E. (2015) Functional integration of adult-born hippocampal neurons after traumatic brain injury. *eNeuro* 14: 0056-15.

Viola-Saltzman M and Watson NF. (2012) Traumatic brain injury and sleep disorders. *Neurol Clin* 30(4): 1299-1312.

Vyazovskiy VV, Achermann P, Borbely AA, and Tobler I. (2004) The dynamics of spindles and EEG slow-wave activity in NREM sleep in mice. *Arch Ital Biol* 142(4): 511-523.

Wagner AK, Miller MA, Scanolon J, Ren D, Kochanek PM, Conley YP. (2010) Adenosine A1 receptor gene variants associated with post-traumatic seizures after severe TBI. *Epilepsy Res* 90: 259-272.

Walf, A.A. and Frye, C.A., 2007. The use of the elevated plus maze as an assay of anxiety-related behavior in rodents. *Nat. Protoc*. 2(2): 322-328.

Wang F, Wang X, Shapiro LA, Cotrina ML, Liu W, Wang EW, Gu S, Wang W, He X, Nedergaard M, and Huang JH. (2017) NKCC1 up-regulation contributes to early post-traumatic seizures and increased post-traumatic seizure susceptibility. *Brain Structure and Function* 222: 1543-1556.

Wang X, Gao X, Michalski S, Zhao S, and Chen J. (2016a) Traumatic brain injury severity affects neurogenesis in adult mouse hippocampus. *J Neurotrauma* 33(8): 721-733.

Wang X, Wang Y, Zhang C, Liu C, Zhao B, Wei N, Zhang J, and Zhang K. (2016b) CB1 receptor antagonism prevents long-term hyperexcitability after head injury by regulation of dynorphin-KOR system and mGlurR5 in rat hippocampus. *Brain Res* 1646: 174-181.

Wang X, Wang Y, Zhang C, Liu C, Yang H, Hu W, Zhang J, and Zhang K. (2016c) Endogenous cannabinoid system alterations and their role in epileptogenesis after brain injury in rat. *Epilepsy Res* 128: 35-42.

Wat R, Mammi M, Paredes J, Haines J, ALasmari M, Liew A, Lu VM, Arnaout O, Smith TR, Gormley WB, Aglio LS, Mekary RA, and Zaidi H. (2019) The effectiveness of antiepileptic medications as prophylaxis of early seizure in patients with traumatic brain injury compared with placebo or no treatment: a systematic review and meta-analysis. *World Neurosurg* 122: 433-440.

Weber W. (2010) Cancer epigenetics. *Prog Mol Biol Transl Sci* 95: 299-349.

Webster KM, Shultz SR, Ozturk E, Dill LK, Sun M, Casillas-Espinosa P, Jones NC, Crack PJ, O'Brien TJ, and Semple BD. (2019) Targeting high-mobility group box protein 1 (HMGB1) in pediatric traumatic brain injury: Chronic neuroinflammatory, behavioral, and epileptogenic consequences. *Exp Neurol* 320:112979.

Wei H, Duan G, He J, Meng Q, Liu Y, Chen W, and Meng Y. (2018) Geniposide attenuates epilepsy symptoms in a mouse model through the PI3K/Akt/GSK3β signaling pathway. *Exp Ther Med* 15: 1136-1142.

Wei G, May Lu X-C, Yang X, and Tortella FC. (2010) Intracranial pressure following penetrating ballistic-like brain injury in rats. *J Neurotrauma* 27(9): 1635-1641.

West, S., Nolan, S.J., and Newton, R., 2016. Surgery for epilepsy: a systematic review of current evidence. *Epileptic Dis*. 18(2), 113-121.

Wilder RM. (1921) High fat diets in epilepsy. *May Clin Bull* 2: 308.

Williams AJ, Hartings JA, May Lu X-C, Rolli ML, Dave J, and Tortella FC. (2005) Characterization of a new rat model of penetrating ballistic brain injury. *J Neurotrauma* 22(2): 313-331.

Witkin JM, Li G, Golani LK, Xiong W, Smith JL, Ping X, Rashid F, Jahan R, Cerne R, Cook JM, and Jin X. (2020) The Positive Allosteric Modulator of *α*2/3-Containing GABAA Receptors, KRM-II-81, Is Active in Pharmaco-Resistant Models of Epilepsy and Reduces Hyperexcitability after Traumatic Brain Injury. *J Pharamcol Exp Ther* 372(1): 83-94.

Witkin JM, Smith JL, Ping X, Gleason SD, Poe MM, Li G, et al. (2018) Bioisosteres of ethyl 8-ethynyl-6-(pyridine-2-yl)-4H-benzo[f]imidazo[1, 5-a][1, 4]diazepine-3-carboxylate (HZ-166) as novel alpha 2,3 selective potentiators of GABAA receptors: Improved bioavailability enhances anticonvulsant efficacy. *Neuropharmacology* 137: 332-343.

Wolf JA, Johnson BN, Johnson VE, Putt ME, Browne KD, and Mietus CJ, et al. (2017) Concussion induces hippocampal circuitry disruption in swine. *J Neurotrauma* 34: 2303-2314.

Woodcock T and Morganti-Kossmann MC. (2013) The role of markers of inflammation in traumatic brain injury. *Front Neurol* 4: 18.

World Health Organization. (2002) Genomics and World Health: Report of the Advisory Committee on Health research. Geneva, WHO.

Wu Z, Wang Z, Liu X, Zhang Z, Gu X, Yu SP, Keene CD, Cheng L, Ye K. (2020) Traumatic brain injury triggers APP and tau cleavage by delta-secretase, mediating Alzheimer's disease pathology. *Prog Neurobiol* 185: 101730.

Wyler A.R., Hermann B.P., Somes G., (1995) Extent of medial temporal resection on outcome from anterior temporal lobectomy: a randomized prospective study. *Neurosurgery*. 37, 982–990.

Xiong Y, Mahmood A, and Chopp M. (2013) Animal models of traumatic brain injury. *Nat Rev Neurosci* 14(2): 128-142.

Xu, A., Sun, Q., Fan, J., Jiang, Y., Yang, W., Cui, Y., Yu, Z., Jiang, H., and Li, B., 2019. Role of astrocytes in post-traumatic epilepsy. *Front. Neurol*. 10(1149).

Xu J, Zhang H, and Zhang Y. (2018) Vorinostat: a histone deacetylase (HDAC) inhibitor ameliorates traumatic brain injury by inducing iNOS/Nrf2/ARE pathway. *Folia Neuropahtol* 56(3): 179-186.

Yang L, Afroz S, Michelson HB, Goodman JH, Valsamis HA, and Ling DS. (2010) Spontaneous epileptiform activity in rat neocortex after controlled cortical impact injury. *J Neurotrauma* 27(8): 1541-1548.

Yarlagadda A, Alfson E, and Clayton AH. (2009) The blood brain barrier and the role of cytokines in neuropsychiatry. *Psychiatry* 6(11): 18-22.

Yen, T, Chang C, Chung C, K W, Yang C, and Hsieh C. (2018) Neuroprotective effects of platonin, a therapeutic immunomodulating medicine, on traumatic brain injury in mice after controlled cortical impact. *Int J Mol Sci* 19(4): 1100.

Younus I and Reddy DS. (2017) Epigenetic interventions for epileptogenesis: A new frontier for curing epilepsy. *Pharmacol Ther* 177: 108-122.

Yu T-S, Zhang G, Liebl DJ, and Kernie SG. (2008) Traumatic brain injury-induced hippocampal neurogenesis requires activation of early nestin-expressing progenitors. *J Neurosci* 28(48): 12901-12912.

Yun Ng S and Lee AYW. (2019) Traumatic brain injuries: pathophysiology and potential therapeutic targets. *Front Cell Neurosci* 27: 00528.

Zeng LH, McDaniel S, Rensing NR, and Wong M. (2010) Regulation of cell death and epileptogenesis by the mammalian target of rapamycin (mtor): a double-edged sword? *Cell Cycle* 9: 2281-2285.

Zeng LH, Rensing NR, and Wong M. (2009) The mammalian target of rapamycin signlaing pathway mediates epileptogenesis in a model of temporal lobe epilepsy. *J Neurosci* 29: 69-64-6972.

Zhang B, West EJ, Van KC, Gurkoff GG, Zhou J, Zhang XM, Kozikowski AP, and Lyeth BG. (2008) HDAC inhibitor increases histone H3 acetylation and reduces microglia inflammatory response following traumatic brain injury in rats. *Brain Res* 1226: 181-191.

Zhang R, Sun L, Hayashi Y, Liu X, Koyama S, Wu Z, and Nakanishi H. (2010) Acute p38-mediated inhibition of NMDA-induced outward currents in hippocampal CA1 neurons by interleukin-1beta. *Neurobiol Dis* 38(1): 68-77.

Zhang, S., Fujita, Y., Matsuzaki, R., and Yamashita, T. (2018) Class I histone deacetylase (HDAC) inhibitor CI-994 promotes functional recovery following spinal cord injury. *Cell Death Dis*. 9(5): 460.

Zhang ZY, Zhang Z, Fauser U, Schluesener HJ. (2007) Global hypomethylation defines a sub-population of reactive microglia/macrophages in experimental traumatic brain injury. *Neurosci Lett* 457: 8-11.

Zhao H, Li G, Zhang S, Li F, and Wang R et al., (2019) Inhibition of histone deacetylase 3 by MiR-494 alleviates neuronal loss and improves neurological recovery in experimental stroke. *J Cereb Blood Flow Metab* 39(12): 2392-2405.

Zhu B, Eom J, and Hunt RF. (2019) Transplanted interneurons improve memory precision after traumatic brain injury. *Nat Comm* 10: 5156.

Zhu O, Wang L, Zhang Y, Zhao F, Luo J, Xiao Z, Chen G, and Wang X. (2011) Increased expression of DNA methyltransferase 1 and 3a in human temporal lobe epilepsy. *J Mol Neuro* 46: 420-426.

Ziino C and Ponsford J. (2005) Measurement and prediction of subjective fatigue following traumatic brain injury. *J Int Neuropsychol Soc* 11: 416-425.

Zijlmans M, Jiruska P, Zelmann R, Leijten FS, Jefferys JG, Gotman J. (2012) High-frequency oscillations as a new biomarker in epilepsy. *Ann Neurol* 71(2): 169-178.

Zimmerman LL, Martin RM, and Girgis F. (2017) Treatment options for posttraumatic epilepsy. *Curr Opin Neurol* 30: 580-586.